Department of Chemical Engineering

Rondebosch, Cape Town, South Africa

Dissertation submitted in fulfilment of the requirements of the degree of

MASTER OF SCIENCE IN ENGINEERING

The effect of hydrocarbon exposure and temperature on the behaviour of elastomeric seals

---

Author: Christopher Scully

Supervisor: Dr Chris Woolard

August 2013

The financial assistance of the National Research Foundation (NRF) towards this dissertation is hereby acknowledged. Opinions expressed and conclusions arrived at are those of the author and are not necessarily attributed to the NRF.

PLAGIARISM DECLARATION

1. I know that plagiarism is wrong. Plagiarism is using another's work and to pretend that it is one's own.

2. Each significant contribution to, and quotation in, this project from the work, or works of other people has been attributed and has cited and referenced.

3. The work, presented here, is my own work.

4. I acknowledge that copying someone else's assignment or project, or part of it, is wrong, and declare that this is my own work.

Christopher Scully

SIGNATURE: Signed by candidate

DATE: 26 August 2013

ACKNOWLEDGEMENTS

This dissertation has been made possible through the help and support of a number of people. The author would like to thank his supervisor, Dr Chris Woolard, for his continual assistance, guidance and support throughout the duration of this project. Additionally, I would like to thank all my colleagues at the Sasol Advanced Fuels Laboratory (SAFL) for their help and assistance throughout. In particular, I would like extend my gratitude towards Mr Gerhard Lourens for his continued assistance both inside and outside of the laboratory. The author would also like to acknowledge the assistance of Mr Ross Burnham who demonstrated many of the methods used in this study.

The author would like to express a special thank you to Sasol Technology Fuels Technology and the University of Cape Town for their generous financial support. Without such support this dissertation would not have been possible. Additionally, the author would like to acknowledge the Department of Chemical Engineering for its support of this study.

Finally, the author would like to thank his partner and family for their continual support and many hours spent proof reading this document.

ABSTRACT

Synthetic jet fuels have been proposed as alternatives to petroleum Jet A-1. Compatibility issues, however, are of concern; specifically the interaction of synthetic fuels with polymeric materials which are commonly used to seal fuel systems. This is because of differences between the composition of synthetic fuels and petroleum-derived fuels. Synthetic fuel streams contain no or very low aromatics, unlike petroleum-derived fuels. This investigation was consequently initiated to gain a greater understanding of the factors affecting seal swell in the aviation industry. The study focussed interactions between fuel components from various fuel classes and nitrile rubber (NBR) as well as a restricted set of investigations on fluorocarbon (FKM) rubber. No comprehensive study of the temperature sensitivity of fuel composition on swelling has been attempted prior to this study.

NBR and FKM were swollen in petroleum Jet A-1, synthesised paraffinic kerosene (SPK) and a variety of blends of pure components with SPK. These components were selected from aromatic species (monoaromatic, diaromatic and heterocyclic), cycloparaffins, aromatic oxygenates and other oxygenates. Aromatic species were blended at 8% (v/v) while all other species were blended at 15% (v/v).

Within the class of aromatic hydrocarbon components, it was found that decreasing molecular size, increasing the number of ring structures (particular aromatic rings) as well as increasing all Hansen solubility parameters increased swelling. Of the Hansen solubility parameters, the greatest correlation was found with the hydrogen-bonding (electron exchange) parameter. Nonetheless the dispersion parameter which is strongly affected by the number of aromatic rings and length of any aliphatic side-chain was also important. A very good correlation was found between swelling and the density of the aromatic species. It was found furthermore that introducing oxygen atoms increased swelling. The introduction of cycloparaffins also increase swelling although to a much lesser extent than aromatics. Cyclisation together with a polar moiety was observed to increase swell significantly. With FKM elastomers, fuel composition had less influence.

Temperature sensitivity was explored by performing swelling at 20^{o}C, 35 ^{o}C and 50 ^{o}C. Van't Hoff plots were used to obtain enthalpies of mixing. It was found that all hydrocarbons swelled more as temperature rose. This is indicative of endothermic interactions between these species and polar NBR. However, it was observed that species with high polar and hydrogen-bonding Hansen solubility parameters had lower sensitivity to temperature. It is postulated that in these species, less aromatic concentration in the NBR occurs at elevated temperatures, contributing to lower sensitivities. Aromatic oxygenates were observed to decrease in swelling with temperature. This is ascribed to a strong exothermic interaction. This behaviour was in

contrast to non-aromatic oxygenates. It is possible that blends of these non-aromatic oxygenates with SPK are less stable at elevated temperatures leading to component separation into the NBR and thus more swelling. Similar trends were observed with fluorocarbon elastomers (FKM).

Physical property measurements were made on swollen NBR O-rings. A distinct relationship between decreased glass transition temperature and the extent of swelling was observed. Fuel which had adsorbed into the elastomer was observed to act as an effective plasticiser. Not only did increased swelling lower the glass transition temperature but it reduced the modulus of NBR O-rings in a predictable fashion. A significant decrease in storage modulus was associated with increased swelling. Increased swelling was found to be associated with increased compression set although the mechanism by which this manifests itself is unclear.

TABLE OF CONTENTS

LIST OF FIGURES

LIST OF TABLES

Abbreviations

ASTM	ASTM International (formerly American Society for Testing and Materials)
BB	n-butyl benzene
BTL	biomass-to-liquids
b.p.	boiling point
CR	co-polymeric resin
CTL	coal-to-liquid(s)
DCM	dichloromethane
Def Stan	Defence Standard
DMA	dynamic mechanical analysis
DSC	differential scanning calorimetry
E*	complex modulus
E’	storage modulus
E’’	loss modulus
EPDM	ethylene propylene diene monomer rubber
EVA	poly(ethylene-*co*vinyl acetate)
FKM	fluorocarbon elastomer
FSJF	fully synthetic jet fuel
FT	Fischer-Tropsch
GC-MS	gas chromatography-mass spectrometry
GTL	gas-to-liquids
HEFAs	hydroprocessed esters and fatty acids
HNBR	hydrogenated nitrile rubber
HSP	Hansen solubility parameter
HTFT	high temperature Fischer-Tropsch
i.d.	inside diameter
IPK	iso-paraffinic kerosene
Jet A	civil aviation turbine fuel used domestically in the United States of America
Jet A-1	civil aviation turbine fuel used outside the United States of America and for international flights to and from the USA
JP-5	high flash point kerosene meeting the requirements of the U.S. Military Specification MIL-PRF-5624S Grade JP-5
JP-8	US military equivalent of Jet A-1 with the addition of corrosion inhibitor and anti-icing additives
LPG	liquid petroleum gas
LTFT	low temperature Fischer-Tropsch
max.	maximum

Merox	mercaptan oxidation
min.	minimum
M_w	molecular weight/molar mass
NBR	nitrile butadiene rubber
NR	natural rubber
PEA	pol(ethylacryalate)
PEM	polymer electrolyte membrane
phr	parts per hundred rubber (by volume)
PMA	poly(methylacryalte)
PVA	poly(vinyl alcohol)
SBR	styrene butadiene rubber
SMDS	Shell middle distillate synthesis
SP	solubility parameter
SPD	slurry phase distillate
SPK	synthesised paraffinic kerosene
SSJF	semi-synthetic jet fuel
T_g	glass transition temperature
tan δ	ratio of storage to loss modulus
TGA	thermogravimetric analysis
THF	tetrahydrofuran
TMA	thermomechanical analysisg
v/v	volume per volume
vol%	percentage by volume
VLE	vapour-liquid-equilibrium
wt%	percentage by weight/mass

CHAPTER 1

1. Introduction

1.1 Motivation for this study

Unprecedented demand for transportation fuels, political instability in oil-rich countries and serious environmental impacts associated with the use of conventional petroleum products have spurred the development of alternative fuels to the forefront of research worldwide [1]. The successful adoption of alternative fuels require a number of factors to be considered. For example, safe and reliable engine function cannot be compromised with the introduction of alternative fuels. The fuel must be fully fungible with current engine technology, prosee no negative impacts on the life-cycle of fuel system components and cause no adverse environmental effects such as increased emissions and particulate matter [2]. It is desirable that these alternative fuels be "drop-in" replacements, i.e. require no modification to existing engine technology [3].

Alternative fuels can be produced from carbon-rich materials such as coal, natural gas and biomass. Currently major production of alternative fuels is carried out via the Fischer-Tropsch (FT) process which converts carbon-rich coal or natural gas to synthetic liquid fuel. The synthetic FT fuel, produced, may require further processing and addition of blending components before implementation [3]. Such fuels have found application in gasoline, jet fuel and diesel markets.

The introduction of non-petroleum-based jet fuel took place in 1999 when a semi-synthetic jet fuel (SSJF), produced by Sasol, was used at O.R Tambo International Airport in Johannesburg, South Africa [4]. The SSJF comprised a blend of petroleum jet fuel and synthetic hydrocarbons derived from coal through Sasol's FT process. Since then SSJF has been accepted and recognised under DEF-STAN 91-91 [5] and ASTM D7566 [6].

Following the success of the SSJF, Sasol launched qualification test work into fully synthetic jet fuel (FSJF) which was approved in September 2008 [7]. The FSJF contains kerosene streams containing aromatics which satisfy the property requirements of international jet fuels. A minimum of 8% (v/v) aromatic content is required in both SSJF and FSJF to ensure compatibility with existing fuel components [7]. The addition of a minimum 8% (v/v) aromatic

compounds has been subject to numerous investigations. This has partly been because the addition of these blending compounds increases the propensity of the fuel to produce soot and particulate matter as well as increasing the overall price of the synthetic fuel [8]. Absence of aromatic compounds, however, reduces the propensity of the fuel to swell elastomeric components such as seals and O-rings. This is of particular concern as the use of synthetic fuels with limited aromatic content may cause elastomeric seals to shrink, harden and fail when fuel is switched from a petroleum jet fuel to a synthesised paraffinic kerosene (SPK). This could compromise the integrity of the system by causing fuel leaks [8]. Whether 8% (v/v) aromatic content constitutes a true minimum acceptable performance limit is uncertain. The specification limit appears to be based on historical experience rather than real performance [3].

Considerably less elastomeric seal swell has been observed for synthesised paraffinic kerosene (SPK) compared to conventional petroleum Jet A-1 resulting in different performance behaviour if fuel is switched from conventional to synthetic fuels that contain limited aromatic content [9]. This is especially true of aged seals which may have experienced a degree of compression set which could further diminish the sealing ability of the elastomer.

The quantity of aromatic species is not the only factor which affects the chemistry and interaction of synthetic fuels with polymeric materials. The reduced elastomeric swell of paraffinic hydrocarbons, compared to aromatic compounds, is driven by the higher polarity and hydrogen bonding character of aromatic compounds.

The processing of synthetic fuels via high temperature Fischer-Tropsch (HTFT) and low temperature Fischer-Tropsch (LTFT) routes produce SPK products, different in paraffinic nature which may cause differences in the performance of elastomeric components compared with conventional petroleum fuels [4, 8]. Synthetic fuels may differ in the ratio of iso to normal paraffins, the level of cycloparaffins and in carbon number distribution. These differences contribute to differences in swelling performance of elastomer materials.

Seals and O-rings, required for dynamic sealing operations, are required to display adequate flexibility, elastic modulus and should not experience a large shift in the glass transition temperature. When seals are used in static sealing operations, exposure to synthetic fuels has been shown to soften the seals leading to a decrease in modulus and tensile strength. Such a change in modulus decreases the applied force on the sealing material and ultimately decreases the overall sealing force and performance of the material [7].

1.2 Objectives

The objectives of the study were to:

- investigate the effects that blending differing aromatic compounds with SPK have on elastomeric seal swell compared to conventional Jet A-1 fuel,
- investigate the effects of molecular size, polarity, hydrogen bonding of these compounds on the swelling of nitrile rubber (NBR) O-rings,
- investigate the effect of ring substituents on the swelling of NBR O-rings by cycloparaffinic compounds,
- investigate the temperature sensitivity of solvent uptake by NBR O-ring specimens,
- assess the impact of these blending components on the physical properties of NBR O-rings such as modulus, tensile strength, elasticity and compression set,
- assess the impact of different fuels on changes in swelling that result when fuels are switched, and
- compare the swelling behaviour of fluorocarbon (FKM) elastomers to that of NBR for a selected set of compounds.

1.3 Scope of investigation

While some investigations were performed using fluorocarbon O-rings, the bulk of this study was performed using nitrile rubber (NBR) O-rings. This was because NBR has been shown to exhibit good fuel resistance and is thus widely used yet it displays a distinct sensitivity to changing fuel chemistry [1].

Initial swelling experiments were performed using blends of SPK and a wide range of compounds to assess the impact of molecular size and solubility parameters. Temperature sensitivity work, however, was performed on subset of these compounds. The compounds for these tests were chosen as representative of different chemical classes. Later experiments using fluorocarbon O-rings and switch-loading experiments were in turn performed on a further reduced subset. For budgetary reasons, experiments could not be performed on fluorosilicone elastomers.

Solvent uptake (swelling) experiments were restricted to gravimetric and volumetric measurements. No attempt was made to determine which specific components were taken up. Recommendations for further work in this regard are made at the end of this dissertation.

A number of physical properties, although by no means exhaustive, were used to assess the impact of solvent exposure on O-rings. Physical property measurements were restricted to

measurements on NBR O-rings because this material had been demonstrated to be the most sensitive to fuel composition. Physical property measurements, which were made, were glass transition measurements, modulus (using dynamic mechanical analysis (DMA) and tensile testing), ultimate tensile strength and compression set.

CHAPTER 2

2. Literature review

2.1 Petroleum fuels

Figure 2.1 illustrates current worldwide energy dependence by source per region and per capita. In the transport sector, crude-derived fuels currently dominate the fuel pool with over 95% gasoline or distillate derivatives such as diesel, kerosene and jet fuel [10]. With demand for transportation increasing, alternative fuels will become more important. A number of challenges face the adoption of such fuels as replacements for petroleum fuels which have long been established. Existing transport infrastructure (distribution networks as well as vehicles) have been developed around petroleum fuels. Any replacement fuel should preferably not cause significant disruption to this infrastructure.

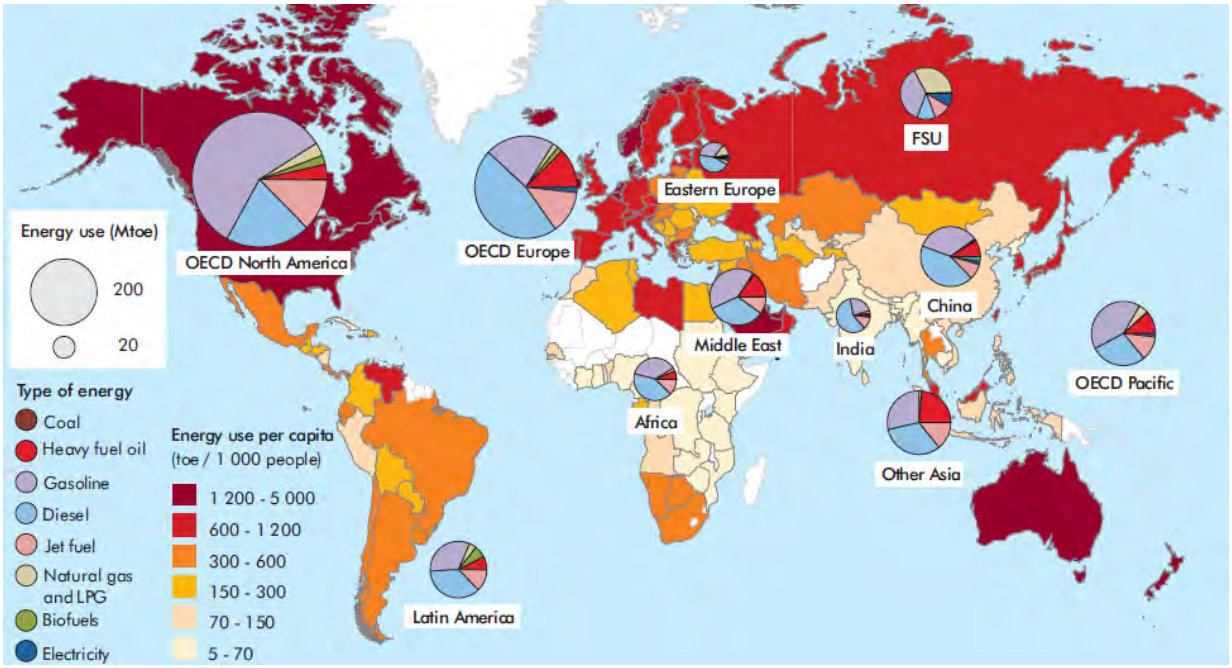

Figure 2.1: Energy use per region and per capita, (reproduced from IEA, 2010 [10])

Gasoline, diesel and jet fuel are typically produced from crude oil. Crude oil consists primarily of hydrocarbons which contain between 5 and 70 carbon atoms per molecule. Depending on

the type of hydrocarbon (linear, branched or cyclic) the fuel may be classified as paraffin base, naphthene base, asphalt base or mixed base [11]. Beside the hydrocarbons present in crude oil, trace metals like vanadium, nickel and chromium are present. Despite occurring in very low concentrations (few parts per million), trace metals are of considerable importance. Even minute quantities can cause severe refining and in-service issues including catalyst poisoning and corrosion of turbine blades, refractory stacks and linings [11]. Table 2.1 describes typical commercial products obtained from conventional crude oil.

Table 2.1: Typical commercial products produced from crude oil refining [9]

Carbon number range	Product produced	Boiling point range (°C)
C_3 to C_4	LPG	<45
C_5 to C_{10}	Gasoline	45-155
C_9 to C_{13}	Kerosene	165-260
C_{10} to C_{24}	Diesel fuel	240-360
C_{13} to C_{40}	Fuel oil	>360

2.1.1 Jet and turbine fuels

Aviation is expected to be the fastest growing transport sector with air miles per passenger set to increase four-fold by 2050 [10]. Currently several grades of jet fuel exist for commercial and military use. These include Jet A-1, Jet A, Jet B and JP-8. Jet A-1 is an international jet fuel employed in nearly all parts of the world. Jet A is restricted to use within the United States of America where the cruising altitude of domestic planes is generally lower than international flights. Jet B is a distillate fuel cut, covering the naphtha and kerosene fractions. Jet B has a lower maximum freezing point specification (-51°C) than Jet A-1 and Jet A and is therefore commonly used in extremely cold climates such as Canada and Alaska [5, 11].

Jet fuel is a complex mixture of hydrocarbons, typically with a carbon distribution between 8 and 16 carbon atoms per molecule. Because of the complexity of jet fuel mixtures, product specifications have evolved to purely performance specifications rather than being compositional based specifications. As such, jet fuels are produced to international standards such as those set out by Defence Standard 91-91 [5] and ASTM D1655 [12]. Despite international standards using performance specification, jet fuels do contain some compositional specifications. These limit the total aromatic content to below 25% (v/v) and the naphthalene content to a maximum of 3.0% (v/v). Note, the maximum of 3.0% (v/v) naphthalene content is related to achieving minimum smoke point value of 19mm [5]. Furthermore, the maximum freezing point for commercial jet fuels is set at -47°C [13] which

indirectly constrains the normal paraffin content of jet fuel. These specifications are summarised in

Table 2.2 which highlights the important specifications and characteristics associated with turbine fuel.

Table 2.2: Key specifications for aircraft turbine fuels [13]

Property	Jet A/A-1	JP-5	JP-8
Aromatics (vol%, max.)	25	25	25
Naphthalenes (vol%, max.)	3.0	-	3.0
Flashpoint (°C) min.	38/40	60	38
Freeze Point (°C) max.	-40/-47	-46	-47
Sulfur, wt%, max.	0.30	0.4	0.3

A typical carbon number distribution for a Merox-treated Jet A-1 may be found in Figure 2.2.

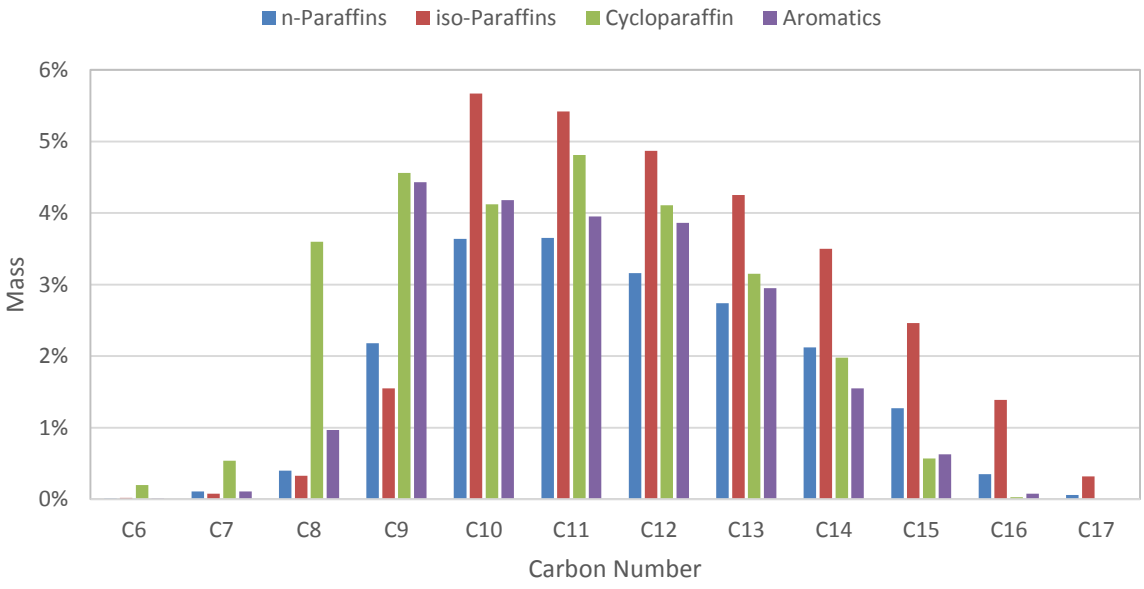

Figure 2.2: Hydrocarbon distribution in a straight run Merox kerosene (adapted from van der Westhuizen *et al.* [14])

A wide variety of chemical species are present in petroleum Jet A-1 with the bulk of the molecules in the C_9 to C_{15} range.

2.2 Alternative hydrocarbon fuels

Substitutes for conventional petroleum can be classified into two distinct groups: (1) synthetic crude oils produced primarily from low-grade (unconventional) petroleum resources and (2) synthetic liquid fuels produced through gasification and catalytic reforming of carbon-rich materials [15]. For the latter, processes and sources include enhanced oil recovery, tar sands, extra heavy-oil and gas-to-liquids (GTL), coal-to-liquids (CTL) and shale oil. Over 1.5% of the total global petroleum production is produced from Canadian tar sands and Venezuelan extra-heavy oil. Upwards of 500,000 bbl/day of synthetic liquid fuels are produced via FT processes, with approximately 260,000 bbl/day produced from the Shell Pearl GTL plant in Qatar [15, 16].

A number of alternative petroleum sources have been touted as the next major source for petroleum production [15]. Shale oil is formed from sedimentary rock that contains hydrocarbon-like material thought to originate from sediment which creates oil naturally. The conversion of shale oil to usable hydrocarbons is an energy intensive process, adding cost and CO_2 emissions to an already costly and energy intensive equation. While technologies to produce synthetic crude oil from shale oil at significantly reduced costs and emissions have been developed, these technologies are still in their infancy [15].

In addition to unconventional petroleum sources, synthetic liquid fuels produced mainly through FT processes have attracted attention worldwide as a possible route for major production of fully fungible synthetic fuels. FT processes typically uses carbon-rich material such as coal, natural gas and biomass to produce a liquid fuel with coal and natural gas leading as primary sources used to produce this fuel [15]. The CTL process of synthetic fuel production is more costly than GTL due to inherent difficulties in handling and processing coal. Further, the high carbon to hydrogen ratio of coal results in higher CO_2 emissions during CTL production [17]. GTL technology is set up to produce high-quality straight chain diesel which adds to the attractiveness of GTL [15, 17].

Biomass feedstock, and in particular, lignocellulosic biomass has been identified as a promising alternative to petroleum-derived products. Utilisation of domestic biomass offers the potential to produce affordable fuels, diversify energy sources and ultimately reduce the dependence on oil [18]. The reducing oil-dependence in turn offers several spin offs such as the ability to mitigate climate impacts, enhance sustainability, increase energy security and stimulate local economies through improved trade-deficits and product innovation [19].

Biomass may be processed in a variety of ways which includes the use of FT biomass-to-liquids technology (BTL) [19].

2.2.1 Fischer-Tropsch (FT) processes

In Fischer-Tropsch processes, a mixture of carbon monoxide and hydrogen (synthesis gas) are reacted in the presence of catalyst (usually Fe or Co) to produce a mixture of higher molecular weight hydrocarbons and oxygenates often referred to as FT syncrude [2, 20]. The properties of the syncrude differ depending on the FT catalyst employed and the operating conditions of the process [16].

The synthesis gas used at the start of the FT process originates from carbon-rich materials such as coal and natural gas. The use of coal to produce a FT syncrude is referred to as coal-to-liquid (CTL) while the use the natural gas is coined as gas-to-liquid (GTL). These technologies produce a wide array of end-products and the choice of technology to use is typically based on resource availability and economic viability of the process and final product [21].

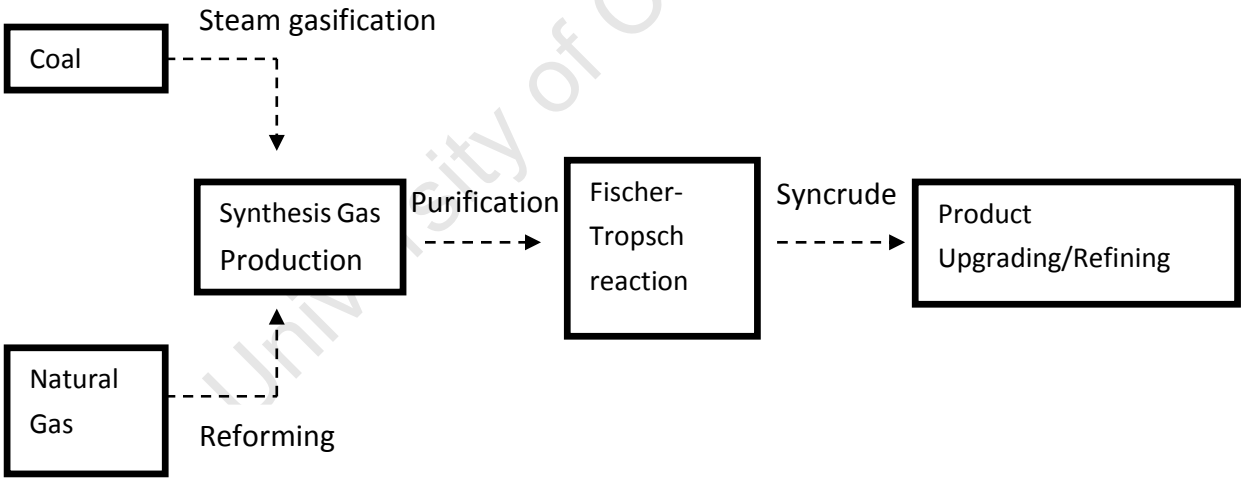

Figure 2.3: Fischer-Tropsch process schematic (adapted from Lamprecht *et al.*, 2007 [20])

Although the application of FT technology is inherently complex, 3 basic steps may be identified as summarised in Figure 2.3. Additionally, the FT process may be run via two distinctive methods namely, high temperature and low temperature FT [20, 22].

2.2.1.1 High temperature Fischer-Tropsch (HTFT) processes

HTFT processes operate in a temperature range between 310-340°C. Known reactor types for the production of HTFT syncrude include circulating bed or fixed fluidised bed systems [20]. Currently the HTFT process employed by Sasol is the largest commercial scale operation of the HTFT technology. Sasol employ Sasol Advanced Synthol (SAS) process using a fixed fluidised bed reactor and an iron catalyst [23]. The hydrocarbon fraction produced through this technology consists of linear paraffins and linear α-olefins as primary products. Aromatics and branched paraffins are also formed [16]. Products derived from HTFT processes generally are of lower molecular weight than those derived from Low Temperature Fischer-Tropsch (LTFT) processes.

HTFT products are distinctly more unsaturated than LTFT products. The FT product stream may be separated into naphtha and distillate fractions. This distillate is then subject to downstream upgrading to produce two distillates in the diesel boiling range. These diesel products are of inferior quality to LTFT diesel and are often used as blending components in final petroleum products [20, 17]. The major refinery products of HTFT processes are geared towards production of gasoline boiling range products.

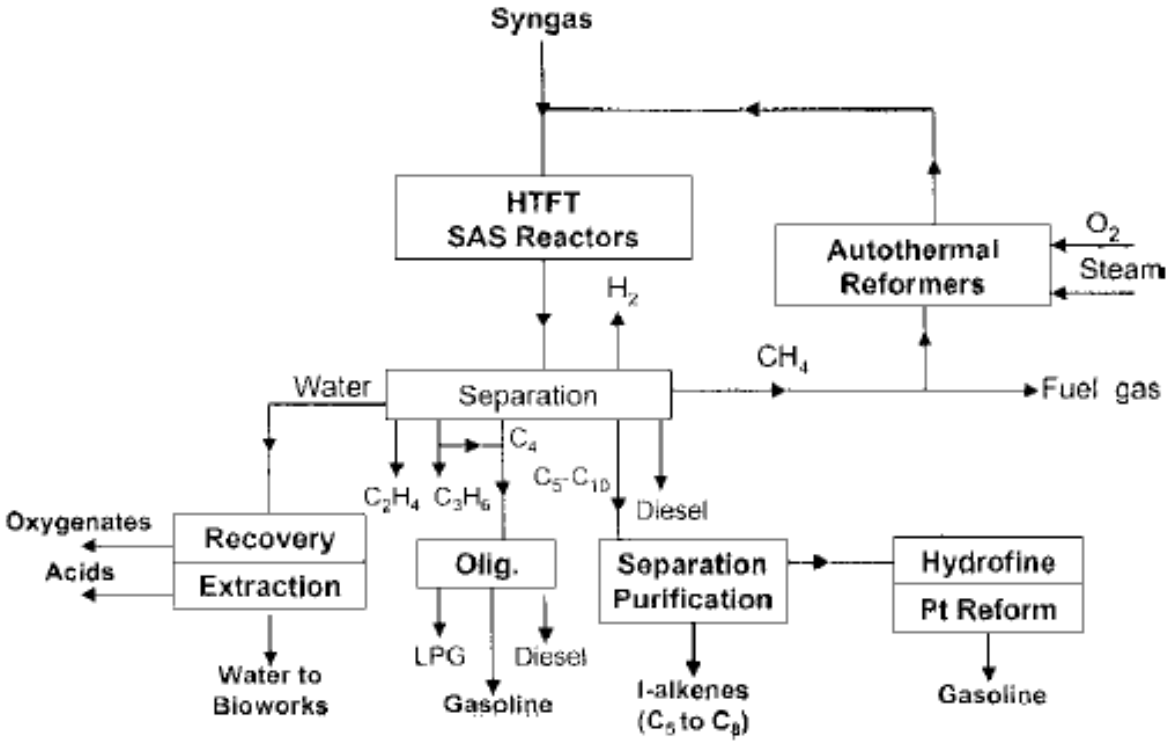

Figure 2.4: Flow diagram of a typical HTFT process (reproduced from Dry, 2001 [21])

Figure 2.4 shows a schematic of the HTFT process while Table 2.3 highlights the product distribution of HTFT and compares this directly with the product distribution of LTFT. The bias of HTFT towards gasoline production, with about 40% of the total product presiding in the gasoline boiling range, can be seen. Jet fuel is produced to a lesser extent. The kerosene fraction produced requires additional downstream processing such as isomerisation in order to meet final jet fuel specifications [23].

Table 2.3: Summary of products produced from LTFT and HTFT processes [16]

Products	LTFT Arge (wt %)	HTFT Synthol (wt %)
Carbon number distribution		
C_3-C_4, LPG	10	30
C_5-C_{10}, naphtha	19	40
C_{11}-C_{22}, distillate	22	16
C_{22} and heavier	46	6
Aqueous products	3	8
Compound classes		
Paraffins	Major product	>10%
Olefins	>10%	Major product
Aromatics	<1%	5-10%
Oxygenates	5-15%	5-15%
S- and N- species	None	None
Water	Major by-product	Major by-product

2.2.1.2 Low temperature Fischer-Tropsch (LTFT) processes

LTFT processes operate in a lower temperature range than HTFT of 210-260°C utilising either an iron or cobalt catalyst with predominantly GTL technology. The process typically includes the use of a slurry bed reactor. In industry practice, Sasol combines this reactor with their Slurry Phase Distillate (SPD) technology, whereas Shell makes use of their proprietary Shell middle distillate synthesis (SMDS) [20, 24]. LTFT processes produce high molecular weight n-paraffins, olefins and oxygenates. These straight chain paraffins may be cracked into lighter fractions while the olefins and oxygenates may be hydrogenated [20]. LTFT technology is ideal for producing high quality diesel fuels since ideal diesel consists primarily of linear paraffins [17]. The kerosene product is derived from cracking straight chain paraffins and thereby requires extensive downstream processing such as isomerisation in order to meet current jet fuel specifications. Figure 2.5 outlines a typical LTFT process using a cobalt catalyst.

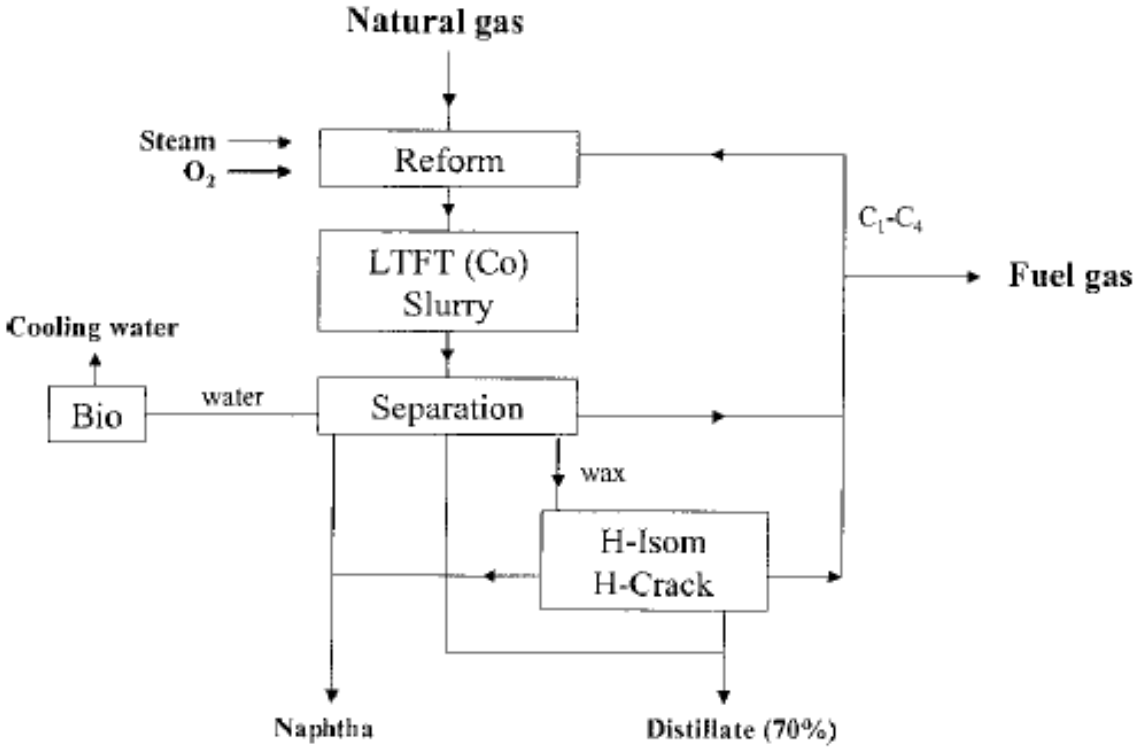

Figure 2.5: Flow schematic of an LTFT process (reproduced from Dry, 2001 [21])

2.2.2 Synthetic jet fuels

When interest in synthetic fuels for aviation first arose during the 1980s the aviation industry raised some major concerns. These concerns included issues of low lubricity, insufficient volume seal swell and low fuel density [25]. In 1999 Sasol became the first company to produce a semi-synthetic jet fuel (SSJF). Its approval addressed the aforementioned concerns from the aviation industry [4, 8]. This SSJF consists of up to 50% (v/v) of an iso-paraffinic kerosene (IPK), largely produced using HTFT processes blended with conventional crude-derived Jet-1 fuel.

IPK consists of largely iso-paraffins although normal and cyclo-paraffins are present in fuel component [4]. Additionally, a minimum of 8% (v/v) aromatics are blended into the final fuel to ensure suitable elastomer compatibility and this aromatic addition is required to stem from conventional crude oil derived petroleum sources [7, 26]. Since this first approval, several other semi-synthetic jet fuel components have been issued for approval which has led to the use of the more generic synthesised paraffinic kerosene (SPK). Sasol's CTL SPK component is produced via polymerisation of C_3 and C_4 olefins. After this, hydrogenation and fractioning occur to produce SPK, which is blended accordingly [7]. The flow diagram in Figure 2.6 illustrates the process of production of SPK.

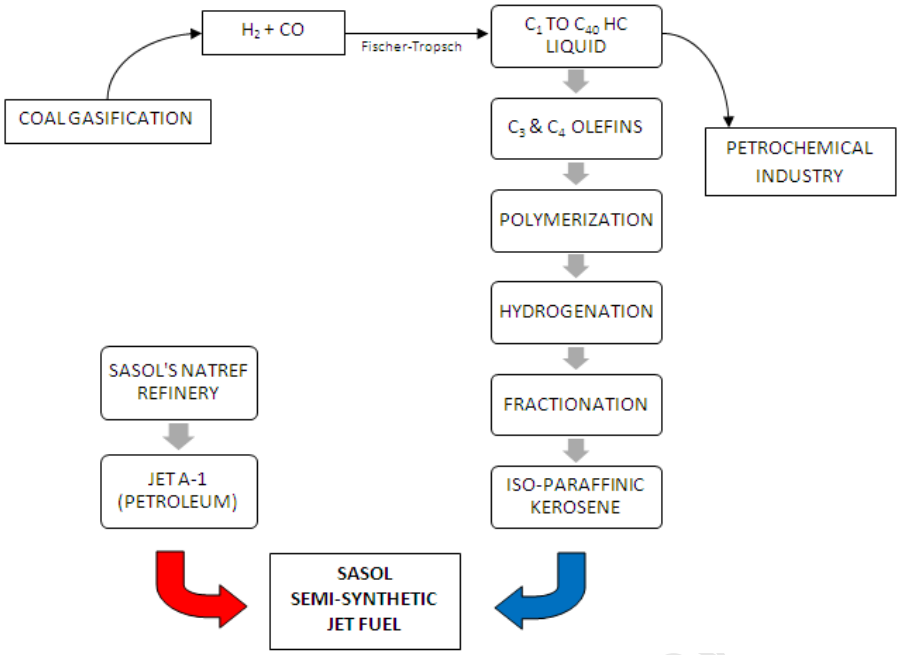

Figure 2.6: Schematic of Sasol synthesised paraffinic kerosene production (reproduced from Moses *et al.*, 1997 [25])

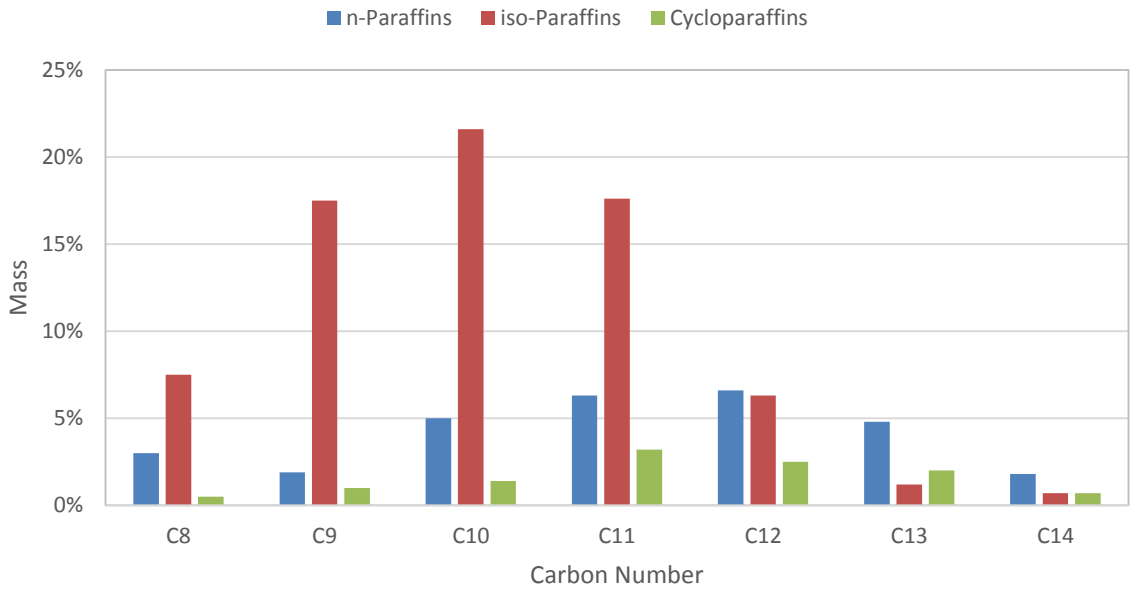

Figure 2.7: Typical hydrocarbon distribution found in SPK (adapted from Moses *et al.*, 1997 [25])

The SPK product produced from the process shown in Figure 2.6 typically consists of a carbon range between C_8 and C_{13} with a bias towards higher iso-paraffin content. SPK has no aromatic content. Figure 2.7 indicates a hydrocarbon distribution of FT produced SPK.

If compared to conventional petroleum jet fuel (see Figure 2.2), a difference in hydrocarbon distribution and, in particular, the absence of aromatic content may be readily observed. Calls for environmentally cleaner fuels, with heavily reduced aromatic content has resulted in increased interest in FT technology and the technologies ability to produce cleaner fuels without the use of crude oil feedstock.

Following the release of SSJF, Sasol applied for approval of a fully synthetic jet fuel (FSJF) that was approved in 2008. This FSJF was also produced via HTFT using coal feedstock. The major difference between the SSJF and FSJF regards the 8% (v/v) aromatic content. SSJF requires aromatics derived from petroleum sources whereas FSJF does not. Specified aromatic content may be obtained from heavy naphtha and light distillate derived from coal tar, a by-product of coal gasification [7]. The SPK is still derived from polymerisation and hydrogenation of C_3 and C_4 olefins as described earlier.

Table 2.4: Summary of SPK fuels from different production processes [4]

Property	Limits	Sasol CTL	Sasol GTL	Syntroleum S-8	Shell Bintulu
Production					
Source material		coal	natural gas	natural gas	natural gas
FT process		HTFT, iron catalyst	LTFT, cobalt catalyst	LTFT, cobalt catalyst	LTFT, cobalt catalyst
FT product		C_3-C_4 olefins	n-paraffinic waxes	n-paraffinic waxes	n-paraffinic waxes
Chemistry					
Aromatics (v%)	25.0	0.5	0	0	0.2
Total sulfur (v%)	0.03 (max)	<0.001	<0.01	0.002	<0.01
Other					
Flash point (°C)	38 (min)	53	48	45	43
Density @ 15°C (kg/m^3)	771-836	765	735	756	736
Fluidity					
Freezing point (°C)	-47 (max)	<-65	-52.5	-51	-53.8

Other refiners, such as Shell, are developing their own FT plants in order to produce synthetic hydrocarbons. This differs from Sasol's product in that their LTFT processes are using GTL

technology and cobalt catalysts, rather that CTL and iron catalysts [7]. Table 2.4 provides a summary of a variety of SPKs.

2.2.3 Hydroprocessed esters and fatty acids (HEFAs)

Another route to SPKs involves the hydroprocessing of esters and fatty acids. The hydroprocessing of esters and fatty acids is a novel technology that converts feedstock of vegetable oil, algae oil and animal fat from triglycerides into hydrocarbons suitable for use in jet fuels [27, 28]. The basic process for HEFA production is depicted by Figure 2.8. As of 2011, bio-derived HEFA joined Fischer-Tropsch (FT) fuel as the only acceptable substitutions for conventional petroleum-derived jet fuel [29]. Bio-derived HEFA fuel is produced through the removal of oxygen and breakdown of the bio-oils into their component pieces. The product is a highly paraffinic bio-wax. The bio-wax is hydroprocessed in a similar way to FT syncrude to give the resultant bio-derived HEFA fuel. This fuel is almost indistinguishable from the FT syncrude, both are highly paraffinic and neither contain aromatic species. Like FT-derived jet fuels, HEFA fuels require addition of aromatic species supplied through conventional petroleum feedstock. Because of the similarity of HEFA to FT syncrude, the bio-derived fuel has been recognised and adopted as a component for FSJF [29].

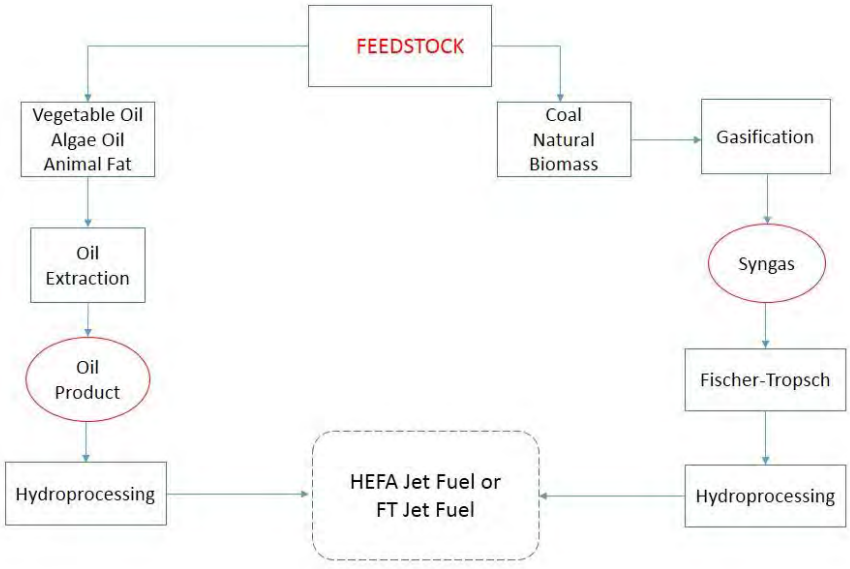

Figure 2.8: Basic processing routes to produce synthetic jet fuel component using differing feedstock (adapted from Pearlson et al. [27])

2.3 Polymeric materials

Polymers are long-chain molecules constructed from many smaller structural units called monomers. Monomers are covalently bonded together in many conceivable patterns to form a polymer of large molecular weight. Due to the size of the polymer molecule, they are often referred to as macromolecules [30, 31]. The process of converting monomer units into a polymer is called a polymerisation reaction and can occur via two distinct reactions; step-growth and chain-growth reactions [30]. Step-growth reactions occur when the monomer contains functional groups such as carboxylic acids and alcohols. The reaction commonly consists of a sequence of condensation reactions producing a by-product molecule in the reaction process [30]. In chain-growth reactions the monomer is predominantly olefinic and occurs via free radical or ionic initiator reaction with the olefin double bond to form a polymeric product. In addition, the reaction proceeds without the elimination of a small molecule typically witnessed in step-growth reactions. The monomer acrylonitrile produces polyacrylonitrile via a chain-growth reaction type shown in Figure 2.9. This polymer constitutes a monomer of nitrile butadiene rubber (NBR), an elastomer that will be discussed in later sections and is thoroughly researched on throughout this dissertation.

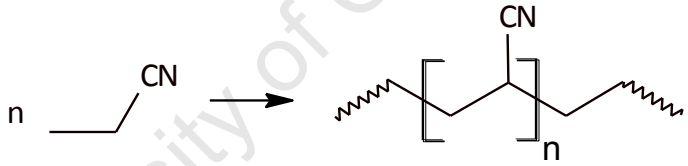

Figure 2.9: Chain-growth polymerisation reaction to produce polyacrylonitrile [30]

Several polymer classes exist including thermosets, thermoplastics and elastomers. The last class finds use as sealing materials which are often exposed to fuels and forms the basis for the discussion to follow.

Elastomers are known for their characteristic low glass transition temperatures (T_g), ability to stretch and retract rapidly without permanent deformation and are identified by their negligible crystalline content [30, 31]. As a consequence they are highly amorphous. Elastomers have glass transition temperatures well below ambient temperatures where most practical elastomers have a T_g below -40°C allowing a versatile operating range. Chain mobility of the elastomer is greatly increased when being used above their T_g as polymeric chains become increasingly mobile [30]. This chain mobility allows elastomers to be deformed elastically with elongations often in the region of several hundred *per cent*. Elastomers are lightly cross-linked. Introducing cross-links severely restricts the elastomers ability to flow

under stress. Because of their flexibility, elastomers are used as both static and dynamic sealants within major industries [30].

2.3.1 Oil-resistant elastomers

Oil-resistant elastomers have gained significant market share within the aviation and automobile industries where these polymeric materials are used as seals between two mating surfaces which are exposed to a range of solvents/fuels. Neoprene and nitrile butadiene rubber (NBR, also known as nitrile rubber or poly(acrylonitrile-*ran*-butadiene)) are two well-known commercial elastomers which display oil and solvent resistance [32]. NBR is superior to Neoprene in resisting oil, gasoline and aromatic solvents, while Neoprene is favoured when exposed to ozone and inorganic solvents. Neoprene and NBR are just two of many commercially available oil-resistant elastomers. Figure 2.10 highlights the oil- and heat-resistance of several other elastomer types. NBR's position as one of the most oil-resistant elastomers on the market should be noted. Consequently NBR has historically been used throughout the automotive and aviation industries.

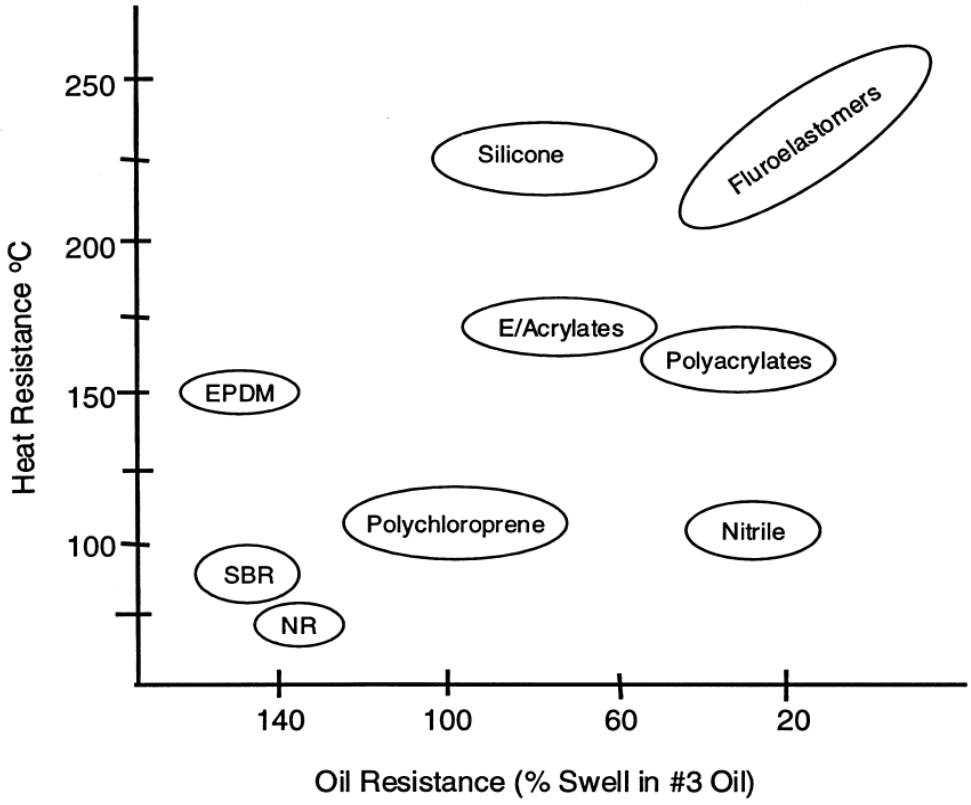

Figure 2.10: Elastomer performance map showing oil- and heat-resistance of typical elastomers submerged in common motor oil (reproduced from Patil and Coolbaugh, 2005 [32])

2.3.2 Nitrile rubber

Nitrile rubber (NBR) is a complex unsaturated copolymer formed when two monomers, butadiene and acrylonitrile, undergo free radical emulsion polymerisation [33]. Aviation and automobile components that experience high fuel exposure are made using NBR due to NBR's inherent fuel and oil resistance. Furthermore, NBR has desirable mechanical properties with a wide temperature range of -40-125°C allowing it to be used in extreme conditions [32]. The polymerisation reaction leading to NBR formation is depicted in Figure 2.11.

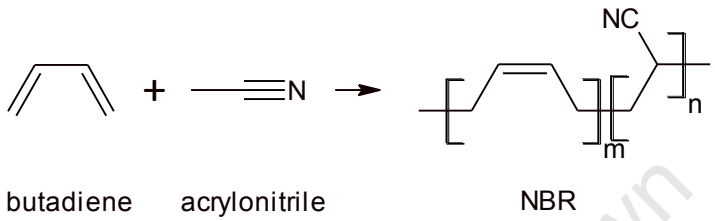

Figure 2.11: Polymerisation reaction of butadiene and acrylonitrile

The acrylonitrile portion of the polymer can vary from a minimum of 15% to a maximum of 50% although typical NBR polymers contain between 30-35%. The acrylonitrile content plays a large role in determining the final properties of the NBR blend. As the acrylonitrile content increases, the polymer becomes increasingly polar thereby increasing resistance to permeation by hydrocarbon solvents such as oils and petroleum fuels [34, 35]. Additionally, properties such as the T_g and solubility parameters increase with increasing acrylonitrile content thereby affecting the performance of NBR in differing environments. Decreasing the acrylonitrile content enhances the low-temperature performance, heat resistance and increases plasticiser compatibility [35]. A brief summary of the effect that varying acrylonitrile has on basic properties of NBR is displayed in Table 2.5.

Table 2.5: Effect of acrylonitrile content on properties of NBR [34]

Acrylonitrile content	
High	**Low**
Favours melt processability	Increased swelling in aromatic compounds
Improved tensile strength	Improved low-temperature properties
High oil and fuel resistance	Improved plasticiser compatibility

Although important, acrylonitrile is not the only component of NBR that affects the final properties of the polymer. NBR is made up of several different constituents, which together determine the final properties and guide the elastomers performance in differing

environments. A typical formulation of NBR is given in Table 2.6 where special attention to the plasticiser content should be noted as this has an influence on elastomer swelling as will be discussed in later sections [34].

Table 2.6: Generic formulation for a typical NBR polymer [34]

Component	Parts per hundred rubber (phr)
NBR elastomer	100
Fillers	20-175
Zinc or Magnesium Oxide	3.0-5.0
Stearic acid	0.5-1.0
Protective agents	2.0-6.0
Plasticisers	0-50
Vulcanising agents	1.0-4.0

NBR is an extremely versatile elastomer which has found use in numerous applications. Most commonly NBR is used within industries that require an oil/fuel resistant material which displays a wide operating temperature range and acceptable mechanical performance during solvent exposure. The result of NBR's inherent versatility is that the polymer often demonstrates a wide range of mechanical properties and can be tailored to specific requirements. The application of these mechanical properties are discussed in later sections.

Table 2.7: Typical mechanical properties for NBR [34]

Property	Value
Tensile strength	2-5MPa
Elongation at break	100-700%
Hardness	25 Shore A to 50 Shore D
Density	0.60-2.00g/cm^3

The resistance of NBR polymers to solvent and gas permeation is well-understood with acceptance that increasing acrylonitrile content leads to increased permeation resistance [35]. In fact it has been observed that NBR with about 40% acrylonitrile content has similar permeation resistance to that of butyl rubber. Additionally, permeation resistance can be further increased by the addition of fillers and even further resistance by surface treatment of these fillers [35]. Resistance to solvent permeation is an attractive factor of NBR which has led to wide-spread use in both the aviation and automobile industries.

Table 2.8: Relative gas permeability for NBR [35]

Relative permeability for gas					
Elastomer	**H_2**	**N_2**	**O_2**	**CO_2**	**Air**
Natural rubber*	100	100	100	100	100
Nitrile rubber (41% ACN)	15	2.9	4.1	5.7	3.4
Butyl rubber	15	4	5.6	4	4.8

* Natural rubber is assigned value of 100

2.3.3 Fluorocarbon elastomers

Fluorocarbon elastomers (FKM) are compounds that contain carbon, hydrogen and fluorine bonded together with high-energy carbon-fluorine bonds. CH_2 groups present in FKM elastomers are responsible for flexibility and low temperature performance [36]. DuPont Viton™ fluoroelastomer was originally introduced in 1957 to meet the stringent standards set out by the aerospace industry [36]. FKM elastomers are produced via polymeric reactions with perfluorocarbon monomers. Typically, the two most common monomers used in the production of FKM are hexafluoropropylene and tetrafluoroethylene [37].

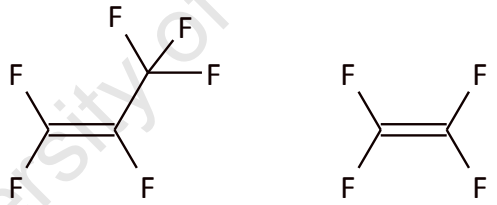

Figure 2.12: Typical monomers for Viton production:hexafluoropropylene (left) and tetrafluoroethylene (right)

Fluorocarbon elastomers are known to offer extraordinary levels of resistance to chemicals, oils and hydraulic fluids. Further, FKMs boast excellent heat resistance, having useful service lives under temperatures in excess of 200°C [38]. This is due to the high ratio of fluorine to hydrogen that exists within their structure. Coupling this with high-strength carbon-fluorine bonding and extensive saturation within the backbone, FKMs are relatively inert when submerged in aromatic and aliphatic hydrocarbons or when exposed to high temperatures [36, 38].

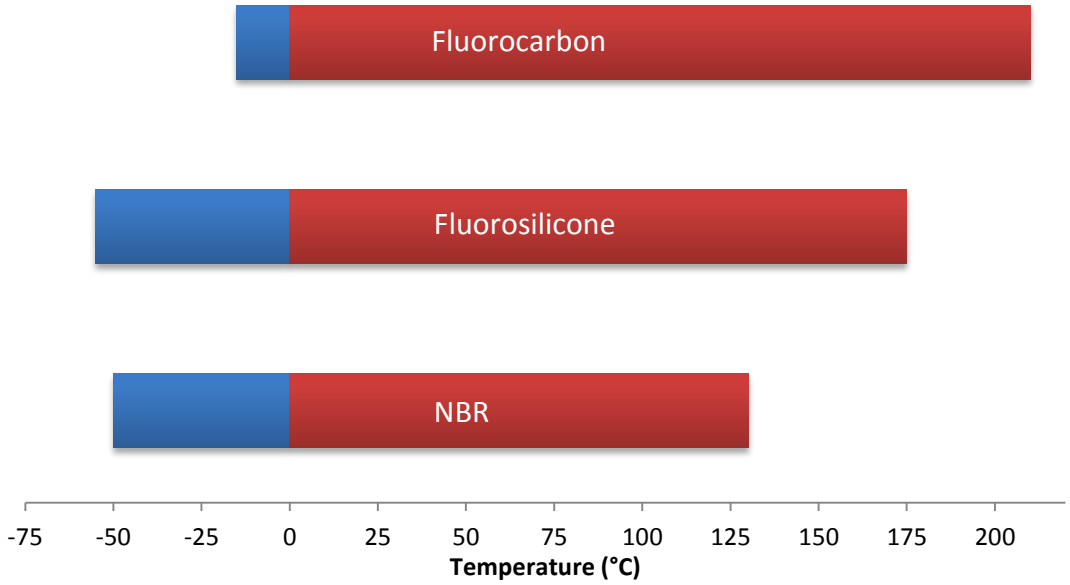

Figure 2.13: Operational temperature range for elastomers commonly found within the aerospace industry (adapted from Parker Hannifin Corporation, 2007 [36])

Despite having an inherent resistance to the aforementioned compounds, fluorocarbon elastomers are susceptible to degradation when exposed to glycol based fluids and low molecular weight organic acids. Additionally, the sealing abilities of FKMs rapidly diminish when exposed to low temperatures. The operational temperature profile of FKMs is compared with NBR and fluorosilicone rubber in Figure 2.13 [36].

2.4 Elastomer additives

Additives are often blended within the make-up of an elastomer for reasons such as easing the manufacturing process, stabilising the final polymer product or to change the physical or mechanical properties of the pure elastomer compound. Common additives include fillers, stabilisers and plasticisers with the latter being most important in terms of elastomer studies [39].

Typically elastomers are plasticised with low molecular weight resins or liquids which are able to form secondary bonds to polymer chains. These bonds disrupt the primary polymer-polymer chain bonding providing greater mobility for macromolecules. Increased mobility can cause softening in the final polymer compound improving flexibility and allowing for easier processing [40]. Generally, plasticisers are expected to reduce physical properties such as the

elastomers modulus, tensile strength and Tg while increasing properties such as the elastomers elongation at break and toughness. Additionally, ideal plasticisers should be compatible with the elastomer while also showing resistance to temperature extremes, oxidation and leaching [40, 41].

Typical plasticisers added to elastomeric compounds include phthalates and adipates, examples of which are indicated in Figure 2.14.

Phthalates are characterised by having high compatibility with the elastomer matrix and are usually inexpensive. Adipates supply superior low temperature flexibility. They tend, however, to be volatile and easily extractable. This fact needs to be appreciated as plasticiser leaching may cause altering of physical properties and dimension changes in the elastomer [40].

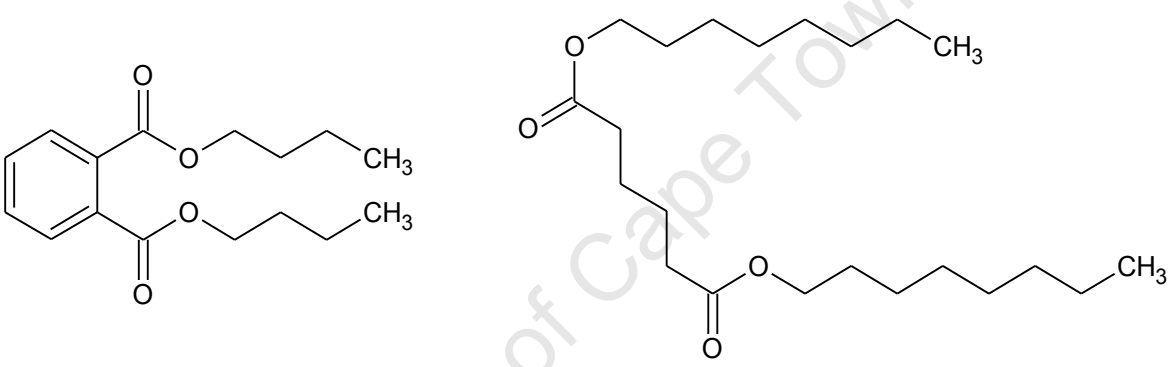

Figure 2.14: Molecular structure of typical phthalate and adipate plasticiser molecules present in elastomer components

2.5 Polymer-solvent interactions

The interaction between polymer and solvent is a key performance parameter in the overall evaluation of the material especially when the solvent concerned is a hydrocarbon. Elastomers are often employed in environments where continual exposure to fuels and other hydrocarbon solvents can result in undesirable changes in the inherent properties of the elastomer. In particular, two solvent-polymer interactions are of interest namely; polymer ageing and polymer swelling. These phenomena are discussed below.

2.5.1 Polymer ageing

Ageing, in polymer science, refers to change of physical properties that occur over time. Ageing is typically a complex chemical process that occurs in the presence of heat, oxygen and

mechanical stress and results in a time-dependent change in the chemical and physical properties of the polymer [42, 43]. Ultimately deterioration of the polymer occurs during the ageing process and this may be due to molecular scission of polymer chains, increased crosslinking and removal of polymer additives such as plasticisers.

Polymer ageing can occur via several distinct modes namely: Physical ageing, curing, thermal ageing and natural ageing. Physical ageing is the most common type of ageing and occurs when a polymer is in a non-equilibrium state caused by molecular relaxations which drive the polymer to equilibrium [43]. Physical ageing can be accelerated by an increase in temperature that can displace the polymer equilibrium and shift the ageing regime. Ageing is also accelerated by exposure to harsh and highly reactive chemical environments through a process commonly known as photo-oxidation [43]. Exposure to either condition can lead to chain scission and molecular relaxations which will have a changing effect on properties of the elastomer.

Thermal ageing occurs when polymer component is exposed to elevated temperatures, not usually experienced in the service life of the material. Prolonged thermal exposure may induce cross-linking within the polymer resulting in increased embrittlement and vast reductions in elasticity [44]. More concerning, however, is the potential exposure of elastomer components to oxygen-rich environments in the presence of elevated temperature. Elastomers with weak bond-energies (Table 2.9) in the back-bone are highly susceptible to chain scission forming active radicals which under the thermally oppressive conditions possess the required activation energy to promote further destructive reactions. Increased chain scission allows release of molecular chain segments from entanglements facilitating a conformational re-arrangement of chains into a lower energy state. This lower energy state is representative of an aged elastomer species [43, 44]. NBR is an example of an elastomer with weak bond-energies between the carbon double bonds in the polymer backbone. Typically, NBR is hydrogenated if the material is intended to face elevated thermal exposure as carbon single bonds exhibit greater bond energies as seen in Table 2.9. Finally, elevated temperatures have the tendency of increasing the activity of polymer additives resulting in accelerated desorption from the polymer component [45].

Table 2.9: Overview of bond energy in the role of thermal ageing in NBR elastomers [44].

Elastomer	Backbone bond	Bond energy (kcal/mol)	Operational range (°C)
NBR	C=C	63	-45-125
HNBR	C-C	83	-30-160

Another type of ageing that is experienced by many elastomers during service is the loss of small molecules such as curatives and plasticisers. The loss of these materials causes an increase in the glass transition temperature of the elastomer as well as an increase in the stiffness of the elastomer.

2.5.2 Polymer swelling

When a liquid and polymer come into contact, mass transfer is generally observed. This behaviour may be intensified when the solvent is hydrocarbon in nature such as automobile and aviation fuels [46]. The transfer of liquid onto polymer is referred to as swelling. A critical performance factor for elastomers is the ability to swell upon coming into contact with a solvent. Although swelling is sought-after behaviour for solvent-exposed elastomers, over-swelling can cause undesirable consequences. As little as 20% volume swell in elastomers can lead to a marked decreases in properties such as tensile strength, hardness and sealing ability and therefore it is important to understand and appreciate the parameters which govern polymer swelling [46, 47].

Thermodynamically, elastomer swelling is driven by the Gibbs free energy which itself is governed by enthalpy, entropy and elastic retraction energy. Elastomer swelling is typically entropically driven since the enthalpy of mixing (ΔH_m) between rubber and solvent is often endothermic ($\Delta H_m > 0$) [33]. The swelling of an elastomer sample is therefore a reflection of the tendency of the sample to interact and mix with the solvent through thermal motion. The result of such an interaction leaves the pure solvent to permeate between elastomer chains pushing them apart and thereby causing a swelling phenomenon. This is illustrated by the schematic diagram in Figure 2.15.

Both solvent dilution and rubber chain stretching events must be taken into account and looked at thermodynamically to have a greater appreciation of rubber swelling behaviour. Solvent dilution is described by the Flory-Huggins [48] model while the stretching effects of polymer chains are described by the complex Flory-Rehner model [49]. Finally, the understanding of elastomer swelling is not complete without a thorough grasp of solubility

parameters. Models by Hildebrand, Scott [50]and Hansen [51] can predict the solubility of a solvent within elastomer species via the determination of enthalpy and its connection to the physical properties of the elastomer and solvent [33]. The impact of elastomer additives on final swelling behaviour is also fundamentally important.

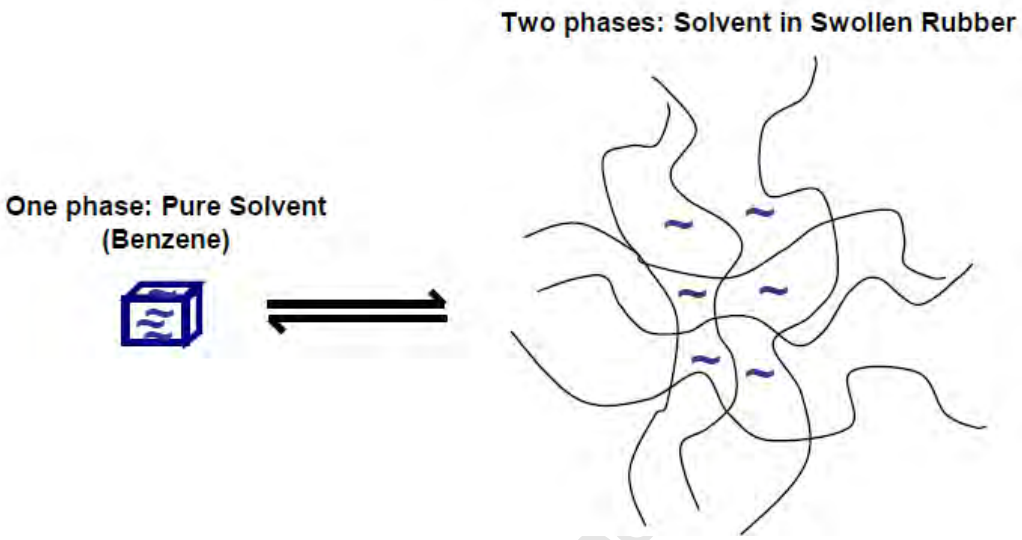

Figure 2.15: Dilution of solvent into a polymer matrix (reproduced from Lachat, 2008 [33])

2.5.3 Factors affecting elastomer swelling

From the above discussions it becomes clear that transport phenomena of solvent molecules through elastomer materials are heavily relied upon the thermodynamics which govern the solvent-elastomer interactions. Despite this, there remain additional factors which strongly influence the dissolution of an elastomer in a solvent environment and require discussion to form a more complete understanding of the elastomer swelling process.

2.5.3.1 Elastomer conformation

The extent of saturation in the elastomer backbone has a direct influence on the transport properties of solvents wishing to permeate the elastomer matrix. Solvent diffusion into an elastomer matrix relies on the segmental mobility of the elastomer chains. Mobility of these chains is hindered by hydrogenation of unsaturated elastomer backbones which leads to decreased solvent permeation [52]. *George* et *al.*. indicated that solvent diffusivity of octadecane through polyisoprene decreased three-fold when the elastomer backbone was exposed to excessive hydrogenation reinforcing the fact that saturated elastomer backbones restrict segmental chain mobility and influence the extent of solvent permeation through

elastomer compounds [52]. Segmental motion is also reliant on the T_g of the elastomer which has a profound influence on the diffusion characteristics of solvent-elastomer systems. Elastomers which display lower T_g values generally allow elastomer chains greater segmental mobility which in turn facilitates greater solvent permeation through the elastomer matrix [52].

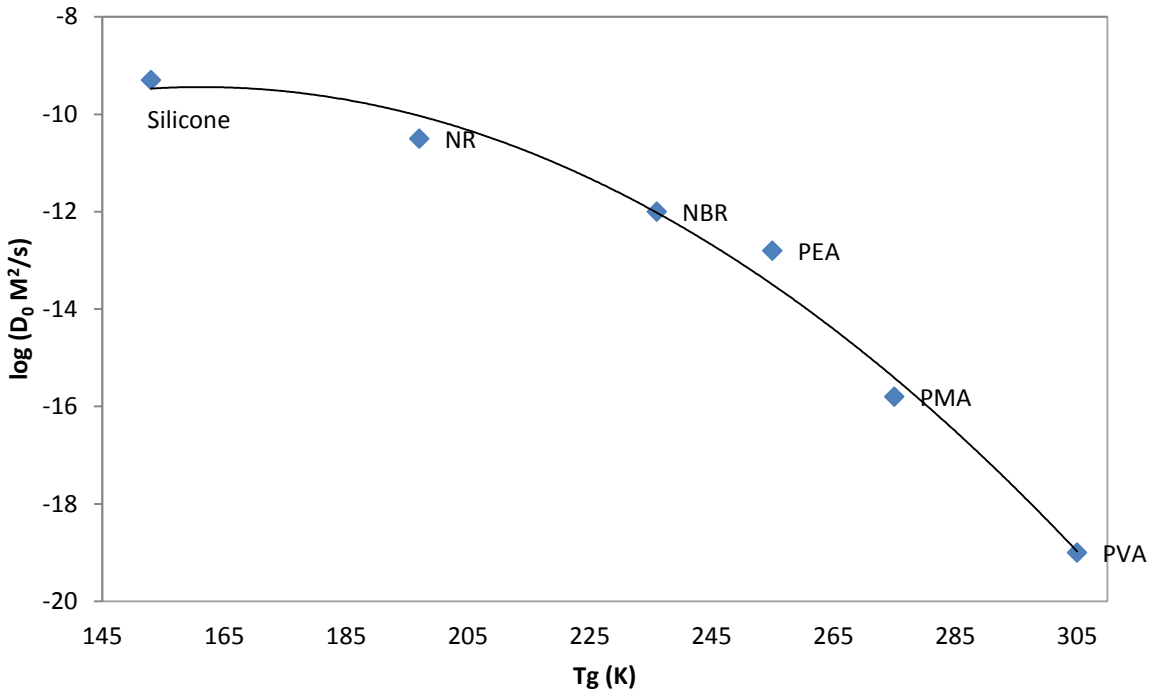

Figure 2.16: Correlation of the diffusion coefficient of benzene versus glass transition temperature of various species (adapted from George and Thomas, 2001 [52]). NR = natural rubber; NBR = nitrile rubber; PEA = poly(ethylacrylate); PMA = poly(methylacrylate); PVA = poly(vinyl alcohol)

Figure 2.16 illustrates the considerable change in permeation characteristics of benzene with decreasing T_g for various elastomer species. The reasoning attributed to the vast difference in diffusion coefficients was the large decrease in T_g from poly(vinyl acetate) to silicone rubber [52].

2.5.3.2 Steric hindrance and penetrant size

The addition of bulky side-groups on either the solvent or elastomer can influence the degree of solvent diffusion and by extension influence the extent of elastomer swelling. Elastomers

with methyl groups are known to exhibit lower permeability which is reflected in the low swelling of butyl rubber which has two methyl groups on every other carbon atom in the rubber backbone [52]. Decreases in solvent permeability are a result of increasing rigidity of the elastomer backbone by the addition of substituted methyl groups or equivalent.

Sterically hindered side-chains on the polymer backbone suppress the extent of solvent permeation through an elastomer matrix to a greater extent than backbone rigidity. A plausible reason for this is the increasing molecular weight or molar volume of the solvent as increasingly hindered side chains are added [52].

The molar volume of a compound is defined as the volume of one mole of that particular substance. Molar volume is therefore a reflection of the size of a particular substance. As the molar volume of a solvent molecule increases so the solvent becomes increasingly hindered increasing the difficulty for the solvent to penetrate the elastomer matrix. Molecules of smaller molar volume are able to pack inside the elastomer matrix with a greater packing factor which results in a greater overall solvent uptake by the elastomer [8].

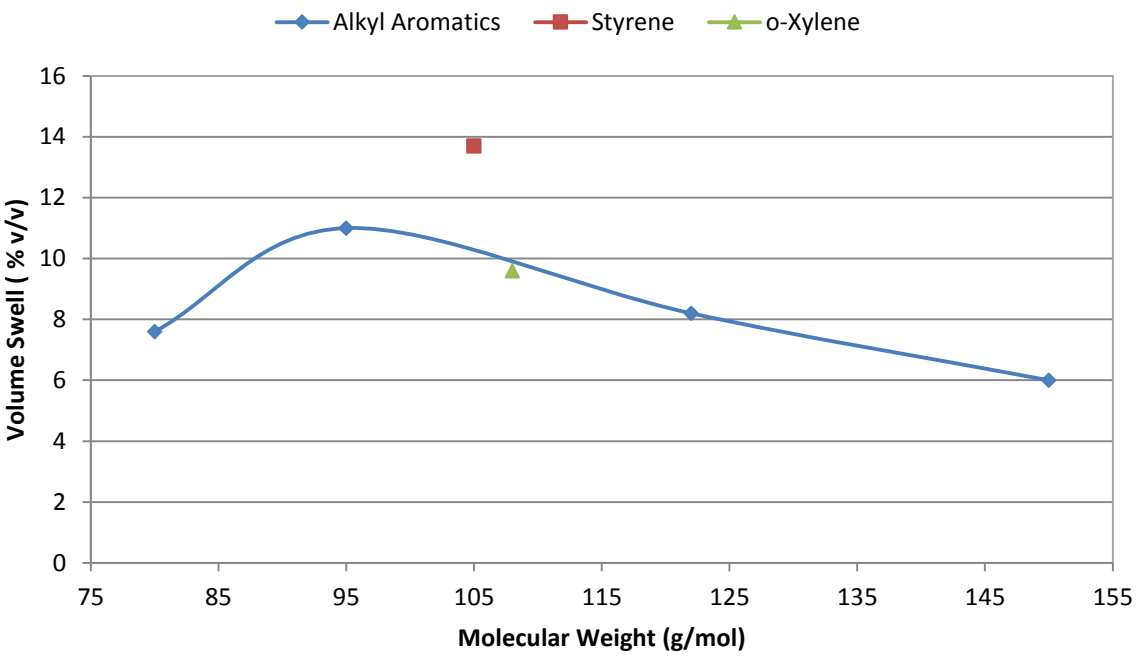

Figure 2.17: Impact of molecular weight on the swelling on standard nitrile rubber submerged in blended S-5 fuel (adapted from Graham *et al.*, 2006 [8])

Figure 2.17 shows the volume swell behaviour for a standard NBR elastomer in contact with blended fuels. As expected elastomer swelling decreases with increasing molecular weight of the alkyl aromatics series, however, a sharp increase in swelling is observed for styrene

exposure. This swelling increase can be attributed to the solubility parameters of styrene which are in close proximity to those of NBR. Furthermore, styrene is able to interact with NBR's electronegative cyano group through hydrogen bonding interactions, thereby increasing the extent of permeation [8, 53]. One exception to the decreasing trend in swelling with increasing molecular weight is benzene (M_w = 78 g/mol). This anomaly may be ascribed to the fact that experiments by Graham *et al*. [8, 54] were conducted on as-received O-rings. These contain plasticisers which, when extracted, cause a volume reduction. The data in Figure 2.17 reflects the greater extraction of plasticisers during benzene exposure at the point of measurement.

2.5.3.3 Effect of temperature

A temperature increase results in higher polymeric chain mobility within the polymer. Subsequently, solvent molecules can penetrate the polymer matrix more easily and often a greater rate of volume swell is observed as illustrated by Figure 2.18 [55].

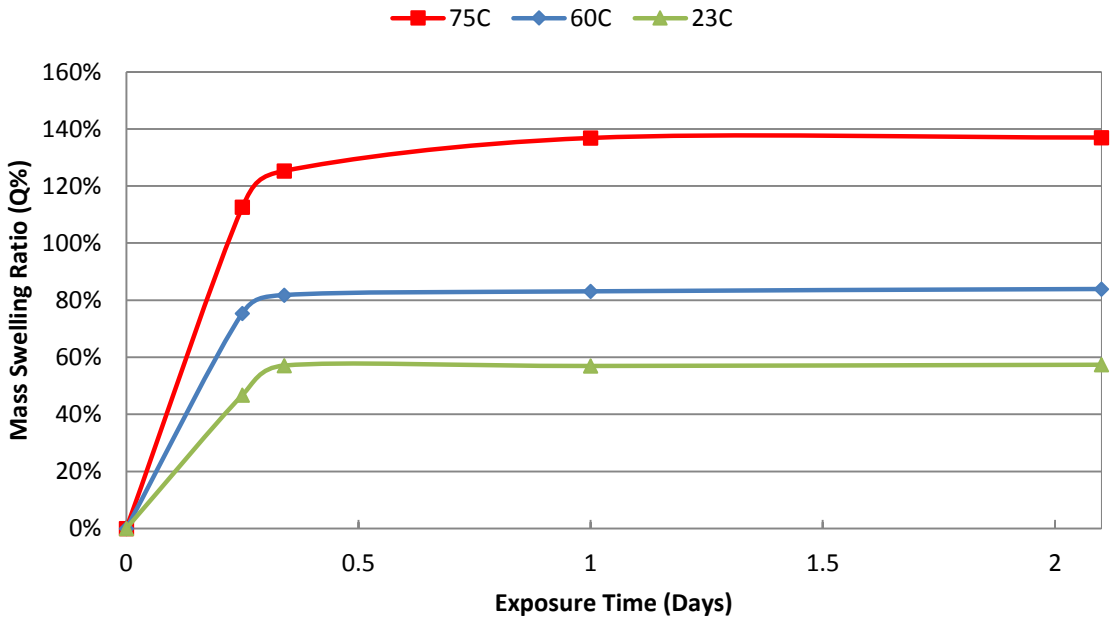

Figure 2.18: Effect of temperature on the sorption of p-xylene into NBR/EVA blends (adapted from Joseph *et al.* 2003 [55])

Temperature effects regarding sorption of a solvent are explained by the Van't Hoff equation shown below. Here enthalpy of mixing is considered to be endothermic and therefore an increase in temperature results in an increasing sorption coefficient and subsequently an increase in swelling observed at equilibrium.

$$\ln K_s = \frac{\Delta S}{R} - \frac{\Delta H}{RT}$$

where:

ΔS	=	entropy of sorption
R	=	universal gas constant
ΔH	=	enthalpy of reaction/process
T	=	temperature in Kelvin
K	=	thermodynamic equilibrium constant

The sorption constant is heavily reliant on the enthalpy of association between species and therefore it may be observed that increasing temperatures can lead to a decrease in net swelling. This is most commonly observed when the solvent concerned is a liquid fuel blended with an aromatic alcohol. It is likely that enthalpy of association between elastomer and fuel is negative culminating in decreased elastomer swelling at increased temperatures. Additional factors contributing to this observation could be increased leaching of elastomer additives or the process of thermal cross-linking [47, 56].

The application of elastomers under conditions of elevated temperature runs the risk of excessive cross- linking of associated chains. Cross-linking occurs when polymer chains fuse together through an ionic or covalent bonding mode often caused by the exposure to prolonged increases in temperature. The result of cross-linking leads to limited mobility of elastomer chains which are now bound by network bonds and hence the ability for the elastomer matrix to accommodate potential solvent permeation decreases. Decreases in the solvent permeation have added repercussions of inherent dimension change of the elastomer and in the case of O-rings a dimension change could lead to potential failure of the material [52, 57].

2.5.4 Performance response of solvent exposed elastomers

Elastomers are often employed within automobile and aviation industries as seals, gaskets and membranes. When used, elastomers are exposed to aggressive solvents or fuels, mechanical compressive pressures and cyclic temperature environments. A high demand is placed on both physical and chemical long-term stabilities of these materials which is a crucial quantitative factor in determining the overall performance of the elastomer. The performance response of elastomers exposed to variety of solvents is two-fold; firstly, it is important to review the dynamic response of solvent exposed elastomers. Secondly, the static response of

solvent exposed elastomers allows basic mechanical properties such as tensile strength and elastic modulus to be evaluated.

2.5.4.1 Dynamic property response

Elastomeric seals used within fuel housings typically undergo oscillating compressive loads from neighbouring contact surfaces. The seals must exhibit flexibility to allow adequate compression thus ensuring intimate contact between mating surfaces remains intact [58]. If the dynamic mechanical properties of the elastomeric seal were to change due to solvent interactions, the material might lose its sealing ability and compromise the entire fuel system. The use of dynamic mechanical analysis (DMA) allows changes in these properties to be tracked and evaluated. DMA measures a materials response to an applied dynamic sinusoidal force most notably evaluating the ability of the material to store energy elastically, known as the storage modulus (E') and the ability of material to dissipate energy, referred to as the loss modulus (E'') [58, 59].

The ratio of E'' to E' is known as tan δ which gives a measure of the damping ability of a material. The peak of the tan δ versus temperature curve is also a useful way of determining the T_g of the material under evaluation. In a recent study performed by Lin *et al* [58] the effect of long term solvent exposure on the storage modulus and tan δ of 5 elastomeric materials under consideration for use in polymer electrolyte membrane (PEM) fuel cell stacks was investigated. The use of DMA was fundamental in tracking the sealing performance of the studied materials. Two materials, namely, co-polymeric resin (CR) and ethylene propylene diene monomer rubber (EPDM) were identified as potential candidates for the use in PEM fuel cell stacks.

Figure 2.19 shows that the storage modulus of CR remained essentially unchanged when exposed to the regular solution. A notable decrease, however, was observed when exposed to a highly acidic solution. The decrease in storage modulus affects the sealing ability of the material as a higher modulus allows greater pressures to be applied to the material ultimately achieving a greater sealing force between the elastomer and mating surfaces [58].

a)

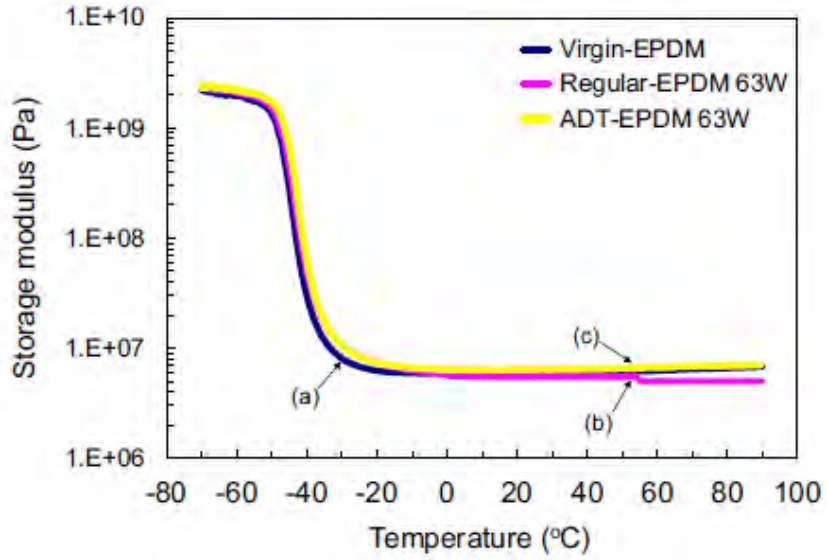

b)

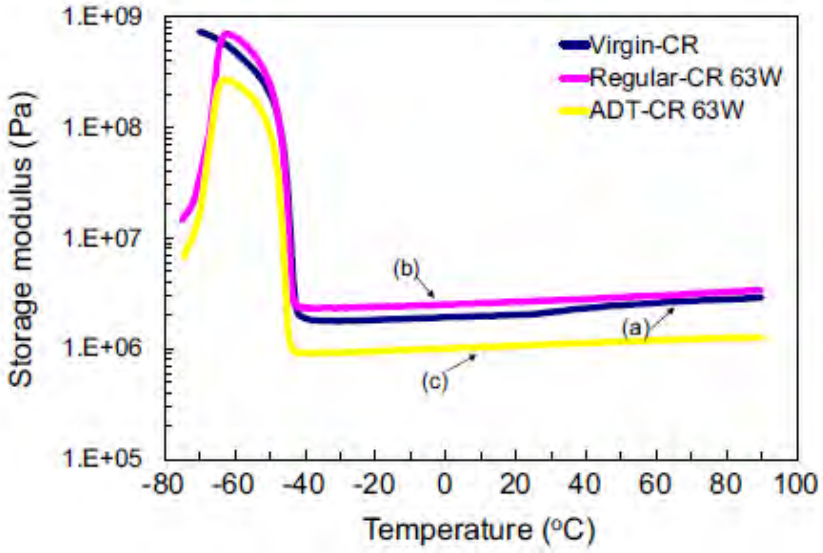

Figure 2.19: Storage modulus as a function of temperature for CR and EPDM. (a) Virgin/no solvent exposure; (b) Exposure to a solution typical of PEM fuel cell environment; (c) Exposure to strongly acidic medium aimed at accelerating ageing process (reproduced from Lin *et al.* [58])

EPDM showed very little change in storage modulus when exposed to either the regular or highly acidic solution. This is preferred behaviour in a material intended for solvent exposure. The effect of solvent exposure on the T_g is also of importance as increasing T_g values decrease the service temperature range of the material.

a)

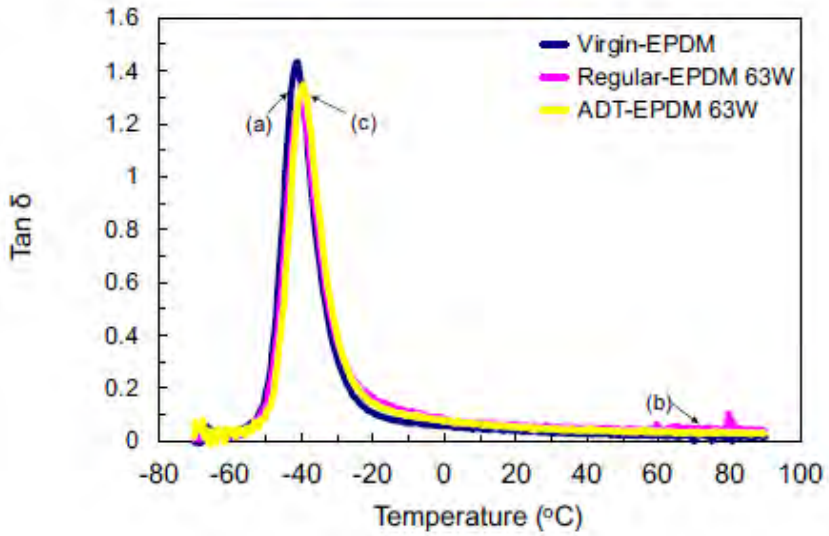

b)

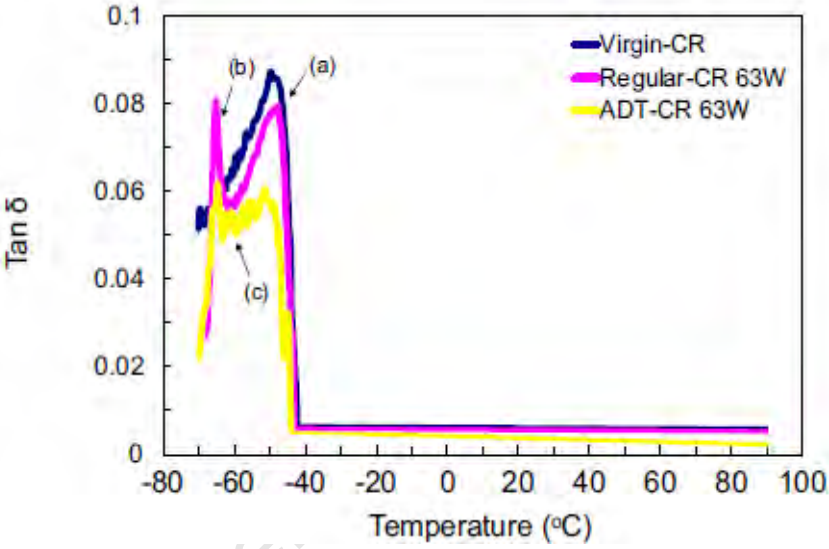

Figure 2.20: tan δ versus temperature for a) CR and b) EPDM exposed to varying environments (reproduced from Lin *et al*. [58])

The value of the T_g remained relatively unchanged for both CR and EPDM materials exposed to the differing environments. For this specific application, it is preferred that the T_g remain unchanged as the storage modulus increases rapidly upon entering the glassy region. Such a rapid increase can render the material highly brittle and useless in desired sealing performance.

On the basis of the DMA results EPDM was deemed as the more suitable material for implementation in a PEM fuel stack. Similar intuition can be applied to various other elastomers in contact with differing solvents. Dynamic properties are best coupled with static

responses to solvent exposure to gain a more fulfilled understanding of the sealing performance of an elastomer.

2.5.4.2 Swelling response

Static properties are most notably characterised by the swelling response of a solvent exposed elastomer. The ability to swell an elastomer is a key compatibility characteristic for alternative fuels undergoing screening tests for implementation into a specified fuel pool [7]. Excessive swelling is often accompanied with a decrease in hardness and tensile strength while volume shrinkage can diminish the contact area between elastomer and adjacent surfaces resulting in fuel leakage [7].

Elastomers used in static applications are allowed a maximum of 30% (v/v) swelling, while elastomers designed for dynamic applications are permitted between 15-20% (v/v). Nitrile elastomers are often used in fuel screening tests due to their significant sensitivity to changing fuel chemistry.

Moses *et al*. [7] immersed NBR O-rings in a number of synthetic jet fuel blends with petroleum jet fuel and observed the swelling response. Each blend contained increasing amounts of aromatic content in an aim to observe the concentration effect that aromatic species had on swelling of the NBR O-rings.

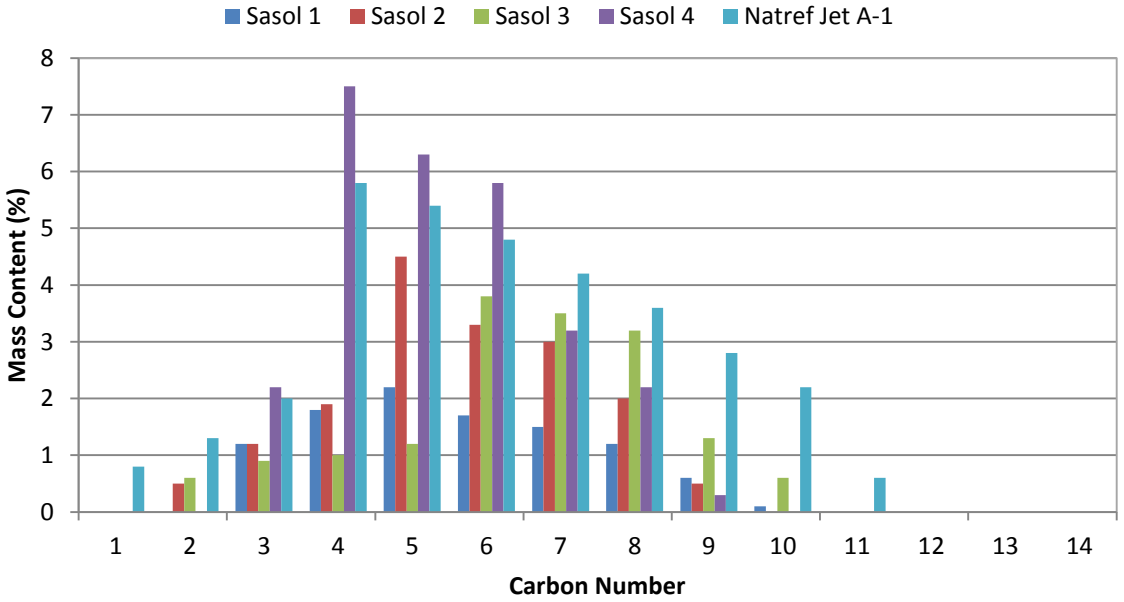

Figure 2.21: Aromatic distribution in various synthetic jet fuel blends (adapted from Moses *et al*.2008 [7])

Figure 2.21 illustrates the aromatic content of each blend used while Figure 2.22 indicates the swelling response of NBR in each fuel blend. The NBR samples showed increasing swelling behaviour with increasing aromatic content. Furthermore swelling of the samples is below the allowable swell for both dynamic and static applications.

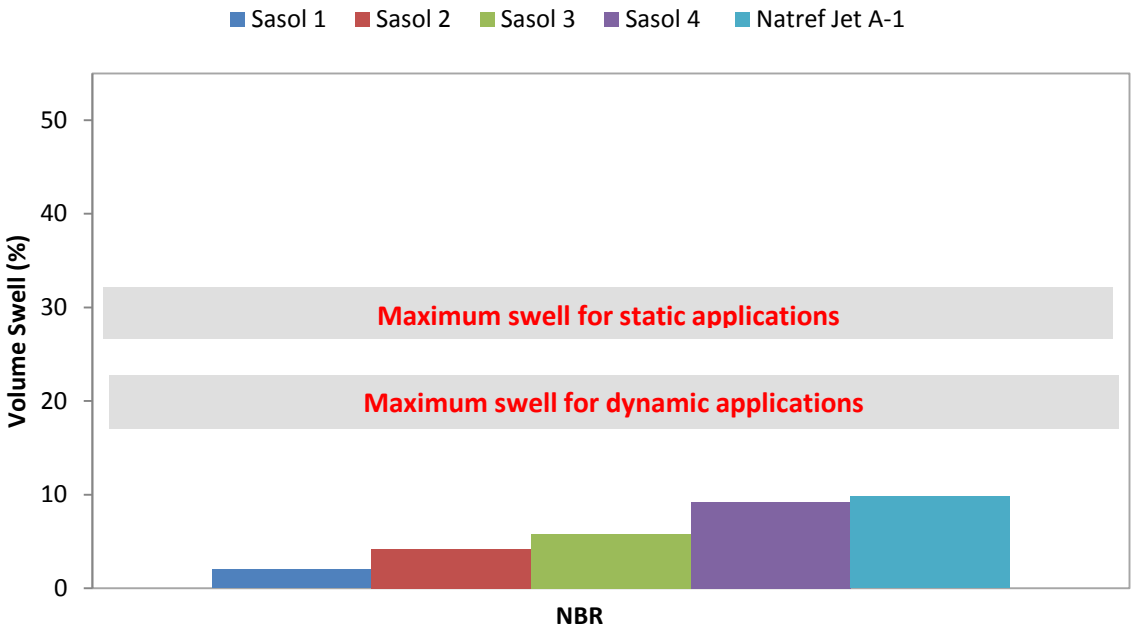

Figure 2.22: Swelling of NBR O-rings exposed to various synthetic jet fuel blends (adapted from Moses *et al.* 2008 [7])

It has been well demonstrated that the swelling of an elastomer depends heavily on the chemical nature of the elastomer and the chemical nature of the solvent/fuel to which it is exposed. It has been found that the alchemical aphorism, *similia similibus solvuntur* or *like dissolves like* applies to swelling since swelling obeys the same rules as dissolution except that cross-linking prevents the polymer chains from completely separating. In general, it has been found that solvents with similar chemical interactions to those displayed by an elastomer are likely to swell that elastomer the most. However, in extremely complex systems like jet fuel, collision frequencies between like molecules may be quite low resulting in come unexpected behaviour. In this case, we often see very strong interactions between dissimilar penetrants and polymers.

This concept can be neatly described using the concept of solubility parameters such as those of Hildebrand [50] or Hansen [51]. Because these concepts underpin much of the analysis in this dissertation, solubility parameters are discussed in more detail in Chapter 3.

2.5.4.3 Tensile behaviour

Tensile properties are primarily used as a means of quality control but are also useful as indication of a materials response to fuel exposure. Elastomers employed as dynamic seals are required to maintain a minimum tensile strength of 6.9MPa in accordance with ASTM D1414-94 [60]. In an extension of the aforementioned swelling work, Moses *et al.* [7] observed the effect that exposure to synthetic jet fuels had on the tensile behaviour of three commonly used elastomeric seals. Samples were exposed to fuel for 14 days under ambient temperature conditions. The tensile results are illustrated in Figure 2.23 where aromatic content of the synthetic fuel increases in each Sasol blend.

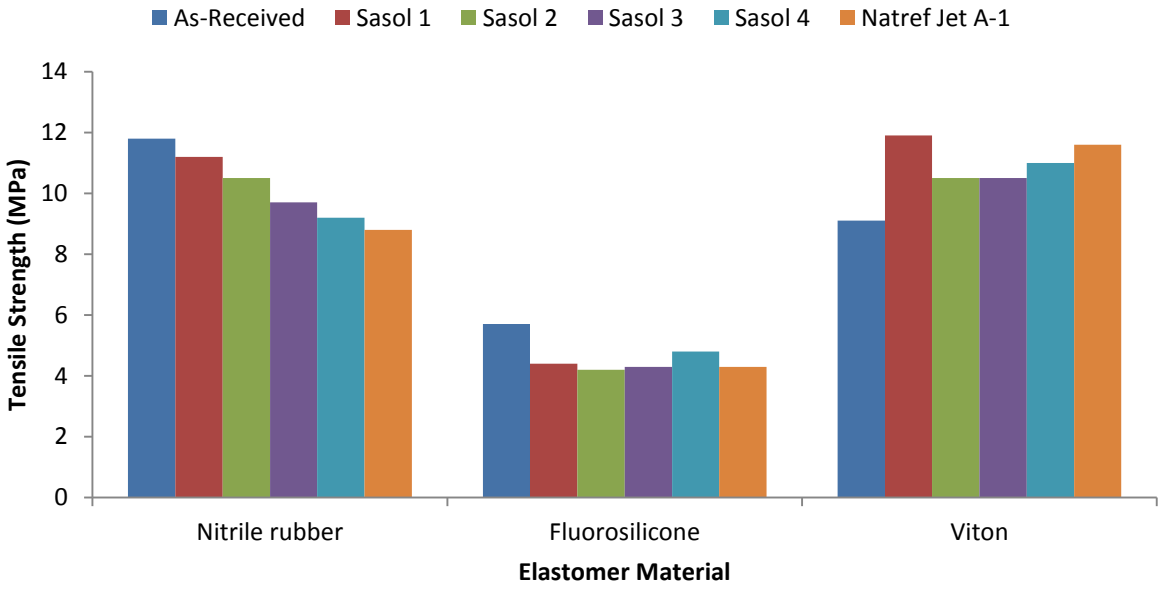

Figure 2.23: Tensile response of common elastomer materials exposed to synthetic and crude oil derived jet fuels (adapted from Moses *et al.* [7])

Each material displayed some minor changes in tensile properties upon exposure to the different fuel blends. NBR and Viton exhibited tensile strength well above the minimum requirements for dynamic seals. Fluorosilicone failed to meet the minimum prescribed value. This material, however, is used in static rather than dynamic applications [7]. As expected NBR exhibited greater sensitivity compared to the other materials. A constant decrease in tensile strength when exposed to fuels of increasing aromatic content was observed. Although the variation was well within the guidelines specified by ASTM D1414-94 [60], increases in tensile strength when exposed to synthetic fuels compared to the petroleum Natref jet fuel could indicate undesirable responses such as increased cross-link density, reduced flexibility and an increase in the glass transition temperature [7]. These responses represent a potential

problem for the implementation of synthetic jet fuels which is defined in more detail in the following section.

2.6 In-service performance

An important source of fuel vapour emissions stems from the sealing performance of elastomer seals and represents an important contributor to the overall hydrocarbon emissions profile of the automobile and aviation industries [61]. In extreme cases, poor sealing may lead to liquid fuel leaks. The sealing performance of elastomeric components is heavily influenced by two parameters namely; the low-temperature sealing performance and the response to fuel switching.

2.6.1 Low-temperature sealing behaviour

Demands on elastomeric seals are continually increasing with a goal of achieving consistently wider ranges of operation. Adequate sealing function of sealing materials at temperatures above the critical glass transition temperature is typical. Upon dropping below the T_g the sealing ability of the material may be lost and fuel leakage may occur. Below the T_g the resilience of the compressed elastomer is lost which results in the material being unable to maintain the adequate tensile forces on the outer diameter resulting in a loss of sealing function [61]. A potential solution to low temperature sealing and performance is the use of highly fluorinated silicone elastomers which combine superior low temperature performance with negligible activity when exposed to solvents and fuels [61, 62].

Although it is highly unlikely that elastomeric sealing materials will experience such low temperature environments, it is possible that the swelling of elastomeric seals by synthetic and other fuels is temperature dependent. Changes in swelling with temperature will affect the flexibility of the sealing materials as well as their sealing ability.

2.6.2 Switch loading behaviour

Switch-loading is a term used to describe the switching of fuel-wetted elastomers from conventional crude oil derived to synthetic fuels [63, 64]. Observation of the performance and behaviour of switch-loaded elastomers is a key parameter in the overall evaluation of the materials compatibility with unconventional fuels. Elastomers have varying degrees of resistance and sensitivity to the composition of conventional fuels. The inherent aromatic content in conventional fuels causes elastomeric seals and O-rings to expand volumetrically

or swell as absorption of the aromatic solute occurs. Synthetic FT fuels are aromatic free by nature and thus the process of solvent absorption may reverse and the material may shrink [64]. Reductions in seal dimensions can diminish the sealing performance and in severe cases lead to fuel leakages. Additionally, aged seals which may experience compression set could accelerate the diminishing sealing performance increasing the chance of seal failure.

The switch-loading performance of general purpose NBR O-rings exposed to a fuel pair of JP-5/S-5 was thoroughly investigated by Muzzell *et al.* [63]. JP-5 is used in naval aircraft which comprised of approximately 18% (v/v) aromatic compounds was used in this study. S-5 is a FT derived copy of JP-5 produced using LTFT technology which yields a fuel free of aromatics. The volumetric dimension change of the NBR samples when exposed to each fuel is illustrated by Figure 2.24. The swing in swelling between JP-5 and S-5, combined with an aged seal or O-ring that has experienced compression set, might result in severe degradation of the materials sealing performance [63]. The authors repeated switch-loading experiments with S-5 blended with 10% (v/v) aromatic agent and observed a decrease in swelling between the fuel pairs illustrating the importance of aromatic content on the swelling performance of elastomer materials.

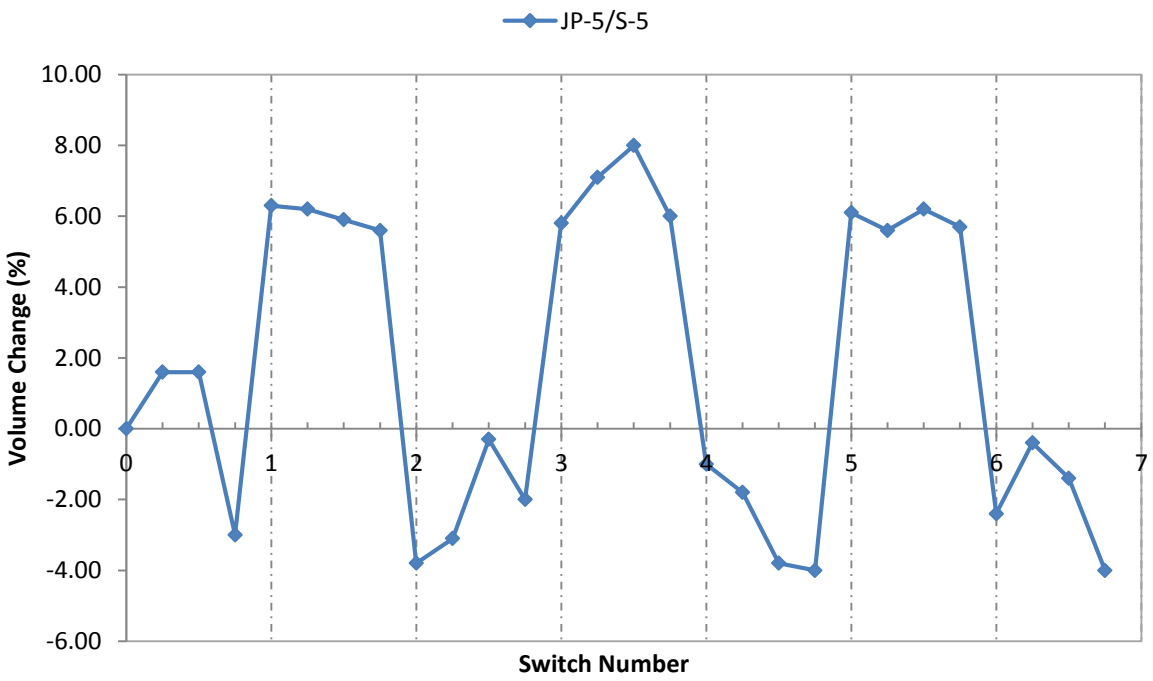

Figure 2.24: Switch-loading behaviour of NBR O-rings in JP-5/S-5 fuel pair. Odd switch-numbers represent a switch from S-5 to JP-5 (adapted from Muzzell *et al*. [63])

One needs to bear in mind that the degree of swelling swing is exaggerated in new seals and O-rings which are susceptible to leaching of plasticisers and fillers by fuels such as S-5. It is likely that swelling changes of such magnitude will not be observed in older less compliant O-rings. Older, O-rings, however, suffer from the problem of compression set, leading to leaks on fuel switching.

2.6.3 Compression set testing

Compression set occurs as the result of progressive stress relaxation which leads to a gradual decline in the sealing force of an elastomer. Typically, elastomer seals, used under dynamic or static compression, are susceptible to compression set which results in permanent deformation of the elastomers shape; thus potentially compromising their ability to act as a functional sealing material [65].

Figure 2.25: Elastomer seal which has experienced compression set and loss of original shape and sealing ability (Adapted from [66])

Compression set is specified by ASTM standard D395 [67]. The concept is illustrated by Figure 2.26. The compression set value represents the residual deformation of the elastomer at a specified time after release from compression. The lower the compression set value the greater shape recovery has occurred within the elastomer [66]. Compression set is defined as

$$\text{compression set}(\%) = \left(\frac{t_0 - t_1}{t_0 - t_s}\right) \times 100$$

where:

t_0 = original thickness of the sample
t_1 = final thickness of the sample after removal from compression
t_s = thickness to which sample is compressed (spacing between the compression plates)

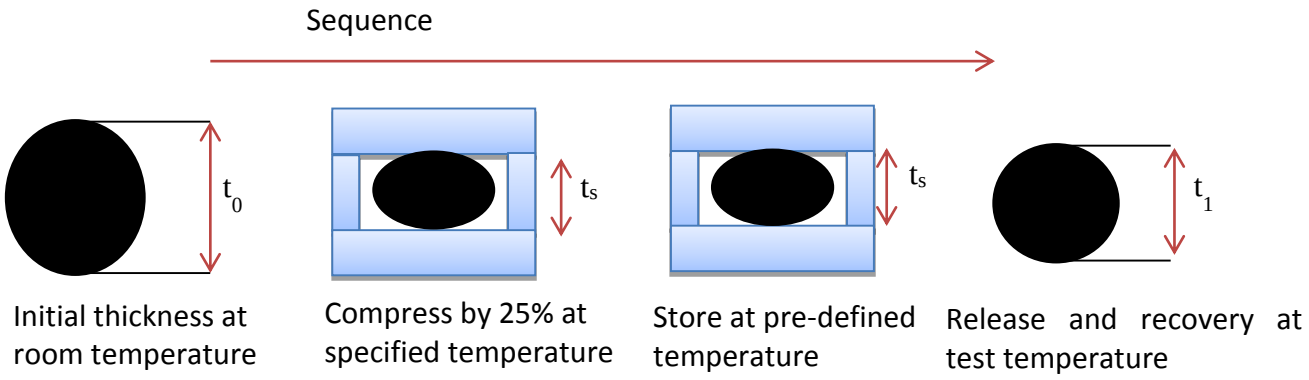

Figure 2.26: Typical compression set measurement procedure (adapted from Jaunich *et al*. [66])

The common mechanisms that result in compression set are plasticiser loss and additional crosslinking [66]. Additional crosslinking can be affected by both the presence of plasticisers and fillers as well as the influence of temperature.

Mostafa *et al.* [68] investigated the effect of carbon black loading on the compression set behaviour of styrene-butadiene rubber (SBR) and NBR. It was found that as increasing amounts of the filler were added to the rubber compounds the compression set value increased. In general filler loading increases the crosslink density with the elastomer resulting in a decrease in chain mobility and ultimately an increase in elastomer stiffness [68]. Increased crosslink density causes resistance to compressive loading during which many of these crosslinks are severed. Upon the load being relieved, the crosslinks responsible for the strain recovery are depleted and the specimen fails to recover to its original dimensions. In the case of NBR it can be expected that crosslink density can increase further when under compressive loads due to the presence of the nitrile group [68]. This study exclusively looked at carbon black loading. The presence of most fillers can have the effect of increasing the crosslinking density of elastomers under compressive loads.

Compression set is also affected by the presence of plasticisers within the elastomer matrix. Of particular importance is the presence of solvent or fuels with the ability to permeate the elastomer matrix and have hydrogen bonding potential. Slater *et al.* [69] observed a noticeable difference in compression set of polyurethane exposed to laboratory air and samples submerged in water. Compression set was far greater in the water-submerged samples compared to the samples exposed to air. Compression set was also observed to increase with increasing temperature. The authors attributed this behaviour to the increased diffusion of the liquid into the polymer matrix at higher temperatures allowing a greater concentration of the fluid to interact with the existing crosslinks through hydrogen bonding

[69]. Such interactions cause a disruption in the crosslink density, reducing the ability of the polymer to recover dimensions upon released compressive load.

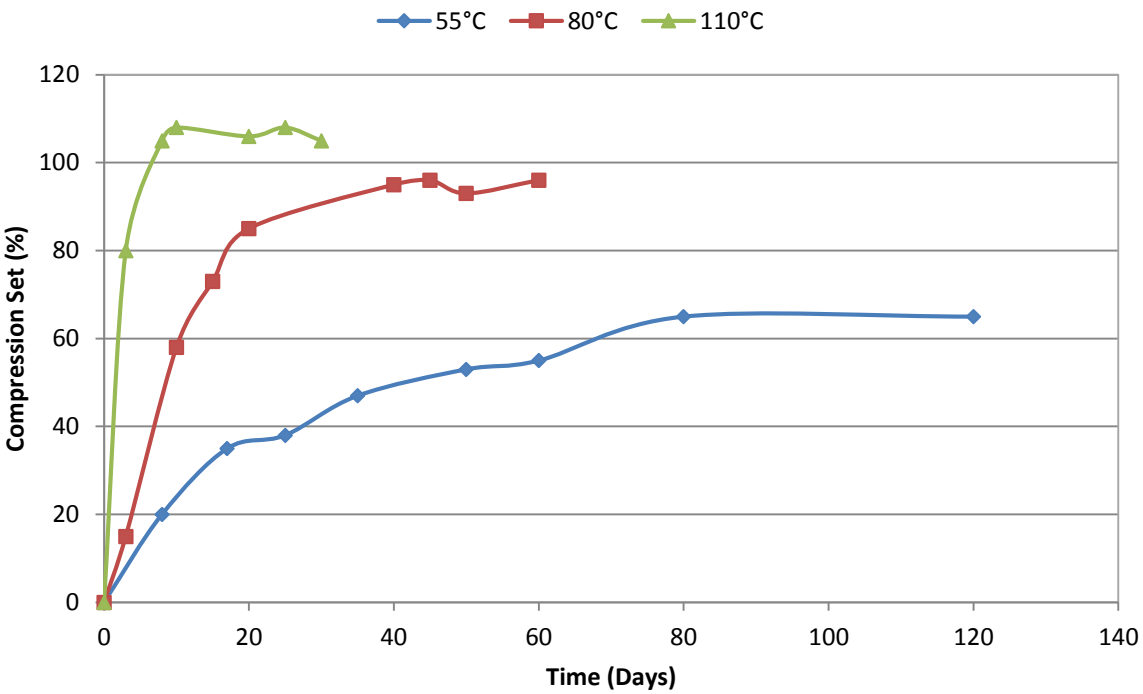

Figure 2.27: The time-temperature effect on compression set of NBR elastomer (adapted from Morrell *et al.* [70])

Compression set is time-temperature dependant. Compression of an elastomer under increasingly high temperatures allows excessive crosslinking to occur, where the crosslink density is directly proportional to the temperature of the surrounding environment [66]. The time-temperature dependence of compression set is illustrated by Figure 2.27 where it is readily observed that higher temperatures result in greater compression set occurring over a shorter time interval.. In general, elastomer samples are unaffected by compression set at low temperatures as mostly reversible effects take place and increased crosslink initiation is unlikely [66].

2.7 Exposure of elastomers to petroleum and synthetic jet fuels

A number of studies have been conducted which have investigated the effect of jet fuel on aviation elastomers [7, 8, 71, 72]. Although a range of elastomers have been investigated, most studies have focussed on NBR [7, 8, 71, 72]. Some of these studies have already been referred to. Many of the more recent studies have investigated the effect of blending aromatics and other compounds with SPK on gravimetric and volumetric swelling [8, 72].

Extensive research has been performed on the swelling of NBR elastomers in various fuel and solvent blends by Graham *et al*. [8] and more recently by Seehra *et al*. [72]. Both studies concluded that swelling was highly reliant on both the bulk fuel and the minor doping agent. Graham *et al.* [8] noted that not all aromatic species interact with NBR to the same degree. Increasingly polar aromatic solvents showed greater propensity to swell the NBR samples while aromatics demonstrating hydrogen-bonding character were likely to interact strongly with the electronegative cyano-group of NBR. Seehra *et al.* [72] attributed the observed results to the role of solubility parameters. Aromatic solvents with Hansen solubility parameters (HSPs) approaching the value of those for NBR were able to interact to a greater degree than those solvents whose HSP values were distant to NBR.

Seehra *et al.* [72] demonstrated the importance of Hansen solubility parameters (HSPs, discussed in more detail in Chapter 3) by observing the high degree of swelling of NBR exposed to acetone. Acetone has HSP values aligned with those of NBR. The highly polar character of the ketone functional group was also cited as playing a major role in the interaction. Interestingly, the same authors observed the swelling response of NBR samples exposed to a synthetic jet fuel S-8. S-8 is a synthetic jet fuel employed within military aviation. It has similar properties to the crude oil derived JP-8 jet fuel with one major exception; the aromatic content in S-8 is negligible while JP-8 contains close on 20% (v/v). The observed swelling of NBR samples in pure S-8 was near zero and typifies a major concern with elastomer compatibility within synthetic fuels. Doping the synthetic fuel with 20% (v/v) HISOL-15, a commercial aromatic-rich solvent, results in swelling of more than 8% (v/v) [72].

Numerous additional research has been documented on the swelling response of fuel-wetted elastomers. However, the majority of the studies neglect to disclose information regarding the nature of the elastomer, elastomer conditioning procedure and operating temperature of the tests. Additionally, few studies explicitly perform testing on deplasticized elastomer samples.

Work of particular interest to this study was that performed by Graham *et al.* [8] who compared the swelling of as-received and deplasticized samples exposed to conventional Jet A and SPK. The authors tested on a variety of materials such as NBR, fluorosilicone and fluorocarbon elastomers. NBR was found to be the most sensitive to fuel exposure. The authors observed that the elastomer swelling response increased with increasing molar volume and increasing solubility parameters; in particular, increasing δ_p and δ_h [8]. Despite these findings, the authors exposed the elastomer samples to the fuel for 40 hours only. Based on this, it is difficult to know if the swelling response had reached an equilibrium state.

Muzzel *et al.* [63] investigated the solvent uptake of two different NBR elastomer types exposed to synthetic and petroleum derived jet fuels. The authors observed that far less solvent uptake of the synthetic fuel occurred compared to the conventional jet fuel. The addition of aromatic species (C_9-C_{11}) to the synthetic fuel resulted in a large increase in the observed swelling response of the elastomer samples [63]. Leading on from this research, Visram [56] investigated the change in swelling response of elastomer samples when additional blending aromatic components were added to the synthetic fuel. The author observed that blending SPK with aromatic oxygenates of concentrations as low as 1-2% (v/v) resulted in elastomer swelling similar to that achieved with exposure to Jet A-1. Additionally, the author concluded that longer compounds such as alkylbenzenes would impart an inferior swelling response on elastomer materials due to their large molar volume [56].

In a report composed by the Boeing Company [73], the authors examined the overall response of NBR O-ring samples to exposure to SPK and SPK fuel blends. Elastomer samples were exposed to a set of 12 Jet A fuel types and 4 SPK fuel types. The Jet A samples had aromatic content that ranged from 8.7% to 23.1%. Ten species of aromatic where chosen to blend with the SPK and these are listed in Table 2.10. The selection emphasized the relative roles of molar volume, polarity and the affinity for hydrogen bonding. A limitation of the study centred on the exposure time of the elastomer samples. The NBR O-rings were submerged in the fuel samples for 40 hours at room temperature [73]. This indicates that the swelling response measured was not indicative of an elastomer sample that has reached an equilibrium swelling value. However, as this was a comparative study, achieving true equilibrium was not needed.

Table 2.10: Aromatic compounds used in the Boeing study [73].

Characteristic	Aromatic	Conc. (v/v)	δ_d	δ_p	δ_h	δ_{total}	Molar Volume (cm^3/mol)
Molar Volume	Propylbenzene	8%	17.6	0.2	1.3	17.6	139
	Butylbenzene	8%	17.4	0.1	1.1	17.4	157
	Pentylbenzene	8%	17.1	0.0	0.8	17.1	173
Polarity	1,3,5- Trimethylbenzene	8%	18.0	0.0	0.6	18.0	140
	1,2,4- Trimethylbenzene	8%	17.8	0.4	1.0	17.8	137
	1,2,3- Trimethylbenzene	8%	17.6	0.8	1.4	17.7	134
Hydrogen Bonding	Tetralin	8%	19.6	2.0	2.9	19.9	136
	Naphthalene	3%	19.2	2.0	5.9	20.2	112
Other	Indan	8%	17.8	0.6	2.1	17.9	123
	Methylindene	3%	20.1	1.0	7.2	21.4	134

Despite this perceived limitation, valuable data was extracted from the report. The authors found that molar volume, polarity and the role of hydrogen bonding were influential in the swelling response of the NBR samples. In particular, volume swell was found to increase as the molar volume of the blending aromatics decreases and the polarity and affinity to hydrogen bond increased [73]. The role of hydrogen bonding was concluded as constituting a greater influence to the overall volume swell compared to the other two factors. This theme is reiterated by Hansen [51] and will be discussed further in sections to follow.

Most recently, Burnham [9] performed work that focussed on the interactions between fuel components from various fuel classes and NBR elastomer. As with the Boeing report, Burnham [9] observed that solubility parameters and molar volume were influential in the resultant swelling response of the elastomer material. In particular, if the elastomer and fuel component had similar solubility parameters it was likely a large swelling response would be observed. Additionally, compounds with large molar volumes imparted a reduced swelling response on the NBR sample [9].

The author further observed that temperature had an effect on the overall swelling dynamics. In particular, aromatic oxygenates were found to show reduced swelling on the elastomer sample with increasing temperature. The author concluded that the largely exothermic hydrogen bonding interactions associated with aromatic oxygenates would result in a decreasing equilibrium swelling constant as temperature increased [9]. The conclusions of the author are further investigated in this study.

CHAPTER 3

3. Thermodynamics of elastomer swelling

A critical performance factor for elastomers exposed to liquid fuels or solvents is their ability to absorb the surrounding fuel resulting in swelling of the elastomer material. Swelling results from competing processes of sorption, diffusion and permeation which minimise the free energy of the liquid and elastomer system [52]. There are several factors which contribute to these transport processes. These are discussed in this chapter.

3.1 Flory-Huggins theory

Flory-Huggins theory [48] models the interactions occurring in polymer solutions. The model estimates the enthalpy of mixing (ΔH_{mix}) using lattice parameters associated with the polymer-solvent system [30, 48]. Flory and Huggins described ΔH_{mix} using the relationship below.

$$\Delta H_{mix} = kT\chi N_A N_B = RT\ \chi n_A \phi_B$$

where:

- χ = Flory interaction parameter
- k = the Boltzmann constant
- R = the universal gas constant
- N_A = number of molecules of component A, the solute
- N_B = number of molecules of component B, the polymer
- n_A = number of moles of component A
- ϕ_B = volume fraction of component B

The Flory interaction parameter may be used to characterise the interaction between polymer and solvent. A positive χ value indicates repulsive interactions between the two components. Consequently ΔH_{mix} is positive. Flory and Huggins developed their theory for endothermic mixing. A negative χ value, however, is indicative of attractive forces between the components which actively promotes the dissolution process between component A and B [48].

A similar approach exists for the entropy of mixing where Flory and Huggins considered that dissolution of a polymer in a solvent can be regarded as a two-stage process dependent on (1) the transfer of a polymer chain from an ideal ordered state to a state of disorder randomly placed within the lattice and (2) the mixing process of these newly disordered chains with the surrounding solvent [30]. ΔS_{mix} is obtained as:

$$\Delta S_{mix} = -k (N_A \ln \phi_A + N_B \ln \phi_B)$$

where:

N_A = number of molecules in component A
N_B = number of moles of component B
ϕ_A = Volume fraction of component A
ϕ_B = Volume fraction of component B

Combining the above equations allows the free energy of mixing to be calculated. This is the basis of the Flory-Huggins theory.

$$\Delta G_{mix} = RT (N_A \ln \phi_A + N_B \ln \phi_B + \chi N_A N_B)$$

In practise Flory-Huggins theory has limitations because the assumption that solution property data can be predicted using a single value of χ is fundamentally flawed. This parameter is often concentration dependant which is ignored by the theory [30, 74].

3.2 Flory-Rehner Theory

After early observations of elastomer swelling performed by Frenkel [75], a general theory for the swelling of cross-linked elastomers was developed by Flory and Rehner. The Flory-Rehner theory was developed because of two distinct properties of elastomers which distinguish them from more typical solids. The first is that elastomers are able to absorb large quantities of solvent without dissolving themselves. This is accounted for in the theory by a polymer-solvent interaction term. Secondly, elastomers are able to undergo large deformations with correspondingly small stress, accounted for by an elastic retraction term [76]. Flory and Rehner hypothesised that the free energy change associated with swelling an elastomer

consisted of the aforementioned terms which were to be treated as separable and additive as summarised:

$$\Delta G_{swelling} = \Delta G_{mixing} + \Delta G_{elastic}$$

The theory accounts for:

(1) the change in entropy caused by polymer-solvent mixing. This change is positive and thus favours elastomer swelling.

(2) the change in entropy caused by reducing the number of possible chain formations upon elastomer swelling. This change is inherently negative and opposes swelling.

(3) the heat or enthalpy of mixing between elastomer and solvent. This was first demonstrated by the Flory-Huggins theory as described earlier. Usually this parameter in positive and opposes swelling.

Consolidation of the above parameters gives rise to the Flory-Rehner equation for quantifying the interaction of an elastomer with a solvent [31].

$$-\left[\ln(1-\upsilon_2)+\upsilon_2+\chi\upsilon_2^{\,2}\right] = V_1 n_{XLD}\left[(\upsilon_2)^{1/3}-\frac{\upsilon_2}{2}\right] = 0$$

where:

V_1 = molar volume of the solvent

υ_2 = volume fraction of polymer in the swollen sample

χ_1 = Flory-Huggins interaction parameter

n_{XLD} = network or cross-link density

Flory-Huggins interaction parameters are widely available for many elastomer-solvent pairs which allow the equilibrium swelling behaviour of an elastomer to be readily determined. The method is typically used to determine cross-link density.

3.3 Solubility parameters

3.3.1 Hildebrand Solubility Parameters

The solubility parameter (SP) is a quantitative indication of the cohesive energy density of a solvent, *i.e.* the strength of molecular interaction between molecules. SPs have proved useful in determining and predicting key physical properties such as solubility and swelling of polymers by solvents [77]. The use of SPs may be summarised by the maxim that "like dissolves like." Polymer and solvent having similar SP values are likely to interact to a greater extent resulting in increased observed swelling whereas, in contrast, a polymer-solvent mixture which display vastly different SP values will show limited interaction [77, 51]. Two concepts of SP will be discussed further which include Hildebrand and Hansen solubility parameters.

The solubility parameter concept was first developed by Hildebrand who defined the Hildebrand solubility parameter (δ_H) as the square root of the cohesive energy density of a solvent. This relationship is only valid for positive heats of mixing and the theory breaks down for negative heats of mixing which represents a limitation of the theory [31].

$$\delta_{HILDEBRAND} = \sqrt{\left(\frac{\Delta H_{fus} - RT}{V}\right)}$$

where:

ΔH_{fus} = enthalpy of fusion
R = universal gas constant
T = temperature in Kelvin (K)
V = molar volume

Group contributions, osmotic pressure, swelling and intrinsic viscosity are all plausible methods of evaluating the Hildebrand solubility parameter. The intrinsic viscosity parameter has been found to be most effective in measuring SP of polymeric materials which display extremely low vapour-pressures [77]. While SP is not the only factor contributing to elastomer swelling it is frequently found that solvents will swell elastomers more where they have similar SP values. As a rule of thumb a solvent-polymer pair should interact favourable provided their SP values fall within 1 unit of each other.

Although a general correlation between elastomer swelling and SP values emerged, several limitations of Hildebrand solubility parameters remained. Firstly, the entropy of mixing

between solvent and elastomer is ignored as it is assumed all solvent molecules had the same size and shape and formed regular solutions. Additionally, it emerged that elastomers such as poly(acrylonitrile-*co*-butadiene) or NBR, seems to exhibit two SP values. This may be ascribed to the fact that NBR is a block copolymer [47]. Finally, as increasing experimental work was undertaken it was found that swelling measurements could not be reliably computed as some solvents were found to impart large swelling on elastomers showed limited interaction with others having similar SP values [47, 77]. One further limitation of $\delta_{HILDEBRAND}$ is the inability to account for elastomer swelling in multicomponent systems. In a study by Gee *et al.* [78] the behaviour of a cross-linked elastomer network exposed to single- and multicomponent solutions was examined with no quantitative agreement between elastomer swelling [47, 78].

3.3.2 Hansen solubility parameters

Charles Hansen proposed extensions to the existing SP model to address some of the limitations by introducing the concept of Hansen solubility parameters (HSPs) which are an extension of the Hildebrand solubility parameter. HSPs are expressed using the sum of energy contributions originating from hydrogen-bonding (and similar interactions), permanent dipole-dipole interactions and non-polar dispersion (van der Waals) forces. They may be using the relationship below [47, 51].

$$\delta_{total}^2 = \delta_d^2 + \delta_p^2 + \delta_h^2$$

where:

δ_d = dispersion component
δ_p = polar component
δ_h = hydrogen bonding component

Materials with similar HSP values tend to have a higher affinity for one another and the extent of this affinity ultimately determines the overall magnitude of the interaction between the two solvents [51]. For many linear and branched paraffins where the general type of interaction is non-polar, $\delta_{total} = \delta_d$. For these solvents, the Hansen and Hildebrand theories predict the same behaviour [51].

The polar component (δ_p) results from permanent dipole interactions. The dipole moment between two materials is the primary interaction used to calculate δ_p. The most polar solvents are ones with high solubility parameters. The third major cohesive energy source is that of

hydrogen bonding (δ_h) which is also often more accurately referred to as an electron exchange parameter [51]. Other than accounting for the hydrogen bonding interactions, this parameter includes cohesive energies not accounted for by the dispersion and polar parameters [51].

Although of global acceptance and use, HSPs ignore other interactions to a greater-or-lesser degree such as induced dipole, metallic bonding, electrostatic interactions and organometallic bonding [51]. Despite this, HSPs have found to be widely used within the industries of coating and surface applications as well as predicting the behaviour of polymeric components in the presence of a given solvent [79]. With the use of HSPs one can estimate the extent of which a particular solvent may swell a polymer sample. Table 3.1 presents solubility parameters for NBR rubber consisting of 30% acrylonitrile, which is representative of typical NBR O-rings and seals found within aviation fuel systems [8].

Table 3.1: Hansen solubility parameters for NBR and the associated homopolymers [8]

Polymer	**Solubility parameter ((MPa)$^{1/2}$)**			
	δ_{total}	δ_d	δ_p	δ_h
poly(acrylonitrile)	25.3	18.2	16.2	6.8
poly(butadiene)	18.0	17.0	0.0	1.0
nitrile rubber (30% acrylonitrile)	18.3	17.4	4.9	2.7

By comparing the solubility parameters of NBR with parameters of typical fuel blending components founds in petroleum and synthetic fuels, a prediction regarding the interaction and potential swelling that may occur as a result of solvent-polymer interaction may be made. HSP values for typical blending components and fuels are listed in Table 3.2.

From the solubility parameters one notices that aromatic compounds have much similar solubility parameters to NBR and would consequently be expected to impart greater swelling than a paraffinic compound such as n-octane. The paraffin contains only dispersion interactions whereas aromatics can interact with NBR via all 3 interaction channels.

Table 3.2: Solubility parameters for typical blending components [8, 51]

Solvents	**Solubility parameter ((MPa)$^{1/2}$)**			
	δ_{total}	δ_d	δ_p	δ_h
JP-5 (Petroleum)	16.5	16.5	0.2	0.5
S-5	16.0	16.0	0.0	0.0
n-octane	15.5	15.5	0.0	0.0
benzene	18.5	18.4	0.0	2.0
toluene	18.2	18.0	1.4	2.0
naphthalene	20.2	19.2	2.0	5.9
benzyl alcohol	23.8	18.4	6.3	13.7

3.3.3 Hansen solubility parameters and χ_{12}

The Flory-Huggins interaction parameter, χ, has historically been used to estimate polymer-solvent activity. Nonetheless, this parameter is inherently flawed and has since been replaced by χ_{12}, the Flory-Rehner interaction parameter [51]. χ_{12} is historically evaluated using Hildebrand solubility parameters and is described by the equation below. Notably, a small interaction parameter indicates that increased polymer swelling is likely. χ_{12} is driven by both temperature and nature of the Hildebrand solubility parameters for the solvent and polymer respectively.

$$\chi_{12} = \beta + \frac{\left[V\left(\delta_1^2 - \delta_2^2\right)\right]}{RT}$$

where:

- V = molar volume of the solvent
- δ = Hildebrand solubility parameters for the solvent and polymer
- R = universal gas constant
- β = term which accounts for entropic effects. Usually set equal to 0.3
- T = absolute temperature in Kelvin

The use of Hildebrand solubility parameters is only applicable to nonpolar systems and as such this model is not representative of many polymer-solvent systems. With the use of HSPs and

by taking into account interactions associated with polar and hydrogen bonding energies, an extension on the interaction parameter was subsequently proposed [80].

$$\chi_{12} = \alpha\frac{V_1}{RT}\left[(\delta_{d1}-\delta_{d2})^2 + 0.25(\delta_{p1}-\delta_{p2})^2 + 0.25(\delta_{h1}-\delta_{h2})^2\right]$$

where:

V_1 = molar volume of the solvent
$\delta_{d,p,h}$ = Hansen solubility parameters
α = fitting parameter. Often 0.6 is assumed.

From the relationship proposed above, polymer swelling will be maximised when individual HSP terms are minimised. The practicality of the expanded interaction parameter model allows χ_{12} to be readily estimated provided the HSP values for the solvent and polymer are available. However, shortcomings of the model persist. HSP values cannot be estimated using known χ_{12} values as the basis for these values derives from Hildebrand solubility parameters. Further, the failure of Hildebrand solubility parameters to account for concentration effects on the swelling response of the polymer material remain a drawback [51, 80].

3.3.4 The importance of concentration

Preferential solvent uptake has been reported previously and readily occurs in a non-ideal solution containing mixed solvents [47]. The importance of solvent concentration is illustrated by Figure 3.1.

All concentration experiments were run at 50°C. It is possible that solvent-solvent associations exist between solvent pairs. In order for any of the aforementioned models to prosee an appropriate estimate of polymer swelling additional coefficients accounting for this deviation are required.

Finally, the interaction parameter model predicts an increase in swelling with increasing temperature. The model fails to account for those systems which deviate from ideal behaviour and show a decreased swelling response with increased temperature.

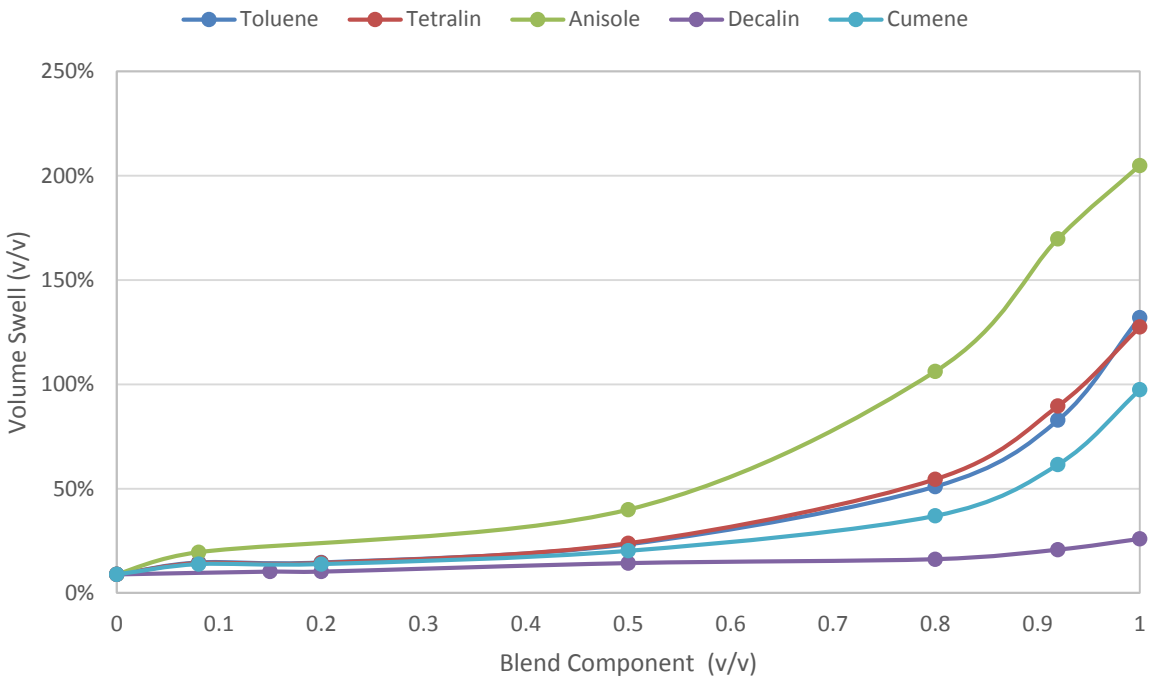

Figure 3.1: Influence of solvent concentration on the swelling response of NBR elastomer

Interestingly, tetralin and toluene follow a very similar swelling profile despite their obvious difference in chemical structure. It was observed that volumetric swelling was profound when the pure compounds were used. Additionally, the profile of Figure 3.1 begin to resemble Gaussian behaviour. Gaussian behaviour has been observed previously as indicated in Figure 3.2 where volumetric swelling was observed to increase with increasing magnitude in total solubility parameter. This trend was observed until a critical point, after which, swelling decreased with increasing total solubility parameter. It has been suggested that the maximum volumetric swelling corresponds to the point of minimization of the interaction parameter, χ. Once this point is surpassed, a drop off in swelling can be expected [56, 52].

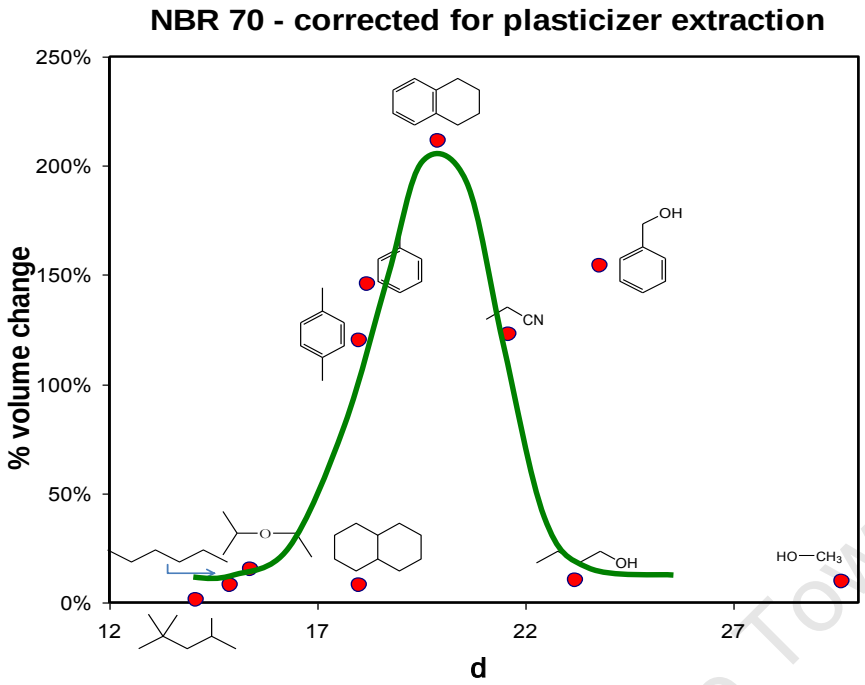

Figure 3.2: Volumetric swelling response to pure component exposure (Adapted from Visram [56])

3.3.5 Limitations of solubility parameters

Although widely used within industry as an estimate for predicting solvent-elastomer activity, the SP theories of Hildebrand and Hansen presented above embody numerous assumptions which limit their applicability.

All SP models estimate solvent-elastomer activity by taking into account only the positive enthalpy of mixing while ignoring contributions to the Gibbs free energy from entropy of mixing and the elastic retraction energy of the elastomer network. This assumption is counter-intuitive since solvents which are predicted to interact favourably with elastomers often have enthalpy of mixing values close to zero. Therefore a reliable prediction of elastomer swelling using SP theories would include taking the aforementioned parameters into account [47]. Additionally, the HSP model fails to represent exothermic interactions associated with solvent-elastomer interactions. By ignoring these negative heats of mixing, it is assumed that an elastomer will interact with a mixed-solvent matrix to the same extent as with each of the pure solvents populating the matrix [47]. Previous studies have reported deviations in swelling of elastomers exposed to multicomponent systems when compared with swelling induced by the single solvent in question. Poly(butadiene-*co*-styrene) elastomers exposed to chloroform/n-butyl acetate systems and natural rubber in chloroform/diethyl ether systems

are examples of elastomer systems showing these deviations. These systems are found to exhibit exothermic heats of mixing. As such, the HSP model is unable to yield reliable quantitative estimates of swelling interactions for these types of systems [47, 51].

Furthermore HSPs do not adequately account for elastomer exposed to a multi-component solvent mixtures like real fuels. It is assumed that solvent which enters the elastomer matrix has the same bulk properties as the bulk solvent or has the best matching SP value with the elastomer. This approach ignores the possibility that solvent permeation relies on the unique orientation of each solvent molecule [47]. Further, the possibility of preferential solvent uptake it not addressed by this model.

The assumption that solvents and elastomers with similar SP values are likely to show greater interaction is widely accepted for both Hildebrand and Hansen SPs. This matching concept is flawed when using HSPs. Although the matching concept works well for dispersion and dipole forces, the ability of compounds to form other interactions such as acid-base interactions is not taken into account [47, 81]. The HSP model also fails to take into account the influence of changing environments on the SP values. Hansen concedes that SP values are susceptible to variation with increasing temperature. In particular, polar cohesive and hydrogen-bonding parameters are most strongly influenced by increasing temperature [51].

CHAPTER 4

4. Experimental procedures

4.1 Fuels and materials

Nitrile rubber (NBR) O-rings were supplied by Bearing Man Ltd (Johannesburg, South Africa). Two sizes of O-rings were used in this study: small sized O-rings with an inside diameter (i.d.) of 4.48mm, cross-sectional diameter of 1.78mm and Shore A hardness of 70 were used for swelling and DMA studies while large O-rings with an i.d. of 34.65mm, cross-sectional diameter of 1.78mm and Shore A hardness of 70 were used for tensile testing. O-rings were used in a deplasticised form. A procedure to remove plasticisers and other fuel extractable additives is described in later sections. Shore A 70 hardness FKM elastomers with the same dimensions were used for a sub-set of exposure experiments.

Commercial fuels used in this investigation include petroleum-derived Jet A-1 and CTL SPK supplied by Sasol. Solvent classes used within this investigation include aromatics, cyclo-paraffins and n-paraffins which were supplied by Sigma-Aldrich (St. Louis, MI, USA), unless specified otherwise. Other suppliers were Merck (Darmstadt, Germany) and Kimix (Cape Town, South Africa). A comprehensive list of solvents and fuels used can be found in Table 4.1.

Table 4.1: Description of the fuels and solvents used

Class	Purity	Solubility parameters ((MPa)$^{1/2}$)				Molar volume at 20°C (cm^3/mol)$^{\$}$
Fuels		δd	δp	δh	δtotal	
CTL SPK	-	15.4$^{\#}$	0.0$^{\#}$	0.0$^{\#}$	15.4$^{\#}$	212.5$^{\#}$
Jet A-1	-	16.5$^{\#}$	0.1$^{\#}$	0.3$^{\#}$	16.5$^{\#}$	193.7$^{\#}$
Hydrocarbons						
n-paraffins						
n-decane*	99%	15.7	0.0	0.0	15.7	195.9
n-dodecane*	99%	16.0	0.0	0.0	16.0	227.1
*						
monocyclic paraffins						

cyclohexane	99%	16.8	0.0	0.2	16.8	108.8
methylcyclohexane	99%	16.0	0.0	1.0	16.0	127.6
1,2-dimethylcyclohexane	99%	16.7[#]	0.0[#]	0.0[#]	16.7[#]	143.7
iso-propylcyclohexane	99%	16.3[#]	0.0[#]	0.5[#]	16.3[#]	157.4
n-butylcyclohexane	99%	16.2	0.0	0.6	16.2	176.7
bicyclic paraffins						
decalin	99%	18.8	0.0	0.0	18.8	156.9
monocyclic aromatics						
benzene	99%	18.4	0.0	2.0	18.5	89.1
toluene**	98%	18.0	1.4	2.0	18.2	106.3
o-xylene	99%	17.8	1.0	3.1	18.1	120.6
m-xylene	99%	17.7[#]	0.5[#]	3.1[#]	18.0[#]	123.5
p-xylene	99%	17.6	0.0[#]	3.1	17.9[#]	123.3
ethylbenzene	99%	17.8	0.6	1.4	17.9	122.5
styrene	99%	18.6	1.0	4.1	19.1	114.6
1,3,5-trimethylbenzene	99%	18.0	0.0	0.6	18.0	139.1
1,2,4-trimethylbenzene	99%	18.0	1.0	1.0	18.1	137.2
n-propylbenzene	99%	17.6	0.4	1.2	17.6	139.4
cumene	99%	18.1	1.2	1.2	18.2	139.4
α-methylstyrene	99%	18.5	2.4	2.4	18.8	129.9
n-butyl benzene	99%	17.4	0.1	1.1	17.4	156.1
s-butyl benzene	99%	17.9[#]	0.8[#]	1.1[#]	18.0[#]	155.5
p-cymene	99%	17.6[#]	1.2[#]	1.2[#]	17.7[#]	156.6
diaromatics						
indene	99%	18.7	2.6	9.0	20.9	116.5
napthalene	99%	19.2	2.0	5.9	20.2	128.0
1-methylnaphthalene	95%	20.6	0.8	4.7	21.1	138.8
hydroaromatics						
indane	95%	19.6[#]	1.3[#]	1.6[#]	19.7[#]	122.8
tetralin	99%	19.6	2.0	2.9	19.9	136.3
Oxygenates						
benzyl alcohol	99%	18.4	6.3	13.7	23.8	103.6
anisole	99%	17.8	4.1	6.7	19.5	108.7
dibenzyl ether	99%	19.6	3.4	5.2	20.6	190.1
furan	99%	17.8	1.8	5.3	18.7	71.6
tetrahydrofuran	99%	16.8	5.7	8.0	19.5	81.1
n-hexanol	99%	15.9	5.8	12.5	21.0	125.6

cyclohexanol	99%	17.4	4.1	13.5	22.4	104.1
Others						
dichloromethane**	99%	18.2	6.2	6.3	20.2	63.9
pyridine	99%	19.0	8.8	5.9	21.8	80.6

[#] estimated

* supplied by Merck

** supplied by Kimix

$ Molar volumes calculated from densities [82]

Where solubility parameters in Table 4.1 were estimated, they were usually estimated using group contributions in Hansen [51]. In the case of *p*-xylene, the δ_p value has been replaced with a more realistic value. Hansen [51] reports δ_p for *p*-xylene to be 1.0, yet p-xylene has no permanent dipole. The values for *m*-xylene have been estimated as being between the two extremes. The values for *sec*-butyl benzene were from those for *n*-butylbenzene by analogy form the cumene/*n*-propylbenzene pair. Although naphthalene is a solid at 20°C, its molar volume is estimated using the density of liquid naphthalene which would be more representative of naphthalene in solution.

Solubility parameters of the fuels were estimated from their molecular compositions as measured by GC-MS. The solubility parameters of the component molecules were first estimated using the group contributions in Hansen [51]. The overall solubility parameters were found by using the volume weighted average of the individual solubility parameters. Fuel molar volume was estimated as an average of the molar volumes of component molecules.

4.2 Instruments used

In order to perform the required testing for this investigation a variety of standard and advanced laboratory equipment was utilised. The swelling response of O-ring samples exposed to varying synthetic fuel blends and temperature environments required use of standard laboratory equipment whereas the sealing and mechanical performance of the elastomer samples were inferred from use of advanced laboratory equipment.

4.2.1 Gravimetric measurements

Mass measurements of elastomer samples were recorded and tracked using a *Mettler Toledo AT20* analytical microbalance with an accuracy of ± 2μg.

4.2.2 Volumetric measurements

Volumetric changes of the elastomer samples were analysed using *Nikon ShuttlePix P-MFSC* microscope with an accuracy of ±1µm.

4.2.3 Temperature measurements

The temperature dependence of elastomer swelling was tracked by placing various fuel blends in laboratory ovens set at various temperatures. For experiments conducted at 50°C a standard laboratory oven was used whereas a *Labotec Ecotherm* laboratory oven was used for experiments at 35°C. Experiments performed at 20°C were placed in a temperature controlled room. Temperature readings were validated using a type K thermocouple connected to a *Fluke 179 True RMS Multimeter* with an uncertainty of ± 1°C.

4.2.4 Thermogravimetric analysis

Thermogravimetic analysis (TGA) was used to determine if residual fuel/solvent remained in the O-rings after drying. A Q5000 IR TGA supplied by TA Instruments (New Castle, DE, USA) was used to measure mass loss (or the absence thereof). The instrument was calibrated for mass using high quality mass standards and was calibrated for temperature using the Curie points of nickel (358^{o}C) and iron (770^{o}C).

4.2.5 Differential scanning calorimetry

Differential scanning calorimetry (DSC) allows temperature and heat flow measurement of a desired sample essentially outputting major thermal events occurring through a specific temperature range. A Q2000 DSC supplied by TA Instruments (New Castle, DE, USA) was used to measure the T_g of the studied materials. The instrument was calibrated for temperature using the melting points of high purity mercury (-38.8^{o}C) and indium (156.6^{o}C).

4.2.6 Dynamic mechanical analysis

DMA works by applying a sinusoidal deformation to a sample of known geometry. The sample can experience either a controlled stress or strain and allows measurement of a materials response to stress, frequency and temperature. The overall deformation of the material is a function of its inherent flexibility. This study made use of a Q800 DMA with a temperature uncertainty of ±1°C. The DMA was supplied by TA Instruments (New Castle, DE, USA).

4.2.7 Tensile testing

Tensile testing is used to determine the basic tensile strength, elongation and Young's modulus of material subject to a tensile load. An *Instron 3365* tensile tester equipped with spool grips was used to carry out tensile testing in this investigation. The instrument was supplied by Instron (Norwood, MA, USA).

4.2.8 Compression set testing

Compression set testing was performed using compression plates [65]. The plates were designed according to ASTM D395 specifications allowing approximately 25% compression of the rubber sample. The plates were made from Al 6061 T6 allowing circulation holes of 2mm to be machined into the plates to ensure free flow of fluid.

4.3 Testing methods

Test procedures used to allow swelling and performance properties of elastomer materials followed ASTM methods where applicable. Deviations from standard methods are described accordingly where applicable.

4.3.1 O-ring conditioning

NBR O-rings, in the as-received condition, contain a varying amount of additives such as plasticisers and fillers which increase the flexibility and generally decrease the tensile strength and hardness. Additives often leach out of the elastomer when exposed to fuels and solvents during in-service conditions. All NBR O-rings where exposed to a conditioning procedure prior to testing to accelerate the ageing procedure, remove the additives and ensure a sample more representative of those found in in-service conditions. The conditioning procedure was used for all as-received O-rings used within this study.

The conditioning procedure was performed as follows [9]:

- As-received O-rings were placed in a 1 litre media bottle and continuously submerged in 800ml of dichloromethane (DCM) at ambient conditions for 3 days.
- After 3 days the DCM was decanted and replaced with a fresh batch. O-rings were submerged under the same conditions for an additional 2 days.
- After 5 days of submersion, the samples were removed from DCM and allowed to air dry in a fume hood for 3 days at ambient temperatures.

- Dried O-rings were placed in a vacuum oven at a temperature of 50°C and pressure of -0.80 bar for an additional 3 days to ensure complete solvent removal.

4.3.2 Swelling response to solvent and fuel exposure

Conditioned O-rings, subject to fuel and solvent exposure, were investigated on methods, adapted from ASTM method D1414-94 [60] and ASTM method D471-06 [83]. Swelling was tracked using both gravimetric and volumetric techniques.

Gravimetric changes in the fuel wetted elastomer were recorded using the procedure described below:

- The initial mass of the O-ring was recorded after which the sample was placed in solution.
- At specified time periods the fuel wetted elastomer was removed from solution.
- The solvent was removed by blotting the sample with tissue on both sides.
- The interior of the sample was dried using cotton buds.
- The mass of the dry sample was recorded and sample was placed back into solution.

The change in mass of the fuel exposed elastomer samples was calculated using the following equation.

$$Q(\%) = 100\left(\frac{m_t - m_0}{m_0}\right)$$

where:

Q = mass swelling of sample
m_0 = initial mass of sample
m_t = mass at specified time period

Changes in volumetric swelling were observed and recorded after the sample was dried according to the procedure described above. To track the changes in volume, a digital optical microscope was used to capture images of the elastomer of interest at prescribed time periods. This method was adapted from that of Graham *et al.* [8] by Burnham [9]. The outer and inner area of the swollen elastomer O-ring was calculated using the average of 3 individual points as shown in Table 4.1.

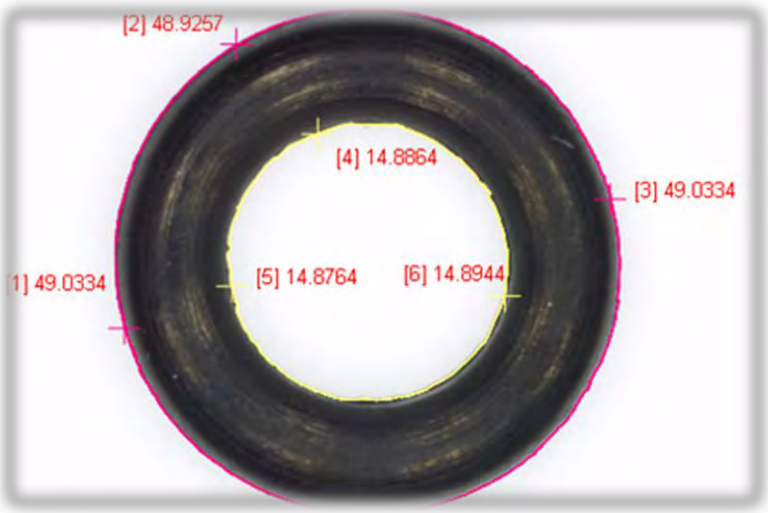

Figure 4.1: ShuttlePix software analysis of elastomer sample.

Software analysis of the images allowed the volume swelling change, R%, as follows:

$$R(\%) = 100\left(\left(\frac{A_t}{A_0}\right)^{3/2} - 1\right)$$

where:

A_0 = initial cross-sectional area of elastomer
A_f = cross-sectional area of elastomer at time t

4.3.3 Switch-load testing

Elastomer samples were immersed in a variety of synthetic fuel blends at 50°C. Each blend contained 3 individual elastomer samples. Samples were removed from the synthetic blend and placed into either petroleum or synthetic jet fuel depending on the test in progress. Sample switching occurred every 24 hours until the samples had reached a stable switching pattern. Stability was generally reached after 8 separate fuel switches.

4.3.4 Tensile testing

Tensile testing was performed on elastomer samples in-line according to the ASTM D1414-94 method [60]. A strain rate of 500mm/min was applied. Samples were measured in triplicate. Fuel wetted samples were lightly dried with tissue before being placed on the spool grips.

4.3.5 Thermogravimetric analysis

Samples of approximately 10µg were placed in 50 µl platinum coated pans and subjected to heating. Nitrogen gas (99.999 % purity) was used throughout the analysis using a flow rate of 25mℓ/min. A heating rate of 10°C/min was applied and the percentage mass loss was calculated from room temperature to 650°C. This procedure was used for all thermogravimetric analysis unless otherwise stated.

4.3.6 Differential scanning calorimetry (DSC)

Samples of approximately 2-3mg were placed into sealed *TA Tzero* aluminium pans subject to a modulated DSC running mode. Nitrogen gas (99.999 % purity) running at a flow rate of 40mℓ/min was used throughout this procedure. The temperature range selected was from -90-30°C with modulations of ±1°C every 60 seconds. The heating rate selected for this procedure was 3°C/min and the glass transition temperature is recorded at the midpoint temperature between the extrapolated onset and extrapolated end temperature (half-height).

4.3.7 Dynamic mechanical analysis (DMA)

DMA tests were conducted using a frequency of 1 Hz under tension mode. Samples were cut into pieces approximately 3-4cm in length and mounted onto the supplied tensile clamp. Once clamped, the sample was tightened with a torque wrench using a torque rating of 3-5 in/lb. Conditioned and fuel wetted elastomers were subjected to an initial heating ramp to 25°C at 5°C/min and left isothermal for 5 minutes. Samples were then cooled to a temperature of -90°C at a rate of 3°C/min using liquid nitrogen as the cooling agent. Storage modulus, loss modulus and tan δ were plotted as a function of temperature. The glass transition temperature is reported as the peak of the tan δ curve.

4.3.8 Compression set testing

Compression set testing was performed according to ASTM D395 [60]. Elastomer samples (in triplicate) were placed between two parallel plates and compressed by 25%. The compression jigs were tightened with stainless steel screws with a torque rating of 0.5 Nm.

Pre-conditioning of the compression set samples was performed prior to fuel exposure. Samples were compressed in the jigs and exposed to air at 80°C for ten days. After this time,

elastomer samples were re-measured, placed in the compression jigs and submerged in the relevant fuel blends. Compression set measurements were performed every 3 days until equilibrium values were reached. It is important to allow samples sufficient relaxation time before set measurements arewas taken. Samples were allowed to rest for 30 minutes prior to measurement and compression set was calculated using the method described on page 38.

Images of the compressed samples were captured using a Nikon ShuttlePix P-MFSC microscope. Dimension changes were analysed using accompanying software. All samples were measured in triplicate at different points along the sample surface, as indicated by Figure 4.2.

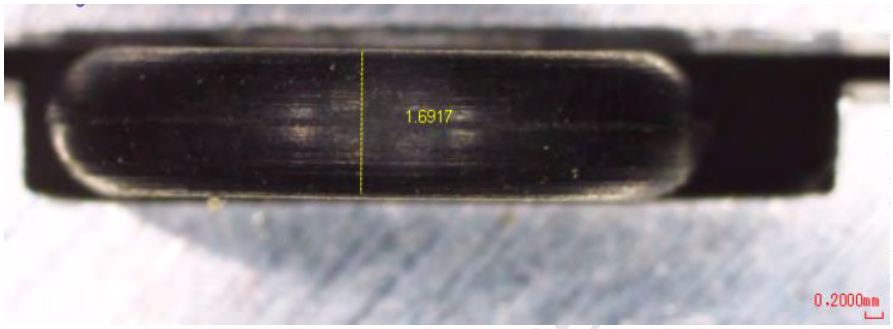

Figure 4.2: Standard thickness measurement of compression set sample

CHAPTER 5

5. Influence of the different chemical classes on the swelling of NBR O-rings

The swelling response of NBR was investigated at 50^{o}C. NBR O-rings were exposed to a wide range of chemical compounds to assess the impact of the chemical nature of a fuel on swelling. Equilibrium swelling data was recorded after 100 days of fuel exposure for all fuel wetted NBR elastomer samples.

5.1 Swelling investigations

NBR elastomer was exposed to a matrix of fuels, pure solvents and blends of SPK and pure solvents. Investigations were performed on a number of classes: (1) base fuels, (2) pure paraffins, (3) 15% cycloparaffin/SPK blends, (4) 8% monocyclic aromatic/SPK blends, (5) 8% bicyclic aromatic/SPK blends, (6) a variety of aromatic oxygenate/SPK blends and (7) 8% blends of other polar compounds with SPK.

SPK, produced via a CTL process, which contains no aromatic species, was used as the base fuel into which 8% (v/v) aromatics or 15% (v/v) cycloparaffins were blended. In contrast, Jet A-1 can contain up to 25% (v/v) aromatic content. The particular Jet A-1 used in this study contained 18% aromatics by volume.

n-Dodecane (b.p. 216.2^{o}C) is a linear paraffin which may be used as a surrogate for SPK. It lies within the boiling range of SPKs and is expected to show similar behaviour with SPK used in this investigation. However, because SPK is not a single component, *n*-decane (b.p. 174.1^{o}C) was included to assess the impact of paraffin molecular size on swelling. *n*-Decane is a lighter paraffin within the jet fuel boiling range.

Another class of important paraffins are naphthenes (cycloparaffins) whose swelling behaviour has not been studied in detail before. n-Decalin (b.p. 186.5^{o}C) was added to the group matrix as a cycloparaffin in the kerosene boiling range.

Table 5.1: Volumetric swelling of deplasticised NBR O-rings exposed to a variety of base fuels and paraffins. (The equilibrium swelling profile for each blend can be found in Appendix A)

Blend	δ_d	δ_p	δ_h	δ_{tot}	Molar volume (cm^3/mol)	Volumetric swell at equilibrium (%) at 50°C**
base fuel						
SPK	15.4	0	0	15.4	212.5	9.0 (0.3)
Jet A-1	16.5	0.1	0.3	16.5	193.7	18.5 (0.5)
n-paraffin						
n-decane	15.7	0.0	0.0	15.7	195.9	9.0 (0.3)
n-dodecane	16.0	0.0	0.0	16.0	228.6	8.7 (0.2)
cycloparaffin						
1,2-dimethyl cyclohexane	16.7	0.0	0.0	16.7	144.2	20.8 (0.4)
decalin	18.8	0.0	0.0	18.8	156.9	25.9 (0.3)

Values in parentheses are the standard deviation of the mean. N = 3

* reproduced from Burnham [9]

** Volume swell is measured to the original volume of the O-ring at room temperature

The significant difference between the swelling caused by SPK and by Jet A-1 is apparent. The data indicates that the swelling induced by SPK is similar to that caused by kerosene boiling range *n*-paraffins although the difference between the two *n*-paraffins tested was not statistically significant. It is apparent that cyclisation of the paraffin causes a significant increase in swelling. As a consequence the addition of cycloparaffins to SPK was explored in more detail. It should be noted that the swelling caused by both cycloparaffins was in excess of that caused by Jet A-1.

5.1.1 15% Cycloparaffin/SPK blends

No comprehensive study exists in the published literature on the effects of cycloparaffin compounds in blends with SPK on the swelling of elastomeric materials. This dissertation examines the swelling behaviour but also the effect of temperature on the elastomer swelling.

Currently, the specifications reported by Def Stan 91-91 [5] and ASTM D7566 [6] allow a maximum of 15% (v/v) cycloparaffin content in the SPK composition. As such, all blends investigated contained 15% (v/v) cycloparaffin content blended with SPK as the base fuel.

Importantly, these compounds are not restricted in the final composition of petroleum Jet A-1.

The data in Table 5.2 indicates clearly that the addition of cycloparaffins to SPK increased the swelling of NBR O-rings. It is clear, however, that as the molar volume increased (cyclohexane (C6) to iso-propyl cyclohexane (C9) to n-butyl cyclohexane (C10)) the extent of swelling decreased until it is no longer statistically distinguishable from SPK. Adding a second ring to make the C10 decalin increased swelling still further. Interestingly, despite the increase in molar volume, methylcyclohexane caused swelling above cyclohexane.

Table 5.2: Swelling of deplasticised NBR O-rings exposed to 15% (v/v) cycloparaffin/SPK blends

Blend component	**C#**	**δ_d**	**δ_p**	**δ_h**	**δ_{tot}**	**Molar volume (cm^3/mol)**	**Volumetric swell at equilibrium (%) at 50°C**
SPK		15.4	0	0	15.4	212.5	9.0 (0.3)
monocyclic							
cyclohexane	6	16.8	0.0	0.2	16.8	108.7	14.2 (0.2)
methylcyclohexane	7	16.0	0.0	1.0	16.0	128.3	14.9 (0.2)
iso-propylcyclohexane	9	16.3	0.0	0.5	16.3	157.4	9.7 (0.4)
n-butylcyclohexane	10	16.2	0.0	0.6	16.2	176.7	9.1 (0.3)
bicyclic							
decalin	10	18.8	0.0	0.0	18.8	156.9	10.3 (0.3)

Values in parentheses is the standard deviation of the mean. N = 3

C# = carbon number

5.1.2 Monoaromatic/SPK blends

Aromatic compounds are under increased scrutiny in terms of their concentration within the general fuel pool. Currently, all synthetic jet fuels require a minimum of 8% (v/v) aromatic content to be present in the final fuel product in accordance with Def Stan 91-91 and ASTM D7566 [5, 6]. All synthetic fuel blends investigated here contain 8% (v/v) aromatic content as a consequence. A wide range of aromatics were investigated to probe molecular size (carbon number) and the influence of solubility parameters.

Table 5.3: Swelling of deplasticised NBR O-rings exposed to 8% (v/v) monoaromatic/SPK blends

Blend	C#	δ_d	δ_p	δ_h	δ_{tot}	Molar volume (cm^3/mol)	Volumetric swell at equilibrium (%) at 50°C
benzene	6	18.4	0.0	2.0	18.5	89.1	16.8 (0.1)
toluene	7	18.0	1.4	2.0	18.2	106.3	14.7 (0.1)
o-xylene	8	17.8	1.0	3.1	18.1	120.6	14.7 (0.4)
m-xylene	8	17.7	0.5	3.1	18.0	123.5	14.2 (0.1)
p-xylene	8	17.6	0.0	3.1	17.9	123.3	14.1 (0.7)
ethylbenzene	8	17.8	0.6	1.4	17.9	122.5	14.2 (0.6)
styrene	8	18.6	1.0	4.1	19.1	114.6	17.6 (0.4)
1,3,5-trimethylbenzene	9	18.0	0.0	0.6	18.0	139.1	13.2 (0.7)
1,2,4-trimethylbenzene	9	18.0	1.0	1.0	18.1	137.2	14.5 (0.4)
n-propylbenzene	9	17.6	0.4	1.2	17.6	139.4	13.6 (0.4)
cumene	9	18.1	1.2	1.2	18.2	139.4	13.9 (0.4)
α-methylstyrene	9	18.5	2.4	2.4	18.8	129.9	16.8 (0.4)
n-butyl benzene	10	17.4	0.1	1.1	17.4	156.1	12.6 (0.4)
s-butyl benzene	10	17.9	0.8	1.1	18.0	155.5	12.9 (0.5)
p-cymene	10	17.6	1.2	1.2	17.7	156.6	11.8 (0.2)

Values in parentheses are standard deviations of the mean. N = 3

C# = carbon number

It should be noted that styrene and α-methylstyrene/ SPK blends form a white waxy deposit when heated which are probably polystyrene polymers. They have been included here to explore the impact of solubility parameters on swelling, rather than as realistic blend components for FSJF.

A general trend that can be seen is that as the carbon number increases and molecular volume increases (down the table), the extent of swelling within the series decreases. The influence of the individual solubility parameters is explored in more detail in section 5.3.

The data indicates that the most swell is observed for the two styrene compounds which have the highest overall solubility parameters.

5.1.3 Bicyclic aromatic/SPK blends

Bicyclic aromatics have high densities and often produce substantial swell of elastomer materials. Two types of bicyclic aromatics were investigated. The first, typified by naphthalene consists of two aromatic rings while in the second class, typified by tetralin, one of the rings is hydrogenated.

Table 5.4: Swelling of deplasticised NBR O-rings exposed to aromatic/SPK blends

Blend	C#	δ_d	δ_p	δ_h	δ_{tot}	Molar volume (cm^3/mol)	Volumetric swell at equilibrium (%) at 50°C
diaromatic							
indene	9	18.7	2.6	9.0	20.9	116.5	21.7 (0.5)
naphthalene*	10	19.2	2.0	5.9	20.2	111.5	12.8 (0.2)
methylnaphthalene	11	20.6	0.8	4.7	21.1	138.8	21.9 (0.3)
hydroaromatic							
indane	9	19.6	1.3	1.6	19.7	122.8	16.7 (0.2)
tetralin	10	19.6	2	2.9	19.9	136.3	14.4 (0.4)

Values in parentheses are standard deviations of the mean. N = 3

C# = carbon number

*Naphthalene was used in 2% (v/v) concentration due to solubility limits

Indene and methylnaphthalene both exhibit much higher swell than monoaromatics of similar carbon number. In the case of methylnaphthalene there are 2 aromatic rings while for indene the second ring is a cyclopentadiene ring. Naphthalene would be expected to produce swelling in the same region as the aforementioned compounds. However, naphthalene becomes insoluble in the SPK base fuel at concentrations greater than 3% (v/v). The data reported in Table 5.5 is for a 2% v/v solution. Replacing one of the rings by a cycloparaffinic ring (tetralin vs. naphthalene (swelling of 8% (v/v) in SPK estimated to be 22-24%) or indane vs indene causes the swelling to decrease. Nonetheless the extent of swell still exceeds that of the equivalent C_{10} (*p*-cymene) or C_9 (cumene) monoaromatics (*see* Table 5.2).

The value for a hypothetical 8% naphthalene/SPK blend was estimated by subtracting the swelling by 100% SPK from that of the 2% naphthalene/SPK blend. This difference was then multiplied by 4 and added back to the value for neat SPK to arrive at swelling that might be expected for a hypothetical 8% naphthalene/SPK blend.

5.1.4 Aromatic oxygenates and other polar compounds blended with SPK

Table 5.5: Swelling of deplasticised NBR O-rings exposed to a range of polar compound/SPK blends

Blend	δ_d	δ_p	δ_h	δ_{tot}	Molar volume (cm^3/mol)	Volumetric swell at equilibrium (%) at 50°C
aromatic alcohol						
benzyl alcohol (0.5%)	18.4	6.3	13.7	23.8	103.6	15.7 (0.4)
aromatic ether						
anisole (8%)	17.8	4.1	6.7	19.5	108.7	19.6 (0.3)
dibenzyl ether (8%)	19.6	3.4	5.2	20.6	190.1	26.6 (0.4)
furan						
furan (8%)	17.8	1.8	5.3	18.7	71.6	14.8 (0.4)
tetrahydrofuran (8%)	16.8	5.7	8.0	19.5	81.1	15.9 (1.1)
pyridine						
pyridine (8%)	19.0	8.8	5.9	21.8	80.6	27.1 (0.7)
cycloparaffinic alcohols						
cyclohexanol (15%)	17.4	4.1	13.5	22.4	104.1	26.2 (0.3)
***n*-alcohols**						
n-hexanol (15%)	15.9	5.8	12.5	21.0	125.6	19.8 (0.4)

Values in parentheses are standard deviations of the mean. N = 3

Burnham [9] suggested that aromatic oxygenates would be ideal blend components which would allow adequate swelling to be achieved at levels below the 8% aromatic limit. While benzyl alcohol and phenols had previously been demonstrated to cause significant swell, Burnham [9] demonstrated the usefulness of aryl and benzyl ethers. These compounds were reinvestigated as well as a number of other oxygenates. Cyclohexanol was included as a member of the class of cycloparaffinic oxygenates while n-hexanol was included to assess the impact of cyclisation on the swelling caused by polar compounds. Pyridine was included as a compound with high solubility parameters. Furan and its hydrogenated relative were added for similar reasons.

The data in Table 5.5 reveals that the incorporation of a heteroatom (O or N) increases the swelling of NBR significantly. This is especially the case if heteroatom is associated with an

aromatic molecule (benzyl alcohol, anisole, dibenzyl ether and pyridine). The cyclisation of n-hexanol to produce cyclohexanol increases swelling as was the case with the cyclisation of paraffins.

5.2 Switch-loading of NBR elastomers

The effect of switching elastomer samples from one fuel type to another was investigated. In particular, the swelling response of fuel changing was monitored. Elastomer samples were exposed to three different fuel blends as listed in Table 5.6. All blending components were added to achieve a solution of 8% (v/v) in SPK. Samples were switched between these blends and neat fuels as well as a 50:50 SPK:Jet A-1 blend. Exchange from one media to the next occurred every 24 hours until stability of the elastomer swelling was achieved.

Table 5.6: Switch-loading conditions

8% blend with SPK	Fuel Component	Switch-Time	Temperature
Toluene	SPK		
Butyl Benzene	Jet A-1	24 hrs	50°C
Tetralin	SPK:Jet A-1*		

*The ratio of SPK-to-Jet A-1 is 50:50

In the figures in the following sections, the first reading and all subsequent odd numbered readings indicate swelling in the neat fuels. Even numbered readings are for elastomer swelling for exposure to blends of 8% (v/v) aromatics in SPK.

5.2.1 Switch from blend to Jet A-1

Figure 5.1 illustrates the swelling behaviour of switching NBR elastomer samples from the pure fuel component, Jet A-1, to blends containing butylbenzene, toluene and tetralin. Curves for Jet A-1 and SPK have been added for comparison. Within 24 hours after switching back to Jet A-1, swelling re-achieves, and in some cases exceeds the value observed for neat Jet A-1. It is believed that aromatic compounds – from blend exposure - may still be present within the polymer matrix upon re-exposure to Jet A-1. Ultimately, permeation of Jet A-1 coupled with residual aromatic content would result in greater observed volumetric swell than would be the case for exposure to pure Jet A-1. The blend values lie between the SPK and Jet A-1 values.

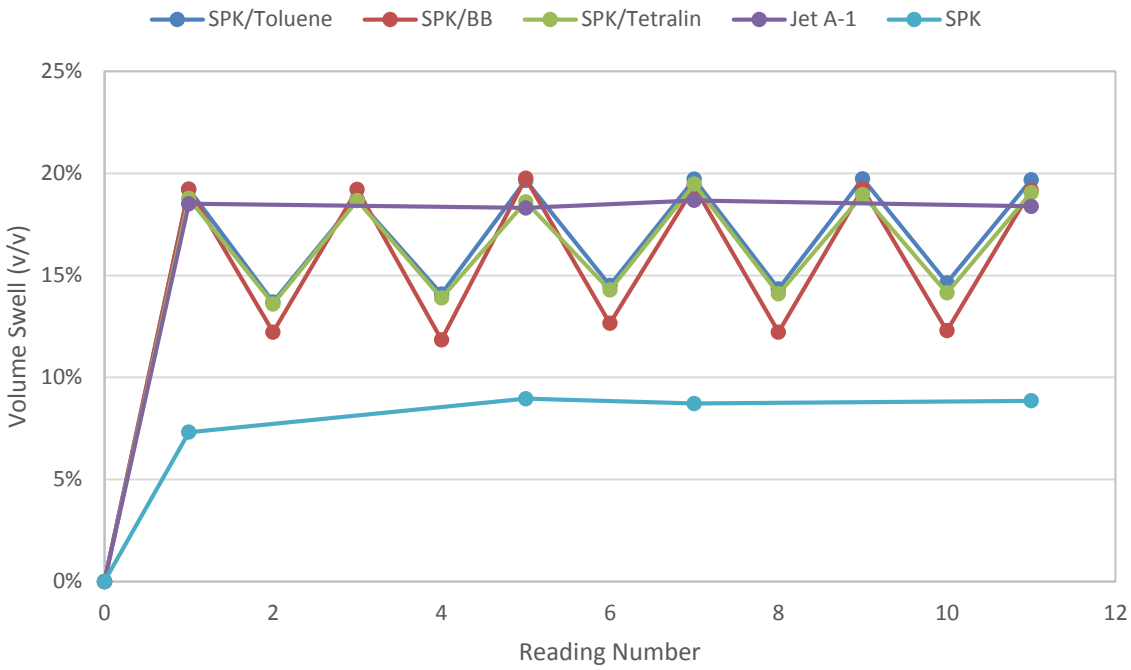

Figure 5.1: Swelling behaviour of NBR O-rings switched between 8% aromatic/SPK blends and Jet A-1. BB = n-butyl benzene

5.2.2 Switch from blends to SPK

The switch-loading performance of NBR elastomers exposed to aromatic/SPK blends and alternately neat SPK is described by Figure 5.2

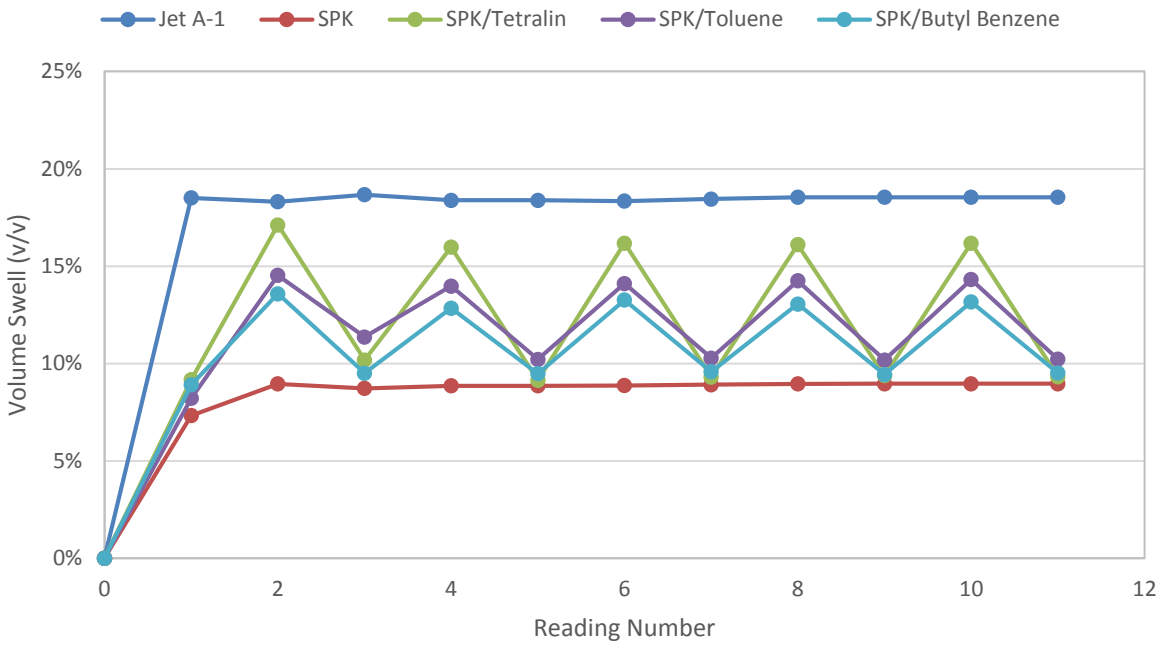

Figure 5.2: Swelling behaviour of NBR O-rings switched between 8% aromatic/SPK blends and neat SPK

Importantly, the effect of switch-loading does not result in the swelling dipping below the response to pure SPK and after the first few readings, perfect swelling oscillation was achieved. Additionally, blends containing tetralin and toluene showed little effect from pure SPK exposure, equilibrating to a similar swelling response as static exposure. The somewhat erratic initial swelling behaviour of tetralin can be attributed to its slower permeation kinetics. A full profile of a SPK/tetralin blend interacting with NBR elastomer can be found in Appendix A.

5.2.3 Switch from blends to 50:50 mixture of SPK and Jet A-1

Elastomers switched between fuel blends and a 50:50 mixture of SPK and Jet A-1 showed little variation in the swelling response. The response of the elastomer samples to switching is highlighted in Figure 5.3. Samples switched between toluene and the fuel mixture showed little change in the swelling response. Once again, perfect volumetric oscillation was observed after the initial readings and the shape of the swelling profile is less dramatic compared to the profiles viewed previously. Additionally, the difference in equilibrium swelling response to the response achieved with static exposure to the 8% (v/v) toluene blend was statistically insignificant. Blends containing tetralin showed somewhat erratic swelling behaviour. The reasons for this are discussed in section 5.1.3.

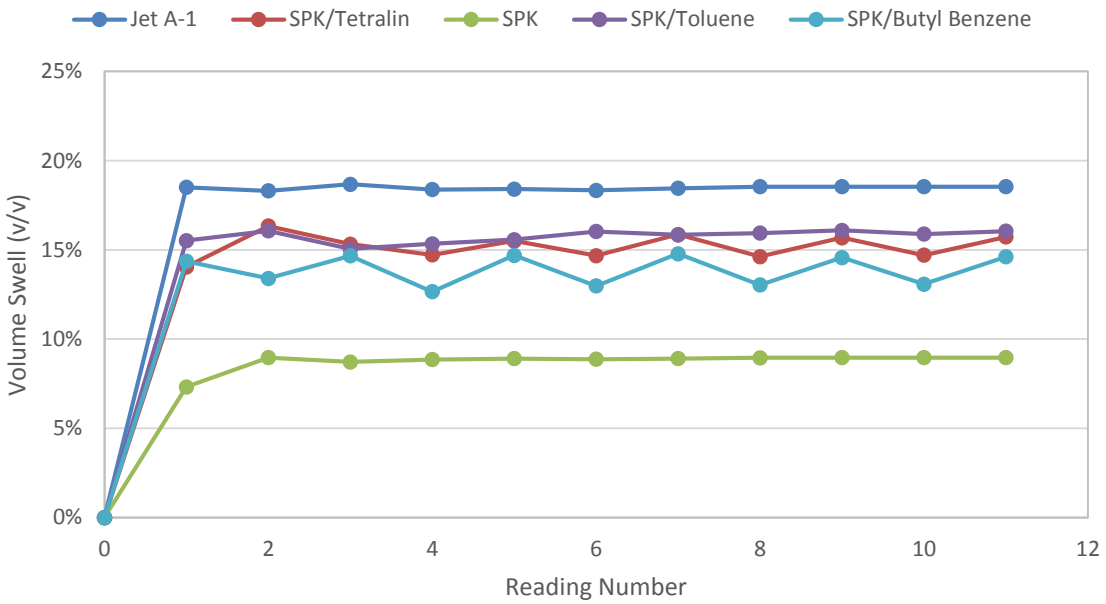

Figure 5.3: Swelling behaviour of NBR O-rings switched between 8% aromatic/SPK blends and a 50:50 mixture of SPK and Jet A-1

5.3 Discussion

5.3.1 NBR O-rings exposed to base fuels and paraffins

The 2-fold increase in swelling caused by Jet A-1 when compared to that caused by SPK (*see* Table 5.1) can be attributed to the presence of 18% aromatics in the Jet A-1 and none in the SPK. It should be noted that, although SPK swelled the NBR O-rings used, the O-rings used were deplasticised. Deplasticisation caused a net shrinkage of 14% in volume. Consequently a net shrinkage would be expected where new plasticised O-rings were used.

The similar swelling obtained for the kerosene boiling range *n*-paraffins and SPK indicate that these species could be used as seal swell surrogates for SPK. Burnham [9] observed that the swelling by *n*-paraffins decreased as the molecular weight (molar volume) of the *n*-paraffin increased although the difference in swell for each extra carbon added decreased as the paraffins became longer. Burnham, in fact, observed a linear correlation between swelling and the reciprocal of density (rather than molar volume) for *n*-paraffins.

The replacement of *n*-paraffins by cycloparaffins increased swell significantly to levels that exceeded neat Jet A-1. This increase in swell can be ascribed to both an increase in the dispersion solubility parameter as well as a reduction in molar volume. Hansen [51] ascribes a group contribution of zero to δ_h for cyclisation yet some cycloparaffins such as methylcyclohexane do have positive δ_h reported. The contribution of δ_h is arguably the most

difficult to assign as it tends to be a left-over term that accounts for cohesive energy density that cannot be accounted for by dispersion and polarity. It is possible that δ_h plays some role but because of large uncertainties in these values no conclusion can be drawn as to the importance of δ_h for the swelling of NBR by cycloparaffins. Further cyclisation (compare the bicyclic decalin to monocyclic 1,2-dimethylcyclohexane) increases swelling even further as a result of further cyclisation increasing δ_d. This is despite the slight increase in molar volume of decalin compared to 1,2-dimethylcyclohexane.

5.3.2 NBR O-rings exposed to 15% cycloparaffin/SPK blends

The increase in solubility parameter, δ_d, may be used to explain the increase in swelling observed when cycloparaffins were added to SPK in addition to a decrease in molar volume. However, for kerosene boiling range cycloparaffins: C9 iso-propyl cyclohexane (b.p. 154.5 ^oC) and C10 n-butyl cyclohexane (b.p. 181^oC) the increase is in fact small. Further cyclisation to form a bicyclic aromatic such as C10 decalin (b.p. 186^oC) is required to increase swelling.

Increased swelling was observed for methylcyclohexane compared to cyclohexane despite a larger molar volume. One may be tempted to ascribe this to the positive δ_h for methylcyclohexane. However, there is uncertainty as to the accuracy of this value and the capacity of other cycloparaffins to form electron exchange interactions. Consequently caution must be taken in assigning a reason for the observed difference

5.3.3 NBR O-rings exposed to 8% aromatic/SPK blends

As with other classes of compounds a molecular size effect was again noted. Increasing molecular weight which is associated with greater carbon numbers and larger molar volumes led to decreased swell within the monoaromatics and in the hydroaromatics (indane and tetralin). The dependence of swelling on carbon number is illustrated in Figure 5.4.

It can be seen that increasing the number of rings, as with cycloparaffins, increases the extent of swell. This increase is driven not only by a reduction of molar volume and an increase in δ_d for bicyclic compounds but also a significant increase in δ_p and especially δ_h for these compounds. The increase in δ_h and δ_p also contributes to the increased swell of the styrenes over the equivalent monoaromatics. Diaromatics swell more than hydrocyclic aromatics because the contribution of the second aromatic ring is more significant than the second aliphatic ring. Figure 5.4 also includes an estimate for the swelling caused by naphthalene were an 8% (v/v) soluble. This is estimated by multiplying the swelling above that of neat SPK (for 2% naphthalene in SPK) by 4 and then adding this product back to that of neat SPK. The

influence of the different solubility parameters can be seen more clearly with the pairwise comparisons in Figure 5.4.

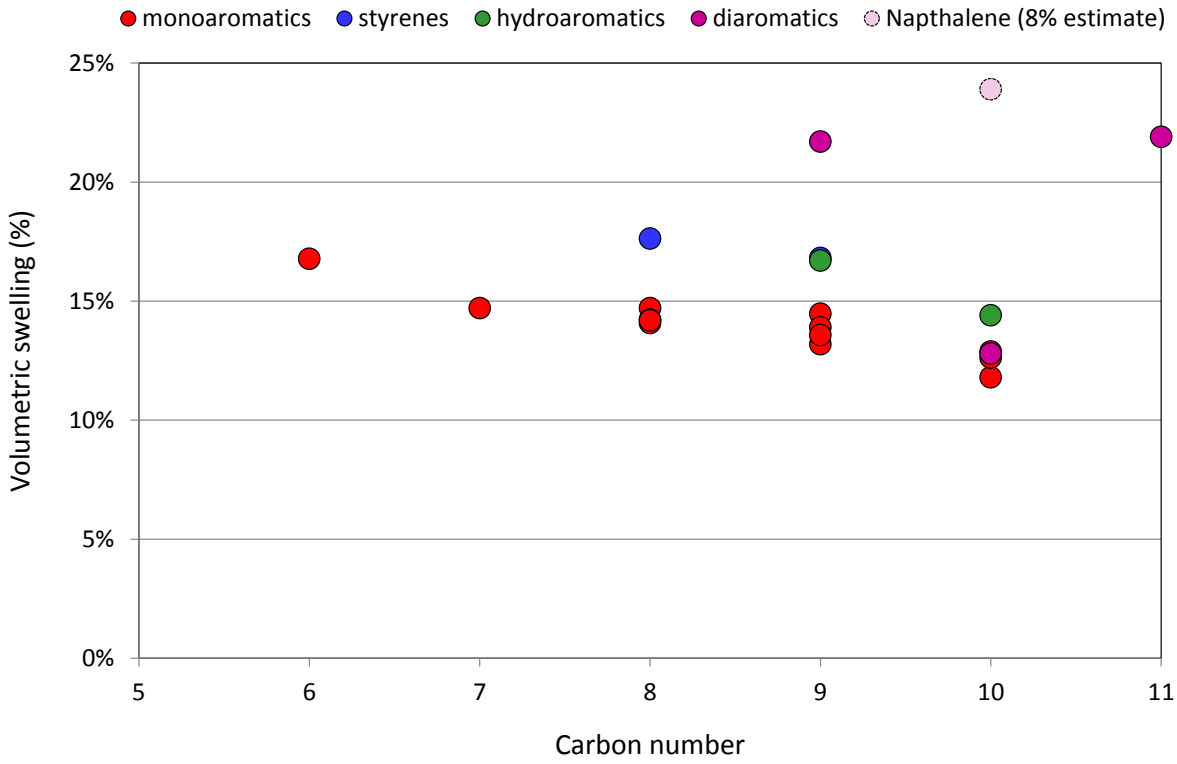

Figure 5.4: Dependence of the swelling caused by 8% (v/v) aromatic/SPK blends on carbon number and aromatic class

The influence of the polar parameter can be seen by considering the xylene molecules and the C9 and C10 monoaromatic isomers. Comparison of α-methylstyrene with o-xylene also reveals the importance of δ_p. This is in spite of α-methylstyrene having a lower δ_h and larger molar volume. Increasing branching in the side-chain increases δ_p which has the effect of increasing swelling.

The one exception is p-cymene. It is suspected that the value measured in this study may be too low. In a repeat set of experiments swelling was measured as 12.9% for *p*-cymene. An old batch of O-rings was used, however. Consequently this result is not reported in Table 5.3.

Table 5.7: Pairwise comparisons of swelling of deplasticised NBR O-rings by 8% aromatic/SPK blends illustrating the influence of δ_p

Blend	δ_d	δ_p	δ_h	δ_{tot}	Molar volume (cm^3/mol)	Volumetric swell at equilibrium (%) at 50°C
o-xylene	17.8	1.0	3.1	18.1	120.6	14.7
m-xylene	17.7	0.5	3.1	18.0	123.5	14.2
p-xylene	17.6	0.0	3.1	17.9	123.3	14.1
α-methylstyrene	18.5	2.4	2.4	18.8	129.9	16.8
n-propylbenzene	17.6	0.4	1.2	17.6	139.4	13.6
cumene	18.1	1.2	1.2	18.2	139.4	13.9
n-butyl benzene	17.4	0.1	1.1	17.4	156.1	12.6
s-butyl benzene	17.9	0.8	1.1	18.0	155.5	12.9
p-cymene	17.6	1.2	1.2	17.7	156.6	11.8

Table 5.8: Pairwise comparisons of swelling of deplasticised NBR O-rings by 8% aromatic/SPK blends illustrating the influence of δ_h

Blend	δ_d	δ_p	δ_h	δ_{tot}	Molar volume (cm^3/mol)	Volumetric swell at equilibrium (%) at 50°C
toluene	18.0	1.4	2.0	18.2	106.3	14.7
o-xylene	17.8	1.0	3.1	18.1	120.6	14.7
α-methylstyrene	18.5	2.4	2.4	18.8	129.9	16.8
indene	18.7	2.6	9.0	20.9	116.5	21.7
1,3,5-trimethylbenzene	18.0	0.0	0.6	18.0	139.1	13.2
1,2,4-trimethylbenzene	18.0	1.0	1.0	18.1	137.2	14.5
indene	18.7	2.6	9.0	20.9	116.5	21.7 (0.5)
indane	19.6	1.3	1.6	19.7	122.8	16.7 (0.2)

The pairs of o-xylene and toluene, and α-methylstyrene and indene illustrate the influence of δ_h on elastomer swelling. Despite the smaller molar volume of toluene, no significant

difference with o-xylene was observed. o-Xylene, however, has a higher hydrogen bonding parameter which compensates for the larger molar volume. The pair of trimethylbenzenes and the pair of indane and indene illustrate a combined δ_p and δ_h effect. Increases in both terms drives an increase in swelling. The higher increase in swelling per percentage aromatic caused by naphthalene compared to tetralin can also be ascribed to the increased δ_p and δ_h parameters.

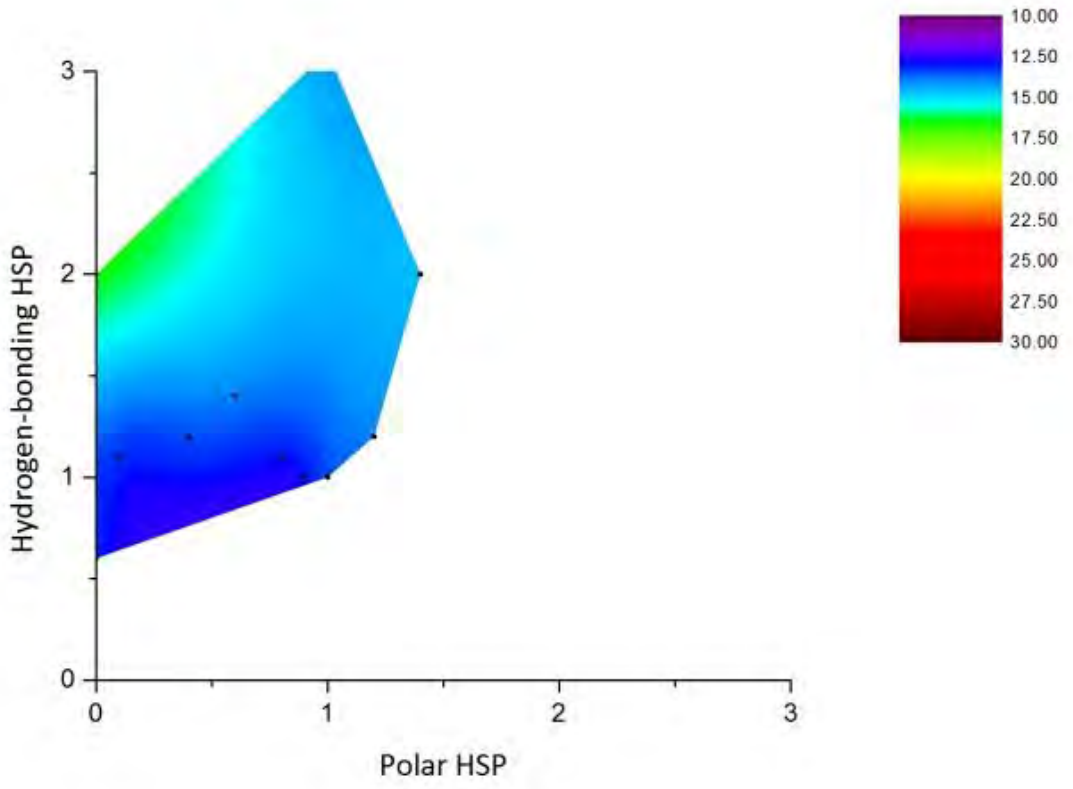

Figure 5.5: The influence of the polar and hydrogen-bonding Hansen solubility parameters on swelling of NBR by 8% (v/v) blends with SPK of monoaromatics only. Black dots indicate data points

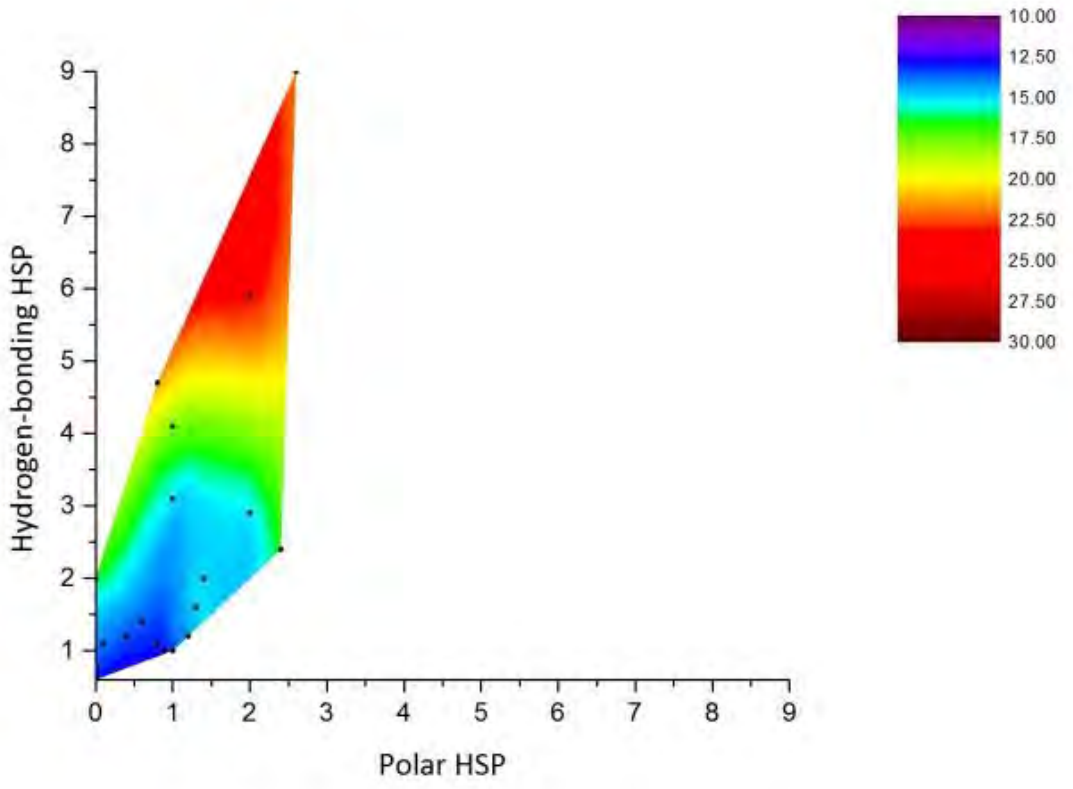

Figure 5.6: The influence of the polar and hydrogen-bonding Hansen solubility parameters on swelling of NBR by 8% (v/v) blends with SPK of all aromatic hydrocarbons. Black dots indicate data points.

Figure 5.5 and 5.6illustrate the dependence of percentage volumetric swelling on the polar and hydrogen-bonding HSPs. It can be seen that as both parameters increase swelling increases. The rate of increase is greater for the hydrogen-bonding HSP than the polar HSP as can be seen in Figure 5.5 for the monoaromatics. Note that indene (δ_p = 2.6) is the aromatic hydrocarbon with the highest polar HSP.

In order to better understand the drivers for swelling, a correlation analysis was performed which investigated the influence of carbon number, molecular size, the inverse of molar volume and solubility parameters.

The analysis was performed for a number of extended data sets: starting with the monoaromatics and progressively adding styrenes, hydroaromatics and bioaromatics to the data set. This is presented in Table 5.9. In Table 5.9 and Table 5.10, shading indicates the level at which the correlation co-efficient is significant: 99.9% (red), 99% (blue), 98% (green), 95% (orange) and 90% (pink).

Table 5.9: Correlation co-efficients of various parameters with swelling

Parameter	Only monoaromatics	Plus styrenes	Plus hydroaromatics	Plus di-aromatics	Plus naphthalene estimate
carbon number	-0.916	-0.651	-0.546	0.035	0.161
molar mass	-0.918	-0.682	-0.589	-0.056	0.053
density	0.481	0.785	0.534	0.816	0.852
(molar volume)$^{-1}$	0.922	0.725	0.697	0.363	0.292
δ_d	0.689	0.846	0.614	0.728	0.716
δ_p	-0.013	0.354	0.347	0.433	0.510
δ_h	0.478	0.669	0.577	0.811	0.830
δ_{tot}	0.817	0.915	0.679	0.890	0.872
N	13	15	17	19	20

A poor correlation was observed between swelling and the polarity solubility parameter when benzene was included. Benzene causes significant swelling but has $\delta_p = 0$. It was decided to repeat the analysis with benzene excluded. These results are presented in Table 5.10.

Table 5.10: Correlation co-efficients of various parameters with swelling (with benzene removed)

Parameter	Only monoaromatics	Plus styrenes	Plus hydroaromatics	Plus di-aromatics	Plus naphthalene estimate
carbon number	-0.854	-0.555	-0.442	0.136	0.249
molar mass	-0.854	-0.598	-0.499	0.027	0.122
Density	0.657	0.905	0.625	0.850	0.876
(molar volume)$^{-1}$	0.839	0.682	0.676	0.384	0.337
δ_d	0.439	0.821	0.619	0.731	0.717
δ_p	0.502	0.610	0.561	0.515	0.574
δ_h	0.571	0.721	0.612	0.827	0.840
δ_{tot}	0.693	0.917	0.699	0.900	0.877
N	12	14	16	18	19

The analysis reveals that within the monoaromatics, with aliphatic substituents, it is in fact the inverse of molar volume which correlates strongly with carbon number that is the best predictor. Nonetheless increasing solubility parameters of all types lead to increasing swelling. Adding aromatics of other classes causes the dependence on molar volume to become weaker as the solubility parameters become more important. The analysis reveals that with the exception of when styrenes are included the highest correlation is found with the hydrogen-bonding solubility parameter. Nonetheless there is a strong dependence on the dispersion solubility parameter too. This is to be expected since this parameter increases as more aromatic rings are added but it decreases as the side chains become longer. This can be rationalised by considering that as the side chains become longer the fraction of carbons in the molecule which are aromatic reduces and the molecule becomes more aliphatic.

Interestingly the total solubility parameter is a better predictor of swelling for the overall set of compounds. This is likely the result of this parameter smearing out uncertainties in the individual parameters. It should be remembered that δ_h is determined as a residual.

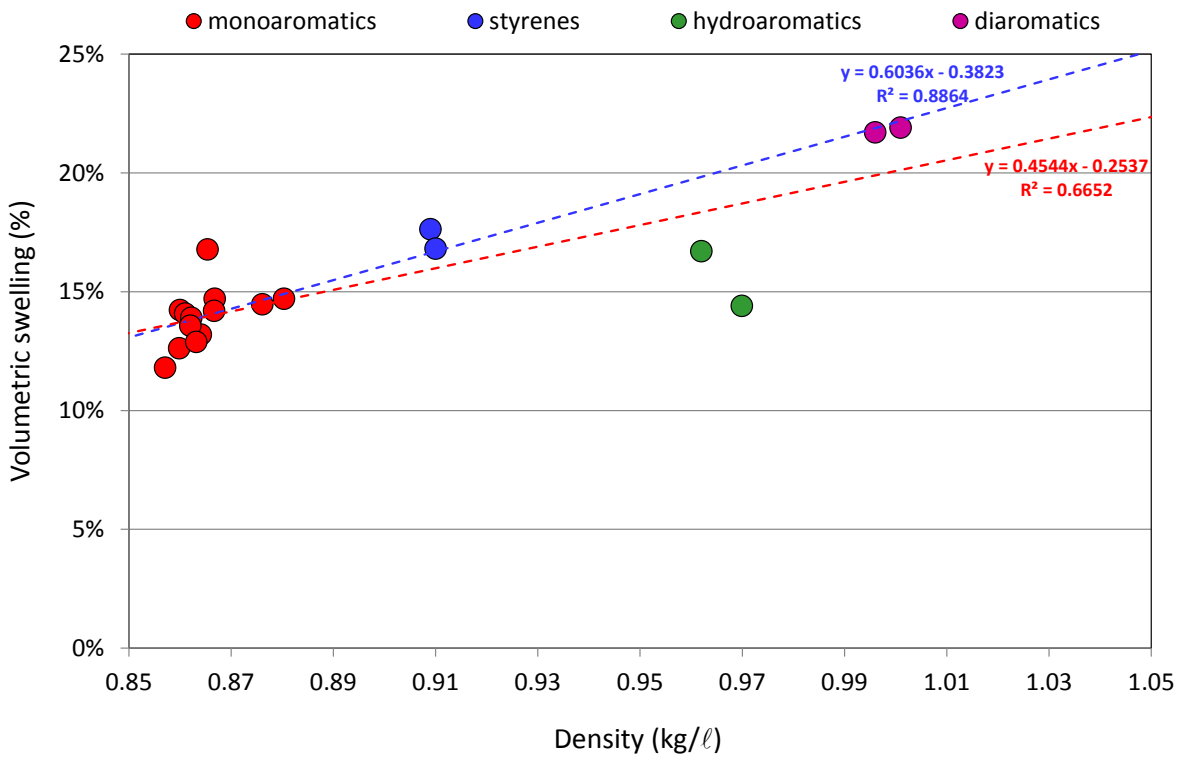

Figure 5.7: Correlation between volumetric swelling and density by aromatic class

Another interesting observation is that as density increases swelling increases. Denser molecules have smaller molar volumes but density in itself is driven by the cohesiveness of

the compound. A highly cohesive compound will have a higher cohesive energy density causing high solubility parameters. Density is thus a composite of these two sets of parameters which are known to strongly influence swelling. This is reminiscent of the correlation observed between density and swelling by Burnham [9] for linear paraffins.

Another way to present the dependence of swelling on Hansen solubility parameters is to use a Teas plot. A Teas plot is a ternary plot where the axes are the dispersion, polar and hydrogen-bonding forces. A force is defined as

$$f_i = \frac{\delta_i}{\delta_d + \delta_p + \delta_h}$$

where δ_I is the particular HSP for the force being defined, *i.e.* the dispersion HSP is used to determine the dispersion force. One limitation of the Teas approach is that it is possible to have two very different solvents have the same Teas forces, *e.g.* the forces will be the same for two solvents whose HSPs are (16.0; 1.0; 1.0) and (24.0, 1.5, 1.5). Nonetheless the approach is usually instructive.

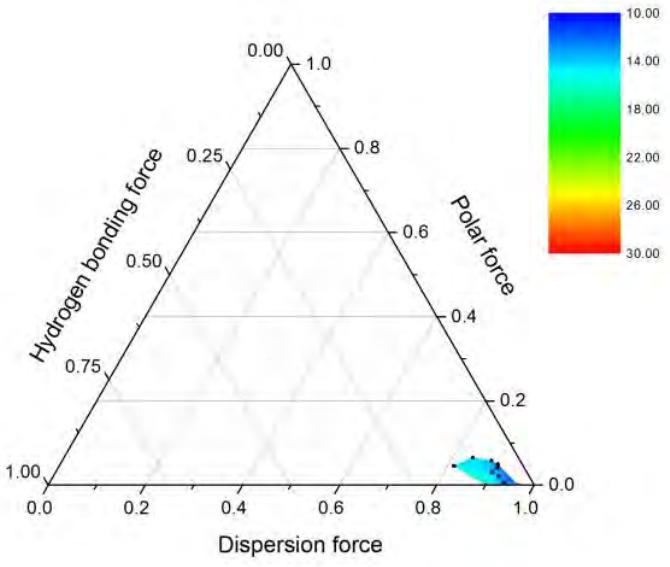

Figure 5.8: Teas plot illustrating the influence of the different Hansen solubility parameters on the swelling of NBR by 8% (v/v) blends with SPK of monoaromatics only. Black dots indicate data points.

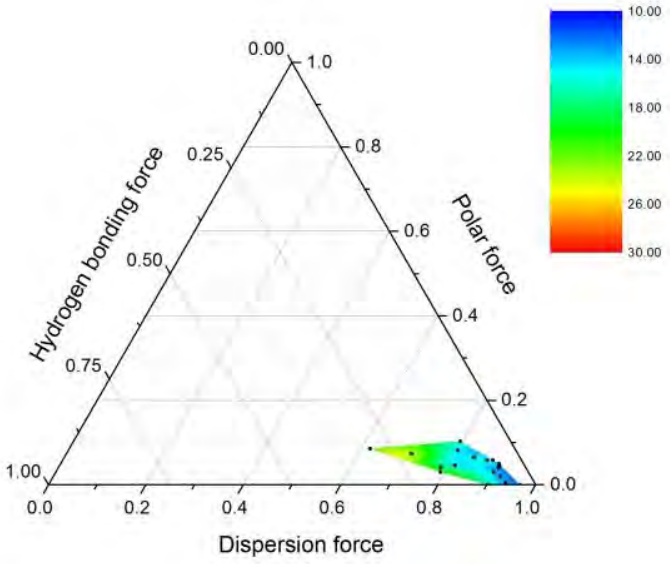

Figure 5.9: Teas plot illustrating the influence of the different Hansen solubility parameters on the swelling of NBR by 8% (v/v) blends with SPK of all aromatic hydrocarbons. Black dots indicate data points

What the Teas plots show is that within the 8% (v/v) blends with SPK, increasing the hydrogen bonding force, *i.e.* the size of δ_h relative to the other HSPs and increasing f_p increases swelling. It would appear though that increasing f_h is more effective than increasing f_p. Similar conclusions were drawn in from a report published by the Boeing Company [73], where the authors compared the swelling response of various elastomer materials exposed to blends aimed at highlighting polarity and hydrogen bonding factors. In almost all cases, the authors noted that compounds with large hydrogen bonding forces imparted greater swell on the elastomer materials than was observed for the compounds with large polar forces [73].

5.3.4 NBR O-rings exposed to polar compound/SPK blends

The addition of a polar species to SPK increased the swelling of NBR significantly. This can be ascribed to the significantly higher δ_p and δ_h of these compounds. Anisole has a similar molar volume and δ_d to toluene but because of significantly larger δ_p and δ_h the swelling observed is approximately 5% higher. The contribution that can be ascribed to the component added to SPK is twice as large when anisole is added than when toluene is added. Despite being a larger molecule, the addition of dibenzyl ether causes even more swell. Although dibenzyl ether has lower δ_p and δ_h than anisole, it has two aromatic rings. These have the effect of increasing δ_d

which is consistent with the observation in section 5.3.3 that the dispersion solubility parameter is also a good predictor of the swelling of NBR.

Cyclisation of n-hexanol to cyclohexanol increased the extent of swell. This is likely the result of the combination of a smaller molar volume and a higher dispersion solubility parameter. The same observations were made for the cyclisation of n-paraffins. The high degree of swell observed suggest that higher alcohols could also be used to increase the swelling of SPK blends. It is estimated that a 3-4% blend of cycloparaffinic alcohol would cause similar swell to a SPK with 8% aromatics added.

Usually hydrogenation of a cyclic structure decreases swell. One exception is the hydrogenation of furan to form tetrahydrofuran (THF). This is because in the case of aromatic compounds, hydrogenation reduces δ_h significantly. However, in the case of THF a large dipole is introduced which is much smaller in furan. This raises the likelihood of polar interactions. δ_p is much larger for THF than furan causing more swelling in spite of a large molar volume and smaller δ_d.

The influence of δ_h and δ_p can be seen more clearly when Figure 5.5 and Figure 5.6 is re-plotted but with 8% (v/v) blends with SPK of the polar species: anisole, dibenzyl ether, furan, tetrahydrofuran and pyridine. This is illustrated in Figure 5.10. It is clear that increasing both δ_h and δp will increase swelling. The addition of oxygen allows higher δ_ps to be explored than can be found with hydrocarbon aromatics alone. Interestingly there is a zone at high δ_h and d_p where THF can be found where the overall swelling appears to decrease again. It must, however, be borne in mind that swelling is maximised when the sum of the square of the differences in HSPs is minimised. Increasing d_p and d_h too far causes this sum to increase again and hence swelling is reduced.

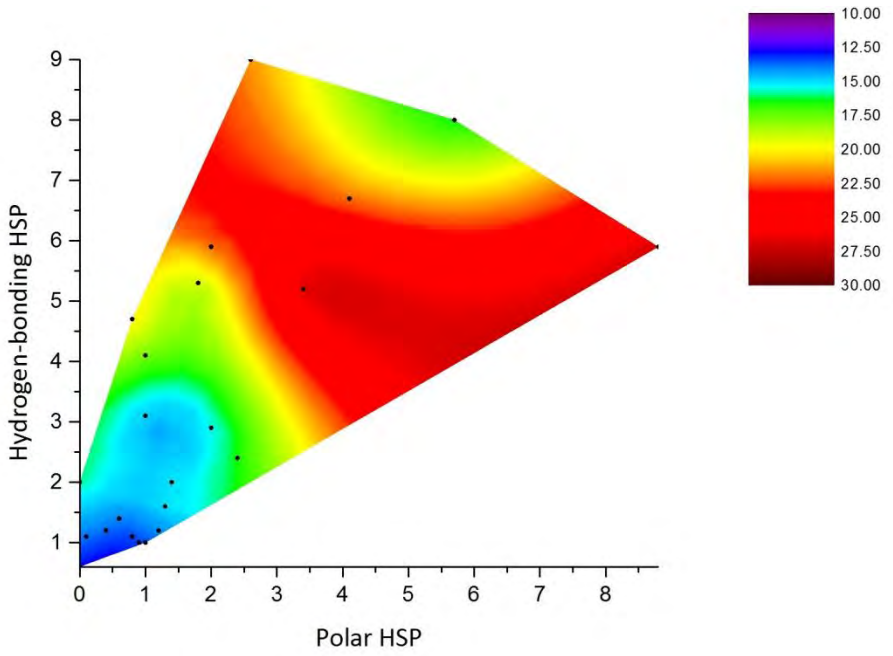

Figure 5.10: The influence of the polar and hydrogen-bonding Hansen solubility parameters on swelling of NBR by 8% (v/v) blends of monoaromatics, bicyclic aromatics, and cyclic polar species (including aromatic oxygenates) with SPK. Black dots indicate data points

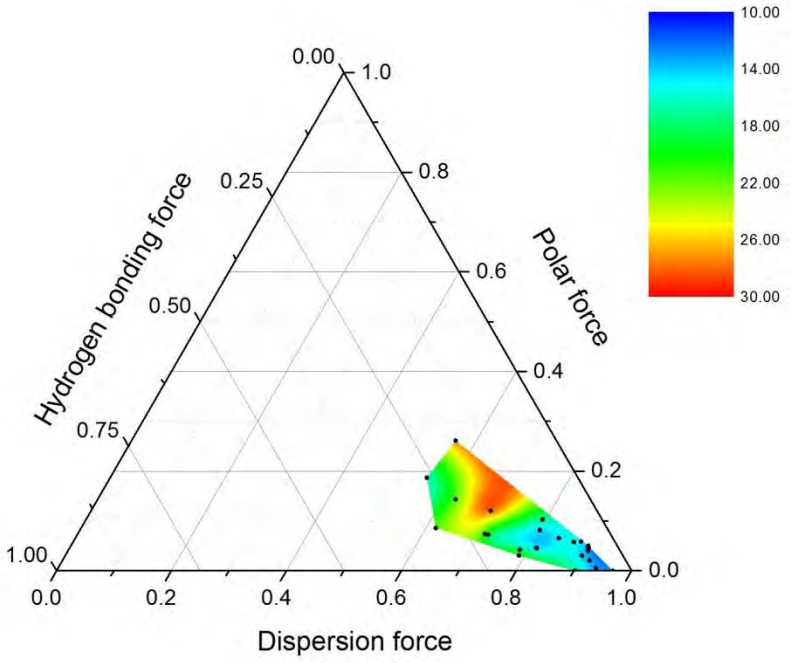

Figure 5.11: Teas plot illustrating the influence of the different Hansen solubility parameters on the swelling of NBR by 8% (v/v) blends of monoaromatics, bicyclic aromatics, and cyclic polar species (including aromatic oxygenates) with SPK. Black dots indicate data points

The Teas plot in Figure 5.11 illustrates this further. If the size of f_d becomes too small, *i.e.* the relative size of δ_d is too small, then swelling starts to fall again. Looking at the figure one can

see that as one progresses further away from the bottom right apex, swelling passes through a maximum and then begins to fall again. The bottom right apex is the point at which $f_d = 1$ and $f_p = f_h = 0$.

5.3.5 Switch-loading

The final section of this chapter examines the switch-loading performance of NBR elastomer switched between three different fuel combinations.

Previously, switch-loading in the extreme case i.e. switching elastomers from exposure to Jet A-1 to SPK was performed by Burnham [9]. The resulting swelling response showed an 8% gravimetric decrease when fuel was switched from Jet A-1 to SPK. This suggests that switching from conventional Jet A-1 to neat SPK may produce unsatisfactory behaviour likely leading to decreased sealing performance [9, 20, 56].

This report investigated the switch-loading performance of NBR elastomers switched from three different fuel blends to pure Jet A-1, pure SPK and a 50:50 blend of SPK and Jet A-1. In all three cases, the swelling response did not drop below swelling values for exposure to pure SPK. However, in the case of switching from blend to pure SPK, a large volumetric decrease in the swelling response was observed. This type of behaviour is undesirable for use in service. The rapid decrease in swelling when the elastomer sample is switched from the blend to pure SPK indicates that SPK may exhibit preferential uptake, however, additional testing is required to confirm this hypothesis. The best switch-loading performance was observed when switching between fuel blends and a 50:50 blend of SPK and Jet A-1. Little oscillation in the swelling response was observed under this condition, likely due to the presence of the aromatic-rich Jet A-1. This type of response is preferred and will yield little change in the sealing performance of the elastomer material.

5.4 Conclusions

Cycloparaffins have been demonstrated to increase the swelling of NBR. Although current specifications limit the content of cycloparaffins in FSJF to below 15% (v/v), were this specification to be relaxed, it is suggested that a FSJF with high cycloparaffin content could for see swelling greater than an 8% aromatic/SPK blend and even equivalent to that of Jet A-1. The swelling caused by a 50% decalin/SPK blend is greater than any of the 8% aromatic/SPK blends.

When blending cycloparaffins at a level of 15% with SPK, kerosene boiling range cycloparaffins with alkyl chains displayed a slight increase in swelling. This would suggest that an SPK that contains a higher degree of cycloparaffins would swell more [73]. However, the addition of 15% cycloparaffins is not nearly as effective as 8% aromatics unless light cycloparaffins are added. The flash point specification for jet fuel would, however, restrict the quantity of light cycloparaffins that could be blended. Bicyclic cycloparaffins, as exemplified by decalin, however, swell more and are capable of achieving swelling on a par with some 8% C11 monoaromatic blends with SPK. This would suggest that the addition of such bicyclic cycloparaffins could potentially allow the production of an FSJF in which adequate swelling is achieved with less than 8% aromatics. It is also suggested that the addition of higher alcohols can also reduce the requirement for aromatics. Here too, cyclisation is likely to result in higher degrees of swelling of NBR where such compounds are blended with SPK.

Solubility parameters were demonstrated to be effective predictors of swelling. For aromatic hydrocarbons, the most predictive of the Hansen solubility parameters was the hydrogen-bonding HSP, followed by the dispersion HSP and then the polar HSP. Correlation analysis showed that the overall solubility parameter turned out to be the most predictive, probably because uncertainties in the individual HSPs were smoothed out.

Within the class of aromatic compounds, decreasing molecular size and increasing all solubility parameters have been shown to correlate with increased swelling. These are associated with high density and polyaromaticity. This analysis would suggest that the aromatic species which when blended with SPK to maximise swelling of NBR should be as small (as low molecular weight) as possible with as high a degree of ring structures as possible. FSJF, however, is constrained by flash point specifications and smoke point considerations. These imply that light aromatics such as benzene and toluene and heavy polyaromatics would not be ideal. Combining this with the analysis here, would suggest that the most ideal aromatics would be hydrocyclic aromatics such as indane and tetralin, and there substituted relatives. Furthermore density appears to be a very useful predictor for swelling of NBR elastomers.

CHAPTER 6

6. Effect of temperature on the swelling of fuel-wetted elastomers

The swelling response of NBR and Viton elastomers was investigated as a function of temperature. Elastomer swelling is dependent on both kinetic and thermodynamic parameters and the extent to which each blend- reviewed previously- is reliant on these parameters is investigated below.

6.1 The swelling response of NBR elastomers

A sub-set of the molecules, investigated in Chapter 5, were further investigated to probe how swelling depends on temperature. Exposure was to six classes of fuels/solvents: (1) base fuels and paraffins, (2) 15% cycloparaffin/SPK blends, (3) 8% aromatic/SPK blends, (4) 8% bicyclic aromatic/SPK blends, (5) 8% aromatic oxygenate/SPK blends, other oxygenates. Equilibrium swelling data was recorded after 100 days of fuel exposure for all fuel wetted NBR elastomer samples. Testing was performed at 20^{o}C and 35^{o}C in addition to 50^{o}C.

6.1.1 Base fuels and paraffins

The influence of temperature on the swelling by SPK/Jet A-1, the *n*-paraffins (n-decane and n-dodecane) and a cycloparaffin (decalin) was probed.

The raw data is presented in Table 6.1 and graphically in Figure 6.1 it can be seen that unlike Jet A-1, the paraffinic SPK, the pure n-paraffins and the cycloparaffin, decalin, all cause increasing swell as the temperature increases from 20-35°C. However, for the same compounds little change in swelling was observed from 35-50°C. The significantly greater swelling due to Jet A-1 can be seen. The high swelling of neat decalin at all temperatures should be noted.

Table 6.1: Swelling of deplasticised NBR O-rings exposed to base fuels as a function of increasing temperature

Solvent	δ_d	δ_p	δ_h	δ_{tot}	Molar volume (cm^3/mol)	Volumetric swell at equilibrium (%)		
						20°C	35°C	50°C
Base fuels								
SPK	15.4	0.0	0.0	15.4	212.5	5.7 (0.1)	8.9 (0.3)	9.0 (0.3)
Jet A-1	16.5	0.1	0.3	16.5	193.7	18.9 (0.1)	18.7 (0.2)	18.5 (0.5)
n-paraffins								
n-decane	15.7	0.0	0.0	15.7	195.9	7.7 (0.2)	n.d.	9.0 (0.3)
n-dodecane	16.0	0.0	0.0	16.0	228.6	5.8 (0.9)	8.2 (0.4)	8.7 (0.2)
cycloparaffin								
decalin	16.7	0	0	16.7	144.2	20.5 (0.5)	24.9 (0.6)	25.9 (0.4)

Values in parentheses are the standard deviation of the mean. N = 3

n.d. not determined

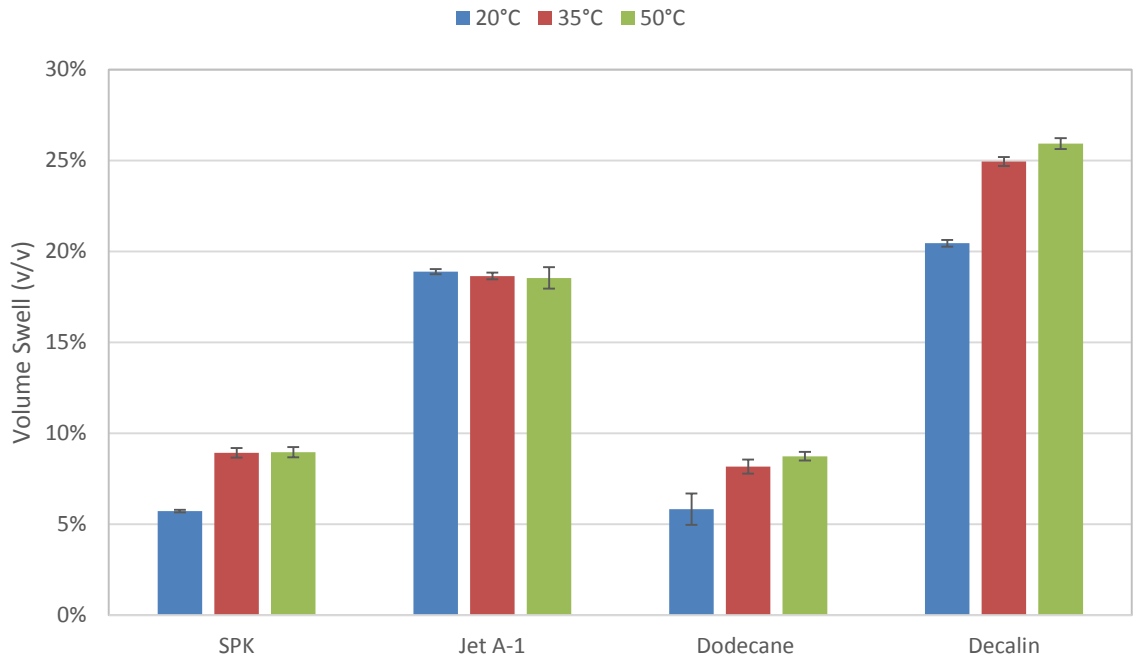

Figure 6.1: Influence of temperature on the swelling of fuel-wetted NBR elastomer samples by base fuels and paraffins. Note: Dodecane and decalin are presented as pure compounds.

6.1.2 Cycloparaffin/SPK blends

Cycloparaffins follow the behaviour of other hydrocarbons (n-paraffins and aromatics) in that increased elastomer swelling with increasing temperature is observed (Figure 6.2).

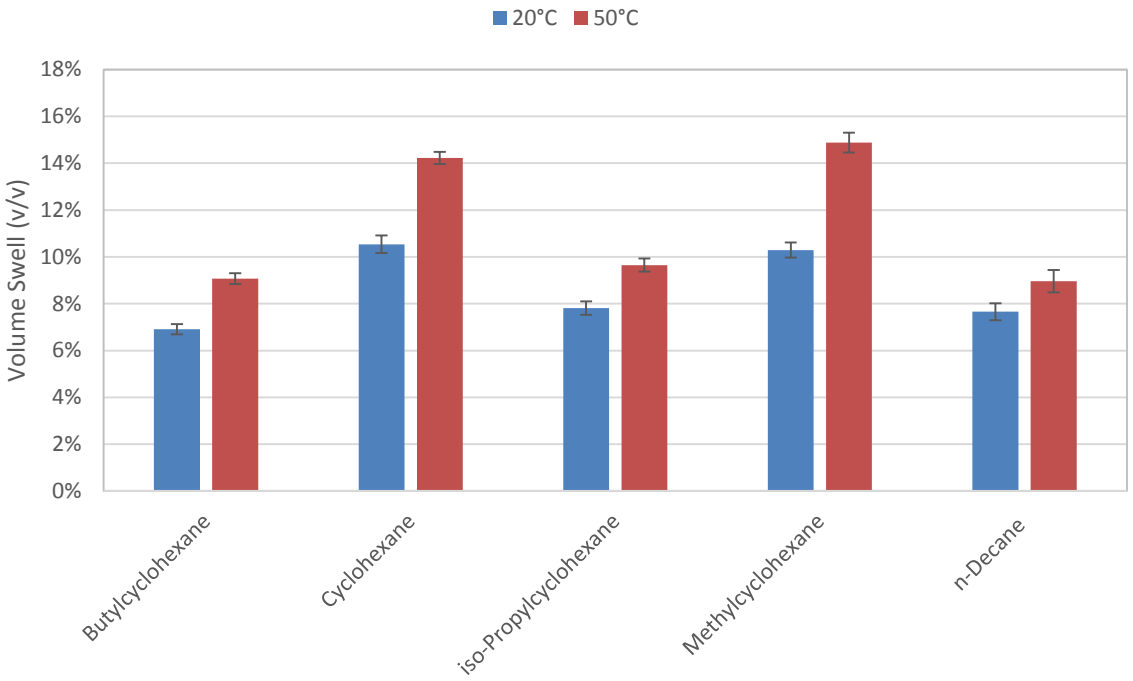

Error bars indicate 1 standard deviation. N=3

Figure 6.2: Effect of temperature on the swelling performance of NBR elastomers exposed to cycloparaffin/SPK blends

Cycloparaffin/SPK blend studies were investigated at 20°C and 50°C. It can be seen that at 20°C the same trend with molar volume as seen at 50°C is again observed. It can again be seen that, also at 20°C, methylcyclohexane has similar swell to cyclohexane, although in this case it is slightly lower. This might suggest a role for δ_h in the swelling of NBR by cycloparaffins but that would require further study on a broader range of cycloparaffins which was beyond the scope of this work.

Table 6.2: Swelling of deplasticised NBR O-rings exposed to cycloparaffin/SPK blends

Blend	δ_d	δ_p	δ_h	δ_{tot}	Molar volume (cm^3/mol)	Volumetric swell at equilibrium (%)	
						20°C	50°C
monocyclic							
cyclohexane	16.8	0.0	0.2	0.2	108.7	10.5 (0.2)	14.2 (0.2)
methylcyclohexane	16.0	0.0	1.0	16.0	128.3	10.3 (0.3)	14.9 (0.2)
iso-propylcyclohexane	16.3	0.0	0.5	16.3	157.4	7.8 (0.2)	9.7 (0.4)
n-butylcyclohexane	16.2	0.0	0.6	16.2	176.7	6.9 (0.2)	9.1 (0.3)
bicyclic							
decalin*	16.7	0	0	16.7	144.2	7.3 (0.2)	10.3 (0.3)

Values in parentheses is the standard deviation of the mean. N = 3

* Swelling of 9.8 (0.3) was measured at 35°C

6.1.3 Monoaromatic/SPK blends

The effect of temperature of monoaromatics blends was performed on a reduced subset of the aromatics which were investigated in Chapter 5. Toluene was chosen because it has been widely studied. Cumene (b.p. 152.4°C) and p-cymene (b.p. 177°C) were chosen because they lie in the kerosene boiling range and have been identified in petroleum Jet A-1.

Table 6.3: Swelling response of deplasticised NBR O-rings exposed to aromatic fuel blends under increasing temperatures

Blend	δ_d	δ_p	δ_h	δ_{tot}	Molar volume (cm^3/mol)	Volumetric swell at equilibrium (%)		
						20°C	35°C	50°C
toluene	18.0	1.4	2.0	18.2	106.3	12.8(0.3)	14.0(0.5)	14.7(0.1)
cumene	18.1	1.2	1.2	18.2	139.4	10.4(0.4)	13.4(0.2)	13.9(0.4)
p-cymene	17.6	1.2	1.2	17.7	156.6	10.1(0.3)	11.5(0.1)	11.8(0.2)

Values in parentheses are standard deviations of the mean. N = 3

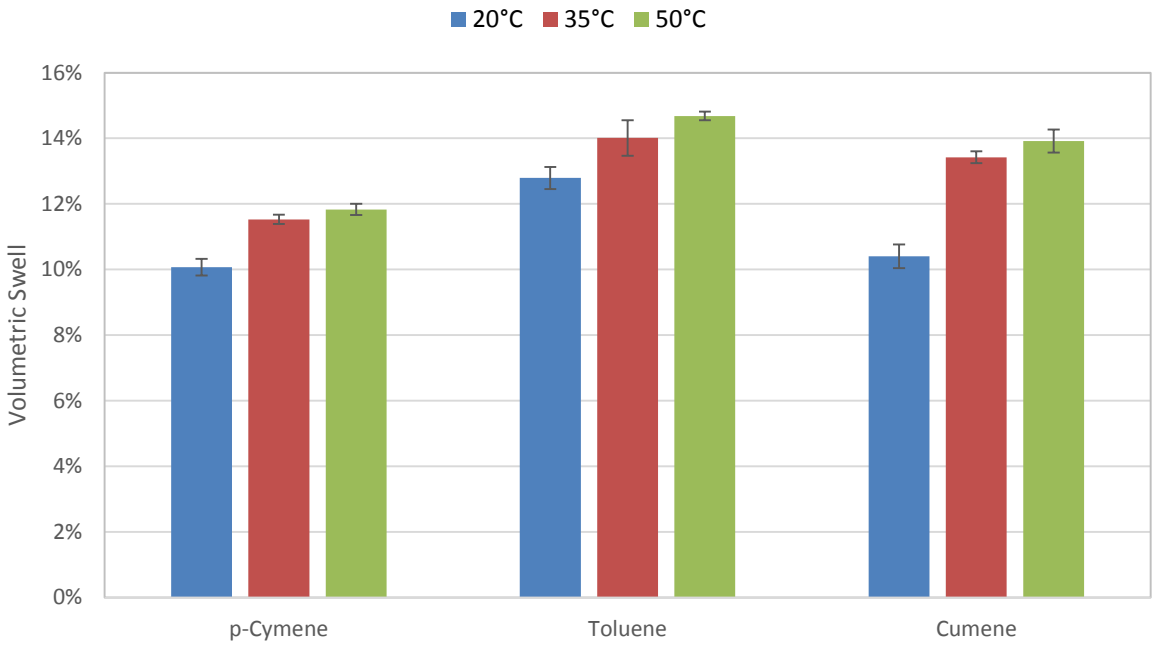

Error bars indicate 1 standard deviation. N=3

Figure 6.3: Effect of temperature on the swelling of deplasticised NBR O-rings exposed to SPK/aromatic fuel blends

Table 6.3 indicates the swelling performance of NBR elastomer when exposed to aromatic blends at various temperatures. The underlying trend in the swelling performance of NBR rubber to these blends is further exposed in Figure 6.3. The most swelling was observed for smallest aromatic, toluene. With the exception of 20°C, where the difference is not statistically significant, the smaller compound, cumene, causes more swelling than *p*-cymene.

6.1.4 Bicyclic aromatic/SPK blends

Bicyclic aromatics have high densities and often produce substantial swell of elastomer materials. All fuel blends investigated here contain 8% (v/v) bicyclic aromatic content unless otherwise noted [9].

The effect of temperature on the swelling characteristics may be observed in Figure 6.4**.** In all cases the extent of swelling increases with temperature although the effect appears to be more pronounced for the C_9 bicyclic aromatics, indane and indene.

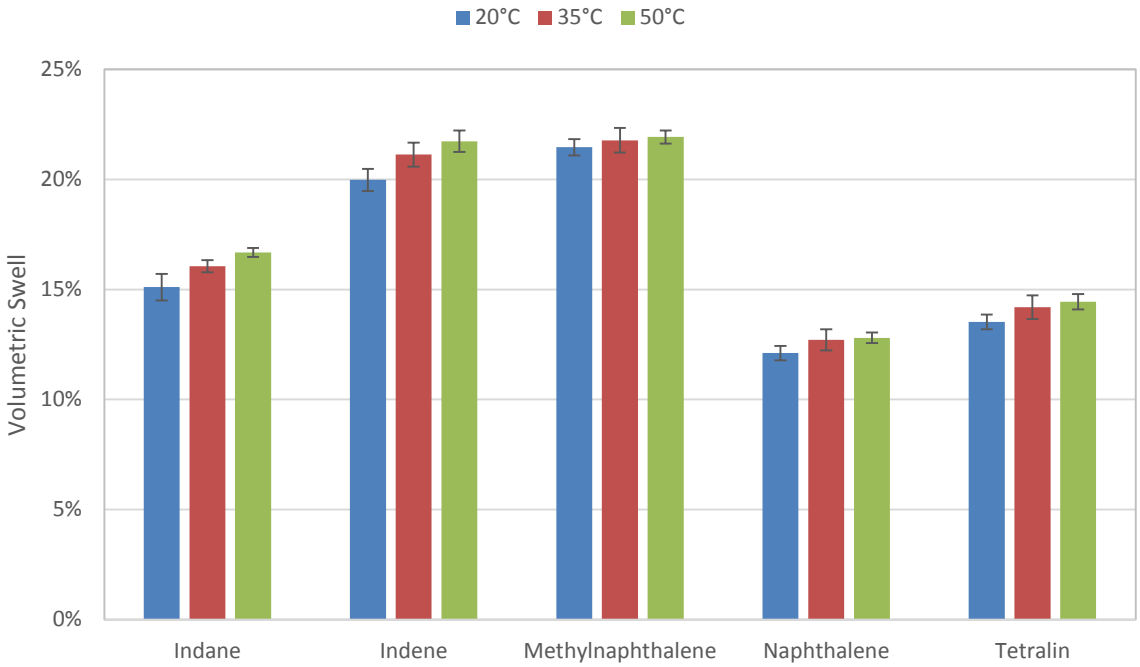

Error bars indicate 1 standard deviation. N=3

Figure 6.4: Temperature effect on the swelling of NBR elastomer samples exposed to bicyclic aromatic blends

Table 6.4: Swelling effect of bicyclic aromatics on deplasticised NBR O-rings

Blend	**δ_d**	**δ_p**	**δ_h**	**δ_{tot}**	**Molar volume (cm^3/mol)**	**Volumetric swell at equilibrium (%)**		
						20°C	35°C	50°C
hydrocyclic aromatic								
indane	19.6	1.3	1.6	19.7	122.8	15.1 (0.6)	16.1 (0.3)	16.7 (0.2)
tetralin	19.6	2	2.9	19.9	136.3	13.6 (0.3)	14.2 (0.5)	14.4 (0.4)
diaromatic								
indene	18.7	2.6	9.0	20.9	116.5	20.0 (0.5)	21.1 (0.6)	21.7 (0.5)
naphthalene*	19.2	2.0	5.9	20.2	111.5	12.1 (0.3)	12.7 (0.5)	12.8 (0.2)
methylnaphthalene	20.6	0.8	4.7	21.1	138.8	21.7 (0.4)	21.8 (0.6)	21.9 (0.3)

Values in parentheses are standard deviations of the mean. N = 3

*Naphthalene was used in 2% (v/v) concentration due to solubility limits

6.1.5 Oxygenate/SPK blends

Aromatic oxygenates present in the fuel pool are residual products derived from the use of crude oil. In diesel and gasoline, these compounds are useful deposit controllers which increase the lubricity of the fuel and are efficient energy density boosters [84]. The ability of oxygen to interact with active cyano-group of NBR may be expected to produce substantial swelling. Note that the data in Table 6.5 is for an 8% (v/v) dibenzyl ether blend with SPK while that for benzyl alcohol is 0.5% (v/v) in SPK. The data for cyclohexanol and n-hexanol is for 15% blends in SPK.

Aromatic oxygenates and display opposite dependence on increasing temperature to the hydrocarbons (paraffins, aromatics and cycloparaffins). With increasing temperature the equilibrium swelling decreases. These results are discussed in depth in Section 6.3.5. The dramatic reverse in trend is best illustrated by Figure 6.5

Table 6.5: Swelling effect of oxygenates on deplasticised NBR O-rings

Blend	**δ_d**	**δ_p**	**δ_h**	**δ_{tot}**	**Molar volume (cm^3/mol)**	**Volumetric swell at equilibrium (%)**		
						20°C	35°C	50°C
aromatic ether								
benzyl alcohol	18.4	6.3	13.7	23.8	103.6	25.7 (0.2)	18.6 (0.5)	15.7 (0.4)
dibenzyl ether	19.6	3.4	5.2	20.6	197.4	33.0 (0.8)	28.5 (0.8)	26.6 (0.4)
paraffinic alcohol								
cyclohexanol	17.4	4.1	13.5	22.4	106.0	19.8 (0.6)	n.d	26.2 (0.3)
n-hexanol	15.9	5.8	12.5	21.04	124.9	14.8 (0.1)	n.d	19.8 (0.4)

Values in parentheses are the standard deviation of the mean. N = 3
n.d = Not determined

In contrast, the other oxygenates that were tested, cyclohexanol and n-hexanol, display increased swelling with temperature. This is indicative that a number of processes influence the temperature dependence of swelling with some increasing swelling with temperature and others decreasing swelling.

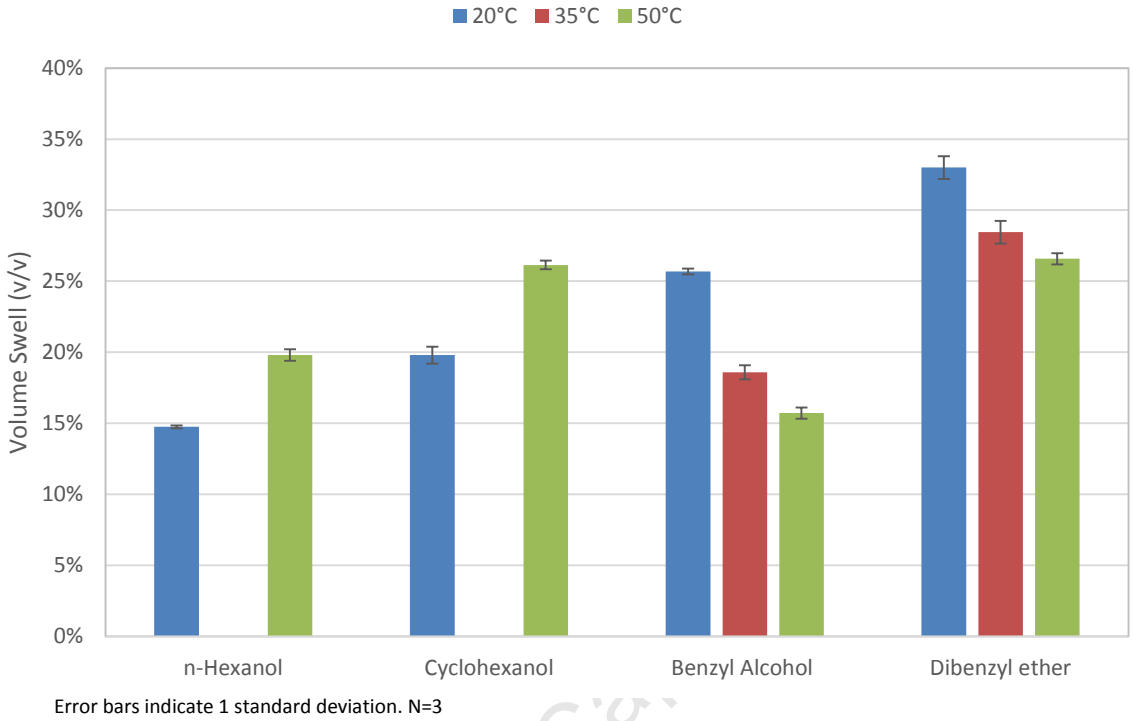

Figure 6.5: Effect of temperature on the swelling of deplasticised NBR O-rings exposed to aromatic oxygenates

6.2 The swelling response of fluorocarbon (FKM) elastomer O-rings

Fluoroelastomers like FKM and fluorosilicone are widely applied within the aviation industry because of their inherent fuel resistance and temperature stability. As such, the swelling response of an FKM elastomer, exposed to a similar matrix of fuels as presented in the case of NBR, was investigated. The fuel matrix was divided into five categories, namely (1) base fuels; (2) general aromatics; (3) aromatic oxygenates, (4) cycloparaffins and (5) a cyclic oxygenate. In the case of FKM, equilibrium swelling values were recorded after 50 days of fuel exposure. FKM samples were exposed to cycloparaffin blends at 50°C only. Table 6.6 presents the swelling performance of the elastomer samples exposed to varying fuel blends and temperature. Unlike NBR, FKM displays a much lower sensitivity to fuel composition. The extent of swelling is much reduced.

Table 6.6: Swelling behaviour of FKM elastomer O-rings exposed to various fuel blends at different temperatures

Blend	δ_d	δ_p	δ_h	δ_{tot}	Molar volume (cm^3/mol)	Volumetric swell at equilibrium (%)		
						20°C	35°C	50°C
Base fuels								
SPK	15.4	0	0	15.4	212.5	1.6 (0.3)	2.0 (0.3)	2.4 (0.4)
CTL Jet A-1	16.5	0.1	0.3	16.5	193.7	1.7 (0.3)	2.7 (0.1)	3.2 (0.1)
aromatics								
toluene*	18.0	1.4	2.0	18.2	106.3	0.8 (0.2)	2.8 (0.3)	5.6 (0.4)
cumene*	18.1	1.2	1.2	18.2	139.4	0.7 (0.3)	1.2 (0.4)	1.4 (0.3)
n-butylbenzene*	17.4	0.1	1.1	17.4	157.0	-0.5 (0.3)	0.6 (0.7)	2.0 (0.3)
tetralin*	19.6	2	2.9	19.9	136.3	-1.7 (0.4)	2.3 (0.2)	2.6 (0.2)
oxygenates								
benzyl alcohol***	18.4	6.3	13.7	23.8	103.6	3.0 (0.1	2.4 (0.3)	1.4 (0.3)
dibenzyl ether*	19.6	3.4	5.2	20.6	197.4	4.1 (0.5)	3.2 (0.5)	3.1 (0.3)
cyclohexanol**	17.4	4.1	13.5	22.4	106.0	-	-	2.7 (0.1)
cycloparaffins								
cyclohexane**	16.8	0.0	0.2	0.2	108.7	-	-	0.9 (0.0)
methylcyclohexane**	16.0	0.0	1.0	16.0	128.3	-	-	1.2 (0.3)
iso-propylcyclohexane**	16.3	0.0	0.5	16.3	157.4	-	-	1.6 (0.2)
n-butylcyclohexane**	16.2	0.0	0.6	16.2	176.7	-	-	1.2 (0.0)

Values in parentheses are the standard deviation of the mean. N = 3

* 8% (v/v), ** 15% (v/v), *** 0.5% (v/v)

The temperature trends of the base fuels, representative aromatics and aromatic oxygenates are displayed in Figure 6.6. As with NBR, FKM swelling shows positive temperature dependence when exposed to common aromatic and cycloparaffinic compounds. FKM also exhibits a negative dependence on temperature when exposed to aromatic oxygenates. Interestingly, a clear increase in Viton swelling was witnessed when exposed to increasing temperatures for the case of Jet A-1. This was not the case for NBR which showed very little change in swelling over the temperature range.

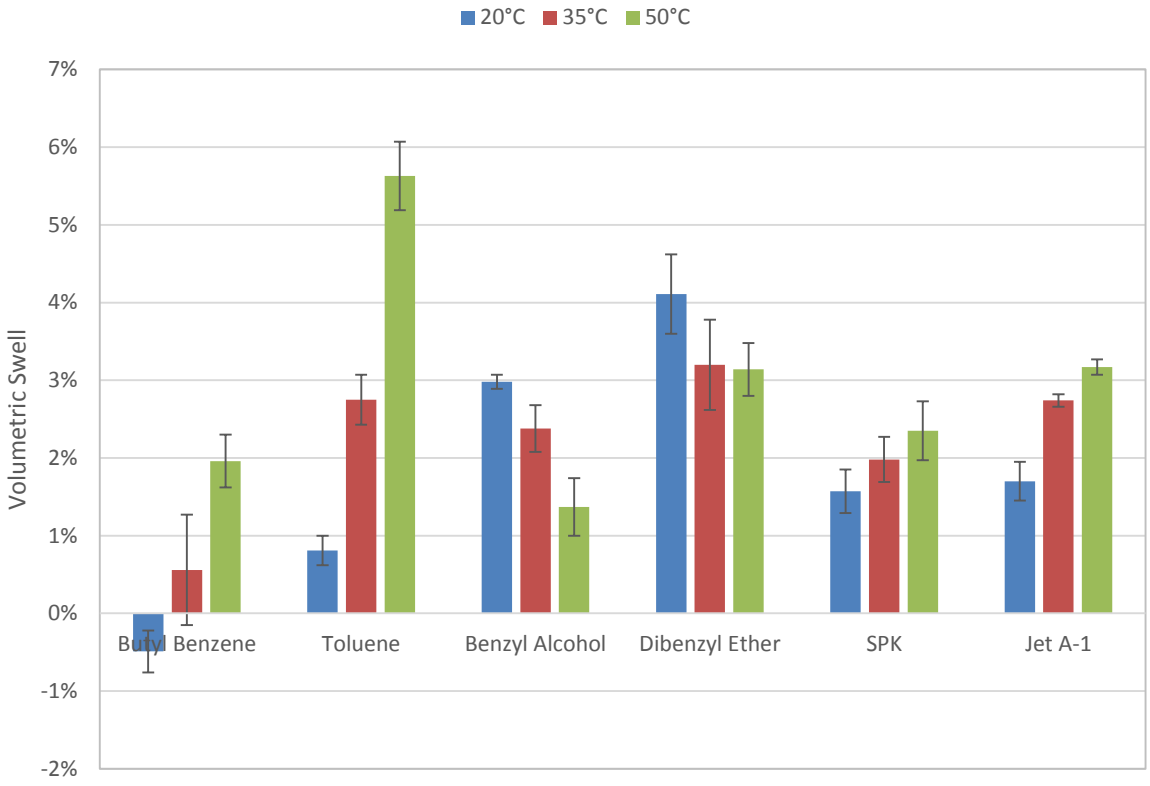

Figure 6.6: Effect of temperature on the swelling behaviour of Viton O-rings exposed to various SPK blends.

6.3 Discussion

6.3.1 NBR O-rings exposed to base fuels

The extent of swelling of NBR O-rings was observed to depend on temperature. Whether swelling increased with temperature or decreased depended on the composition of the fuel to which the O-rings were exposed.

Not only was the extent of swell for SPK and *n*-dodecane similar, but also the dependence on temperature showed similar responses. This is expected since *n*-dodecane is a paraffin and the SPK used is highly paraffinic, albeit iso-paraffinic. The swelling of both *n*-dodecane and SPK showed a positive dependence on temperature which is consistent with an endothermic entropy of mixing. Because both are paraffinic hydrocarbons they are capable of only dispersive (van der Waals) interactions with NBR. Such interactions are typical of endothermic polymer-solvent interactions.

The increased swelling by Jet A-1 is the consequence of the presence of aromatic species in Jet A-1 which are absent in SPK. Interestingly no statistically significant dependence of the

swelling by Jet A-1 on temperature could be observed. This is of note because all of the hydrocarbons added to SPK (cycloparaffins and aromatics) displayed a positive dependence on temperature. Jet A-1 is a far more complex mixture than SPK and the blends of SPK and single aromatic species. Because the enthalpy of mixing for swelling is dependent on not only interactions between the solvent/fuel and elastomer (NBR) but also on interactions between the solvent/fuel constituent molecules, it is possible that this latter may counteract the positive influence of temperature on swelling by hydrocarbons.

The effect of temperature on the sorption behaviour of solvents may be described using the Van't Hoff relationship. If mixing were endothermic, an increase in temperature would result in an increasing sorption coefficient and subsequently an increase in swelling observed at equilibrium [9, 56].

$$\ln Q = \frac{\Delta S}{R} - \frac{\Delta H}{RT}$$

where:

- Q = equilibrium swelling value = number of moles of solute/mass of rubber
- ΔS_{mix} = entropy of mixing
- ΔH_{mix} = enthalpy of mixing
- T = temperature in Kelvin
- R = universal gas constant

Since the number of moles of solute (n) = mass/molar mass = m_{solute}/M_w

$$Q = \frac{n_{solute}}{m_{rubber}} = \frac{m_{solute} / M_{w,solute}}{m_{rubber}}$$

Thus

$$\ln Q = \ln\left(\frac{m_{solute}}{m_{rubber}}\right) - \ln(M_w)$$

Rearranging

$$\ln\left(\frac{m_{solute}}{m_{rubber}}\right) = \ln(M_w) + \frac{\Delta S}{R} - \frac{\Delta H}{RT}$$

A plot of the logarithm of the fraction increase in mass due to swelling versus the inverse of temperature, allows the enthalpy of mixing to be determined from the slope of the plot. Note that the above analysis assumes a homogeneous solvent which is not the case with the fuel. Provided the composition of the fuel in the O-ring is the same at all temperatures, the same result can be obtained with M_w replaced by average molar mass. This assumption may well not be valid for real fuels, as discussed below. Nonetheless, an analysis was performed using the above approach to elucidate any trends.

Table 6.7: Enthalpy of sorption for exposure to base fuels

Fuel	ΔH_{mix} (kJ/mol)
SPK	4.0
n-dodecane	8.0
Jet A-1	0.9

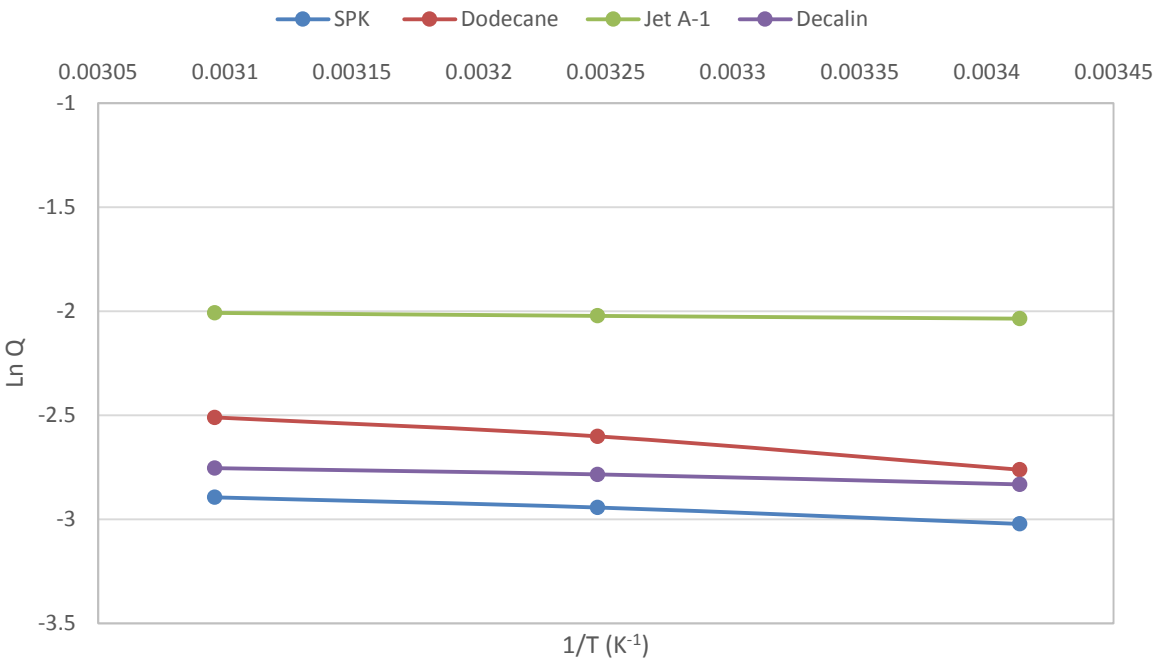

Figure 6.7: van't Hoff plots for the swelling of NBR by base fuels

The enthalpies of sorption for NBR elastomers exposed to the base fuels and neat hydrocarbons are highlighted in Table 6.7. As expected, endothermic mixing has occurred. Henry-type diffusion is likely the underlying diffusion mechanism [55]. Figure 6.7 illustrates that the swelling of NBR by Jet A-1 is less sensitive to temperature than the more paraffinic

fuels (SPK and n-dodecane). The estimated enthalpy of sorption is near zero. The presumption that Jet A-1 follows Langmuir-type diffusion or displays exothermic swelling nature is difficult to make and more research is required to confirm whether this is in fact the case.

6.3.2 NBR exposure to cycloparaffins

This study is the first to detail the influence of temperature on the swelling response of elastomer materials exposed to cycloparaffins. Cycloparaffins are present in the petroleum jet fuel pool where they boost the overall density of the fuel [5, 9]. When exposed to cycloparaffins, the swelling response as a function of temperature increased across the range.

The resulting enthalpy of sorption for NBR exposure to the cycloparaffin blends is endothermic in nature, as shown in Table 6.8.

Table 6.8: Enthalpy of sorption for NBR elastomer exposed to cycloparaffin fuel blends

Blend component	**ΔH_{mix} (kJ/mol)**
cyclohexane	9.6
methycyclohexane	13.2
iso-propylcyclohexane	7.3
n-butylcyclohexane	2.1
decalin	2.5

The temperature sensitivity was greatest for the smaller cycloparaffins as reflected by their larger enthalpies of mixing.

6.3.3 NBR exposed to aromatic compounds

NBR O-rings exposed to 8% (v/v) aromatic blends showed a noticeable temperature dependence. A steady increase in the swelling response was observed. Toluene also imparted the greatest amount of swell observed at equilibrium. Cumene and p-cymene both show significantly positive dependence of swelling on temperature. It should, however, be noted that the increase between 35^{o}C and 50^{o}C is less than that 20^{o}C and 35^{o}C. This deviation from linearity may again be consequence of the relative stability of the fuel mixture of the neat fuel vs the fuel adsorbed at the two temperatures. Experiments to assess the relative amounts absorbed of the aromatic species vs the paraffinic species of SPK at the two temperatures was

beyond the scope of this work. The heat of sorption for NBR exposed to the aromatic fuel blends is noticeably endothermic, indicative of likely Henry-type diffusion.

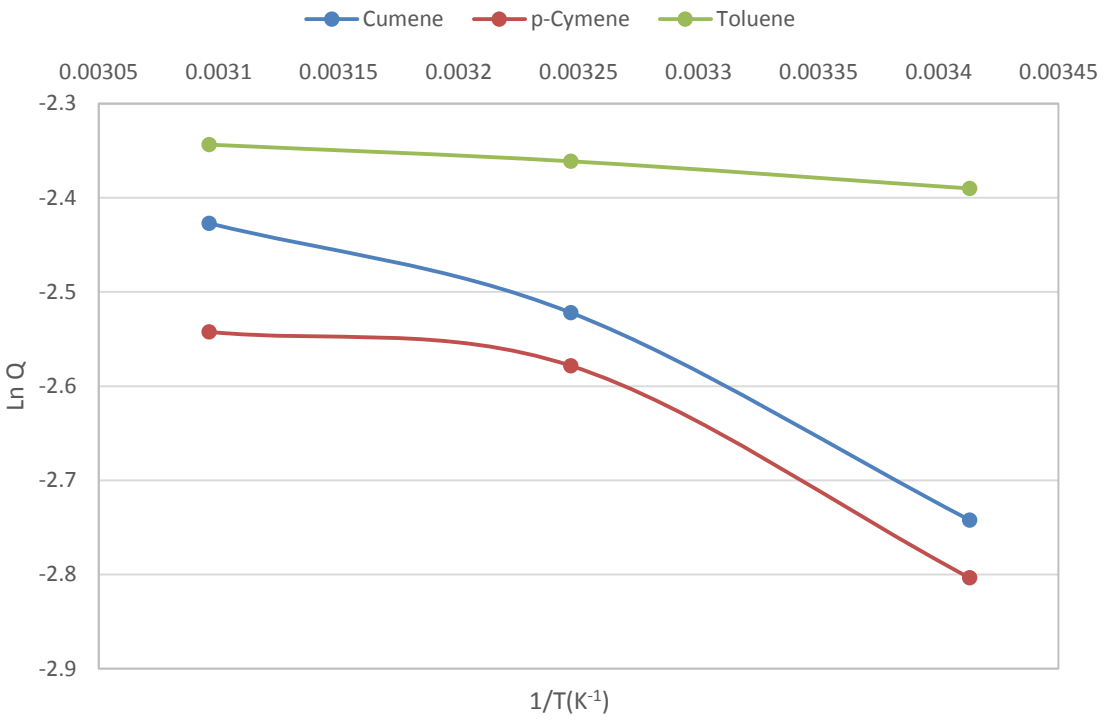

Figure 6.8: van't Hoff plots of the swelling of NBR exposed to SPK/aromatic blends

Table 6.9: Enthalpy of sorption for NBR exposed to aromatic fuel blends

Blend component	ΔH_{mix} (kJ/mol)
toluene	1.5
cumene	10.0
p-cymene	8.3

6.3.4 NBR exposure to bicyclic aromatics

Exposure to bicyclic aromatic blends resulted in sorption behaviour that was endothermic in nature. All blends exhibited a positive dependence on increasing temperature. The sensitivity was greatest for the hydrocyclic aromatics while the dependence for the diaromatics was very small. The diaromatics displayed behaviour very similar to Jet A-1. The exact reasons behind this behaviour are unclear. The latter group of compounds are associated with having large hydrogen bonding character (δ_h = 9.0 and 4.7, respectively) as well as high polar cohesive

energies (δ_p =2.6 and 0.8, respectively). The association of the hydrogen bonding parameter, and therefore the increased interactions with the cyano-group of NBR, has been reported to be a major contributor to large elastomer swelling [9, 3].

Table 6.10: Enthalpy of sorption for NBR exposed to bicyclic aromatic blends

Blend component	**ΔH_{mix} (kJ/mol)**
indane	3.9
tetralin	3.5
indene	0.7
naphthalene	0.4
1-methylnaphthalene	1.7

The enthalpy of sorption for each bicyclic aromatic blend has been estimated in Table 6.10.

Although, all blends exhibit endothermic sorption behaviour, the dependence on temperature is far less pronounced compared to the aromatic blends and base fuels. This may be seen on inspection of Figure 6.9. The curves are almost flat, much like that of Jet A-1. Burnham [9] speculated that compounds with high δ_p and δ_h would display the greatest temperature sensitivity although he did predict negative sensitivity.

It is possible that while the interactions between these compounds and NBR are endothermic, entropic factors become important at higher temperatures. As the temperature rises the system will tend towards a higher entropy state. It is known that concentration of aromatic species occurs within the NBR, *i.e.* there is more aromatics adsorbed in the NBR relative to the paraffins when compared to their ratio in the original blend [73]. This concentration effect has the tendency to reduce entropy. At higher temperatures entropic considerations would drive the system to have less such concentration. This would be achieved by a lower ratio of aromatics to paraffins in the swollen NBR which would translate into reduced swell. Consequently entropic and enthalpic factors would counteract each other providing the result observed. The enthalpies of mixing reported are thus a mix of solute-NBR interactions and solute-solute interactions.

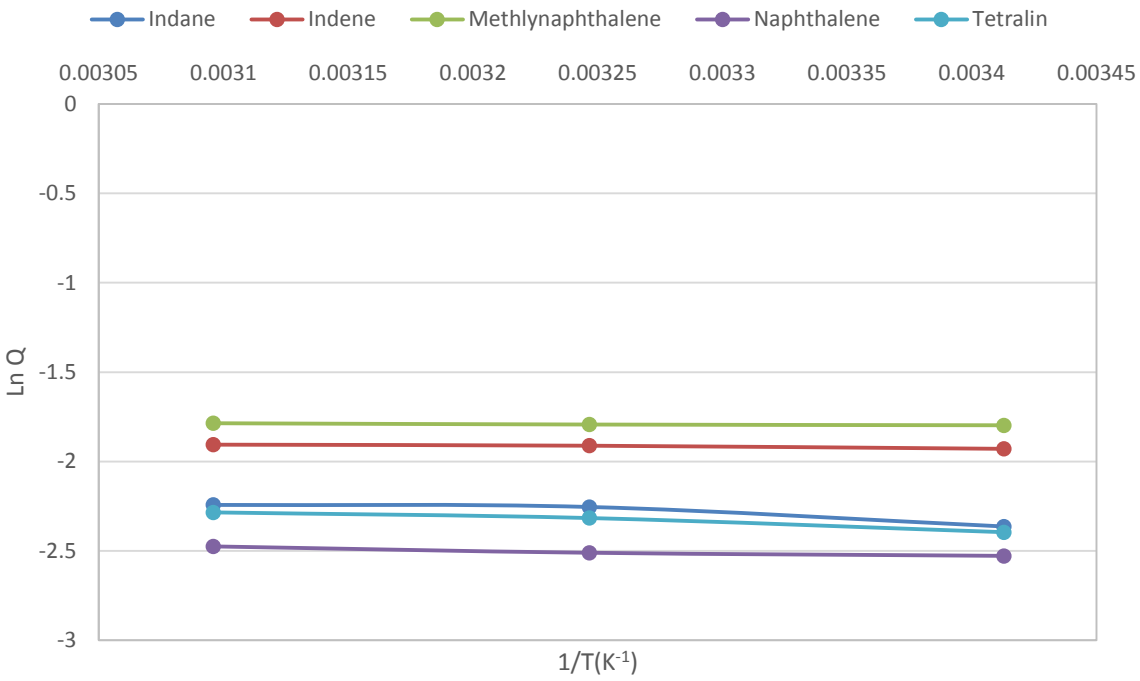

Figure 6.9: van't Hoff plot of the swelling of NBR exposed to SPK/bicyclic aromatic blends

6.3.5 NBR exposure to aromatic oxygenates

The swelling response of aromatic oxygenates has been studied previously [9, 56]. This study is the first to detail the effect of temperature on the equilibrium swelling response of NBR exposed to these compounds. Exposure to SPK/aromatic oxygenate blends produces extremely large swelling values, more so than exposure to any other fuel blends tested. Both dibenzyl ether and benzyl alcohol have large δ_h and δ_p parameters. The presence of such large δ_h energies and propensity of these compounds to readily form hydrogen-bonding interactions is perhaps a significant contributor to the observed swell. Polar forces are inherently molecular interactions found in most systems and are predicted to be a major contributing factor to the sorption process [51]. With this in mind, it is likely that the high swelling response of NBR exposed to these compounds is driven by both polar cohesion and hydrogen bonding energies.

In contrast to the SPK/hydrocarbon blends, SPK/benzyl alcohol and SPK/dibenzyl ether blends both displayed a statistically significant decrease in swelling with increasing temperature. This is illustrated in

Figure **6.5**. A relative swelling reduction of approximately 10% in absolute terms was observed after exposure to benzyl alcohol at 20°C and 50°C. The difference in temperature dependence

may be explained in terms of a difference in the nature of the interaction between these solutes and other compounds with NBR. The enthalpies of sorption for both aromatic oxygenate species are presented in Table 6.11.

Table 6.11: Enthalpy of sorption for NBR elastomers exposed to aromatic oxygenates

Blend component	**ΔH_{mix} (kJ/mol)**
benzyl alcohol	-15.8
dibenzyl ether	-8.8
cyclohexanol	21.5
n-hexanol	21.6

What is immediately obvious is that benzyl alcohol and dibenzyl ether show sorption behaviour which is exothermic in nature. These large and negative enthalpies would suggest a very strong and directed interaction between the aromatic oxygenates and NBR. This is more clearly seen in Figure 6.10 where the linearised plots have much steeper slopes compared to compounds which show little temperature dependency. The exothermic nature of sorption the aromatic oxygenates into NBR points to a different mode of diffusion. Langmuir-type diffusion is assumed for sorption processes exhibiting exothermic nature [55].

n-hexanol and cyclohexanol, are also oxygen-containing compounds which also swell NBR significantly. These oxygen-containing compounds also have both large hydrogen-bonding and polar solubility parameters and thus are expected to impart a large swelling response, conforming to the solubility parameter model proposed by Hansen [51]. In contrast to the aromatic oxygenates these species have a large and endothermic entropy of mixing in spite of large δ_h values. It is known, for instance, that n-hexanol and paraffins displays a positive deviation from Raoult's law and a minimum azeotrope temperature. This is indicative of a highly endothermic enthalpy of mixing for the formation of a blend of paraffin and n-hexanol. It is suggested that in the case of cyclohexanol and n-hexanol, the latter effect dominates due to is δ_h and δ_p values. This is in contrast to the case with diaromatics, where the fuel mixture itself is more thermodynamically stable at elevated temperatures.

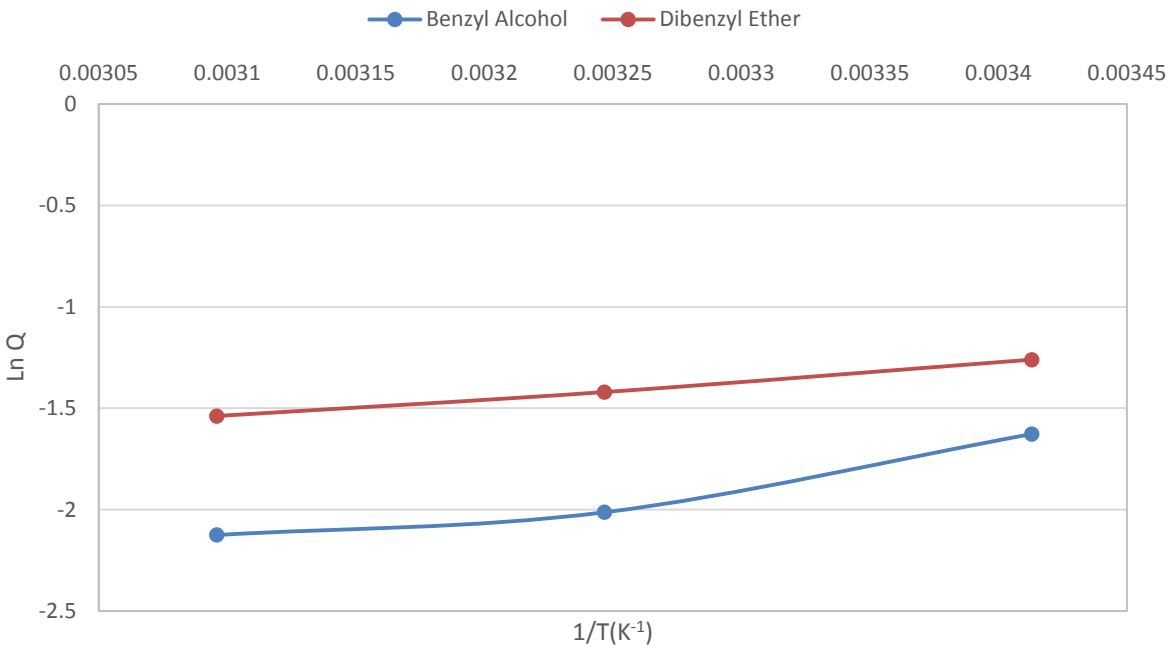

Figure 6.10: van't Hoff plots of the swelling of NBR elastomers exposed to SPK/aromatic oxygenate blends

Hansen [51] noted that at increased temperatures the solubility parameters remained approximately stable. The hydrogen bonding parameter was the exception and showed the greatest sensitivity to increased temperature. Hansen concluded that the hydrogen bonding parameter decreases at a greater rate compared to the other parameters due to cleavage of hydrogen bonds at elevated temperatures [51]. This will also play a role in determining the temperature response.

This result further endorses the hypothesis that the solubility parameter model proposed by Hansen is incomplete. The Hansen solubility approach assumes endothermic interactions between solute and polymer. This is high likely not the case here. Prediction of solvent compatibility with elastomers based on matching of solubility parameters by themselves may not prosee a complete picture. The strong emphasis on the hydrogen bonding and polar cohesive energies as the dominant effect on elastomer sorption is likely incomplete as an explanation and the failure of the model to account for exothermic heats of mixing remain the biggest flaws.

6.3.6 Exposure of NBR to pure components

In order to probe the processes underlying the temperature dependence, swelling was performed where NBR was exposed to a set of pure components, rather than blends with SPK. This was done so that the effect of the thermodynamic stability of the fuel mixture was eliminated. When swelling takes place the equilibrium is determined by the contributions to the overall free energy by i) extension of the elastomer chains, ii) enthalpic interactions between fuel component and elastomer; iii) combinatorial entropy of the polymer-fuel mixture, iv) enthalpic interactions between fuel component and fuel component and v) combinatorial entropy of the fuel component mixture. The last two terms constitute the free energy of mixing of the fuel mixture on its own which is itself temperature dependent. This temperature dependence is determined by (iv) above: enthalpic interactions between fuel component and fuel component.

Table 6.12: Swelling of NBR O-rings exposed to pure components at different temperatures

Solvent	δ_d	δ_p	δ_h	δ_{tot}	Molar volume (cm^3/mol)	Volumetric swell at equilibrium (%)		
						20°C	35°C	50°C
n-paraffin								
n-decane	15.7	0.0	0.0	15.7	195.9	7.7 (0.2)	n.d.	9.0 (0.3)
n-dodecane	16.0	0.0	0.0	16.0	228.6	5.8 (0.9)	8.2 (0.4)	8.7 (0.2)
cycloparaffin								
decalin	16.7	0	0	16.7	144.2	20.5 (0.5)	24.9 (0.6)	25.9 (0.4)
aromatic								
toluene	18.0	1.4	2.0	18.2	106.3	127.3 (0.8)	128.8 (0.8)	132.1 (1.4)
cumene	18.1	1.2	1.2	18.2	139.4	88.2 (0.5)	92.8 (0.9)	97.5 (0.2)
tetralin	19.6	2	2.9	19.9	136.3	119.0 (0.9)	126.3 (0.1)	127.5 (1.8)
oxygenate								
anisole	17.8	4.1	6.7	19.5	108.7	219.1 (0.3)	210.3 (0.8)	205.0 (0.6)
cyclohexanol	17.4	4.1	13.5	22.4	106.0	n.d.*	34.5 (0.7)	43.6 (0.3)

n.d. = not determined

* cyclohexanol is solid at 20°C

It can be seen that the influence of molecular size and solubility parameters as discussed in Chapter 5 for 8% (v/v) aromatic/SPK blends also holds for the pure aromatics. Note that testing was performed using anisole as a model aromatic oxygenate rather than dibenzyl ether because swelling in dibenzyl ether swelled the O-ring to such an extent that it broke apart.

The data in Table 6.12 shows that with the exception of anisole, all solvents caused increased swelling with temperature. This is consistent with the trends that were observed with the blends with SPK for aromatics, aromatic oxygenates and other oxygenates. Table 6.13 contains the enthalpies of sorption which were obtained from van't Hoff plots.

Table 6.13: Enthalpy of sorption for NBR elastomer exposed to pure solvents

Solvent	ΔH_{mix} (kJ/mol)
n-paraffin	
n-decane	4.1
n-dodecane	8.0
cycloparaffin	
decalin	6.3
aromatic	
toluene	1.0
cumene	2.6
tetralin	1.9
oxygenate	
anisole	-1.8
cyclohexanol	13.0

The value for anisole is significantly closer to zero than the value obtained for 8% (v/v) dibenzylether in SPK. While aware of the fact that anisole and dibenzyl ether are different compounds, this suggests that part of the large negative enthalpy of sorption for aromatic oxygenate blends is the result of a change in the uptake of aromatic oxygenate relative to the paraffinic components of SPK with temperature. Preferential uptake of aromatic ethers is likely to be temperature sensitive.

The enthalpy of sorption for cyclohexanol, however, is still endothermic and large. This implies that the large positive enthalpy of sorption observed for the 15% (v/v) cyclohexanol/SPK blends is not solely a function of the cyclohexanol/SPK blend being less stable at elevated

temperatures. Note, however, that the magnitude of the enthalpy of sorption has decreased two-fold so this may well have an effect in the blend. The large enthalpy suggests that there may well be non-combinatorial effects that are temperature sensitive. Investigation of such effects which would require molecular and thermodynamic modelling was deemed beyond the scope of this study.

6.3.7 Fuel exposure of FKM O-rings

FKM O-rings were included in this investigation for comparative purposes. As expected, FKM shows very little swelling response to fuel exposure, regardless of the component, blended with SPK. The high carbon-to-fluorine content within the elastomer backbone is a driver behind the observed fuel resistance. In particular, strong bonding energies exist between carbon and fluorine and the lower energy bonding with fuel components is not favoured on a thermodynamic basis [37]. In terms of swelling behaviour, FKM exhibits similar responses to that of NBR elastomer. A positive-relationship with increasing temperature is observed for base fuels and SPK blends with aromatic compounds. As with NBR, a reversed relationship of swelling with increasing temperature is observed for the aromatic oxygenate fuel blends.

The extent of swelling of FKM is much reduced compared to NBR. NBR exhibited large swelling when exposed to aromatic oxygenates. In the case of FKM, exposure to general aromatics like toluene produced swell of similar magnitude to that of the aromatic oxygenates.

From the swelling response, the enthalpy of sorption can be estimated in the same manner as was used for NBR. The temperature is summarised in Table 6.14 and Figure 6.11 respectively.

All hydrocarbon fuels including the base fuels, Jet A-1 and SPK, have endothermic enthalpies of mixing which are all of a similar size (4-6 kJ mol^{-1}). The aromatic oxygenates show negative heats of sorption and thereby the swelling response is seen to decrease with increasing temperature. This reiterates the shortcomings of the solubility parameter model which neglects taking negative heats of mixing into account [47]. The consequence of this limitation is that such models are unable to adequately predict the swelling response of compounds which exhibit exothermic sorption behaviour.

Table 6.14: Enthalpy of sorption for FKM exposed to selected fuel blends

Blend component	ΔH_{mix} (kJ/mol)
Base fuels	
Jet A-1	5.8
SPK	5.0
Aromatics	
toluene	4.1
cumene	6.1
n-butyl benzene	4.8
tetralin	5.6
Aromatic oxygenates	
benzyl alcohol	-3.6
dibenzyl ether	-3.8

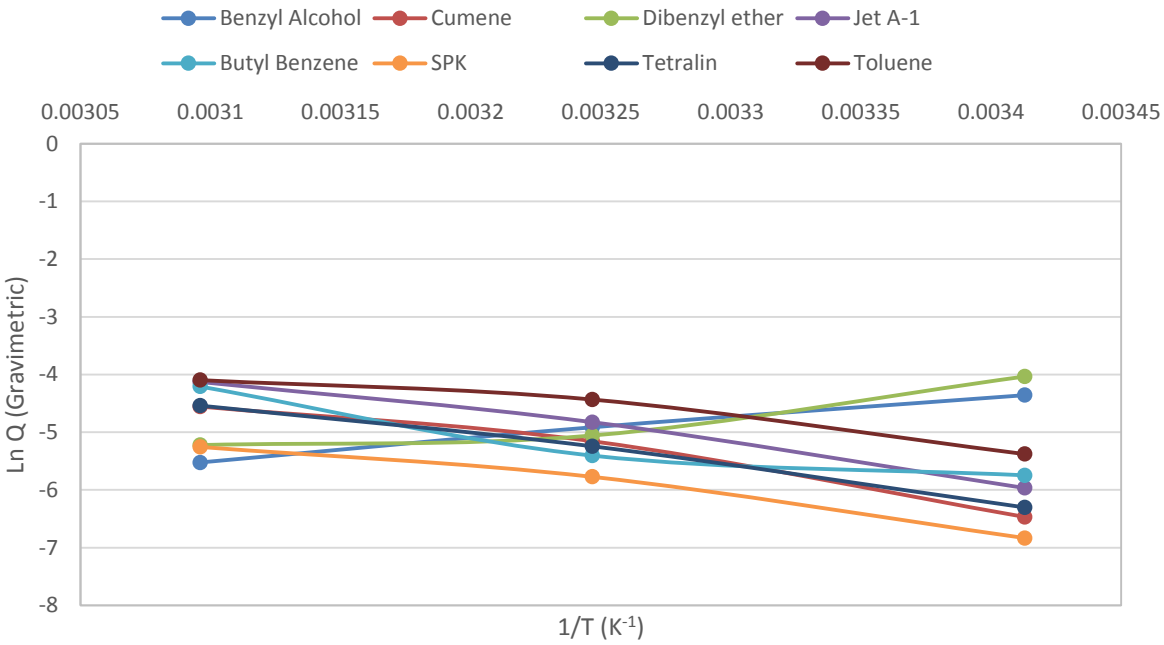

Figure 6.11: van't Hoff plots of FKM elastomer exposed to selected fuel blends.

CHAPTER 7

7. Effect of fuel exposure on the physical properties of NBR

This chapter aims to investigate the influence of fuel exposure on the physical properties of NBR O-rings. Understanding the effect of fuel exposure on the physical properties on elastomers is an integral part of predicting their sealing performance. The effect of fuel exposure on the glass transition temperature, compression set, tensile response and modulus of the elastomer are reported upon.

7.1 Glass transition temperature measurements by DMA and DSC

Monitoring the change in the glass transition temperature (T_g) of an elastomer is a useful way of evaluating the materials change in sealing performance. The T_g of an elastomer is heavily dependent on the surrounding environment. Moreover, the type of solvent the elastomer is exposed to and the surrounding temperature of the solvent both influence the materials T_g. DMA and DSC techniques are widely employed to observe the T_g of an elastomer material. As-received and deplasticised NBR samples have been analysed using both techniques and the resulting T_g values are found in Table 7.1.

Table 7.1: Glass transition temperatures for NBR elastomer samples analysed with DMA and DSC techniques

Condition	**As-Received**		**Deplasticised**	
	T_g(°C)		T_g(°C)	
Sample No.	DMA	DSC	DMA	DSC
1	-28.4	-38.3	-26.7	-32.7
2	-29.1	-38.1	-25.2	-32.1
3	-28.5	-37.1	-25.5	-33.1
4	-28.6	-37.6	-26.8	-33.3
5	-28.7	-36.9	-26.3	-32.4
Mean	-28.7	-37.6	-26.1	-32.7
Standard deviation of mean	0.1	0.3	0.3	0.2

Standard deviation of the mean was calculated using a sample size of N = 5

The difference in T_g values for DMA versus DSC is something that is expected. Literature reports that DMA T_g values are generally 8-10°C higher than those obtained through DSC work [85]. DMA is one of the most valuable methods for evaluating performance properties of polymeric materials. In particular, DMA enjoys the unrivalled ability to determine frequency and temperature effects on the mechanical properties of elastomer materials. By applying an oscillating force to the elastomer material, the resultant displacement is measured. The stiffness of the sample can be determined and the modulus and *tan δ* can be calculated. A drop in the storage modulus - due to a change in the heat capacity of the elastomer- is indicated by the peak of the *tan δ* curve. As a result, the T_g is strongly dependent on frequency and somewhat more sensitive to changing T_g performance compared to DSC techniques. DSC is strongly dependent on the heat flows associated with the elastomer sample and is inherently less sensitive to T_g changes compared to DMA techniques. With this in mind, dynamic mechanical analysis has been used to conduct all further testing on fuel-wetted elastomers.

7.2 Dynamic mechanical response of fuel-wetted NBR O-rings

The DMA response of fuel-wetted NBR elastomer samples is presented in this section. Responses measured include the change in the elastomers ability to store and dissipate energy as well as the change in the T_g of the fuel-wetted samples. Table 7.2 summarises the complete behavioural response of NBR samples exposed to numerous fuel blends. Each blend contains 8% (v/v) of the listed aromatic unless otherwise stated. The remainder of the solution comprises of SPK. ΔT_g is taken as the temperature difference between the T_g of deplasticised NBR and the T_g observed for fuel-wetted samples.

Figure 7.1, 7.2 and 7.3illustrate the changes in the storage modulus, loss modulus and *tan δ* of elastomer samples that have been exposed to the blends listed in Table 6.2. It is important that the elastomer sample retain adequate flexibility in order to allow sufficient contact between adjacent surfaces. The dynamic mechanical properties of elastomer materials exposed to fuel are important indicators of the materials level of functionality under these conditions. It is especially important for elastomers used within the fuel hosing on board an aircraft to maintain a suitable level of sealing properties to prevent potential fuel leakage.

Table 7.2: NBR dynamic property response to fuel exposure

Blend	T_g(°C)	ΔT_g	Storage Modulus (MPa) at 25°C	Loss Modulus (MPa) at 25°C
as-received NBR	-28.8(0.2)	-2.7	10.3 (0.4)	1.8 (0.1)
deplasticised NBR	-26.1(0.6)	0.0	43.5 (0.5)	9.1 (0.3)
SPK	-29.5(0.5)	-3.4	21.1 (0.2)	4.3 (0.2)
Jet A-1	-36.3(0.8)	-10.2	10.2 (0.9)	1.6 (0.1)
methylcyclohexane**	-31.3(0.4)	-5.2	21.2 (0.8)	4.0 (0.3)
toluene*	-37.5(0.6)	-11.4	13.7 (1.0)	2.4 (0.2)
n-butylbenzene*	-32.7(0.7)	-6.6	17.5 (0.2)	3.4 (0.1)
tetralin*	-42.0(0.7)	-15.9	12.8 (0.2)	2.4 (0.1)
dibenzyl ether*	-43.6(0.8)	-17.5	8.7 (0.3)	1.8 (0.1)

Samples is parentheses are standard deviations of the mean. N = 3

* blended at concentration of 8% (v/v)

** blended at concentrations of 15% (v/v)

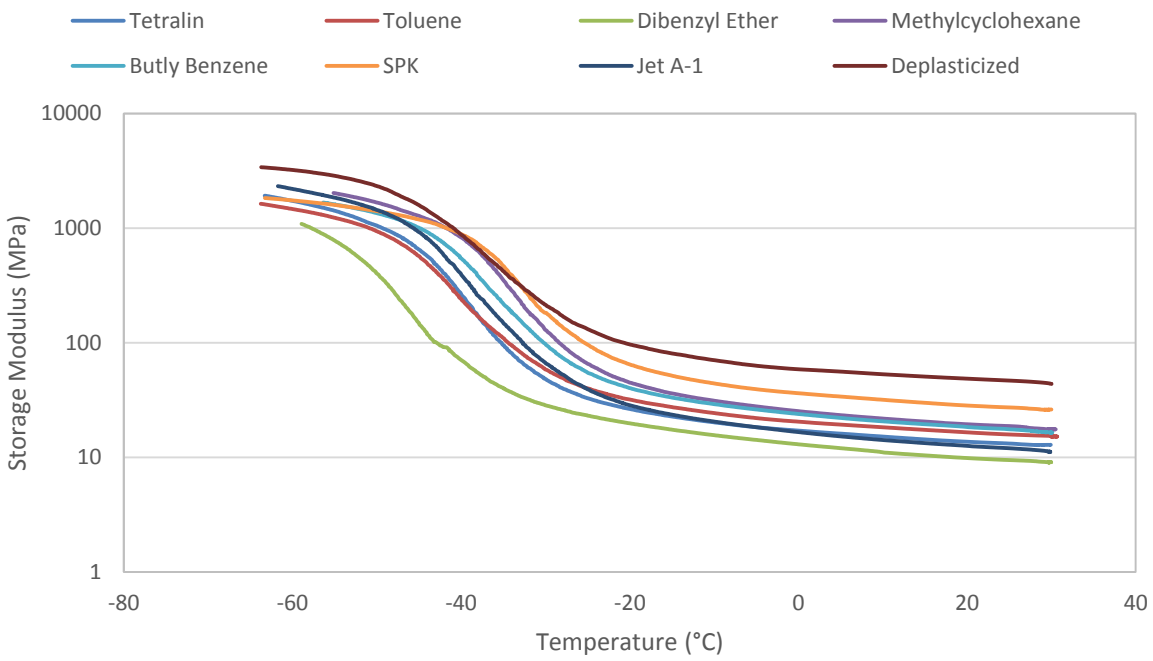

Figure 7.1: Storage modulus as a function of temperature for NBR elastomer samples exposed to 7 different fuel blends

The behaviour of a deplasticised NBR sample has been used as a point of reference for all DMA work. The minimum operating temperature in service is not likely to be less than -10°C. Testing, however, has been conducted from -65°C to assess performance across a wider temperature range. Ideally, the performance of the storage modulus (E') should remain steady through operation above -10°C. Figure 7.1 shows a gradual decay in E' with increasing temperature.

The change in the loss modulus (E'') due to fuel exposure is described in Figure 7.2. E'' represents the ability of the material to convert mechanical energy into heat through viscous frictional forces. E'' is a key indicator of the overall functionality that fuel exposure has on the elastomer materials [58]. Figure 7.2 shows that the deplasticised NBR sample exhibits the greatest E'' at room temperature . Fuel exposure causes a decrease in E'' across the board when measured at 25°C.

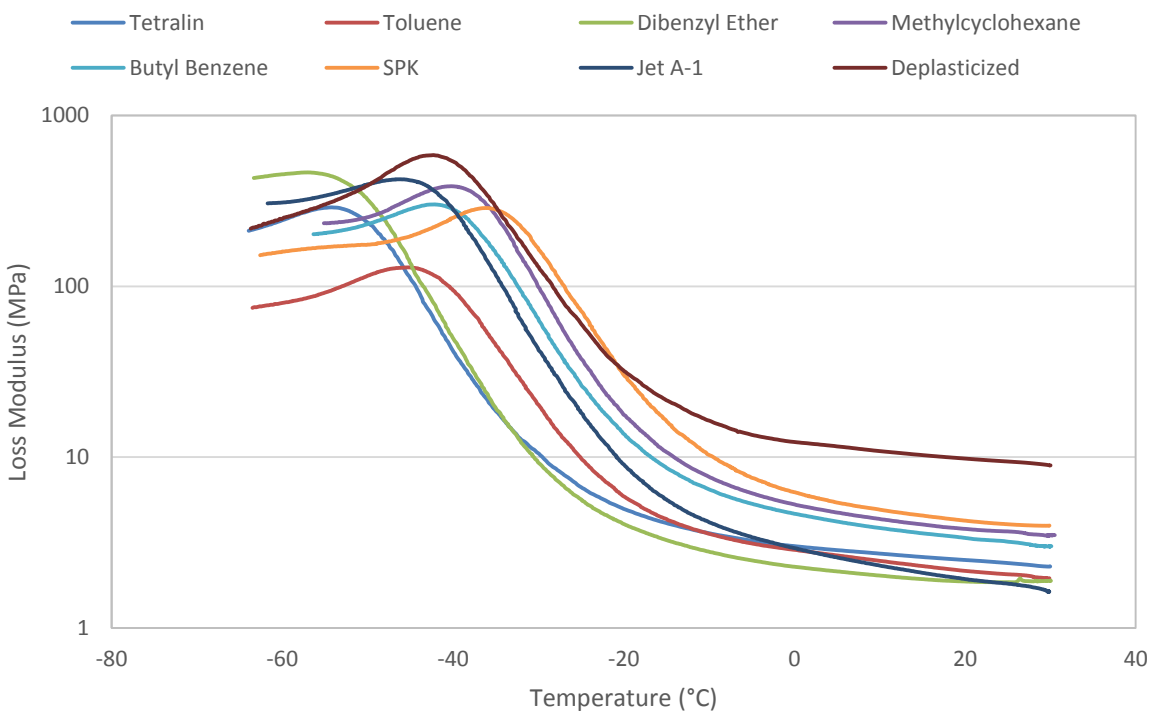

Figure 7.2: Loss modulus performance as a function of temperature of NBR elastomer samples exposed to 7 different fuel blends

The change in tan δ as a function of temperature is illustrated in Figure 7.3. *tan δ* is the ratio of the loss modulus to the storage modulus. Along with the storage modulus, changes in *tan δ* are useful indictors of an elastomer's response to changing environments [58]. In particular,

the peak of the tan δ curve is often recorded as the T_g for the material under testing. The deplasticised NBR sample has again, been taken as the reference point. Deplasticised NBR has a T_g of approximately -26°C and as such it is important that fuel exposure does not cause an increase the T_g value. A greater T_g reduces the operational range of the elastomer material.

All fuel-wetted elastomer samples showed a decrease in the T_g value. This is desired behaviour and indicates that the sealing performance of the elastomer samples will not be hindered by the reduced operational range. Exposure to dibenzyl ether and tetralin blends resulted in the greatest decrease in T_g. The interaction of the dibenzyl ether blend with the elastomer samples has resulted in the greatest overall change in the dynamic mechanical properties of the elastomer.

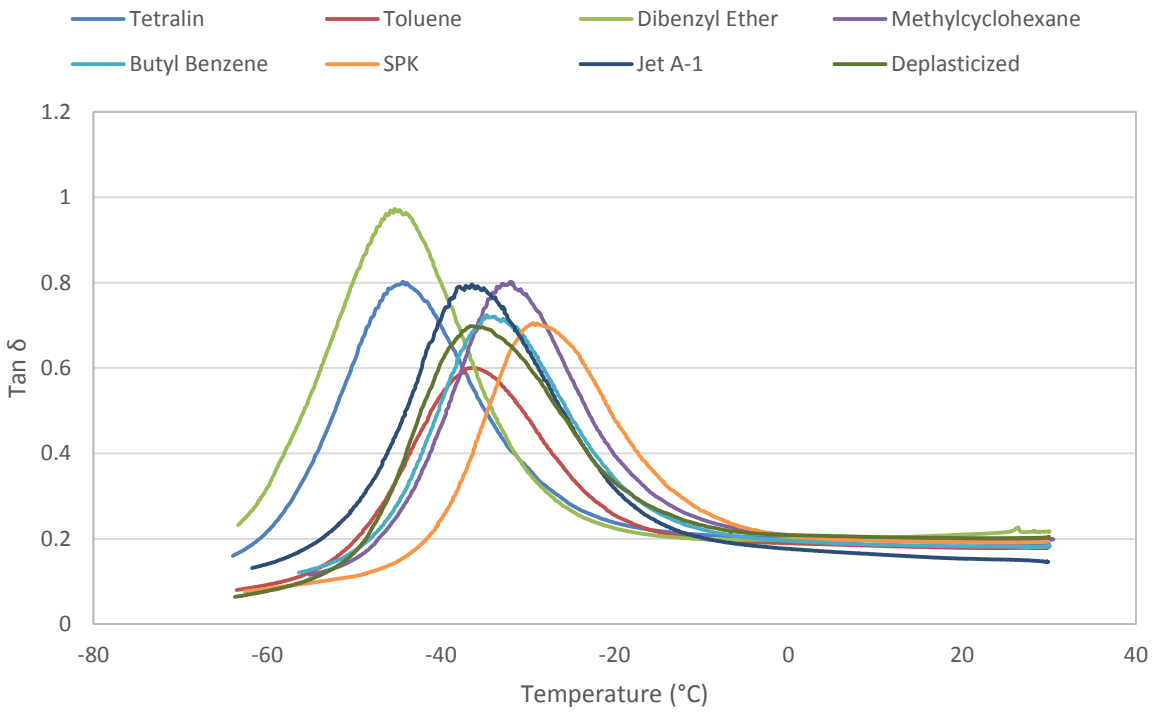

Figure 7.3: tan δ as a function of temperature for NBR elastomer samples exposed to 7 different fuel blends

An analysis of the relationship between the glass transition temperature (determined by DMA) and the change in volume upon swelling can be found in Figure 7.4. The relationship is approximately linear although some species such as tetralin lie off the linear trend.

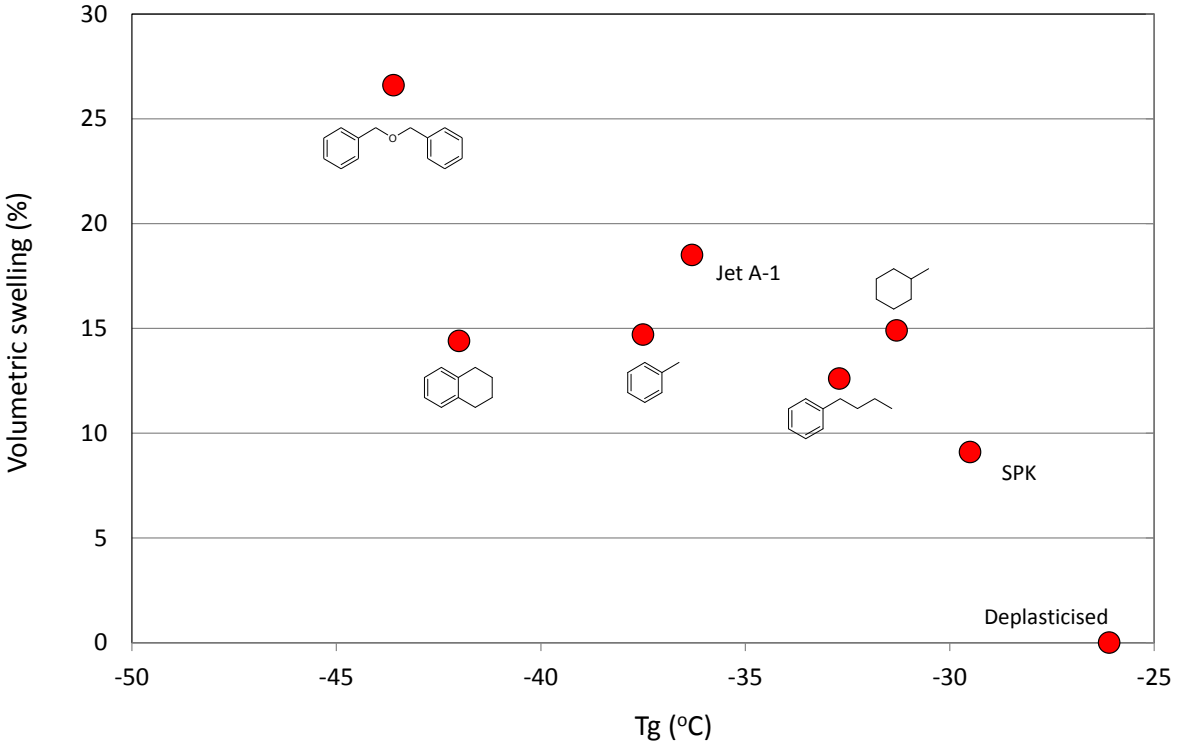

Figure 7.4: Relationship between extent of swelling and glass transition temperature

Because swelling forces the elastomer chains apart, the chains are more able to rotate and slip past each other. This effectively lowers the barrier to chain slippage at any temperature . Consequently the chains acquire sufficient energy to overcome the barriers to slippage at lower temperature. This manifests itself as a reduction in the glass transition temperature.

Figure 7.5 illustrates that as the extent of swelling increases, the complex modulus decreases. Although the relationship might appear to be linear for most of the blends and fuels tested it is in actual fact asymptotic. While swell can exceed 100%, with some pure aromatics, modulus can never be less than zero. A plot of volumetric swelling vs the logarithm of modulus, however, is near a straight line. This has the consequence that as NBR swells, it softens in a near predictable way. Note that the volumetric swell for the as-received sample is the difference in volume between the as-received and deplasticised O-form.

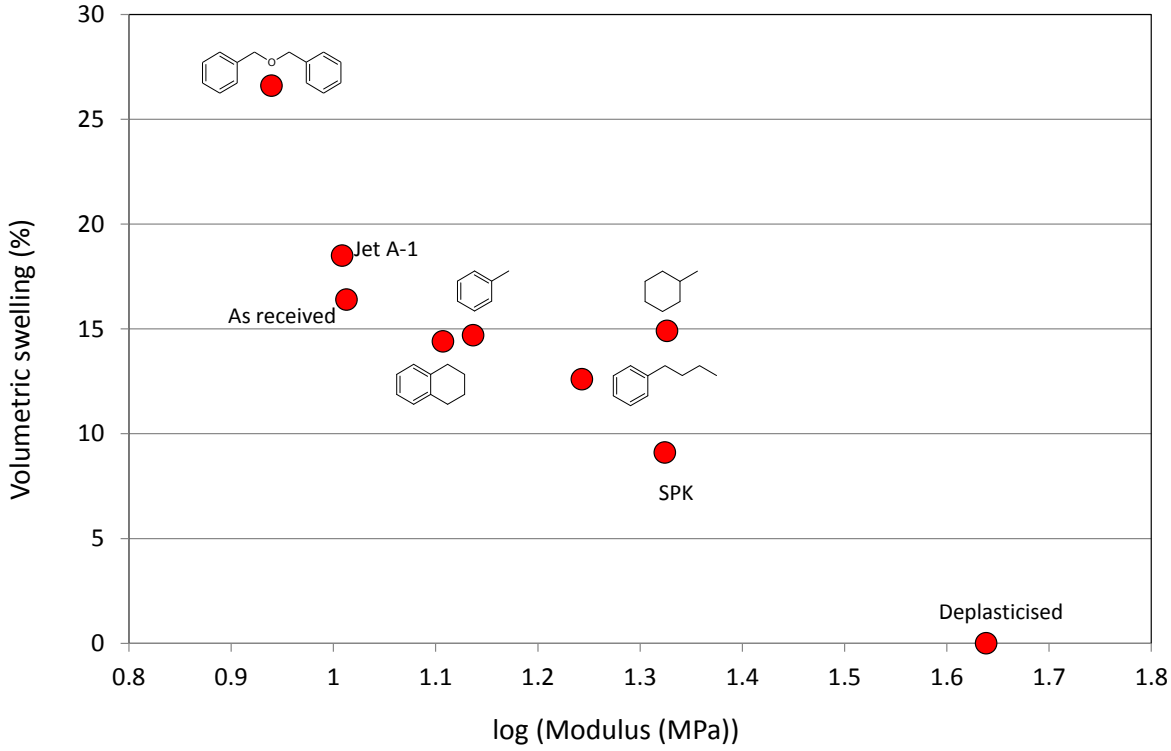

Figure 7.5: Relationship between extent of swelling and complex modulus at 25°C

Volumetric swelling measurements can be used as predictors of changes in the physical properties of NBR O-rings. In particular swelling may be used to predict changes in glass transition temperature and modulus.

7.3 Tensile response of fuel-wetted elastomers

The tensile response of elastomer materials is primarily used as a method of quality control screening. However, for elastomers utilised in dynamic sealing applications a minimum tensile strength of 6.9MPa is required to be maintained [60]. A convenient way to infer the potential change in the sealing ability of an elastomer sample is to monitor the response of the Young's modulus under changing environments. Depending on the sealing application, it is important that the elastomer maintain adequate stiffness and flexibility. In the case of static sealing, increased stiffness, or Young's modulus, potentially allows a greater pressure to be applied to the sample. Moreover, with increased applied pressure, a greater sealing force can be established between the two adjacent surfaces. If, however, a dynamic sealing environment is envisioned, it is appropriate for the elasticity not to change significantly. Elastomers which are required for dynamic sealing applications and show increased stiffness under changing environments are prone to premature failure.

Since seals are designed to operate well away from their breaking point, the discussion that follows focusses on modulus rather than ultimate tensile strength. The force at 100% extension after exposure to various conditions is presented in Table 7.3. The elastomer performance is presented in Figure 7.6 for greater clarity.

Table 7.3: Tensile response of fuel-wetted NBR elastomer samples

Condition	**Wet**	**Dry**
Blend	**Force at 100% extension (N)**	
as-received	20.9(0.8)	
deplasticised	38.7(1.1)	
SPK	34.3(1.4)	39.2(1.0)
Jet A-1	34.7(0.5)	40.7(0.5)
toluene	34.0(0.8)	43.4(0.7)
tetralin	34.2(0.5)	44.4(1.0)

Values in parentheses are the standard deviation of the mean. N = 3

The deplasticised elastomer sample is used as the point of reference for this investigation. The term “Dry” preceding the type of fuel blend refers to samples which have been dried at 50°C for 24 hours following fuel exposure. Force is presented at an extension which is equivalent to 100% extension of a deplasticised O-ring.

Typically, what is observed is that the force at 100% extension decreases across exposure to the varying fuel blends. In comparison to the reference sample a decrease of approximately 12% in the force was observed for all fuel exposed samples. A decrease in stiffness is expected as exposure to fuel will result in elastomer swelling. Swelling increases the free volume within the polymer matrix, allowing chains greater mobility before deformation and failure. The decrease in force was insignificant between different hydrocarbon additives. Moreover, the force reduction is unlikely to impact significantly on the static sealing performance of the elastomer.

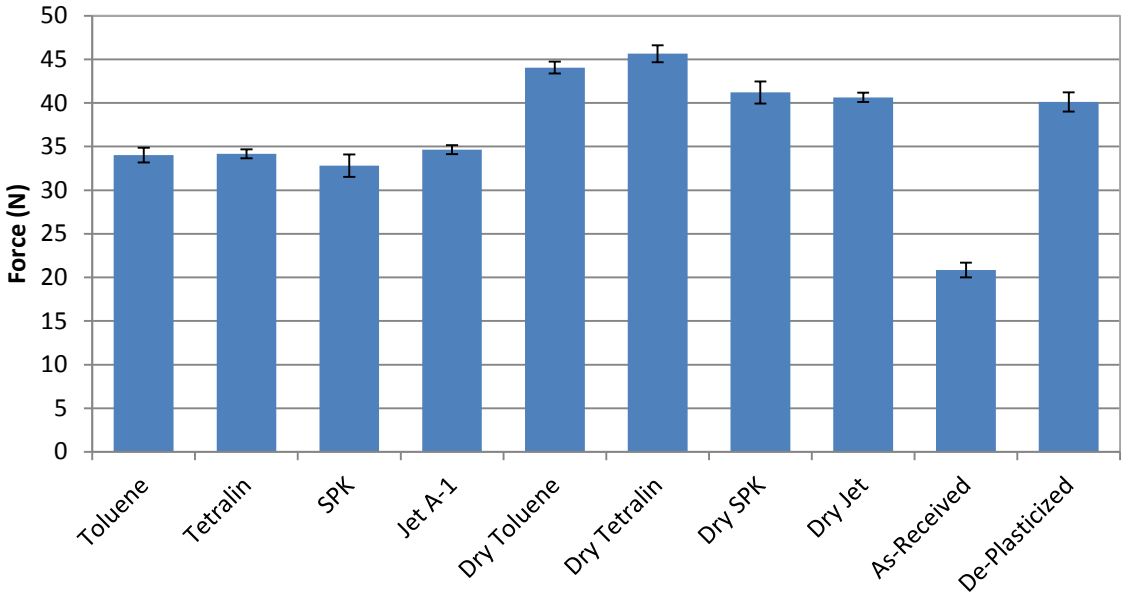

Figure 7.6: Tensile response of elastomer sample to various conditioning methods

As mentioned, drying the sample for 24 hours prior to evaluation of the tensile response was adhered to. Again, all samples are compared against the deplasticised reference sample for performance reviews. Samples dried after exposure to toluene and tetralin, unlike those exposed to SPK and Jet A-1, displayed increases in the force at 100% elongation. These increases were significant when compared to the deplasticised reference sample. The reasons behind the increased force are not clear. It is possible that additional crosslinking has taken place during fuel exposure. An increase in cross-link density would increase the modulus of the dry material thus requiring a greater force for a set extension.

For the base fuel exposed samples, no significant variation from the reference sample was observed. It was thought that 24 hours drying time was insufficient to remove the fuel already present in the polymer. Thermogravimetic analysis was performed and results indicate that all fuel had been removed from the sample.

Because elastomers are non-Hookean, they are often characterised by M_{100} (100% modulus). M_{100} is the stress at 100% extension and reflects an average rather than a true modulus.

Table 7.4 contains apparent M_{100} and real M_{100} values for swollen NBR elastomers. The apparent M_{100} is obtained by dividing the force by the original cross-sectional area of the deplasticised sample. The real value is obtained by dividing the force by the swollen cross-section. Note that in the case of dried samples, the apparent and real M_{100} values are the same.

Table 7.4: M_{100} of fuel-wetted NBR elastomer samples

Condition	Wet		Dry
Blend		M_{100} (MPa)	
	Apparent	Real	Real
as-received		4.2	
deplasticised		9.0	
SPK	8.0	7.6	9.2
Jet A-1	8.1	7.2	9.5
toluene	8.0	7.3	10.1
tetralin	8.0	7.3	10.4

The data would seem to suggest that increased swelling softens the materials (reflected by the reduction in real M_{100}). SPK which swells the least had the highest M_{100}, indicative of a stiffer material. It is also apparent that the swelling with fuel does not compensate for the removal of plasticiser. This would suggest that the deplasticisation process employed had an effect over and above the simple removal of plasticiser. It is unclear whether this is a chemical effect as a result of the use of dichloromethane for extraction or whether it is the result of the fact that during deplasticisation, excessive swelling occurs, leading to a temporarily strained rubber network. Note that 100% extension at which the M_{100} values are reported is significantly greater than the strain induced under normal swelling conditions. Note that because the strain is large at M_{100}, M_{100} can differ significantly from the complex modulus determined by DMA at very small strains.

7.4 Compression set testing

The compression set response of elastomer samples to fuel exposure is described by Figure 7.7. Switching from air to fuel exposure happened after 14 days and is indicated by the dashed line. Most notably, exposure of the fuel blends produces a substantial increase in the compression set response. In particular, the response to dibenzyl ether exposure was in excess of 90%, a relative compression set increase of approximately 41% after air exposure. Exposure to cumene and tetralin produced a compression set response in excess of 80%. Interestingly, elastomer submersion in Jet A-1 resulted in an increase in set of approximately 17% after air exposure, whereas exposure to SPK saw almost no change in the set response.

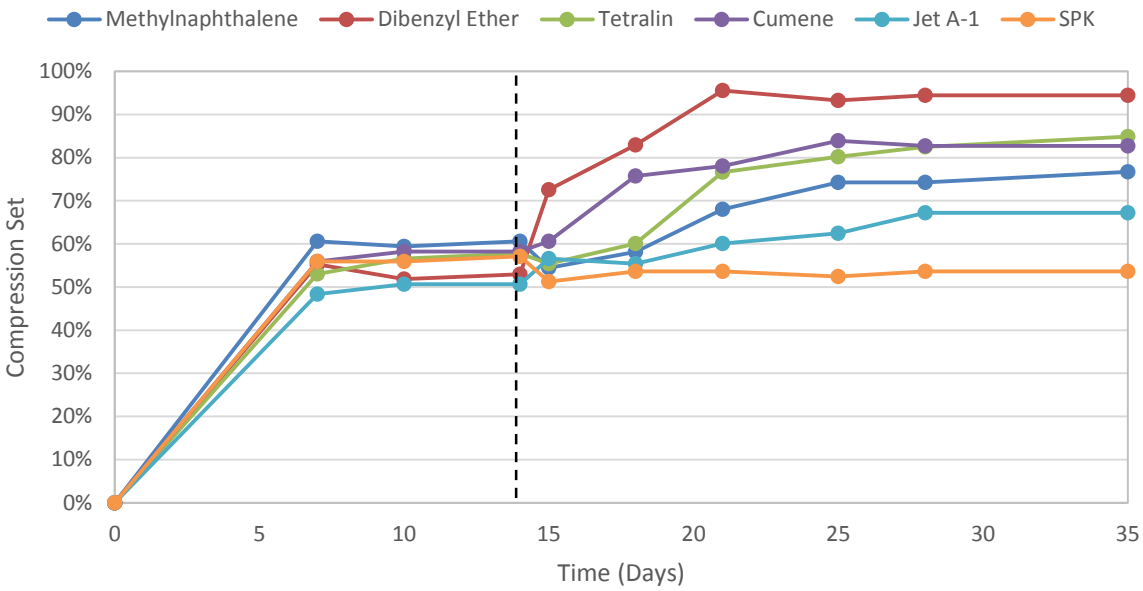

Figure 7.7: Compression set response of NBR elastomer samples exposed to air and fuel blend environments.

Numerous reasons exist to explain the compression set response of NBR elastomers exposed to different fuel blends. The primary effect behind compression set is the formation of additional crosslinks within the polymer backbone [66]. This set behaviour can be more adequately appreciated by viewing the equilibrium swelling profiles in Appendix A. A slight decrease in the swelling is occurring for samples exposed to blends at 50°C. What this suggests, is that additional crosslinking is occurring, driving down the observed volumetric swell but at the same time increasing the observed set behaviour of the elastomer. At even higher temperatures, such as in the case of the compression set testing, greater additional crosslink density can be expected. Numerous other factors may result in increased set including fluid exposure and the presence of plasticisers and fillers loaded into the polymer matrix.

The influence of solvent exposure on the crosslink density of the elastomer materials is potentially a factor contributing to the compression set response. Dibenzyl ether is observed to impact significant set response of NBR samples. In parallel with this, dibenzyl ether also imparts large swelling on the elastomer sample. It is likely that there is a correlation between these observations. The ether compound contains oxygen within its structure. Slater *et al* [69] observed that the compression set response of polyurethane increased when exposed to oxygen-containing compounds. The authors attributed this behaviour to the addition of hydrogen-bonding occurring along the polymer backbone. Similarly, dibenzyl ether has a large hydrogen-bonding energy, or solubility parameter (δ_h = 5.20). As described in earlier

discussions, the presence of such a large δ_h energy – and in particular the oxygen atom - increases the likelihood of strong interactions between the highly polar cyan-group present in the NBR backbone and the ether compound. It is inferred that this strong interaction leads to the formation of new and the severing of old crosslinks existing within the polymer backbone.

As these occur while the sample is under compression, the crosslinks responsible for strain recovery may either be outweighed by these new crosslinks, or even severed by the additional crosslink formation [68, 69]. Reduction in the density of crosslinks responsible for strain recovery is potentially a driving factor in explaining the large set response experienced by elastomer samples exposed to dibenzyl ether. The compression set response for cumene, tetralin and methylnaphthalene fuel blends may be assumed to follow similar reasoning. These three compounds show much smaller δ_h values compared to dibenzyl ether. As such it is assumed that their interaction with the NBR backbone is of a smaller magnitude and the overall set response will be less pronounced.

Temperature is another factor adding to the degree of compression set observed. Generally speaking, set response increases with increasing temperature. Compression set testing was performed at 80°C drive home the temperature effect on compression set. At such elevated temperatures, there is a possibility that crosslink density within the elastomer sample will increase. Faster reaction kinetics at higher temperatures can promote crosslink formation, something that would be unfavourable at ambient temperatures. Slater *et al.* [69] went on to suggest that at elevated temperatures, the profound increase in the rate of solvent/fuel sorption into the polymer matrix can disrupt the chain order, which in turn, affects the strain recovery of the elastomer. In this case, compression set testing was performed at only one temperature. Further work at different temperatures was deemed beyond the scope of this study.

CHAPTER 8

8. Conclusions

This investigation focused on the effect of hydrocarbon and temperature exposure on NBR seals. Additionally, the effect fuel exposure has on the physical properties of NBR seals has been investigated. The following conclusions have been drawn:

8.1 Effect of hydrocarbon type on swelling

The swelling performance of elastomers exposed to a variety of hydrocarbon blends showed some marked trends. Hansen solubility parameters and Flory-Rehner interaction parameter models were used as the basis for the prediction of the swelling behaviour. Minimising the difference in solubility parameters between solvent and elastomer resulted in greater observed swelling. Hydrocarbons that exhibited large δ_d and δ_h parameters were observed to impart greater swelling on the fuel-wetted elastomer samples. Indene, methylnaphthalene and benzyl alcohol are examples of solvents containing large δ_d and δ_h values. The association of these parameters with the highly polar and electronegative cyano-group located on the polymer backbone is sound reasoning behind the observed increase in swelling behaviour.

It is suggested that the most ideal aromatic would have a small molar volume with high polyaromaticity. However, flash point and smoke point restrictions would mean that hydrocyclic aromatics such as tetralin show the most promise followed by C9 monomaromatics.

The addition of cycloparaffins was demonstrated to contribute to increased swelling. As with aromatic compounds, increasing the number of ring structures increased the extent of swelling. This is ascribed to reduced molar volume and increased dispersion interactions. Although cycloparaffins are restricted to a maximum of 15% (v/v) in FSFJ at present, it is possible to achieve acceptable seal swell behaviour with higher concentration blends. It is suggested that blending cycloparaffins in combination with aromatics could reduce the amount of aromatics required for acceptable swelling.

The inclusion of oxygenated species increases the extent of swelling. These species can also allow reduced aromatics to be used, especially where these oxygenates are aromatic. Cyclisation again increases the extent of swell observed.

8.2 Switch-loading behaviour

NBR elastomers were switched from three different fuel blends to pure Jet A-1, pure SPK and a 50:50 blend of SPK and Jet A-1. In all three cases, the swelling response did not drop below swelling values for exposure to pure SPK. In the case of switching from the fuel blend to pure SPK, a large reduction in volume swell was observed. This behaviour is indicative of preferential solvent uptake and the degree of volume oscillation could likely increase the stresses on the elastomer material.

8.3 The effect temperature on the swelling of NBR

For hydrocarbons blended with SPK, increasing temperature increased the extent of swelling observed. This is ascribed to the endothermic nature of the interaction between these species and NBR. Increasing the polar and hydrogen bonding solubility parameters decreased the sensitivity to temperature, notably with d-iaromatics. A similar effect was seen with Jet A-1. It is suggested that in this cases, significant concentration of the aromatic present in the NBR. It is suggested that for entropic reasons, less concentration of the aromatic species in the NBR takes place at elevated temperature. This then leads to an effect which counteracts the endothermic nature of the interactions causing lower temperature sensitivity.

Unlike cycloparaffinic and n-paraffinic oxygenates, aromatic oxygenates decreased in swelling with temperature. A specific interaction between these aromatic oxygenates and NBR is postulated which is destabilised at elevated temperatures. This interaction is expected to be endothermic in nature. By contrast non-aromatic oxygenate mixtures with SPK are expected to become less stable with temperature. As a result increasing the temperature is expected to lead to separation of the constituents through concentration of the oxygenate in the NBR. This in turn increases swelling with increasing temperature.

8.4 Fuel and temperature effects on FKM elastomers

FKM elastomers were less sensitive to fuel composition. Classes that display significant differences when swelling NBR displayed much reduced differences when swelling FKM. However, the sensitivity of the swelling of FKM to temperature was greater. This may be the

result of FKM being more polar than NBR. This would make the enthalpy of sorption for the interaction between FKM and hydrocarbons larger than between hydrocarbons and NBR. An increased ΔH_{mix} would then cause increased temperature sensitivity. It is possible that the interactions of aromatic oxygenates with FKM are in turn more exothermic.

8.5 The effect on physical properties of NBR exposure to fuels

The use of dynamic mechanical analysis was used as an indicator of the change in sealing performance of NBR elastomer seals exposed to a variety of fuel blends. Ideally, fuel exposure should cause as little change in DMA properties as possible. Of particular interest is the change in storage modulus and Tg. It was observed that in general an increase in the extent of swelling caused a greater decrease in the T_g and the storage modulus. These parameters may be used as proxies for the extent of swelling.

8.6 Tensile and compression-set response of fuel-wetted NBR elastomers

The tensile response of fuel-wetted elastomers was used as a method to monitor the change in the static and dynamic sealing properties of the material. The Young's modulus decreased slightly for fuel-wetted samples which could impact the dynamic sealing ability of the material. However, the decrease in Young's modulus was relatively small and, as such, the impact on the dynamic and static sealing behaviour could be expected to be minimal, in the absence of compression set.

The compression set response of fuel-wetted NBR elastomers is an important property contributing to the overall sealing performance of the material. The set response was recorded at elevated temperatures of 80°C. At such high temperatures, the large increase in the rate of solvent permeation into the elastomer matrix has likely disrupted the chain order. While under compression, chain disruption may adversely affect the strain recovery of the elastomer leading to greater compression set observed. Additionally, an increase in the crosslink density due to temperature elevation may be a contributing factor towards the large compression set response observed.

CHAPTER 9

9. Recommendations

A number of recommendations for further investigation are made to address issues that were deemed beyond the scope of the current investigation

9.1 Preferential uptake analysis

This dissertation has eluded to the fact that sorption response and display of sealing properties may be influenced by preferential uptake of certain solvents over others. Acquiring this knowledge would be extremely valuable towards the overall understanding of the swelling behaviour of elastomer materials. The use of TGA-MS, pyrolysis GC-MS and/or standard gas chromatography of extracted components could be employed. It is recommended that such studies be performed on binary blends such as n-dodecane blended with various aromatic species. This would simplify the analysis. It would also reduce the thermodynamic complexity of the system.

9.2 Swelling caused by polar species

Elastomer-aromatic oxygenate systems have been shown to exhibit exothermic heats of mixing. Further, elastomer exposure to aromatic oxygenates has resulted in large changes in the sealing properties of NBR elastomers. It would be of particular interest to observe similar elastomer responses but using additional polar molecules. These could include cyclic ethers for instance as well as aromatic species with other polar moieties. While these components would not be suitable for inclusion in a FSJF, they would shed further light on the processes underlying the temperature sensitivity of swelling.

9.3 Computational modelling of swelling and mixing

Limitations with the Flory-Rehner and Hansen Solubility Models exist. The basis has been covered throughout this dissertation. As such, the framework for preliminary computational

modelling of elastomer swelling behaviour exists. This would require modelling using an appropriate software interface as well as and appropriate theory such as Moller-Plesset. With this in place the ability to model the swelling behaviour of numerous elastomers exposed to various solvent exists. Such modelling could be used to assess the enthalpy of interaction between the various fuel components and NBR as well as with FKM. This is especially true of aromatic oxygenates which do not obey conventional endothermic behaviour. Further modelling could shed light on the stability of fuel mixtures (as represented by their free energies) as a function of temperatures [86]. This would be important in explaining the contrasting behaviour of non-aromatic oxygenates. Vapour-liquid-equilibrium (VLE) modelling of solutions using a model such as UNIFAC could be attempted.

9.4 Submersible DMA testing

DMA testing proved extremely valuable during this investigation. Additional testing using submersible DMA grips is likely to prosee greater depth to the analysis of the elastomers sealing performance. Samples can be submerged in a fuel of choice under ambient conditions and the compression performance of the elastomer is measured. This type of testing would prosee information on both the static and dynamic sealing characteristics of the material and the extent to which fuel exposure affects these properties. Important information on the uptake of components during switch-loading and their effect on physical properties could be obtained. It is also recommend that experiments be performed using thermomechanical analysis (TMA) instrument or using a DMA equipped with a TMA compression clamp.

9.5 Expanded set of blends for FKM swelling

A restricted set of blends were used to swell FKM elastomers. A larger set could be used to investigate further the factors that drive FKM swelling, as was done in this study for NBR. Furthermore, additional experiments would shed light on the thermodynamic factors influencing the temperature sensitivity of swelling. FKM elastomers would be ideal for a general study, given the high sensitivity observed in this study. Furthermore the same set of experiments could be extended to another aviation elastomer, fluorosilicone. Finally, the role of changing crosslink density on the swelling response of these elastomers should be more thoroughly investigated.

9.6 Relationship between compression set and swelling

The relationship between compression set and swelling should be explored further. The work in this study should be extended by performing compression set at other temperatures.

CHAPTER 10

Bibliography

[1] E. Corporan, T. Edwards, L. Shafer, M. J. DeWitt, C. Klingshrin, S. Zabarnick, Z. West, R. Striebich, J. Graham and J. Klein, "Chemical, Thermal Stability, Seal Swell and Emissions Studies of Alternative Jet Fuels," *Energy & Fuels,* vol. 25, pp. 955-966, 2011.

[2] G. Heminghaus, T. Boval, C. Bosely, R. Organ, J. Lind, R. Brouette, T. Thompson, J. Lynch and J. Jones, "Alternative Jet Fuels," Chevron Corporation, San Raman, CA, 2006.

[3] D. Anderson, "How low can you go? Aviation fuel needs to reduce its aromatic content-but by how much?," The University of Sheffield, Sheffield, UK, 2011.

[4] C. Moses, "CRC Project No. AV-2-04a: Comparative evaluation of semi-synthetic jet fuels," Coordinating Research Council, Alpharetta, GA, 2008.

[5] "DEF STAN 91-91, Issue 7, Turbine fuel, aviation kerosene type, Jet A-1," Defence Equipment and Support, UK Ministry of Defence, Glasgow, UK, 2011.

[6] "ASTM Standard D7566. Standard specification for aviation turbine fuel contaning synthesized hydrocarbons," ASTM International , West Conshohocken, PA, 2008.

[7] C. Moses and P. Roets, "Properties, characteristics and combustions performance of Sasol fully synthetic jet fuel," in *ASME Turbo Expo 2008: Power for Land, Sea and Air*, Berlin, Germany, 2008.

[8] J. L. Graham, R. C. Striebich, K. J. Myers, D. K. Minus and W. E. Harrison, "Swelling of Nitrile Rubber by Selected Aromatics Blended in a Synthetic Jet Fuel," *Energy & Fuels,* pp. 759-765, 2006.

[9] R. Burnham, "The effect of different chemical classes on the swelling of NBR O-rings in blends with synthetic paraffinic kerosene," M.Sc. dissertation, University of Cape Town, Cape Town, South Africa, 2012.

[10] "Energy technology perspectives: scenarios and strategies to 2050," International Energy Agency, Paris, 2010.

[11] J. Gary, G. E. Handwerk and M. Kaiser, Petroleum refining: Technology and economics, Boca Raton, FL: CRC Press, 2010.

[12] "ASTM Standard D1655," ASTM International, West Conshohocken, PA, 2009.

[13] "Fuel properties - effect on aircraft and infrastructure," FAA Aviation Rulemaking Advisory Committee, Washington DC, 2008.

[14] R. van der Westhuizen, M. Ajam, P. de Coning, J. Beens, A. de Villiers and P. Sandra, "Comprehensive two-dimensional gas chromatography for the analysis of synthetic and crude-derived jet fuels," *Journal of Chromatography A,* vol. 1218, pp. 4478-4486, 2011.

[15] A. R. Brandt and A. Farrell, "Scraping the bottom of the barrel: greenhouse gas emission consequence of a transition to low-quality and synthetic petroleum resources," *Climate Change,* vol. 84, pp. 241-263, 2007.

[16] A. de Klerk, "Hydroprocessing peculiarities of Fischer-Tropsch syncrude," *Catalysis Today,* vol. 130, pp. 439-445, 2008.

[17] M. Dry, "The Fischer-Tropsch process: 1950-2000," *Catalysis Today,* vol. 71, pp. 227-241, 2002.

[18] "Replacing the whole barrel to reduce US dependence on oil," US Department of Energy, Washington, DC, USA, 2013.

[19] L. Lucia, "Lignocellulosic biomass: a potential feedstock to replace petroleum," *Bioresources,* vol. 3, pp. 981-982, 2008.

[20] D. Lamprecht, L. Dancuart and K. Harrilall, "Performance Synergies between Low-Temperature and High-Temperature Fischer-Tropsch Diesel Blends," *Energy & Fuels,* vol. 21, pp. 2846-2852, 2007.

[21] M. Dry, "High quality diesel via the Fischer-Tropsch process-a review," *Journal of Chemical Technology and Biotechnology,* vol. 77, pp. 43-50, 2001.

[22] A. Steynberg and M. Dry, Fischer-Tropsch Technology, Amsterdam, Netherlands: Elsevier, 2004.

[23] A. Steynberg, R. Espinoza, B. Jager and A. Vosloo, "High temperature Fischer-Tropsch synthesis in commercial practice," *Applied Catalysis,* vol. 186, pp. 41-54, 1999.

[24] B. Jager and R. Espinoza, "Advances in low temperature Fischer-Tropsch synthesis," *Catalysis Today,* vol. 23, pp. 17-28, 1995.

[25] C. Moses, L. Stavinoha and P. Roets, "SwRI-8531: Qualification of Sasol Semi-Synthetic Jet A-1 as Commercial Jet Fuel," South West Research Institute, San Antonio, TX, 1997.

[26] E. Corporan, T. Edwards, L. Shafer, M. DeWitt, C. Kingshirn, S. Zabarnick, Z. West, R. Striebich, J. Graham and J. Klein, "Chemical, Thermal Stability, Seal Swell and Emissions Studies of Alternative Jet Fuels," *Energy&Fuels,* vol. 25, no. 3, pp. 955-966, 2011.

[27] M. Pearlson, C. Wollersheim and J. Hileman, "Modeling and analysis: The techno-economics of renewable jet fuel production Biofuels," *Biofuels, Bioproducts and Biorefining,* pp. 89-95, 2012.

[28] L. Siswati, M.-A. Paivi, J. Beltramini, G. Max-Lu and D.-Y. Murzin, "Transforming Triglycerides and Fatty Acids into Biofuels," *ChemSusChem,* vol. 2, no. 12, pp. 1109-1119, 2009.

[29] "IATA 2011 Report on alternative fuels," International Air Transport Association, Montreal, Canada, 2011.

[30] J. Cowie and V. Arrighi, Polymers: Chemistry and physics of modern materials, Boca Raton, FL: CRC Press, 2008.

[31] L. Sperling, Introduction to physical polymer science, New York, NY: John Wiley & Sons, 2001.

[32] A. Patil and T. Coolbaugh, "Elastomers: A literature review with emphasis on oil resistance," *Rubber Chemistry & Technology,* no. 78, pp. 516-535, 2005.

[33] V. Lachat, "Understanding oil resistance of nitrile rubber: CN group interactions at interfaces," Ph.D. thesis, University of Akron, Akron, Ohio, 2008.

[34] J. A. Brydson, Rubber Chemistry, Barking, UK: Applied Science Publishers, 1978.

[35] H. L. Stephens, Basic Elastomer Technology, Akron, Ohio: The Rubber Division, 2001.

[36] Parker Hannifin Corporation, Parker O-ring Handbook, Cleveland, OH: Parker Hannifin Corporation, 2007.

[37] DuPont Corporation, "Viton and Vamac families: chemical structure and monomer composition," DuPont Corporation, Wilmington, 2010.

[38] R. Ohm, The Vanderbilt Rubber Handbook, Norwalk, CT: R.T Vanderbilt Company Inc., 1990.

[39] D. Teegarden, Polymer Chemsitry: Introduction to an indespensible science, Arlington, V: National Science Teachers Association, 2004.

[40] M. Rahman and C. S. Brazel, "The plasticizer market: an assessment of traditional plasticizers and research trends to meet new challenges," *Progress in Polymer Science,* no. 29, pp. 1223-1248, 2004.

[41] H. Bertram and D. Brandt, "Influence of lubricating oil additives on swell-resistant elastomers," in *Division of Rubber Chemistry, American Chemical Society*, Boston, MA, 1972.

[42] M. Garbarczyk, K. Winfried, J. Klinowski and S. Jurga, "Characterization of aged nitrile rubber elastomers by NMR spectroscopy and microimaging," *Polymer,* no. 43, pp. 3169-3172, 2002.

[43] J. White, "Polymer ageing: physics, chemistry or engineering? Time to reflect," *Comptus Rendus Chemie,* no. 9, pp. 1396-1408, 2006.

[44] Z. Tao, N. Viriyabanthorn, B. Ghumman, C. Barry and J. Mead, "Heat resistant elastomers," *Rubber Chemistry and Technology,* vol. 78, pp. 489-515, 2005.

[45] V. Subramanian and S. Ganapathy, "Aging of vulcanisates of formulations of rubber seals," *Journal of applied polymer science,* no. 70, pp. 985-994, 1998.

[46] K. Azaar, J. Vergnaud and I. Rosca, “Anisotropic swelling behaviour of EPDM rubber disks by absorption of toluene,” *Rubber Chemistry and Technology,* vol. 76, no. 4, pp. 1031-1039, 2003.

[47] P. Westbrook and R. French, “Elastomer swelling in mixed solvents,” *Rubber Chemistry and Technology,* vol. 72, no. 1, pp. 74-90, 1999.

[48] P. J. Flory, Principles of Polymer Chemistry, Ithaca: Cornell University Press, 1953.

[49] P. J. Flory and J. Rehner, “Statistical Mechanics of Crosslinked Polymer Networks II. Swelling,” *Journal of Chemical Physics,* vol. 11, pp. 512-520, 1943.

[50] J. Hildebrand and R. L. Scott, Regular Solutions, Englewood Cliffs, NJ: Prentice Hall , 1962.

[51] C. Hansen, Hansen Solubility Parameters: A User's Handbook, Boca Raton, FL: CRC Press, 2007.

[52] S. George and S. Thomas, “Transport phenomena through polymeric systems,” *Progress in Polymer Science,* vol. 26, pp. 985-1017, 2001.

[53] M. DeWitt, E. Corporan, J. Graham and D. Minus, “Effects of aromatic type and concentration in Fischer-Tropsch fuel on emissions production and material compatibility,” *Energy & Fuels,* no. 22, pp. 2411-2418, 2008.

[54] J. Graham, D. Minus and T. Edwards, “The Effect of Aromatic Type on the Volume Swell of Nitrile Rubber in Selected Synthetic Paraffinic Kerosenes,” in *International Conference on Stability, Handeling and Use of Liquid Fuels*, Sarasota, FL, 2011.

[55] A. Joseph, A. Mathai and S. Thomas, “Sorption and diffusion of methyl substituted benzenes through cross-linked nitrile rubber/poly(ethylene co-vinyl acetate) blend membranes,” *Journal of Membrane Science,* no. 220, pp. 13-30, 2003.

[56] S. Visram, “A novel method to evaluate synthetic fuel options for gas turbines in terms of O-ring swelling.,” M.Sc. dissertation, University of Cape Town, Cape Town, 2009.

[57] R. P. Compton, B. Thomson and J. A. Harris, “Elastomers for fluid containment in offshore oil and gas production: Guidlines and review,” *Health and Safety Excutive,* pp. 1-111, 2005.

[58] C. Lin, C. Chieb, J. Tan, Y. Chao and J. Van Zee, "Dynamic mechanical characteristics of five elastomeric gasket materials in a simulated and an accelrated PEM fuel cell environment," *Hydrogen Energy ,* no. 36, pp. 6756-6767, 2011.

[59] A. Pinheiro and J. Mano, "Study of gass transition on viscous-forming and poweder materials using dynamic mechanical analysis," *Polymer Testing ,* no. 28, pp. 89-95, 2009.

[60] "ASTM Standard D1414-94. Standard test method for rubber O-rings," ASTM International, West Conshohocken, PA, 2008.

[61] M. Achenbach, "Development of a robust fuel circuit sealing system: Defining the problem," *Sealing Technology,* pp. 10-13, 2007.

[62] M. Achenbach, "Development of a robust fuel circuit sealing system: Achieving a solution," *Sealing Technology,* pp. 7-10, 2007.

[63] P. Muzzell, B. McKay and S. E, "The effect of switch-loading fuels on fuel-wetted elastomers," in *SAE World Congress*, Detroit, MI, 2007.

[64] TACOM Research and Development Engineering Centre, "Elastomer impact when switch-loading synthetic fuel blends and petroleum fuels," US Army Tank-Automotive Research, Development and Engineering Centre, Warren, MI, 2006.

[65] D. Louw, "The effect of O-ring conditioning on their physical properties and behaviour when exposed to fuels," B.Sc.(Hons) treatise, University of Cape Town, Cape Town, 2012.

[66] M. Jaunich, W. Stark and D. Wolff, "A new method to evaluate low temperature function of rubber sealing materials," *Polymer Testing,* no. 29, pp. 815-823, 2010.

[67] "ASTM standard D395. Standard Test Methods for Rubber Property - Compression Set," ASTM International, West Conshohocken, PA, 2008.

[68] A. Mostafa, A. Abouel-Kasem, M. Bayoumi and E.-S. M.G, "Effect of carbon black loading on the swelling and compression set behaviour of SBR and NBR rubber compounds," *Materials and Design,* no. 30, pp. 1561-1568, 2009.

[69] C. Slater, C. Davis and M. Strangwood, "Compression set of thermoplastic polyurethane under different thermal-mechanical-moisture conditions," *Polymer Degradation and Stablity ,* no. 96, pp. 2139-2144, 2011.

[70] P. Morrell, M. Patel and A. Skinner, "Accelerated thermal ageing studies on nitrile rubber O-rings," *Polymer Testing,* no. 22, pp. 651-656, 2003.

[71] R. J. Gormley, D. D. Link, J. P. Baltrus and P. H. Zandhuis, "Interactions of jet fuels with nitrile O-rings: petroleum-derived versus synthetic fuels," *Energy & Fuels,* vol. 23, pp. 857-861, 2009.

[72] M. Seehra, M. Yalamanchi and V. Singh, "Structural characteristics and swelling mechanisms of two commercial nitrile-butadiene elastomers in various fluids," *Polymer Testing,* no. 31, pp. 564-571, 2012.

[73] The Boeing Company, "Altnerative Fuels," The Boeing Company, Chicago, 2011.

[74]

[75] J. Frenkel, "A Theory of Elasticity, Viscosity and Swellingin Polymeric Rubber-Like Substances," *Rubber Chemistry and Technology,* vol. 13, no. 2, pp. 264-274, 1940.

[76] N. Neuburger and B. Eichinger, "Critical experimental test of the Flory-Rehner theory of swelling," *Macromolecules,* vol. 21, pp. 3060-3070, 1988.

[77] P. Weerachanchai, Z. Chen, S. Leong, M. Chan and J. Lee, "Hildebrand solubility parameters of ionic liquids: Effects of ionic liquid type, temperature and DMA fraction in ionic liquid," *Chemical Engineering Journal,* no. 213, pp. 356-362, 2012.

[78] G. Gee, J. Herbert and R. Roberts, "Vapour pressure of a swollen cCrosslinked elastomer," *Rubber Chemistry and Technology,* vol. 40, no. 4, pp. 1159-1165, 1967.

[79] C. Hansen, "50 years with solubility parameters-past and future," *Progress in Organic Coatings,* no. 51, pp. 77-84, 2004.

[80] T. Lindvig, M. Michelson and G. Kontogeorgis, "Thermodynamics of paint related systems with engineering models," *American Institute of Chemical Engineering,* vol. 47, pp. 2573-2584, 2001.

[81] M. Belmares, M. Blanco, W. Goddard, R. Ross, G. Caldwell, S. P. J. Chou, P. Olofson and C. Thomas, "Hildebrand and Hansen solubility parameters from molecular dynamics with applications to electronic nose polymer sensors," *Journal of Computational Chemistry ,* no. 25, pp. 1814-1826, 2004.

[82] D. R. Lide, Ed., Handbook of chemistry and physics, Boca Raton, FL: CRC Press, 2004.

[83] "ASTM Standard D471-06. Standard test method for rubber property-effects of liquid," ASTM International, West Conshohocken, PA, 2008.

[84] A. de Klerk, Fischer-Tropsch Refining, Edmonton: Wiley-VCH, 2011.

[85] Perkin Elmer, "Tg of gycerine using a stainless steel gauze scaffold," Perkin Elmer, Waltham, MA, 2011.

[86] T. Yamada, J. Graham and D. Minus, "Density Functional Theory Investigation of the Interaction between Nitrile Rubber and Fuel Species," *Energy and Fuels,* no. 23, pp. 443-450, 2008.

CHAPTER 11

11. APPENDICES

11.1 APPENDIX A – Changes in volumetric swell with time

The evolution in the volumetric swelling response of the elastomer samples was observed through consistent observation and measurement. All changes in volume over the three temperature ranges are plotted in section 11.1.1.The objective of this was to ensure all samples had reached an equilibrium swelling value allowing observation of behavioural changes.

11.1.1 NBR swelling

The following section documents the volumetric swelling response of NBR elastomer to fuel exposure.

11.1.1.1 Base fuels

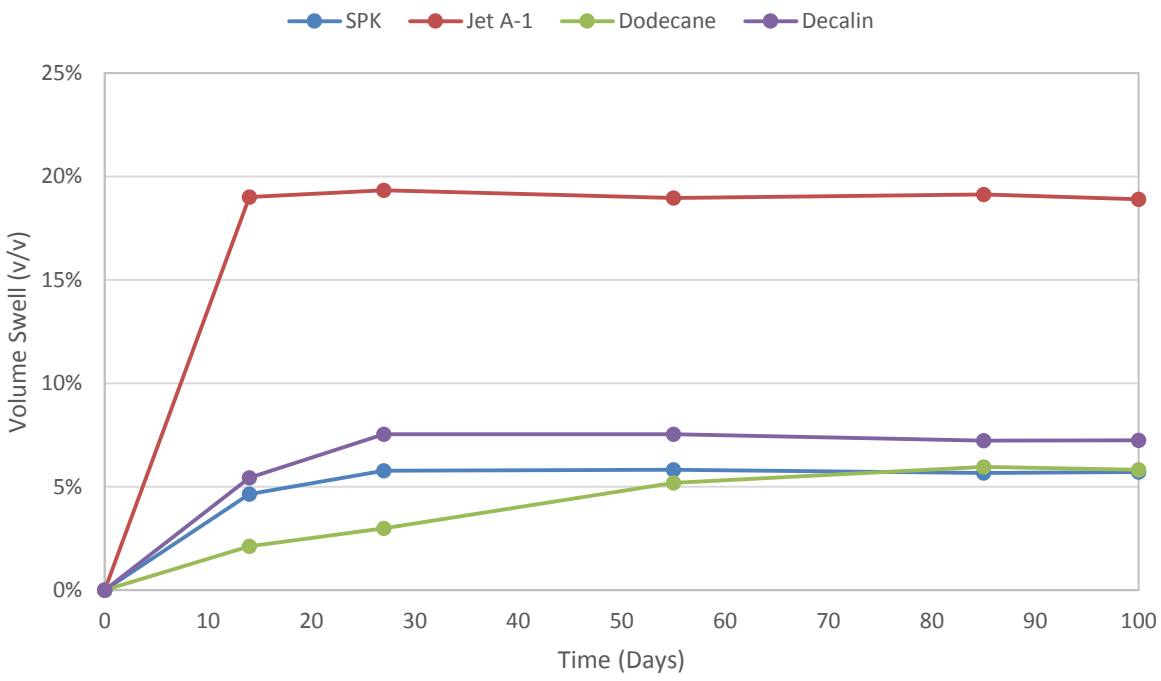

Figure 11.1: Evolution of volumetric swelling response of NBR to base fuel exposure at 20°C. Decalin is a 15% (v/v) blend in SPK

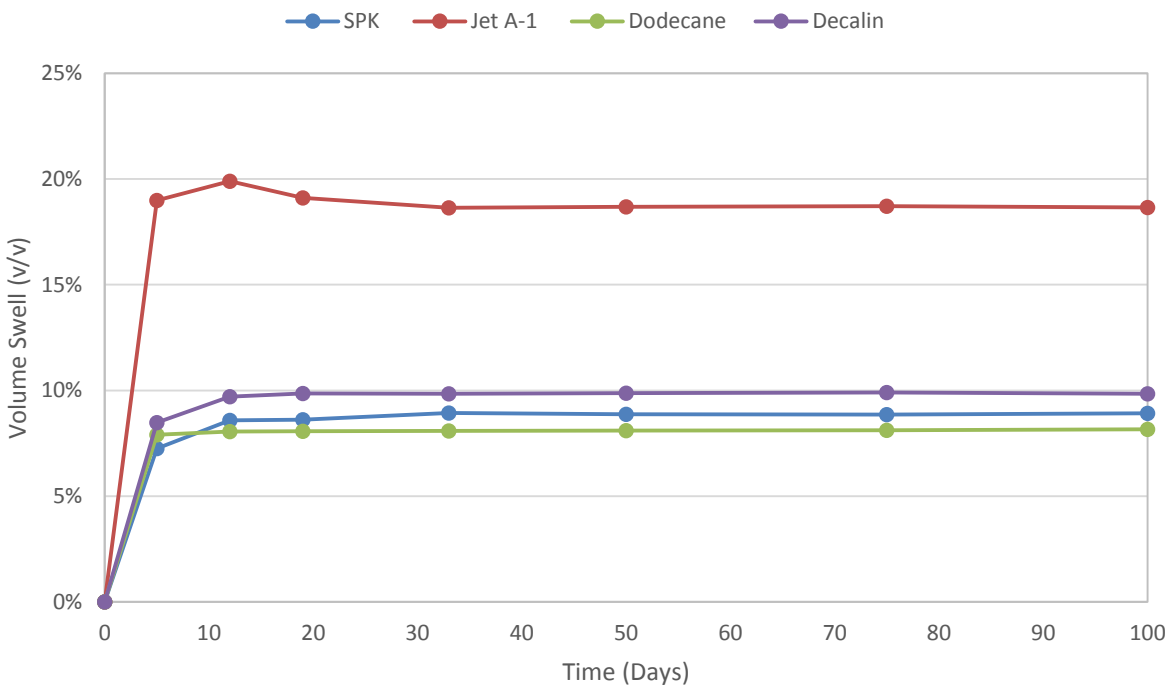

Figure 11.2: Evolution of volumetric swelling response of NBR to base fuel exposure at 35°C. Decalin is a 15% (v/v) blend in SPK

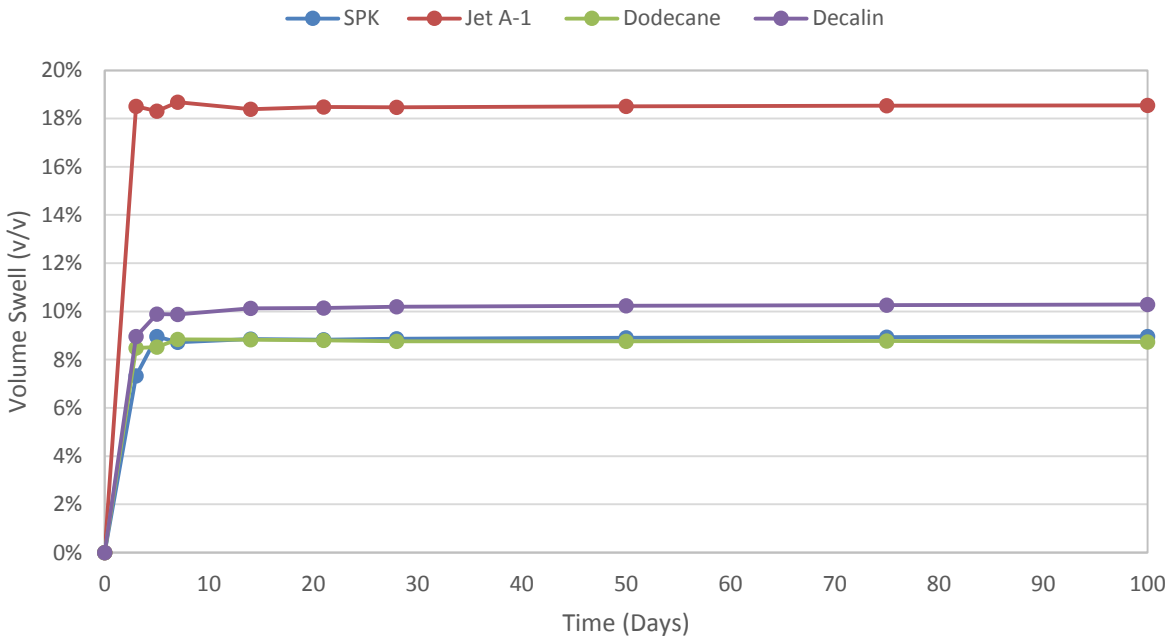

Figure 11.3: Evolution of volumetric swelling response of NBR to base fuel exposure at 50°C. Decalin is a 15% (v/v) blend in SPK

11.1.1.2 15% cycloparaffins/SPK blends

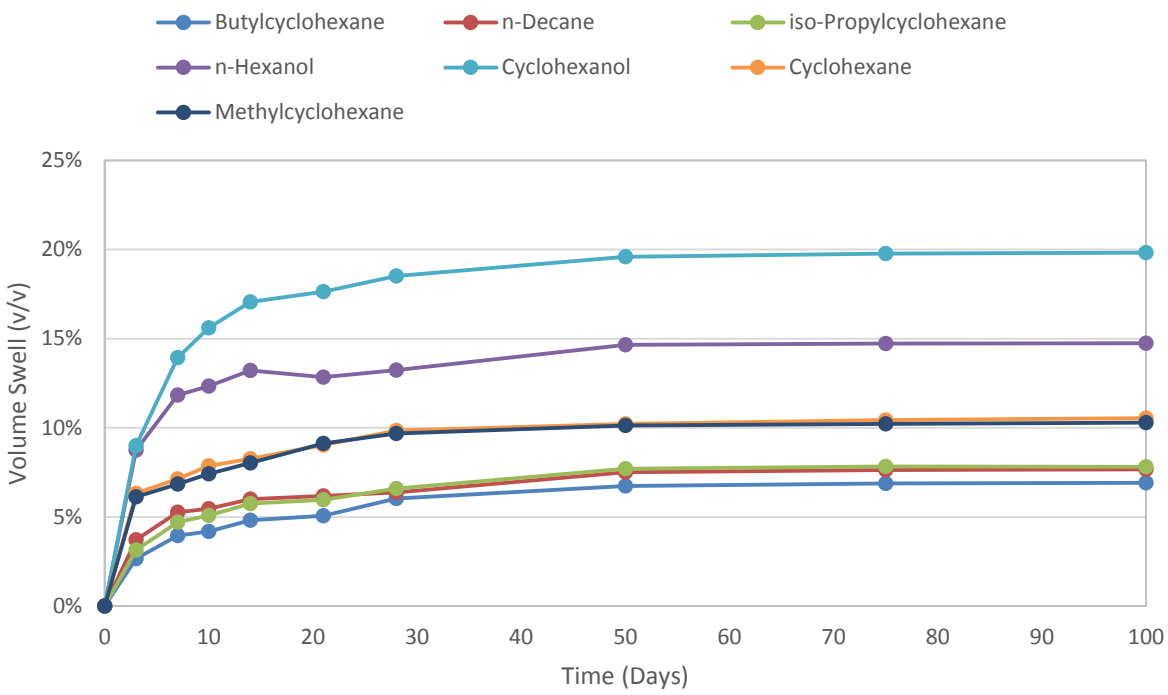

Figure 11.4: Evolution of the volumetric swelling response of NBR to cycloparaffin exposure at 20°C. n-decane is neat

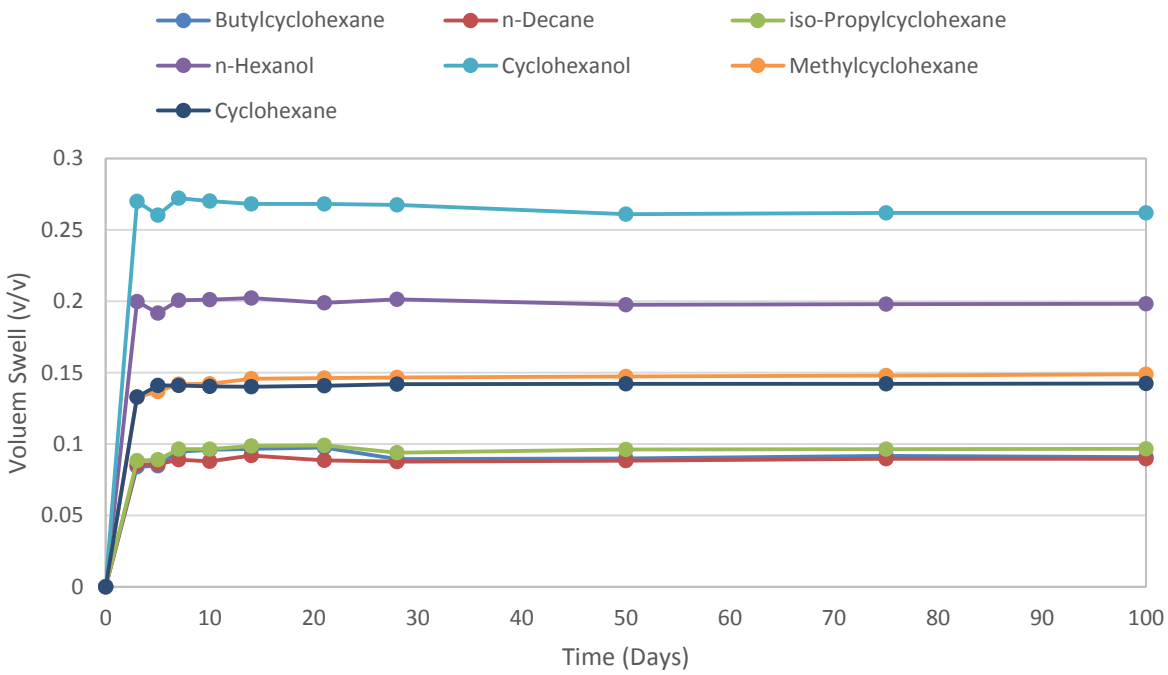

Figure 11.5: Evolution of the volumetric swelling response of NBR to cycloparaffin exposure at 50°C. n-decane is neat

11.1.1.3 8% aromatic/SPK blends

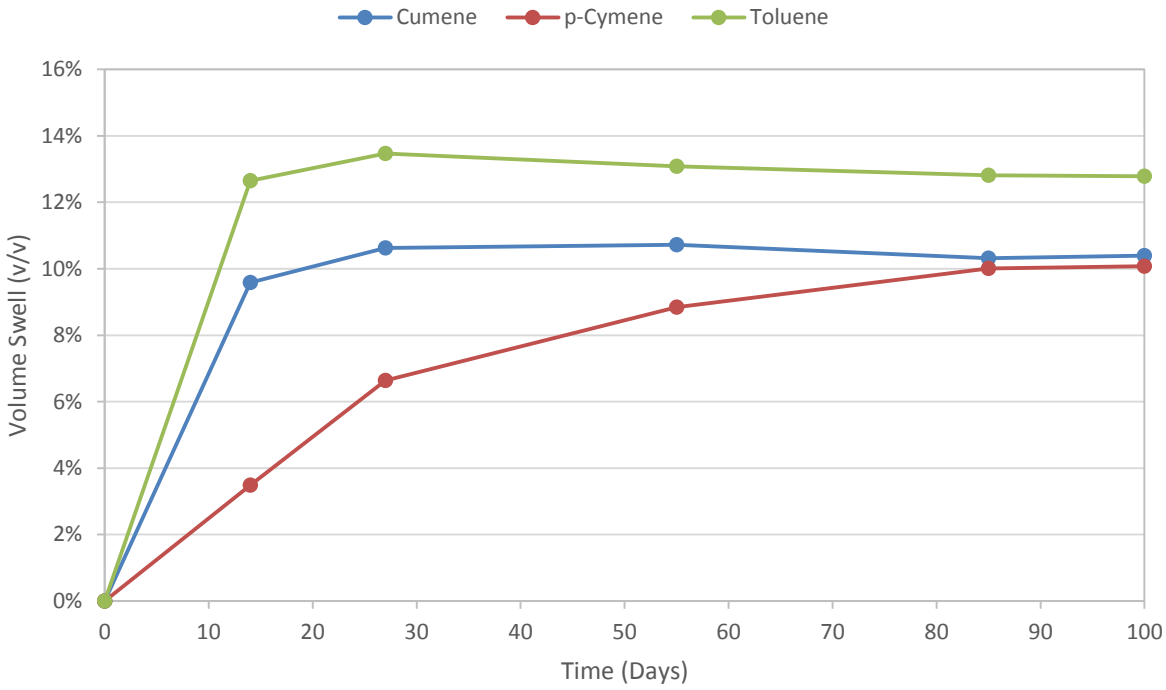

Figure 11.6: Evolution of the volumetric swelling response of NBR to aromatic blend exposure at 20°C

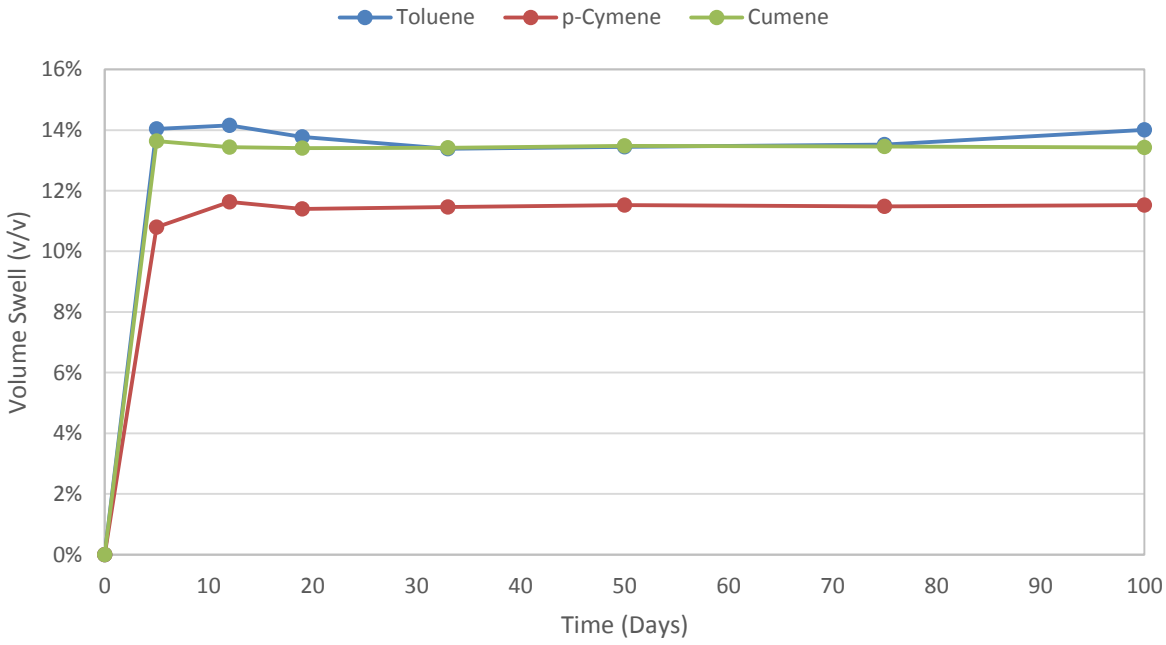

Figure 11.7: Evolution of the volumetric swelling response of NBR to aromatic blend exposure at 35°C

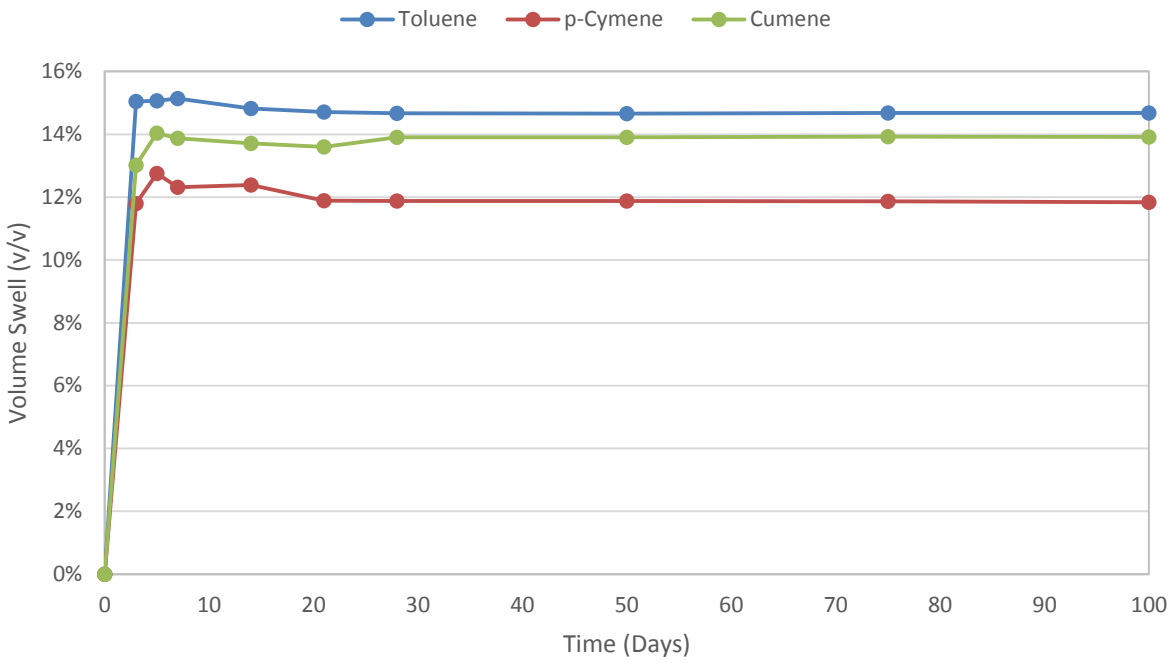

Figure 11.8: Evolution of the volumetric swelling response of NBR to aromatic blend exposure at 50°C

11.1.1.4 8% Bi-cyclic aromatic/SPK blends

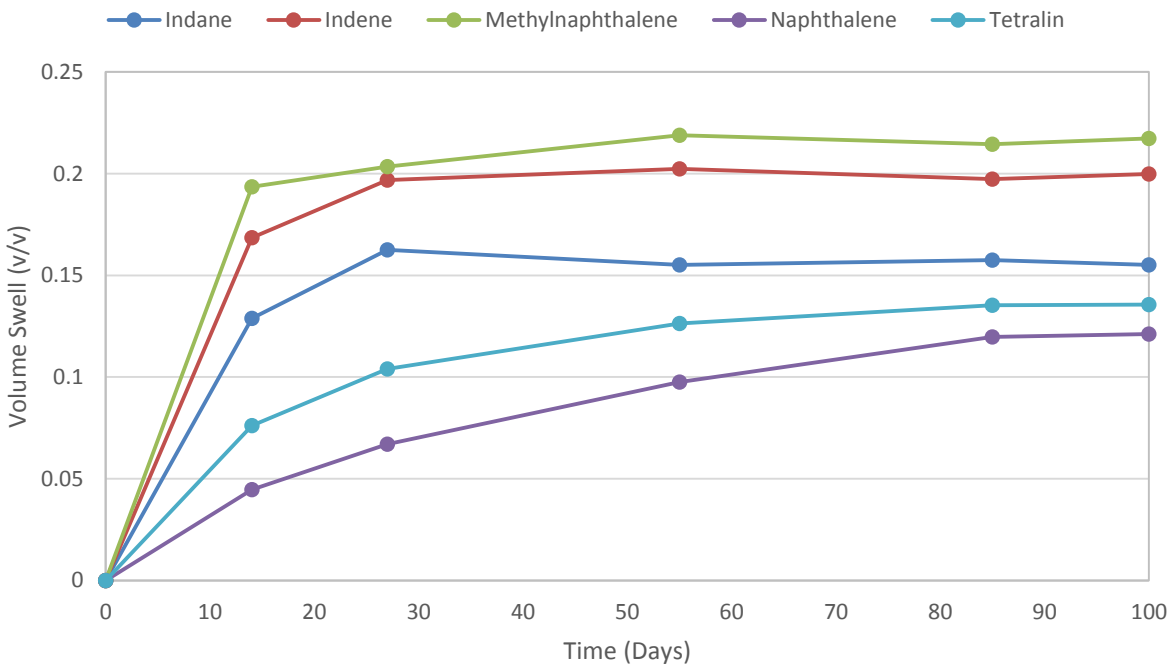

Figure 11.9: Evolution of the volumetric swelling response of NBR to bi-cyclic aromatic exposure at 20°C. Naphthalene is a 2% (v/v) blend with SPK

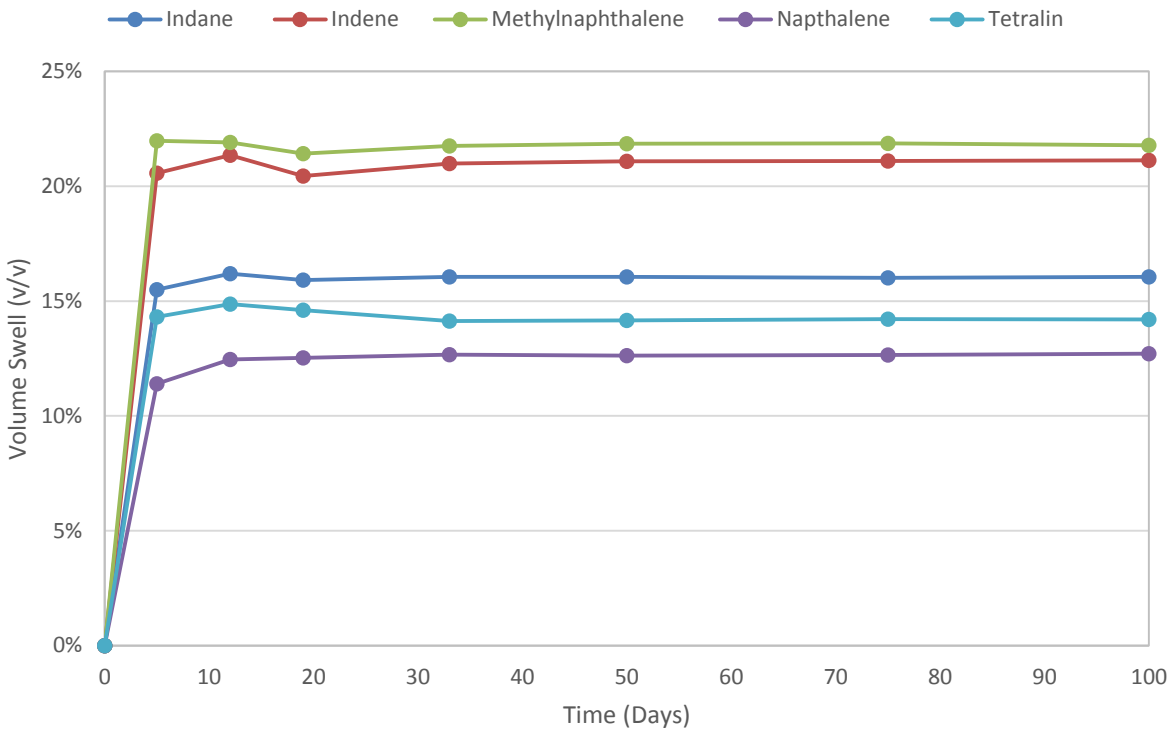

Figure 11.10: Evolution of the volumetric swelling response of NBR to bi-cyclic aromatic exposure at 35°C. Naphthalene is a 2% (v/v) blend with SPK

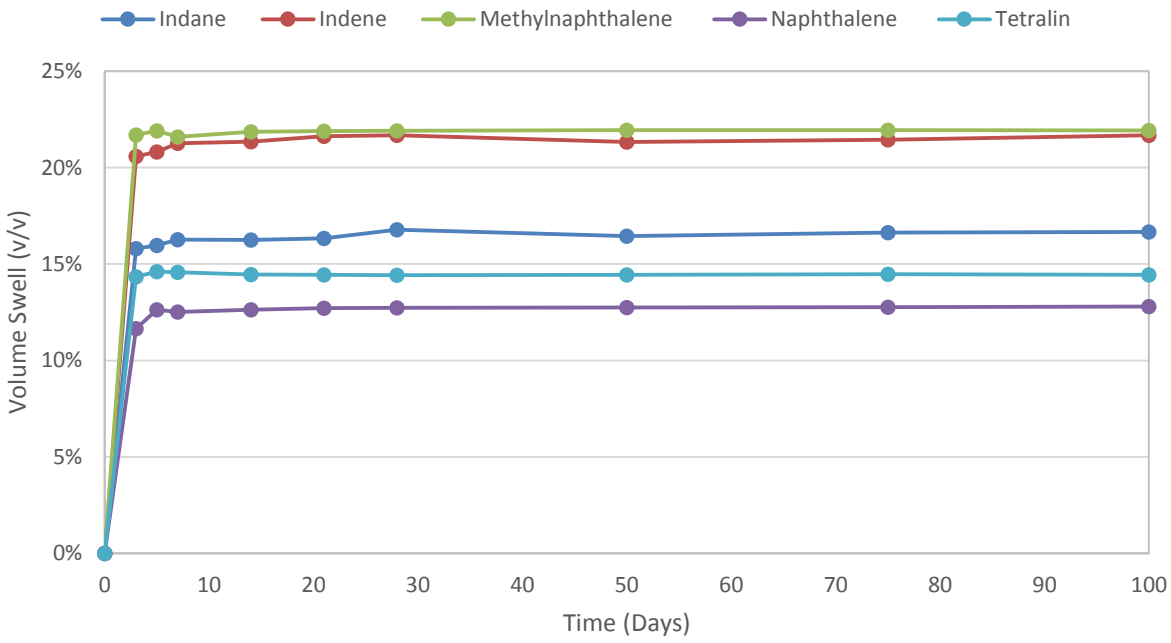

Figure 11.11: Evolution of the volumetric swelling response of NBR to bi-cyclic aromatic exposure at 50°C. Naphthalene is a 2% (v/v) blend with SPK

11.1.1.5 8% Aromatic oxygenate/SPK blends

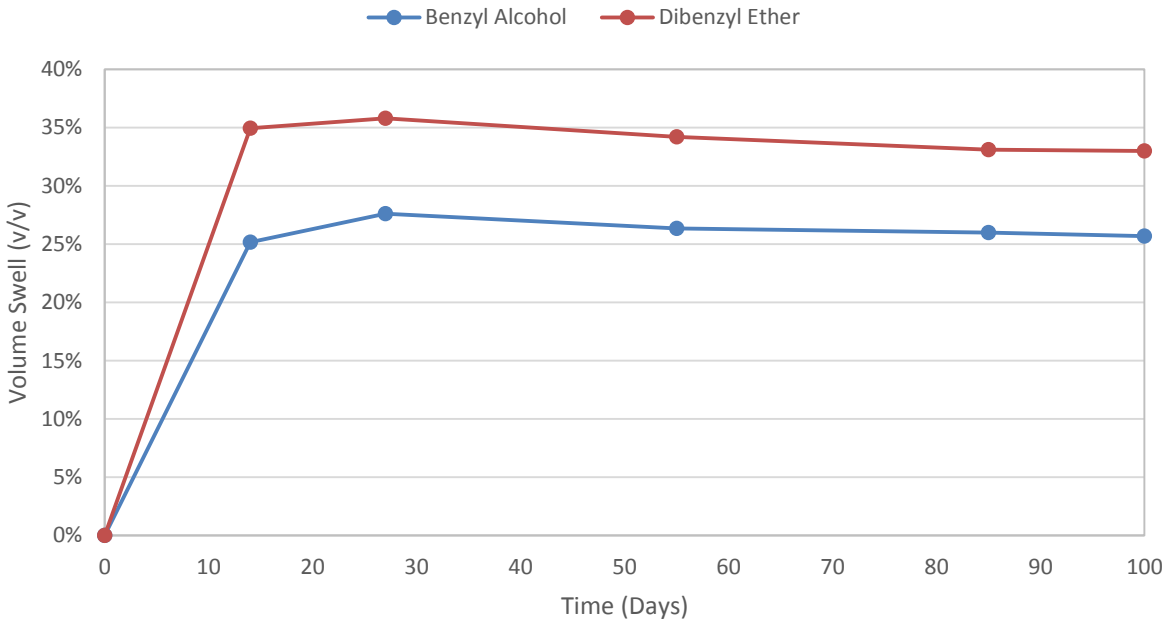

Figure 11.12: Evolution of the volumetric swelling response of NBR to aromatic oxygenate exposure at 20°C. Benzyl alcohol is a 0.5% blend with SPK.

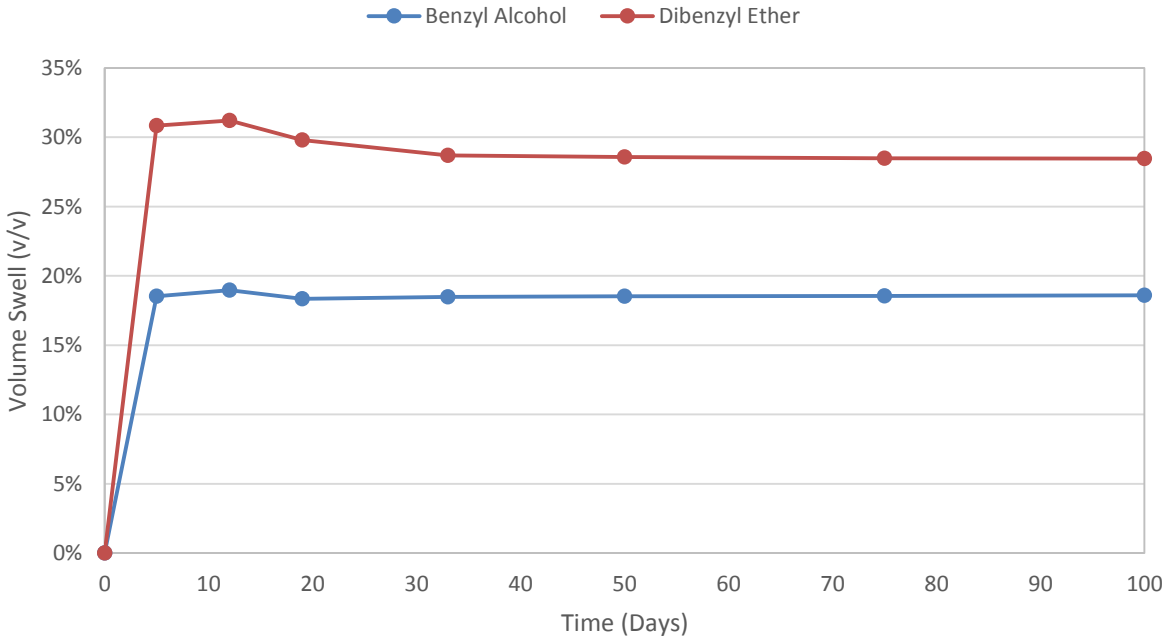

Figure 11.13. Evolution of volumetric swelling response of NBRto aromatic oxygenate exposure at 35°C. Benzyl alcohol is a 0.5% blend with SPK.

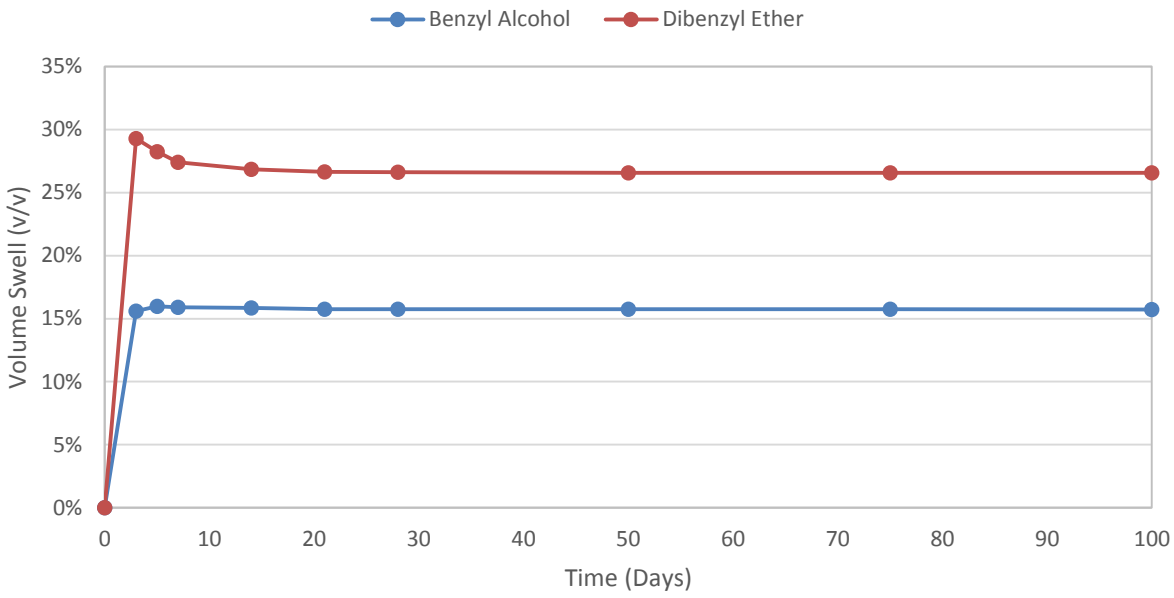

Figure 11.14: Evolution of the volumetric swelling of NBR to aromatic oxygenate exposure at 50°C. Benzyl alcohol is a 0.5% blend with SPK.

11.1.2 FKM elastomer

11.1.2.1 Base Fuel

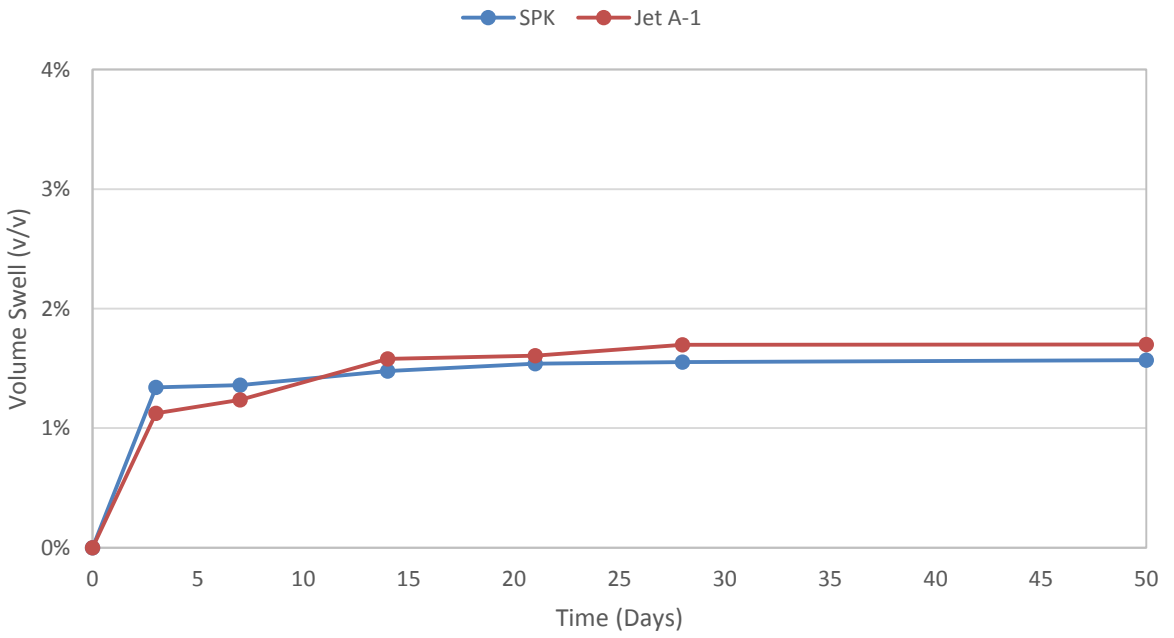

Figure 11.15: Evolution of the swelling response of FKM to base fuel exposure at 20°C

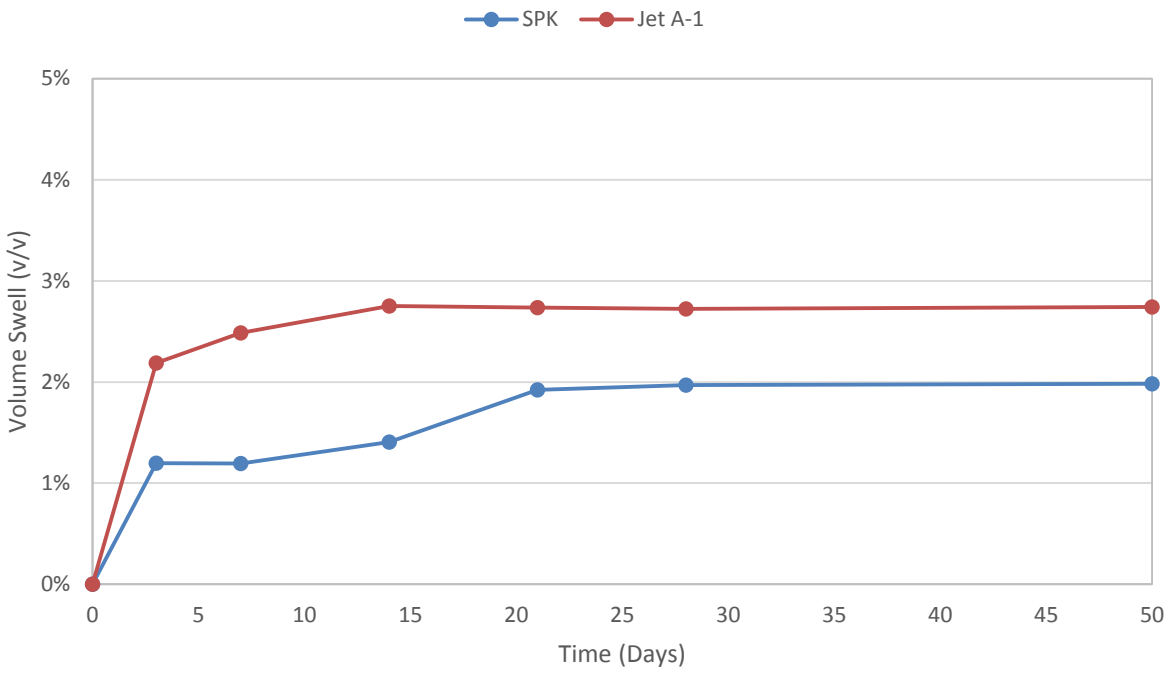

Figure 11.16: Evolution of the volumetric swelling response of FKM to base fuel exposure at 35°C

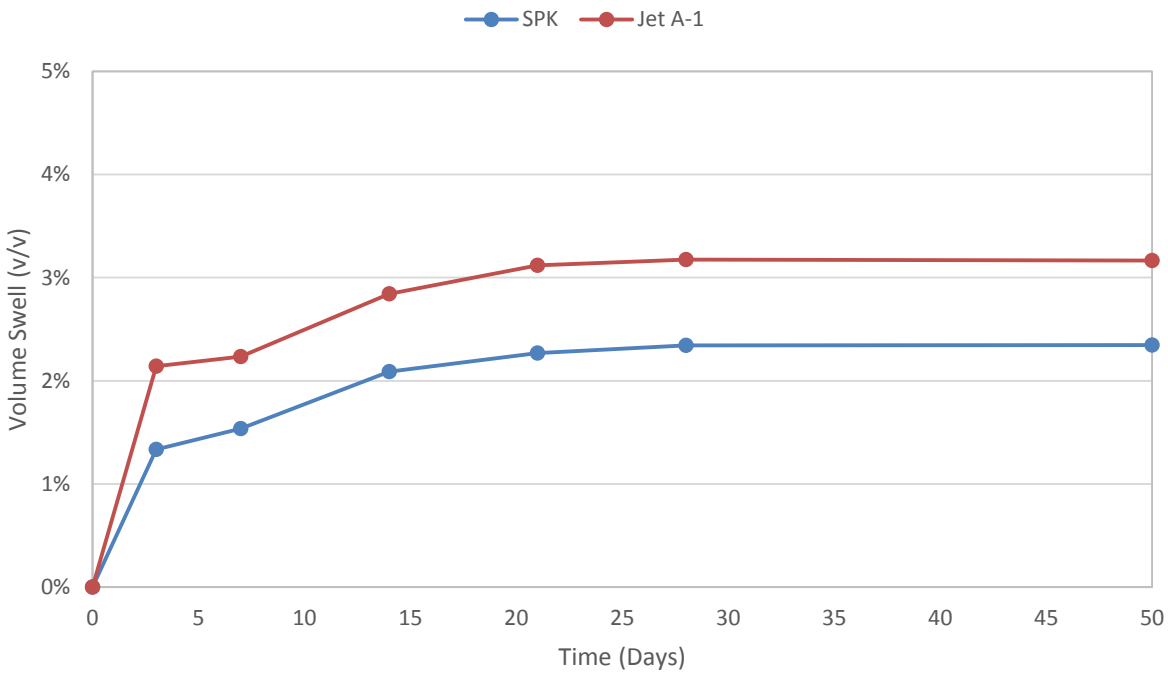

Figure 11.17. Evolution of the volumetric swelling response of FKM to base fuel exposure at 50°C

11.1.2.2 15% cycloparaffin/SPK blends

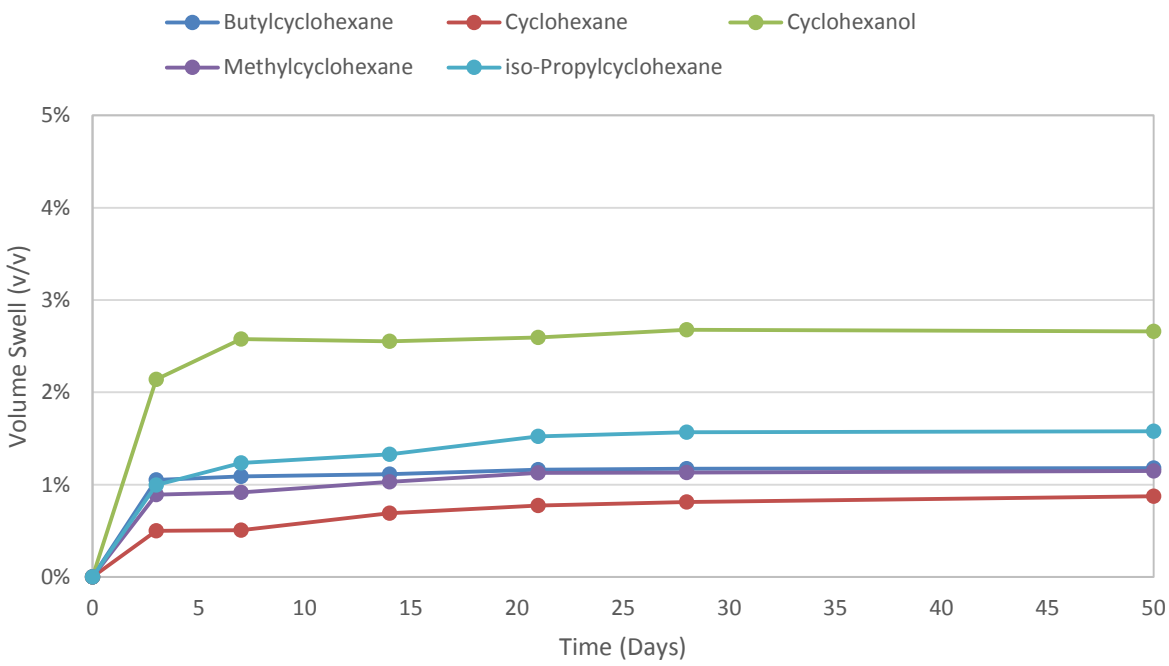

Figure 11.18: Evolution of the volumetric swelling response of FKM to cycloparaffin exposure at 50°C

11.1.2.3 8% aromatic/SPK blends

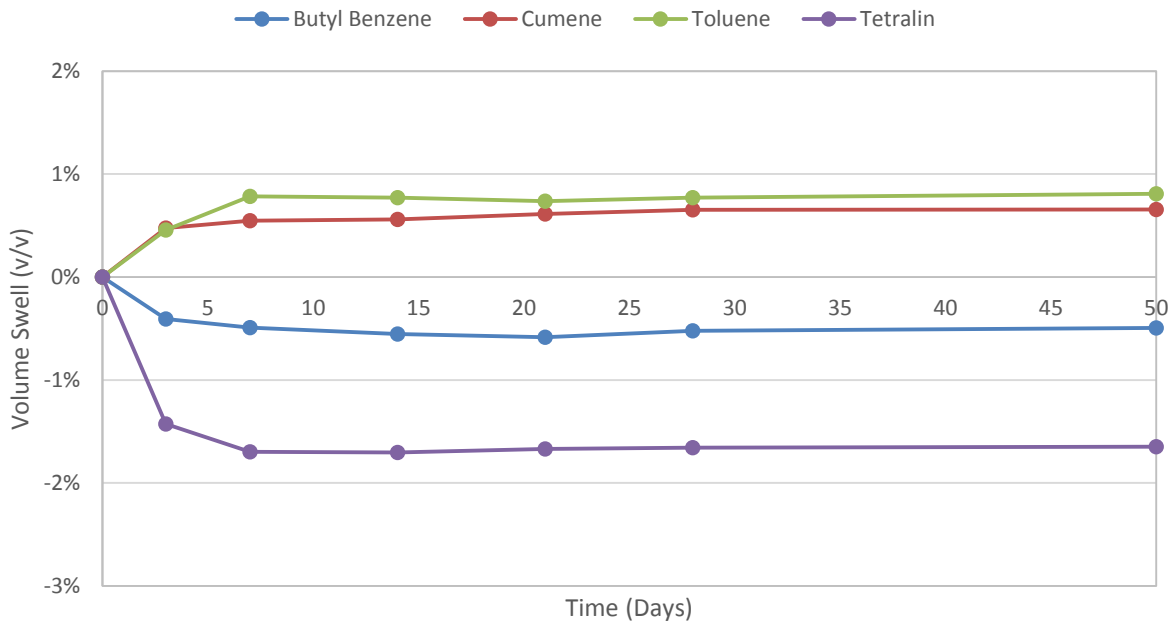

Figure 11.19: Evolution of the volumetric swelling response of FKM to aromatic exposure at 20°C

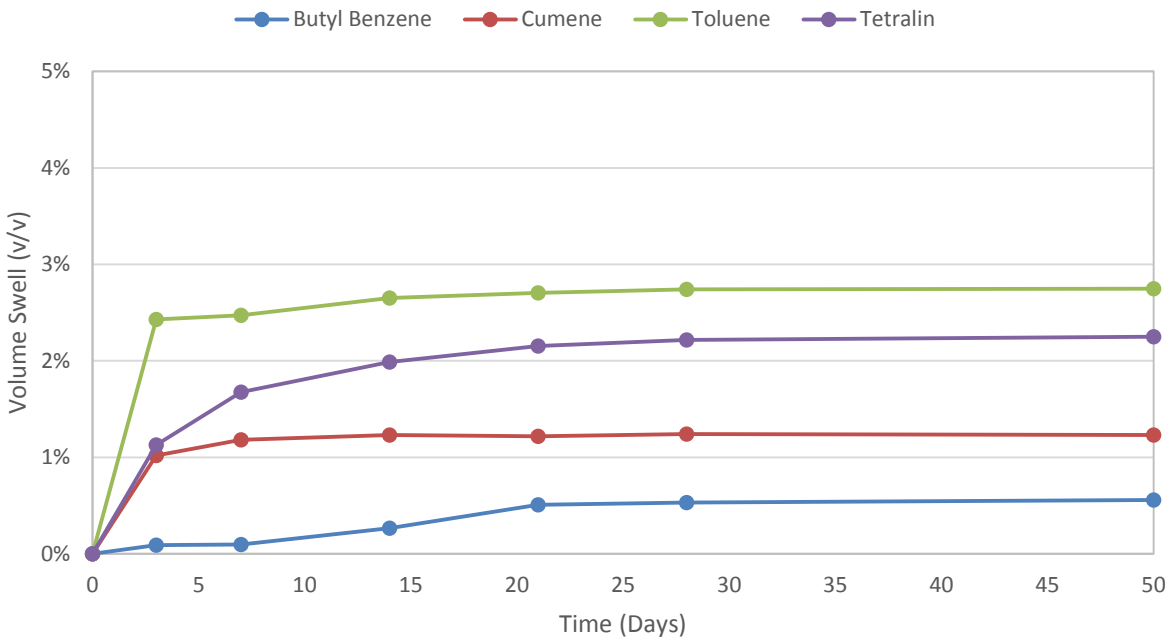

Figure 11.20: Evolution of the volumetric swelling response of FKM to aromatic exposure at 35°C

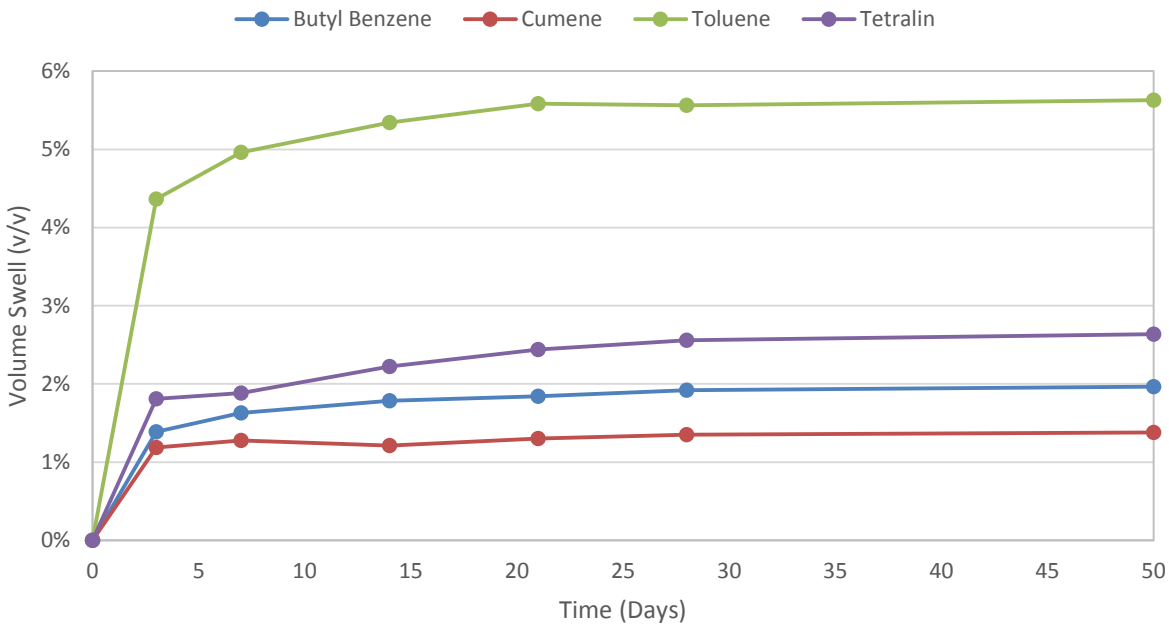

Figure 11.21: Evolution of the volumetric swelling response of FKM to aromatic exposure at 50°C

11.1.2.4 Aromatic oxygenate/blends

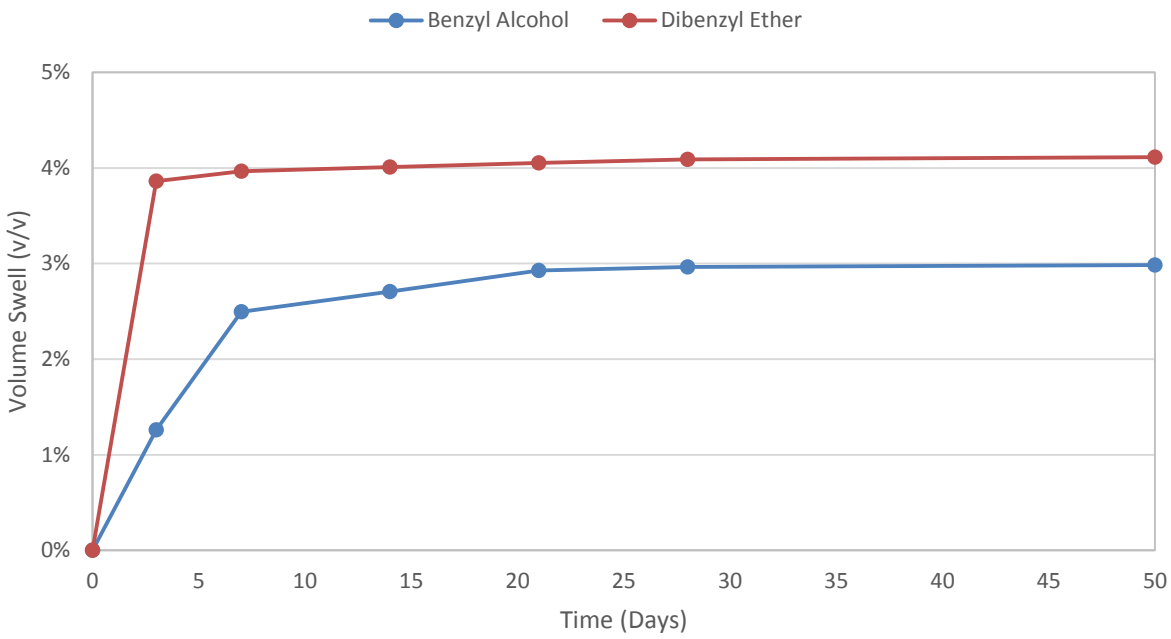

Figure 11.22: Evolution of the volumetric swelling response of FKM to aromatic oxygenate exposure at 20°C. Benzyl alcohol is a 0.5% blend with SPK; dibenzyl ether is an 8% blend

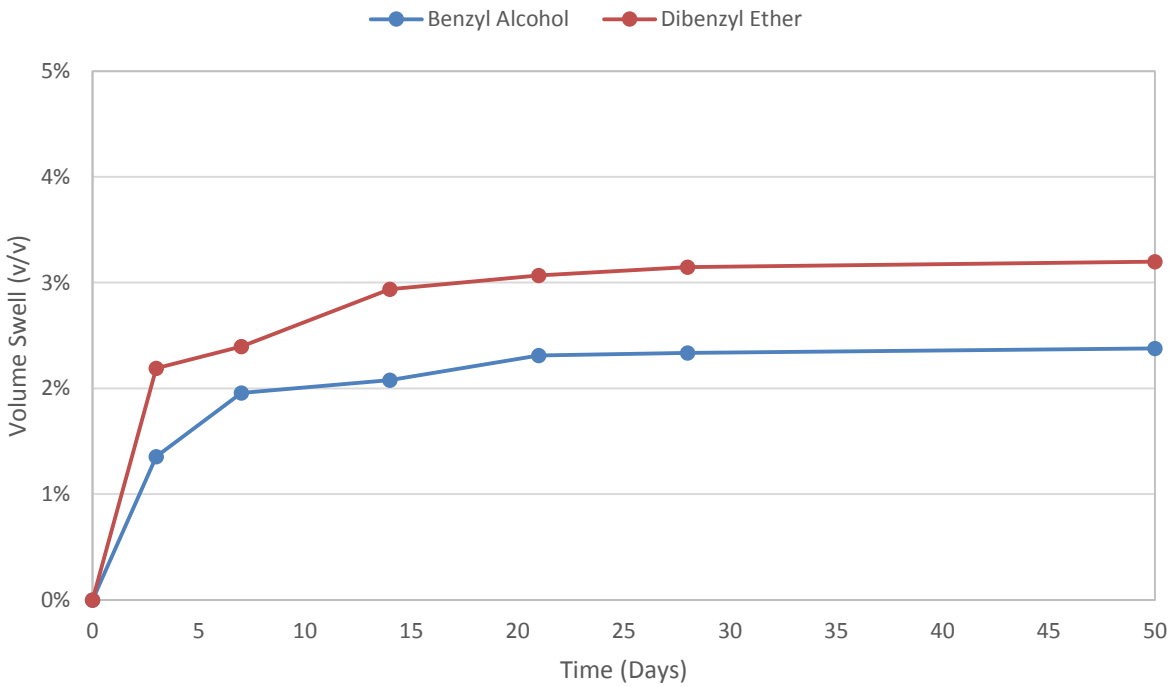

Figure 11.23: Evolution of the volumetric swelling response of FKM to aromatic oxygenate exposure at 35°C. Benzyl alcohol is a 0.5% blend with SPK; dibenzyl ether is an 8% blend

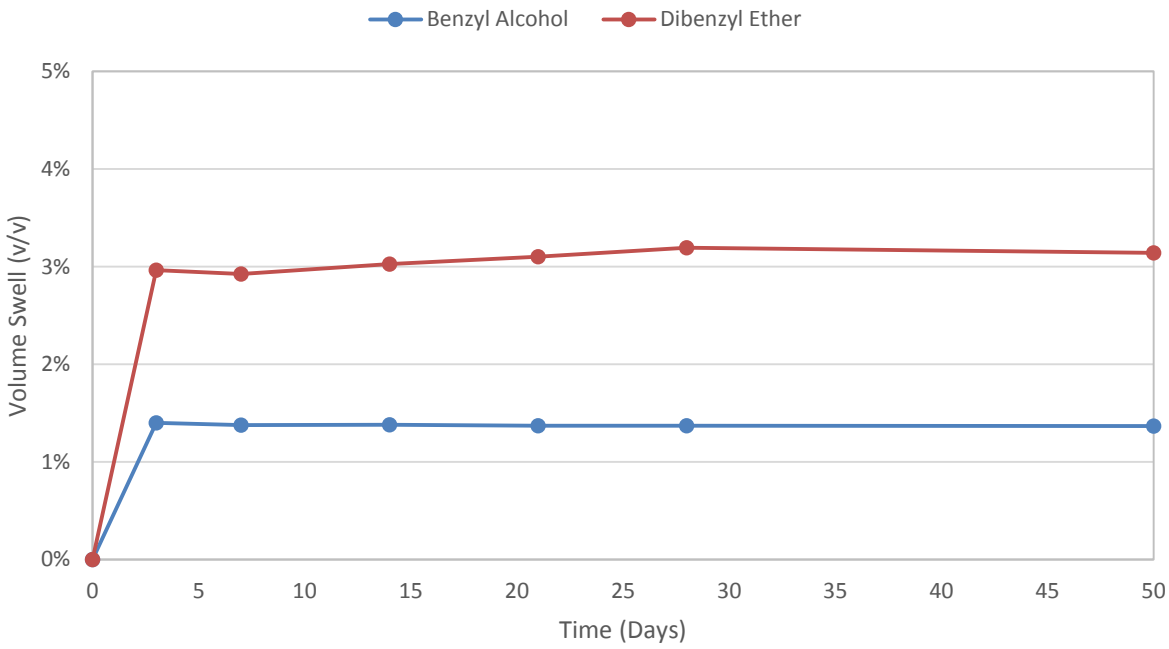

Figure 11.24: Evolution of the volumetric swelling response of FKM to aromatic oxygenate exposure at 50°C. Benzyl alcohol is a 0.5% blend with SPK; dibenzyl ether is an 8% blend

11.2 APPENDIX B – Gravimetric changes with fuel exposure

The change in the mass of the elastomer samples due to fuel exposure was evaluated using the equation below.

$$Q\% = 100\left(\frac{m_2 - m_1}{m_1}\right)$$

where:

m_2 = mass of the elastomer after fuel exposure at some time

m_1 = mass of the elastomer sample before fuel exposure

Table 11.1: Gravimetric swelling response of fuel-wetted NBR O-rings

Fuel Blend	δ_d	δ_p	δ_h	δ_{total}	Molar Volume (cm^3/mol)	Mass swell (%)		
						20°C	35°C	50°C
Base fuel								
SPK	15.4	0.0	0.0	15.4	212.5	3.82	5.31	5.56
Jet A-1	16.5	0.1	0.3	16.5	193.7	13.9	13.2	13.4
n-paraffin								
n-decane	15.7	0.0	0.0	15.7	195.9	4.15		4.50
n-dodecane	16.0	0.0	0.0	16.0	228.6	3.22	8.06	8.22
cycloparaffin								
cyclohexane (15%)	16.8	0.0	0.2	0.2	108.7	8.45		9.92
methylcyclohexane (15%)	16.0	0.0	1.0	16.0	128.3	8.32		10.36
iso-propylcyclohexane (15%)	16.3	0.0	0.5	16.3	157.4	4.48		5.05
n-butylcyclohexane (8%)	16.2	0.0	0.6	16.2	176.7	6.23		6.17
decalin (15%)	16.7	0	0	16.7	144.2	4.75	6.15	6.48
monoaromatic								
toluene (8%)	18.0	1.4	2.0	18.2	106.3	8.91	9.00	9.68
cumene (8%)	18.1	1.2	1.2	18.2	139.4	7.15	8.16	8.35
p-cymene (8%)	17.6	1.2	1.2	17.7	156.6	6.49	7.58	7.95
bicyclic aromatic								
indane (8%)	19.6	2.0	2.9	19.9	136.3	10.04	10.48	10.60
indene (8%)	18.7	2.6	9.0	20.9	116.5	14.84	14.79	15.07
naphthalene (2%)	19.2	2.0	5.9	20.2	111.5	7.48	7.73	8.35
methylnaphthalene (8%)	20.6	0.8	4.7	21.1	138.8	16.21	16.44	16.73
tetralin (8%)	19.6	2.0	2.9	19.9	136.3	9.17	9.86	10.24
aromatic oxygenate								
benzyl alcohol	18.4	6.3	13.7	23.8	103.6	13.51	13.48	11.97
dibenzyl ether (8%)	19.6	3.4	5.2	20.6	197.4	28.52	23.22	21.51
Other oxygenate								
n-hexanol (15%)	15.9	5.8	12.5	21.04	124.9	8.86		12.68
cyclohexanol (15%)	17.4	4.1	13.5	22.4	106.0	12.67		18.12

Table 11.2: Gravimetric swelling response of fuel-wetted FKM O-rings

Fuel Blend	δ_d	δ_p	δ_h	δ_{total}	Molar Volume (cm^3/mol)	Mass swell (%)		
						20°C	35°C	50°C
Base fuel								
SPK	15.4	0.0	0.0	15.4	212.5	0.03	0.26	0.51
Jet A-1	16.5	0.1	0.3	16.5	193.7	0.18	0.72	1.34
cycloparaffin								
cyclohexane (15%)	16.8	0.0	0.2	0.2	108.7			0.73
methylcyclohexane (15%)	16.0	0.0	1.0	16.0	128.3			0.73
iso-propylcyclohexane (15%)	16.3	0.0	0.5	16.3	157.4			0.61
n-butylcyclohexane (8%)	16.2	0.0	0.6	16.2	176.7			0.50
monoaromatic								
toluene (8%)	18.0	1.4	2.0	18.2	106.3	0.27	0.87	1.38
cumene (8%)	18.1	1.2	1.2	18.2	139.4	0.06	0.34	0.72
n-butylbenzene	17.4	0.1	1.1	17.4	157.0	0.31	0.29	0.61
bicyclic aromatic								
tetralin (8%)	19.6	2.0	2.9	19.9	136.3	0.07	0.49	1.00
aromatic oxygenate								
benzyl alcohol	18.4	6.3	13.7	23.8	103.6	0.23	0.66	1.11
dibenzyl ether (8%)	19.6	3.4	5.2	20.6	197.4	0.63	0.93	1.94
other oxygenate								
cyclohexanol	17.4	4.1	13.5	22.4	106.0			1.64

11.3 APPENDIX C – Elastomer dimensions after conditioning procedure

Table 11.3: Elastomer thickness readings after conditioning procedure

	Reading Number					
	1	2	3	4	5	Mean
	Thickness (mm)					
Sample 1	1.64	1.64	1.64	1.65	1.66	1.65
Sample 2	1.67	1.64	1.62	1.65	1.64	1.64
Sample 3	1.66	1.66	1.66	1.66	1.69	1.67
Sample 4	1.67	1.64	1.62	1.67	1.65	1.65
Sample 5	1.68	1.66	1.66	1.62	1.61	1.65

Overall thickness of conditioned elastomer = **1.65mm**

Table 11.4: Elastomer internal diameter readings after conditioning procedure

	Reading Number					
	1	2	3	4	5	Mean
	Internal diameter (mm)					
Sample 1	4.16	4.18	4.18	4.17	4.2	4.18
Sample 2	4.13	4.15	4.15	4.15	4.16	4.15
Sample 3	4.21	4.22	4.19	4.19	4.2	4.20
Sample 4	4.21	4.22	4.21	4.19	4.19	4.20
Sample 5	4.19	4.2	4.18	4.18	4.19	4.19

New internal diameter after elastomer conditioning = **4.18mm**

11.4 APPENDIX D – RISK ASSESSMENTS AND STANDARD OPERATING PROCEDURES

SASOL ADVANCED FUELS LABORATORY

RISK ASSESSMENT

Date: __16 April 2012_____

NOTE:

- **A new risk assesment form needs to be completed for each new activity.**
- **Any relevant Material Safety Data Sheets (MSDS) must be attached.**

Name:	Christopher Scully
Supervisor:	Dr. Chris Woolard
Describe the activity:	Standard elastomer swelling experiments with jet fuel/kerosene
Location:	Wet chemistry lab

A COMPLETED RISK ASSESSMENT REPORT MUST BE HANDED IN WITH THIS FORM

I declare that I am aware of the risks associated with the activity and will take all necessary steps to mitigate these risks.	**Signature**	**Date** **16 April 2012**

This section to be completed by the Project Supervisor		
Level of supervision required: (Tick relevant block)	Work may not take place without trained supervision	
	Work may not take place without 2nd party present	
	No specific extra supervision requirements	X
General comments:		

I am satified that the person responsible for this activity is aware of the risks associated with this activity and grant approval for it to proceed.	**Signature**	**Date** 16 April 2012

This section to be completed by the Area Safety Officer		
General comments:		
A satisfactory risk assessment has been performed and I grant approval for this activity to proceed.	**Signature**	**Date** 16 April 2012

Standard SAFL Risk Matrix		Hazard Effect / Consequence (C) (Where an event has more than one 'Loss Type', choose the 'Consequence' with the highest rating)				
Loss Type (Additional 'Loss Types' may exist for an event; identify & rate accordingly)		1 Insignificant	2 Minor	3 Moderate	4 Major	5 Catastrophic
(S/H) Harm to People (Safety / Health)		First aid case / Exposure to minor health risk	Medical treatment / Exposure to major health risk	Loss time injury / Reversible impact on health	Single fatality or loss of quality of life / Irreversible impact on health	Multiple fatalities / Impact on health ultimately fatal
(EI) Environmental Impact		Minimal environmental harm - L1 incident	Material environmental harm - L2 incident remediable short term	Serious environmental harm - L2 incident remediable within LOM	Major environmental harm - L2 incident remediable post LOM	Extreme environmental harm - L3 incident irreversible
(BI/MD) Business Disruption / Material Damage & Other Consequential Losses		No disruption to operation	Brief disruption to operation	Partial shutdown	Partial loss of operation	Substantial or total loss of operation
(L&R) Legal & Regulatory		Low level legal issue	Minor legal issue; non compliance and breaches of the law	Serious breech of law; investigation/report to authority, prosecution and/or moderate penalty possible	Major breech of the law; considerable prosecution and penalties	Very considerable penalties & prosecutions. Multiple law suits & jail terms
(R/S/C) Impact on Reputation/Social/Community		Slight impact - public awareness may exist but no public concern	Limited impact - local public concern	Considerable impact - regional public concern	National impact - national public concern	International impact - international public attention
Likelihood (L)	Examples (Consider near-hits as well as actual events)	Risk Rating (R)				
5 Almost Certain	The unwanted event has occurred frequently; occurs in order of one or more times per year & is likely to reoccur within 6 months	11 (M)	16 (H)	20 (H)	23 (Ex)	25 (Ex)
4 Likely	The unwanted event has occurred infrequently; occurs in order of less than once per year & is likely to re-occur within 1 years	7 (M)	12 (M)	17 (H)	21 (Ex)	24 (Ex)
3 Possible	The unwanted event could well have occurred in the business at some point within 5 years	4 (L)	8 (M)	13 (H)	18 (H)	22 (Ex)
2 Unlikely	The unwanted event has happened in the business at some time; or could happen within 10 years	2 (L)	5 (L)	9 (M)	14 (H)	19 (H)
1 Rare	The unwanted event has never been known to occur in the business; or is highly unlikely that it could ever occur beyond 10 years	1 (L)	3 (L)	6 (M)	10 (M)	15 (H)

Interpretation of Risk Level

Risk Rating	Risk Level	Guidelines for Risk Matrix
21 to 25	(Ex) – Extreme	Eliminate, avoid, implement specific action plans / procedures to manage & monitor
13 to 20	(H) – High	Proactively manage
6 to 12	(M) – Medium	Actively manage
1 to 5	(L) – Low	Monitor & manage as appropriate

SAFL Risk Assessment Report

No	List the task/activity	List the hazard associated with the task and describe how the hazard can be brought about	Hazard consequence, type of loss/affect	Control measures	Loss Type	C	L	R	Recommended Additional Controls	C	L	R
1	Measuring swelling response of fuel-wetted elastomers	Chemical spill when deplasticizing elastomers	Equipment damage Human injury	1. Use glass funnel to transfer solvent 2. Work inside a fume hood 3. Wear latex gloves and safety glasses at all times	S/H	1	3	4L	1. Wear lab coat and closed shoes 2. Decant solvent into smaller, user-friendly beakers			
		Chemical spill Broken glassware when making up standard solution	Human injury/lacerations	1. Ensure you work in a fume hood with required PPE 2. Ensure glassware is dry before using	S/H	1	3	4L	1. Have working knowledge of the risks associated with each solvent prior to experiment			

No	List the task/activity	List the hazard associated with the task and describe how the hazard can be brought about	Hazard consequence, type of loss/affect	Control measures	Loss Type	C	L	R	Recommended Additional Controls	C	L	R
		Potential combustion of fuel blends whilst in laboratory oven	Equipment damage	1. Try as far as possible to use blends below flashpoint of blending solvent 2. Ensure containers are fastened correctly 3. Be aware of fire exits and fire marshals	MD	1	1	1L	1. Be aware of location of fire extinguisher			
		Chemical spill/chemical inhalation whilst measuring swelling response	Human injury	1. Ensure fresh air is flowing to measuring area 2. Use additional breathing apparatus if deemed necessary	S/H	2	2	5L	1. Try to work in fume hood as far as possible 2. Wear full PPE 3. Work on a clear surface			

SASOL ADVANCED FUELS LABORATORY

RISK ASSESSMENT

Date: __15 August 2012_____

NOTE:

- **A new risk assesment form needs to be completed for each new activity.**
- **Any relevant Material Safety Data Sheets (MSDS) must be attached.**

Name:	Christopher Scully
Supervisor:	Dr. Chris Woolard
Describe the activity:	Filling GCA liquid nitrogen tank for DMA testing
Location:	Analytical Chemistry Lab

A COMPLETED RISK ASSESSMENT REPORT MUST BE HANDED IN WITH THIS FORM

I declare that I am aware of the risks associated with the activity and will take all necessary steps to mitigate these risks.	**Signature**	**Date** **15 August 2012**

This section to be completed by the Project Supervisor		
Level of supervision required: (Tick relevant block)	Work may not take place without trained supervision	
	Work may not take place without 2nd party present	
	No specific extra supervision requirements	X
General comments:		

I am satified that the person responsible for this activity is aware of the risks associated with this activity and grant approval for it to proceed.	**Signature**	**Date** 15 August 2012

This section to be completed by the Area Safety Officer		
General comments:		
A satisfactory risk assessment has been performed and I grant approval for this activity to proceed.	**Signature**	**Date** 15 August 2012

APPENDICES

Standard SAFL Risk Matrix		Hazard Effect / Consequence (C) (Where an event has more than one 'Loss Type', choose the 'Consequence' with the highest rating)				
Loss Type (Additional 'Loss Types' may exist for an event; identify & rate accordingly)		1 Insignificant	2 Minor	3 Moderate	4 Major	5 Catastrophic
(S/H) Harm to People (Safety / Health)		First aid case / Exposure to minor health risk	Medical treatment / Exposure to major health risk	Loss time injury / Reversible impact on health	Single fatality or loss of quality of life / Irreversible impact on health	Multiple fatalities / Impact on health ultimately fatal
(EI) Environmental Impact		Minimal environmental harm - L1 incident	Material environmental harm - L2 incident remediable short term	Serious environmental harm - L2 incident remediable within LOM	Major environmental harm - L2 incident remediable post LOM	Extreme environmental harm - L3 incident irreversible
(BI/MD) Business Disruption / Material Damage & Other Consequential Losses		No disruption to operation	Brief disruption to operation	Partial shutdown	Partial loss of operation	Substantial or total loss of operation
(L&R) Legal & Regulatory		Low level legal issue	Minor legal issue; non compliance and breaches of the law	Serious breech of law; investigation/report to authority, prosecution and/or moderate penalty possible	Major breech of the law; considerable prosecution and penalties	Very considerable penalties & prosecutions. Multiple law suits & jail terms
(R/S/C) Impact on Reputation/Social/Community		Slight impact - public awareness may exist but no public concern	Limited impact - local public concern	Considerable impact - regional public concern	National impact - national public concern	International impact - international public attention
Likelihood (L)	**Examples** (Consider near-hits as well as actual events)	Risk Rating (R)				
5 Almost Certain	The unwanted event has occurred frequently; occurs in order of one or more times per year & is likely to reoccur within 6 months	11 (M)	16 (H)	20 (H)	23 (Ex)	25 (Ex)
4 Likely	The unwanted event has occurred infrequently; occurs in order of less than once per year & is likely to re-occur within 1 years	7 (M)	12 (M)	17 (H)	21 (Ex)	24 (Ex)
3 Possible	The unwanted event could well have occurred in the business at some point within 5 years	4 (L)	8 (M)	13 (H)	18 (H)	22 (Ex)
2 Unlikely	The unwanted event has happened in the business at some time; or could happen within 10 years	2 (L)	5 (L)	9 (M)	14 (H)	19 (H)
1 Rare	The unwanted event has never been known to occur in the business; or is highly unlikely that it could ever occur beyond 10 years	1 (L)	3 (L)	6 (M)	10 (M)	15 (H)

Interpretation of Risk Level

Risk Rating	Risk Level	Guidelines for Risk Matrix
21 to 25	(Ex) – Extreme	Eliminate, avoid, implement specific action plans / procedures to manage & monitor
13 to 20	(H) – High	Proactively manage
6 to 12	(M) – Medium	Actively manage
1 to 5	(L) – Low	Monitor & manage as appropriate

SAFL Risk Assessment Report

No	List the task/activity	List the hazard associated with the task and describe how the hazard can be brought about	Hazard consequence, type of loss/affect	Control measures	Loss Type	C	L	R	Recommended Additional Controls	C	L	R
1	Liquid nitrogen fill of GCA tank	Lifting of heavy equipment/reactor vessels	Human injury Equipment damage	4. Ensure more than 2 people aid in moving equipment. 5. Appropriate methods of transportation of vessel should be used	S/H	2	1	3L	3. Move equipment in daylight hours 4. Exercise caution when vessel is loaded with nitrogen			
		Incorrect or damaged fittings may cause leakage / spillages. Liquid nitrogen may spill onto user	Human injury	3. Leak test before starting every fill	S/H	2	2	5L	2. Ensure fittings are tightly fastened 3. Wear appropriate PPE			

No	List the task/activity	List the hazard associated with the task and describe how the hazard can be brought about	Hazard consequence, type of loss/affect	Control measures	Loss Type	C	L	R	Recommended Additional Controls	C	L	R
		Nitrogen gas displaces oxygen leaving oxygen-deficient environment.	Injury to head, body or limbs	4. Ensure filling door remains open at all times	S/H	2	1	3L	1. Wear breathing apparatus			
		Over fill of GCA tank	Equipment damage	3. Ensure you have a working knowledge of the GCA control software	MD	1	2	2L	4. Adequate training of GCA control software 5. Use “buddy” system			
		Touch frozen equipment during filling process	Injury to limbs	1. Wear cryogenic gloves/equipment	S/H	2	2	5L	1. Indicate that equipment is at dangerously low temperature			

SASOL ADVANCED FUELS LABORATORY

RISK ASSESSMENT

Date: __20 August 2012_____

NOTE:

- **A new risk assesment form needs to be completed for each new activity.**
- **Any relevant Material Safety Data Sheets (MSDS) must be attached.**

Name:	Christopher Scully
Supervisor:	Dr. Chris Woolard
Describe the activity:	Use of DMA for fuel-wetted elastomer analysis
Location:	Analytical chemistry lab

A COMPLETED RISK ASSESSMENT REPORT MUST BE HANDED IN WITH THIS FORM

I declare that I am aware of the risks associated with the activity and will take all necessary steps to mitigate these risks.	**Signature**	**Date** **20 August 2012**

This section to be completed by the Project Supervisor		
Level of supervision required: (Tick relevant block)	Work may not take place without trained supervision	
	Work may not take place without 2nd party present	
	No specific extra supervision requirements	X
General comments:		
I am satified that the person responsible for this activity is aware of the risks associated	**Signature**	**Date**

with this activity and grant approval for it to proceed.		20 August 2012

This section to be completed by the Area Safety Officer		
General comments:		
A satisfactory risk assessment has been performed and I grant approval for this activity to proceed.	**Signature**	**Date** 20 August 2012

Standard SAFL Risk Matrix		Hazard Effect / Consequence (C) (Where an event has more than one 'Loss Type', choose the 'Consequence' with the highest rating)				
Loss Type (Additional 'Loss Types' may exist for an event; identify & rate accordingly)		1 Insignificant	2 Minor	3 Moderate	4 Major	5 Catastrophic
(S/H) Harm to People (Safety / Health)		First aid case / Exposure to minor health risk	Medical treatment / Exposure to major health risk	Loss time injury / Reversible impact on health	Single fatality or loss of quality of life / Irreversible impact on health	Multiple fatalities / Impact on health ultimately fatal
(EI) Environmental Impact		Minimal environmental harm - L1 incident	Material environmental harm - L2 incident remediable short term	Serious environmental harm - L2 incident remediable within LOM	Major environmental harm - L2 incident remediable post LOM	Extreme environmental harm - L3 incident irreversible
(BI/MD) Business Disruption / Material Damage & Other Consequential Losses		No disruption to operation	Brief disruption to operation	Partial shutdown	Partial loss of operation	Substantial or total loss of operation
(L&R) Legal & Regulatory		Low level legal issue	Minor legal issue; non compliance and breaches of the law	Serious breech of law; investigation/report to authority, prosecution and/or moderate penalty possible	Major breech of the law; considerable prosecution and penalties	Very considerable penalties & prosecutions. Multiple law suits & jail terms
(R/S/C) Impact on Reputation/Social/Community		Slight impact - public awareness may exist but no public concern	Limited impact - local public concern	Considerable impact - regional public concern	National impact - national public concern	International impact - international public attention
Likelihood (L)	**Examples** (Consider near-hits as well as actual events)	**Risk Rating (R)**				
5 Almost Certain	The unwanted event has occurred frequently; occurs in order of one or more times per year & is likely to reoccur within 6 months	11 (M)	16 (H)	20 (H)	23 (Ex)	25 (Ex)
4 Likely	The unwanted event has occurred infrequently; occurs in order of less than once per year & is likely to re-occur within 1 years	7 (M)	12 (M)	17 (H)	21 (Ex)	24 (Ex)
3 Possible	The unwanted event could well have occurred in the business at some point within 5 years	4 (L)	8 (M)	13 (H)	18 (H)	22 (Ex)
2 Unlikely	The unwanted event has happened in the business at some time; or could happen within 10 years	2 (L)	5 (L)	9 (M)	14 (H)	19 (H)
1 Rare	The unwanted event has never been known to occur in the business; or is highly unlikely that it could ever occur beyond 10 years	1 (L)	3 (L)	6 (M)	10 (M)	15 (H)

Interpretation of Risk Level

Risk Rating	Risk Level	Guidelines for Risk Matrix
21 to 25	(Ex) – Extreme	Eliminate, avoid, implement specific action plans / procedures to manage & monitor
13 to 20	(H) – High	Proactively manage
6 to 12	(M) – Medium	Actively manage
1 to 5	(L) – Low	Monitor & manage as appropriate

SAFL Risk Assessment Report

No	List the task/activity	List the hazard associated with the task and describe how the hazard can be brought about	Hazard consequence, type of loss/affect	Control measures	Loss Type	C	L	R	Recommended Additional Controls	C	L	R
1	Use of DMA to study response of fuel wetted elastomers	Incorrect furnace input conditions	Equipment damage	6. Understand furnace operation	MD	1	2	2L	5. Consult equipment manuals before use 6. Ask clarifying questions			
		Incorrect or damaged fittings may liquid nitrogen leakage	Human injury	4. Leak test before proceeding with test 5. Ensure correct fittings are used	S/H	2	2	5L	4. Become familiar with equipment differences for nitrogen fill and DMA testing			

No	List the task/activity	List the hazard associated with the task and describe how the hazard can be brought about	Hazard consequence, type of loss/affect	Control measures	Loss Type	C	L	R	Recommended Additional Controls	C	L	R
		Faulty compressor/incorrect compressor use	Equipment damage	5. Ensure compressor unit is turned on 6. Ensure compressor unit reaches desired pressure	MD	1	1	1L				
		Overflow of nitrogen gas	Human injury	4. Ensure extraction system is turned on before testing	S/H	3	1	6M	6. Wear breathing apparatus 7. Ensure air conditioning is switched off 8. Ensure oxygen sensors are turned on			

No	List the task/activity	List the hazard associated with the task and describe how the hazard can be brought about	Hazard consequence, type of loss/affect	Control measures	Loss Type	C	L	R	Recommended Additional Controls	C	L	R
		Chemical spillage/permeation through elastomer material	Human injury	2. Wear full PPE including latex gloves, safety glasses and lab coat	S/H	2	3	8M	2. Attempt to use non-toxic chemicals 3. Wear breathing apparatus if necessary			

University of Cape Town

Sasol Advanced Fuels Laboratory

OPERATING PROCEDURE:

BE AWARE OF RISKS PERTAINING TO TASK

Procedure Number:	
Procedure Description:	**Elastomer swelling and conditioning**
Procedure Compiled by:	Christopher Scully
Procedure Revision Date:	15 August 2013
Safety Officer Approval:	Dr Chris Woolard
Nature of revision:	To include changes made in operating procedure ☐ To include instrument modifications ☐ Changes made to wording in procedure document ☐ Other:_____ X
Re-training required:	**Yes** ☐ **No** X

1. GENERAL

SCOPE

This test method covers the procedures used to test the swelling response of fuel wetted elastomers. Additionally, the conditioning procedure of the elastomers and the make-up of standard solutions is included for completeness.

OBJECTIVE

This procedure is aimed at providing a framework to the safe operation and handling of materials and solvents used when performing elastomer swelling experiments. The objective of elastomer exposure to solvents is to assess the change in the dimensional change and thereby infer the consequences this will have on the materials performance. This test method can be applied to any material that will undergo swelling experiments. The solvents/fuel listed in this document are not exhaustive and any other fuels (within reason) may be used.

REFERENCES

This document serves as the primary reference on the seal swell procedure

2. PRINCIPAL HAZARDS

Volatile solvents

Flammable material

Glassware handling

Spilling of liquids

Petroleum products at elevated temperatures (50°C)

3. PERSONAL PROTECTIVE EQUIPMENT

Safety glasses

Safety gloves (impermeable to solvents)

Lab coat

Long pants

Closed shoes

Sufficient ventilation (use of a fume hood)

4. FIRST AID AND MEDICAL CARE RELATING TO KEROSENE & APPLICABLE SOLVENTS

EYE CONTACT

Check and remove any contact lenses. Flush out eyes with water for at least 15 minutes occasionally lifting the eye lids. Seek medical attention immediately.

SKIN CONTACT

Flush affected area with water for at least 15 minutes. Remove any clothing that may be constrictive or solvent contaminated. Wash affected area thoroughly with soap and water. If burn or irritation continues, seek medical attention as soon as possible.

INHALATION

For mild inhalation, take person to fresh air. If trouble breathing or experiencing breathing irregularities, prosee artificial respiration or oxygen by a trained professional. Seek medical attention immediately if person is unconscious.

INGESTION

Wash out mouth thoroughly with water. Do not induce vomiting unless advised to do so by a trained medical professional. Never give mouth to mouth assistance if person is unconscious. Seek medical help as soon as possible.

LACERATIONS

Any lacerations from broken glassware are to be treated with care. Advise the qualified first aid representative for further assistance. Apply pressure to laceration or keep laceration above the level of the heart for at least 15 minutes to stop the bleeding. For large lacerations, seek medical attention/dispatch of an ambulance.

5. GENERAL PROCEDURE

APPARATUS TO BE USED:

1. Clean volumetric flask
2. Clean 100ml Shott glass bottles
3. Clean Gilson pipette tips
4. Clean Pasteur pipette
5. Appropriate laboratory ovens (vacuum, if required)
6. Desired solvent matrix

ELASTOMER CONDITIONING

The following procedure is applied to ensure the elastomer sample is fully deplasticized

1. Place as-received samples in 1 litre of dichloromethane (DCM)
2. Allow samples to sit in solution for 3 days
3. Replace DCM with fresh batch after 3 days
4. Allow additional 2 days of solvent exposure
5. Remove samples from DCM and dry in fume hood for 24 hours
6. Place samples in drying oven at 50°C for additional 3 days

STANDARD SOLUTION MAKE-UP

The following procedure is recommended for the make-up of standard solutions

1. Obtain clean 100ml volumetric flasks
2. Draw required volume of solvent using electronic Gilson pipette
3. Load the required solvent volume into the clean volumetric flask
4. Fill the volumetric flask to the 100ml mark with desired fuel/solvent
5. Pour 100ml blend into clean 100ml Schott bottle
6. Shake thoroughly to ensure sufficient mixing
7. Place bottles in desired environment

SWELLING MEASUREMENTS

The following procedure is recommended to carry out reliable volumetric and gravimetric changes in the fuel-wetted sample

1. Label elastomer samples with metallic tags for differentiation
2. Measure the mass of the dry samples
3. Measure the volume of the dry samples through the digital microscopy
4. Place desired samples in the fuel blend
5. Place blend and samples in the desired environment
6. To measure changes, remove samples, one-by-one from the blend
7. Dab dry with roller towel
8. Dry samples with cotton swab
9. Measure the mass of the samples

10. Measure the volume of the samples using digital microscopy

11. Compare the changes in volume and mass

12. Continue steps 6 through 11 until equilibrium has been reached

6. TERMINATING A PROCEDURE

To terminate a procedure at any point simply remove the sample from the fuel blend or temperature sensitive environment

7. EMERGENCY SHUT DOWN OF SYSTEM

In the event that a fuel blend catches fire, assess the situation before acting. If fire is localised and small, turn off ovens using main switch. Alert a fire marshal of the fire. Exit through the appropriate exit. If the fire is large, exit the room immediately through the safest exit. Alert the fire marshal and call the fire department.

8. CLEANING EQUIPMENT

Cleaning of the equipment is an important part of the process. The recommended procedure for cleaning fuel/solvent exposed glassware is given below.

1. Dispose of the blend/solvent in the correct manner (Petrol waste, diesel waste, jet fuel waste)

2. Dispose of the elastomer samples in the appropriate manner. (Call EnviroServ)

3. Place methanol/ethanol in the empty Schott bottles. Shake thoroughly and allow to rest for 5 minutes. Dispose of solvent in the “petrol waste” container.

4. Soak bottles in hot water for up to 24 hours. (2-5 is ok)

5. Remove bottles from water and place in drying oven at 100°C.

6. Allow drying time of 24 hours

7. Soak removed metallic tags in acetone/toluene

8. Allow to dry in fume hood and drying oven for 24 hours before next use

SAFETY OPERATING PROCEDURE BLOCK STRUCTURE:

Job Step	Method	Hazard	Risk	Control Measure	Task observation	
					Task executed effectively	Deviations noticed
Elastomer conditioning	Decanting DCM	Chemical spillage	Chemical burns/ Irritations	Latex gloves Full lab coat		
Standard solutions	Decanting into glassware	Chemical spillage Broken glass	Chemical burns/irritations Lacerations	Latex gloves Work in a fume hood Work carefully with glass		
Swelling measurements	Remove elastomers from solution	Chemical spillage Broken glass	Chemical burns Lacerations Chemical inhalation	Latex gloves Full lab coat Additional breathing apparatus		
Cleaning of glassware	ecanting chemicals into glassware	Chemical spillage Broken glass	Chemical burns Lacerations Toxic waste down drain	Latex gloves Full lab coat Use correct waste disposal method		

University of Cape Town

Sasol Advanced Fuels Laboratory

OPERATING PROCEDURE:

BE AWARE OF RISKS PERTAINING TO TASK


Procedure Number:	
Procedure Description:	**Operation of Dynamic Mechanical Analysis (DMA) apparatus**
Procedure Compiled by:	Christopher Scully
Procedure Revision Date:	15 August 2013
Safety Officer Approval:	
Nature of revision:	To include changes made in operating procedure ☐ To include instrument modifications ☐ Changes made to wording in procedure document ☐ Other:_____ X
Re-training required:	**Yes** ☐ **No** X

1. GENERAL

SCOPE

This test method covers the procedure required to carry out testing using a Thermal Analysis (TA) DMA Q800. The procedure is designed to allow testing over the full temperature limits of the machine (-90°C-500°C). In particular, this method describes only testing in which tensile clamps are appropriate. For other modes of testing, the user should consult the necessary references provided below.

OBJECTIVE

This procedure aims to document the safe operation procedure to test the dynamic mechanical response of a material using a DMA Q800 apparatus. Testing temperatures in the range of -90°C - 500°C is obtainable and thus care needs to be given to the testing method. The DMA output includes information regarding the storage modulus, loss modulus and Tan δ response of the material to changing conditions. As such, this procedure can be used for any desired material.

REFERENCES

TA Instruments DMA Q800 operators manual

Official TA Instruments YouTube channel

2. PRINCIPAL HAZARDS

Liquid nitrogen handling

Temperature extremes

Fuel wetted samples (if applicable)

3. PERSONAL PROTECTIVE EQUIPMENT

Safety glasses

Safety gloves (latex or cryogenic for liquid nitrogen fill)

Closed shoes

4. FIRST AID AND MEDICAL CARE RELATING TO LIQUID NITROGEN CONTACT

EYE CONTACT

Immediately flush eyes with warm water for at least 15 minutes. Seek medical attention immediately.

SKIN CONTACT

Remove any clothing that may restrict blood flow to affect area. Do not rub affected area as tissue damage may occur. Apply warm water to the affected area and seek medical attention as soon as possible.

INHALATION

Person suffering from a lack of oxygen should be moved to fresh air immediately. Seek medical attention immediately.

FIRST AID AND MEDICAL CARE RELATING TO FUEL/SOLVENT EXPOSURE

EYE CONTACT

Check for and remove any contact lenses. Continually flush eyes out with water for at least 15 minutes. Consult MSDS for further information however, seeking medical attention is advised on all occasions.

SKIN CONTACT

Immediately flush affected area with water. Remove any contaminated clothing. Wash affected skin area with soap and water. Seek medical attention if required.

INGESTION

Wash out mouth with water. Do not induce vomiting unless directed to do so by medical professional. Seek medical attention immediately.

5. PROCEDURE

LIQUID NITROGEN FILL

When low temperature testing is required, the use of liquid nitrogen as a coolant is required. The following procedure is used to fill TA GCA liquid nitrogen tank (approx.100L)

1. Position tank within close proximity of liquid nitrogen mini-tank.
2. Connect filling pipe to the tank jack labelled “auto fill”
3. Connect opposite end to liquid nitrogen source (mini-tank)
4. An adapter device (provided by Air Products) may be required for some tanks.
5. Tighten filling pipe onto mini-tank using a shifting spanner of appropriate size
6. Power on the TA GCA liquid nitrogen tank by pressing the black “power” switch
7. To fill, the tank needs to be connected to the appropriate GCA interface
8. Connect GCA tank to a laptop/PC using a USB to RS232 connection
9. Ensure the appropriate GCA control software is installed on the electronic device
10. Launch the GCA control software
11. Click “Connect” on top right hand corner of GCA control interface
12. A loud “Klack” sound should be heard as the GCA tank registers connection
13. Once connected, open the liquid nitrogen tap located on top of the mini-tank. Open this fully.
14. Once opened, click the “Fill” located in the centre of the GCA control interface

15. Liquid nitrogen should start to flow to the GCA tank
16. Allow approximately 5-7 minutes for liquid nitrogen to circulate the GCA tank cooling the interior.
17. Monitor the “Tank Level” tab on the top left hand corner of the GCA control interface
18. Once appropriately filled, click the “Stop” button located on the right hand panel of the GCA control interface
19. Shut down GCA tank by clicking “Disconnect” tab on GCA control
20. Shut down GCA tank by clicking “Power” button on the GCA tank
21. Turn off tap to stop liquid nitrogen flow from mini-tank
22. Allow 15 minutes for connector pipe to defrost before removal

GENERAL DMA USE

This section describes the general procedure for use of the DMA Q800. Tension clamps have been used throughout.

1. Ensure flow pipe from GCA tank to DMA Q800 is sufficiently connected
2. Ensure compressor unit is switched on to prosee sufficient drive to furnace motor
3. On the DMA control face, click “open furnace” to allow sample mounting
4. Select the correct clamp to install in the DMA Q800
5. Calibrate the clamp mass and position (For calibration guidance, refer to the suggested references listed above)
6. After calibration, mount the sample in clamp
7. Tighten clamp using provided torque wrench (3-5 in/lb for tensile clamps)
8. Click “close furnace” to close the furnace chamber
9. Proceed to the TA software interface for DMA operation on the host PC
10. Click on the “Experimental Wizard” tab on the interface ribbon

11. Select type of DMA test you require (isothermal, multi-frequency, custom)
12. Select the oscillation frequency you require (typically, 1Hz)
13. Input experimental parameters such as start temperature, hold time, temperature ramp rate and final temperature
14. Input sample dimensions where appropriate
15. Click “Finish”
16. Test parameters will be shown in central box on the interface screen
17. Click “Edit Procedure” to amend your procedure
18. Click “Select Path” to indicate path directory you require the information to be stored
19. Add appropriate comments in the “Comments” tab that pertain to your test (optional)
20. Click “Run” button located on top left side of the interface ribbon
21. Test should run to completion

6. TERMINATING A PROCEDURE

To terminate a procedure which is running normally, simply click the “Stop Run” button located on the left side of the DMA control interface. This must be done from the host PC. The test will immediately cease and liquid nitrogen will automatically stop flowing. The gathered data will be saved under the file path that the user has selected.

7. EMERGENCY SHUT DOWN OF SYSTEM

If emergency situation arises while liquid nitrogen is flowing, simply click the “Power” button on the GCA tank to power the tank down. Nitrogen will cease to flow and the test will automatically stop.

In the event no nitrogen is flowing, click “Stop Run” located on the DMA interface on the host PC or on the screen of the DMA machine.

SAFETY OPERATING PROCEDURE BLOCK STRUCTURE:

Job Step	Method	Hazard	Risk	Control Measure	Task observation	
					Task executed effectively	Deviations noticed
Liquid nitrogen fill	Roll or lift GCA tank to proximity of mini-tank	Lifting of heavy materials	Putting your back out Dropping the tank	Ensure 2 or more people help with moving of the GCA tank		
	Shifting spanner to tighten bolt	Finger pinch Minor frost bite	Frozen tank	Cryogenic gloves		
	Actual filling process	Flowing liquid nitrogen	Frost bite	Cryogenic gloves Closed Shoes		
	Moving GCA tank back to lab	Heavy lifting Liquid nitrogen spillage	Pulled/damaged muscles Frost bite	Ensure more than 2 people aid moving of GCA tank Ensure tank is tied down sufficiently		